SPATIAL AND TEMPORAL DISTRIBUTION OF PARTICULATE POLLUTION IN LONDON FROM HIGH-TEMPERATURE COMBUSTION SOURCES

Thesis submitted for the degree of Doctor of Philosophy in the University of London

by

Alison Helen Berry

University College London

April 2002

ABSTRACT

The urban atmospheric environment contains a complex cocktail of pollution from numerous sources. However, the contribution to this mixture from power stations and other high-temperature combustion point sources is uncertain. Spheroidal carbonaceous particles (SCPs) and inorganic ash spheres (IASs) are uniquely formed as a by-product of high-temperature combustion of fossil fuels and therefore are ideal indicators of fossil-fuel derived pollution in London.

Deposition of SCPs in London from power stations and other combustion processes regulated by the Environment Agencies under Part A of the Environment Act 1990 was modelled using the atmospheric dispersion modelling system (ADMS 3) developed by the Meteorological Office and the Cambridge Environmental Research Consultancy. The results agreed well with the spatial distribution of SCP concentrations in surface sediments from twenty-seven lakes and ponds within the M25. SCP size distributions were used to identify the dominant sources of SCPs for each site. Multivariate statistical analyses showed that lake and pond processes were generally not important variables affecting the concentration of SCPs in the surface sediments.

High resolution SCP and IAS time-series collected by Burkard Spore Traps on a transect linking the centre of London with the power stations in the east Thames Corridor showed the presence of several pollution events, both SCP and IAS, that occurred simultaneously at a number of sites. Potential sources were identified for each IAS and SCP event based on SCP size data and meteorological conditions. The relationship between the IAS and SCP concentrations indicated whether the event was caused by a coal- or oil-fired source. Multivariate statistical analyses of the meteorological data did not consistently extract any one variable that would explain the SCP and IAS profiles. However, a subjective analysis of the data shows that many IAS events in London are caused by emissions from the power stations in the east Thames Corridor.

ACKNOWLEDGEMENTS

I would like to thank the following people:

My supervisors, Neil Rose and Rick Battarbee at UCL and Jimi Irwin at the Environment Agency for their help and guidance throughout this project.

My fieldwork helpers for braving some of the muddiest waters in London; Emma Durham, Simon Dobinson, Sophie Evitt, Al Graham, Ben Goldsmith, Phil Henderson, Kate Heppell, Ian Mulvey and Ewan Shilland.

The members of the Environmental Change Research Centre at UCL for their friendship and support. I would especially like to thank Martin Kernan for all his help with statistical problems.

The lab staff at UCL, in particular Janet Hope and Tula Cloke.

Neil Lucas at Glaxo-Wellcome, Duncan Phillips at Dartford Borough Council, the Air Pollution team at Gravesham Borough Council and Dawn Sutton at Thamesmead Community College for providing sites for the Burkard Trap transect.

John Watt and Sandra Nederbragt for help with analytical techniques.

Peter Burt for top-tips on how to prepare Burkard Trap tapes for counting.

Finally, I would like to thank my parents for constant support in whatever I have chosen to do and Martin Palmer for proof reading, educating me in the correct usage of the comma and for never losing faith in me even when I lost it in myself.

This work was funded by the Natural Environment Research Council and the Environment Agency under the CASE studentship scheme.

CONTENTS

CHAPTER 3: DISPERSION MODELLING IN LONDON OF PARTICLES FROM HIGH TEMPERATURE COMBUSTION SOURCES

CHAPTER 5: SCP AND IAS POLLUTION EPISODES ACROSS LONDON

CHAPTER 6: METEOROLOGY OF POLLUTION EPISODES

LIST OF FIGURES

LIST OF TABLES

CHAPTER 1: INTRODUCTION

1.1 Historical air pollution in London

Urban air pollution is perceived as being a modern problem associated with cars and heavy industry. However, pollution has always been a by-product of human activity and wherever humans settle there will be a pollution problem. As the population size increases then the pollution problem also increases.

In the past urban air pollution was mostly associated with domestic and industrial use of coal as a fuel within the urban area. In medieval London the pollution from coal burning was considered such a serious problem that in 1285 a commission was set up to investigate the matter. Regular meetings of this commission resulted, in 1306, in a ban on the use of sea coal (Brimblecombe, 1988). Coal use remained relatively constant between the 13th and 16th centuries with wood and charcoal being used in preference due to lower emissions of noticeable pollutants. However, shortages of wood and charcoal were not uncommon in cities once the surrounding area became deforested leading to a general rise in timber prices in 1540 (Nef, 1932).

In the 16th century Queen Elizabeth I complained about the taste and smoke of 'sea-coales' from industrial sources. After her death in 1558 and with the accession of James I, coal use became more widely accepted because it was more frequently used in his native Scotland. The lower sulphur content of Scottish coal (0.1% sulphur compared with 1.38% for Lancashire coal) meant that it produced less sulphur dioxide. This would have made coal use more socially acceptable for the upper classes (Brimblecombe, 1988). By the end of the Elizabethan era (c 1600) the shortage of wood meant that coal was needed as a domestic fuel and was no longer used exclusively in industry.

Population growth in the 16th century, in London and countrywide, with its associated increasing demands for coal, both by industry and for use in domestic fires, brought about the start of an 'early industrial revolution'. Without coal the expansion of industry at this time would not have been able to take place. At the end of the 15th century 34 757 tonnes of coal were

imported into London. This had increased to 466 639 tonnes by 1697-98 (Nef, 1932).

In 1661 John Evelyn wrote "Fumifugium" which described the effects of smoke on buildings, clothes, paintings, water, plants and humans. He recommended that fuels such as wood or charcoal should be used in preference to coal but recognised that industries were the major cause of pollution. He recommended that an Act be put to Parliament that the industries be moved to the outskirts of London,

> 'or at the least so far as to stand behind that Promontory jetting out, and securing Greenwich from the pestilent Aer of Plumstead-Marshes'.

For industry that needed to remain within the confines of London, Evelyn recommended that it be situated in 'the Town of Bowe' because of the continual winds that would clear the air (Evelyn, 1661).

By the beginning of the 17th century London was suffering from air pollution problems that have continued through until the modern day. Coal replaced wood as the major domestic fuel and by the end of the century coal imports into London exceeded one million tonnes per annum (Brimblecombe, 1977). In the 18th century, medical writers such as Arbuthnot, Walker and Mead described the effects of air pollution on health and the urban environment. Air pollution had become related to London's fogs, which increased between 1750 and 1890. The fogs of the 19th century were noted to be of a different colour to those of previous times (Brimblecombe, 1977). A fog incident in London during the winter of 1873 caused 700 deaths in addition to those expected at that time of year.

Smogs had become less frequent during the first half of the 20th century. However, in December 1952 a slow moving anticyclone came to a stop over the city of London which then trapped high levels of pollution at low elevations. The 'Great Smog' lasted four days and was held responsible for the deaths of thousands of people. Relocation of large combustion sources

away from the centres of towns and cities along with the introduction of pollution control technology and pollution control legislation has reduced the quantities of smoke, SO_2 and NO_2 emitted within urban areas. However, there are now many pollution sources including road transport, aircraft, power stations and industrial processes and in combination these many sources create a complex cocktail of pollution in urban areas. Long range transport of pollution (e.g. HMIP, 1996) shows that pollution from those sources that were relocated away from urban centres can still contribute to pollution concentrations within the urban area.

1.2 Pollution legislation in London

A number of Acts of Parliament have been passed through the ages to attempt to achieve reductions in air pollution (Brimblecombe, 1988). The pollution problem and legislation to control it has been widespread since the time of Evelyn. The Public Health (London) Act of 1891 was brought in to control emissions of smoke from non-domestic fires and furnaces. This Act was crippled by the fact that the nuisance was defined by the words 'black smoke'. Polluters that emitted brown smoke could therefore get around the legislation. The term 'Great Stinking Fogs' was used in the 19th century to describe the fogs that were thicker and more frequent than in the past. The London County Council (General Powers) Act of 1910 strove to clarify the Act of 1891 but had limited power and little success (Brimblecombe, 1988). In 1926 the phrase 'best practicable means' (BPM) to control pollution appeared in legislation for the first time, and by 1932 there were by-laws in 155 authorities across the country that were concerned with the abatement of black smoke.

Charles Gandy of the National Smoke Abatement Society called for the creation of smokeless zones during the rebuilding of London following World War II. The City of London Act was passed in 1946 which allowed development of smokeless zones and nowadays over 90% of London is covered by these zones (Brimblecombe, 1988). The 'Great Smog' of 1952 prompted major changes in legislation. Before this date legislation had been

weak and public opinion about pollution had been divided between support for cleaner air and the desire for coal fires. In response to the 'Great Smog', Clean Air Acts were introduced in 1956 and 1968 which attempted to control both domestic and industrial sources of pollution. The Control of Pollution Act of 1974 finally recognised the need to treat the environment as a whole and pollution control measures were integrated to protect the environment from air pollution, water pollution, noise pollution and waste disposal (Brimblecome, 1988). Figure 1.1 shows the decrease in black smoke concentrations at a number of sites from 1961 onwards.

Figure 1.1: Annual black smoke concentrations at selected sites (from QUARG, 1996)

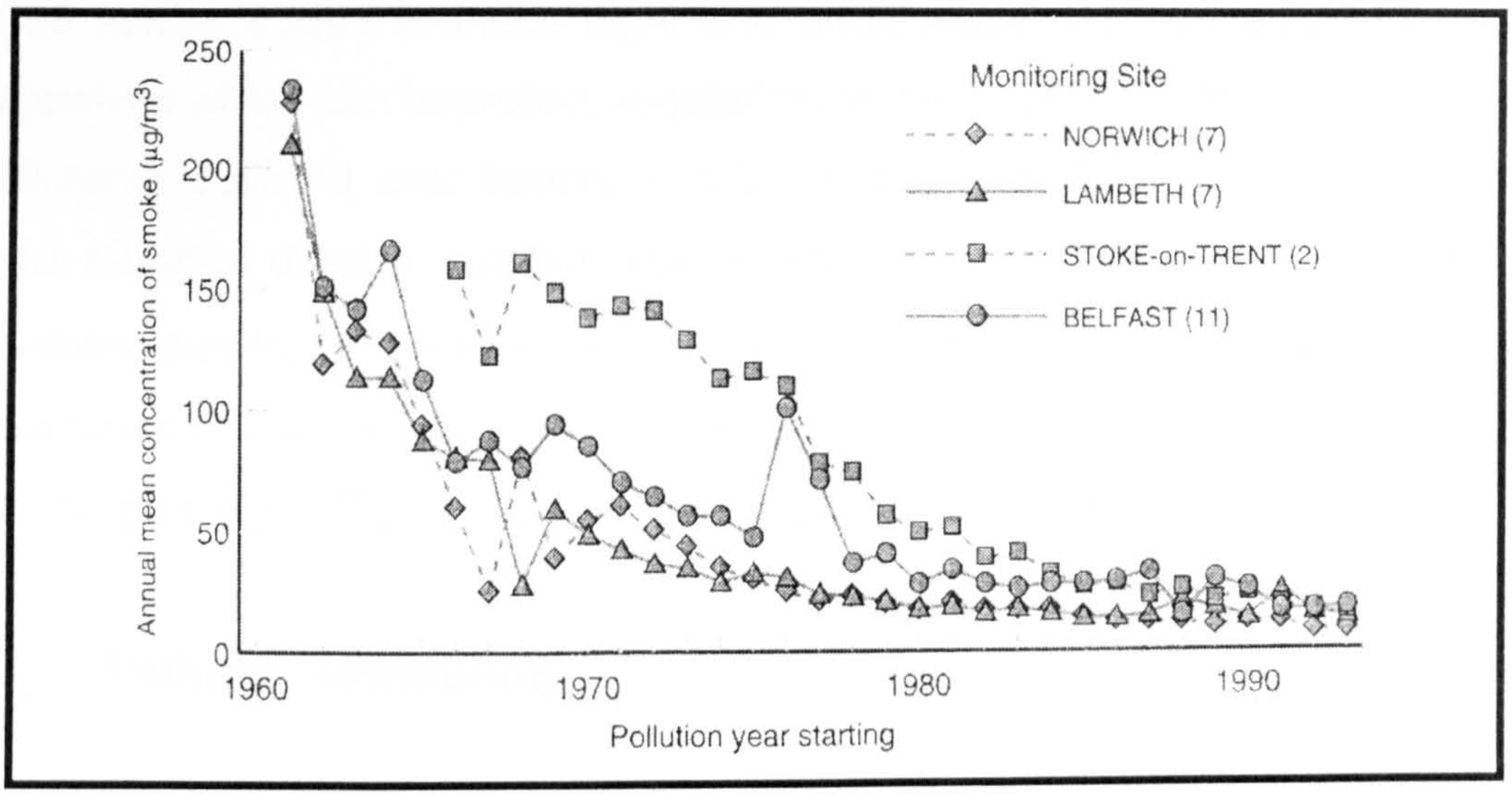

More recently, in 1990, BPM was replaced with BATNEEC - the requirement for pollution control using the Best Available Technology (Not Entailing Excessive Costs). BATNEEC was replaced by BAT (Best Available Techniques) in 1996 by the Integrated Pollution Prevention and Control (IPPC) Directive, which takes away the ability for pollution producers to hide behind economic screens.

In order to comply with Part IV of the Environment Act 1995, the Government produced a National Air Quality Strategy which contained standards and objectives for air quality. The Local Air Quality Management system was also initiated as part of the Act that sets out the obligations for local authorities to meet the air quality standards. There is now a statutory requirement under The Air Quality Regulations 1997 (as amended) (made under Part IV of the 1995 Act) for local authorities to review and assess seven of the objectives and where the objectives are not met to declare an Air Quality Management Area (AQS, 1999).

The National Air Quality Strategy set out objectives to reduce eight main pollutants to protect health and was implemented in the UK in 1997. The 1999 review added to these eight and additionally has suggested two new objectives which aim to protect vegetation and ecosystems (AQS, 1999). The pollutants covered are: benzene, 1,3-butadiene, carbon monoxide, ozone, lead, nitrogen dioxide, sulphur dioxide and particles (PM_{10}). PM_{10} are those particles that have a mean aerodynamic diameter of 10 μm or less. These guidelines are set within the European and wider international contexts. The UK, as part of the EU, is required to comply with European legislation.

1.3 Pollution monitoring

Once pollution is perceived as a problem then it becomes necessary to accurately quantify the extent of the problem through pollution monitoring. Otherwise analysis of the problem is subjective without spatial and historical levels with which to compare any changes. The process of keeping records of atmospheric pollution has been sporadic through time. In Victorian England there was no air pollution monitoring, but evidence for the extent of air pollution is provided by written records describing air pollution events or paintings showing urban scenes with the skies yellowed by sulphur. (Brimblecombe, 1988).

The earliest monitoring of rainwater in London was carried out by R A Smith on samples from 1870. The next measurements were made between 1882

and 1884 with samples of rain collected by Dr W J Russell from a small number of sites in London. These two sets of measurements gave levels of sulphate and chloride deposition higher than those measured in 1956-7. A few measurements of the levels of particulate matter in the air were made by Russell in the 1880's. He found that particulate matter concentrations were higher during dull or foggy conditions and lower during sunny weather. In 1910, the Coal Smoke Abatement Society initiated a monitoring exercise to collect rainwater in what became the forerunner of the deposition gauge, which comprised a funnel with a mesh over the top to prevent birds soiling the sample. Analyses of chloride, sulphate, ammonia, calcium and solid matter were presented in the Lancet by Dr H A Des Voeux. The deposition gauge was further developed and by 1914 there were twelve gauges in operation in the British Isles (Brimblecombe, 1988).

A good relationship between coal use and deposition of black matter led to the filter paper method being established in 1918. Air was drawn through a circle of filter paper and the amount of darkening caused by the deposition of particulate matter was noted. The degree of darkening was calibrated against the amount of suspended particulate matter. The system was automated to make measurements every 15 minutes. A system was installed in Kew Gardens in the 1920's (Brimblecombe, 1988). This relationship works well when pollution is from the same source. However, with the increased contribution that particulates from road transport make to the atmosphere the relationship is less clear (APEG, 1999). Modern filter papers are weighed to compare the mass of particulates with concentration in the atmosphere thus bypassing the problem of particulate colour.

Atmospheric sulphur was first assessed in 1932 by the Building Research Establishment who were interested in the damage that SO_2 did to paint, stone and ironwork. However, this technique did not convert easily to give an estimate of atmospheric SO_2 concentration. Pyatt (1973) used vegetation as a method for monitoring particulate pollution and found particulate matter in up to 50% of laurel leaf stomata.

Qualitative comparisons between historical records and contemporary measurements are difficult because of the lack of continuity in measurements. The number of different methods and observers leads to a certain amount of scepticism of the historical measurements (Brimblecombe, 1977).

The resurgence of an interest in pollution in recent times because of concern over health and environmental impacts has lead to increased pollution monitoring. The United Kingdom's Automatic Urban Air Quality Monitoring Network (AUN) is operated by the Department for Environment, Food and Rural Affairs (DEFRA) and comprised ninety-three sites in 2000. The data from the AUN are collated into a pollution archive, which is available on the Internet (http://www.aeat.co.uk/netcen/airqual, (September, 2001)). In urban areas where the pollution impact from road transport is greatest, specific monitoring networks have been set up. The London Air Quality Network (LAQN) was set up in 1993 with the aim of improving air quality monitoring and to enable London Boroughs to review and assess their air quality (SEIPH, 1999). At the end of 1995 seventeen monitoring sites from the LAQN were selected for inclusion into the AUN. The impact of power stations on the environment has been well monitored over the last 30 years by over 200 long-term air quality monitoring stations (Laxen, 1996). In the Thames estuary in 1994 there were nine monitoring stations.

1.3.1 Particle monitoring

There are a number of different methods available to monitor particles. The type of monitor used depends on whether human health effects are being studied, in which case the airborne concentration of particles is measured, or whether nuisance effects are of interest, in which case particulate deposition is important. Most monitors now measure PM_{10}, which is an aerosol fraction that is small enough to enter the thoracic region of the respiratory system. PM_{10} is defined as the particulate matter that will pass through an inlet with defined characteristics with a 50% sampling efficiency for particles 10 µm in diameter (APEG, 1999) which means that the particles will penetrate the respiratory system beyond the larynx. Recently there has been a greater

focus on monitoring the smaller size fractions of particles (e.g. $PM_{2.5}$, PM_1), which are perceived to be more important in terms of potential health effects (APEG, 1999).

Monitoring methods for PM_{10} can broadly be broken down into gravimetric cumulative samplers and direct reading monitors. Gravimetric cumulative samplers separate PM_{10} (or $PM_{2.5}$) particles from the air stream which are then collected on a filter and weighed (e.g. the SA 1200 PM_{10} High Volume Sampler which is the standard monitor used in the USA for measuring PM_{10} in ambient atmosphere). Direct reading monitors carry out both sampling and analysis within the instrument (e.g. the Grimm Stationary Environmental Dust Analyser 1.200, the Tapered Element Oscillating Membrane (TEOM) and beta particle attenuation) (QUARG, 1996). The TEOM is used at most AUN sites by DEFRA.

The TEOM system is kept at a constant temperature of 50°C to drive off water droplets, however this has caused the TEOM system to come under criticism. APEG (1999) suggests that the TEOM system under-represents the particle mass by 30% due to the evaporation of water from particulates and loss of semi-volatile species. Additionally, the heating system is not totally effective. Jones et al. (2001) linked the presence of $CaSO_4$ and NaCl crystals on TEOM filters to the presence of water in the system, caused by the failure of the internal heating system to exclude water from the collection filter, thereby affecting the particulate mass.

The number of particles per microgram increases with a decrease in particle size and, correspondingly, the surface area to volume ratio of the particle will increase with a decrease in particle size. The weight of deposition measured by PM_{10} analysers (e.g. TEOM, Beta Particle Attenuators) is dominated by a small number of large particles despite smaller particles dominating the particle number (e.g. Harrison et al., 1999a). Size fraction analysis of individual particles is carried out using single-particle optical counters (OPCs). These measure the amount of light scattered by particles as they pass through a tightly focussed beam of light. The scattered light is then converted

into a voltage pulse that is proportional to the size of the particle. Chemical characterisation of individual particles is possible using methods such as single particle mass spectrometry (SPMS) (McMurray, 2000).

1.4 Contemporary gaseous pollution

Fossil fuel power stations are responsible for the emission of significant quantities of gaseous pollutants, including SO_2 and NO_x. The principle gas emitted by these power stations is SO_2 whereas NO_x contributes less to both annual mean concentrations and specific episodes (Laxen, 1996).

SO_2 is a primary pollutant, which means that it is emitted directly from a source. Natural emissions of sulphur, which are then oxidised to SO_2, occur as DMS (dimethyl sulphide) from marine phytoplankton and as H_2S (hydrogen sulphide) from soils and vegetation (Colls, 1997). Power stations are the largest emitters of SO_2 in the UK, however in urban areas there can be a significant contribution to SO_2 concentrations from diesel-powered vehicles. In London, road transport is responsible for the production of 25% of SO_2, 75% of NO_x (SEIPH, 1996) and 96% of volatile organic compounds (VOC's) (QUARG, 1993). In 1991 the total UK anthropogenic emission of SO_2 was 3 731 ktonnes of which 73% (2723 ktonnes) was from power stations. National emissions of sulphur dioxide have decreased by 66% since 1980. In 1997 power stations contributed 62% of the annual UK emissions of SO_2; a reduction in emissions of 1 698 ktonnes to just 1 025 ktonnes (AQS, 1999).

Both NO and NO_2 are pollutants that are generally grouped together as NO_x. NO is produced in two ways:

1. Thermal reaction between nitrogen and oxygen in the air; and
2. From nitrogen in fuel.

Where the oxidising capacity of the environment is limited there will be less NO_2 and more NO. In less polluted areas almost all of the NO will be converted to NO_2.

The nitrogen content of oil and coal is between 0.5% and 1.5%. The nitrogen content of natural gas is much smaller. Power stations in 1997 made up only 20% of the total UK emissions of NO_x and there has been a steady reduction each year since 1990 when the contribution was 29%. The contribution to annual NO_x from road transport has stayed between 46% and 48% for the same period. Both power stations and road transport have reduced total emissions each year from 781 ktonnes in 1990 to 370 ktonnes in 1997 from power stations and from 1 233 ktonnes in 1990 to 883 ktonnes in 1997 from road transport (AQS, 1999).

The fate of nitrogen emissions is further complicated by the presence of ozone in the atmosphere. Natural ozone exists in the troposphere at background levels of 10–20 ppb. The remainder forms photochemically by the reaction of photons on NO_2 (Colls, 1997). Thus during episodes of sunny weather this reaction causes the levels of NO_2 in the atmosphere to decrease.

Other gaseous pollutants that are of concern for their effects on human health are CO, benzene, 1,3-butadiene and lead. The main source for both CO and 1,3-butadiene is road transport and benzene results from petrol distribution and combustion. Petrol-fuelled vehicles were thought to be a significant source of lead in the atmosphere although emissions fell between 1989 and 1995 due to increased usage of unleaded petrol and the reduction of the lead content of leaded fuel. A recent study of the isotopic composition of lead particles in the Straits of Dover has shown that vehicles are a minor source in comparison with industrial sources (Deboudt et al., 1999).

1.5 Contemporary particulate pollution

Airborne particles have a wide range of sizes. PM_{10} is defined above in Section 1.3. $PM_{2.5}$ is the corresponding fraction that has an aerodynamic diameter of less than 2.5μm and is commonly referred to as the fine fraction. The fraction of PM_{10} which is larger than $PM_{2.5}$ is normally considered to be coarse particulate matter. Smoke is defined as particulate matter derived

from the incomplete combustion of fuels smaller than 15μm in size. Total suspended matter (TSP) refers to all airborne particles (QUARG, 1996). Particles with a diameter of less than 0.1μm (APEG, 1999) or 0.05μm (QUARG, 1996) are termed ultrafines. Figure 1.2 shows some typical aerosols and corresponding particle sizes.

Figure 1.2: Diagram of particle sizes (from QUARG, 1996)

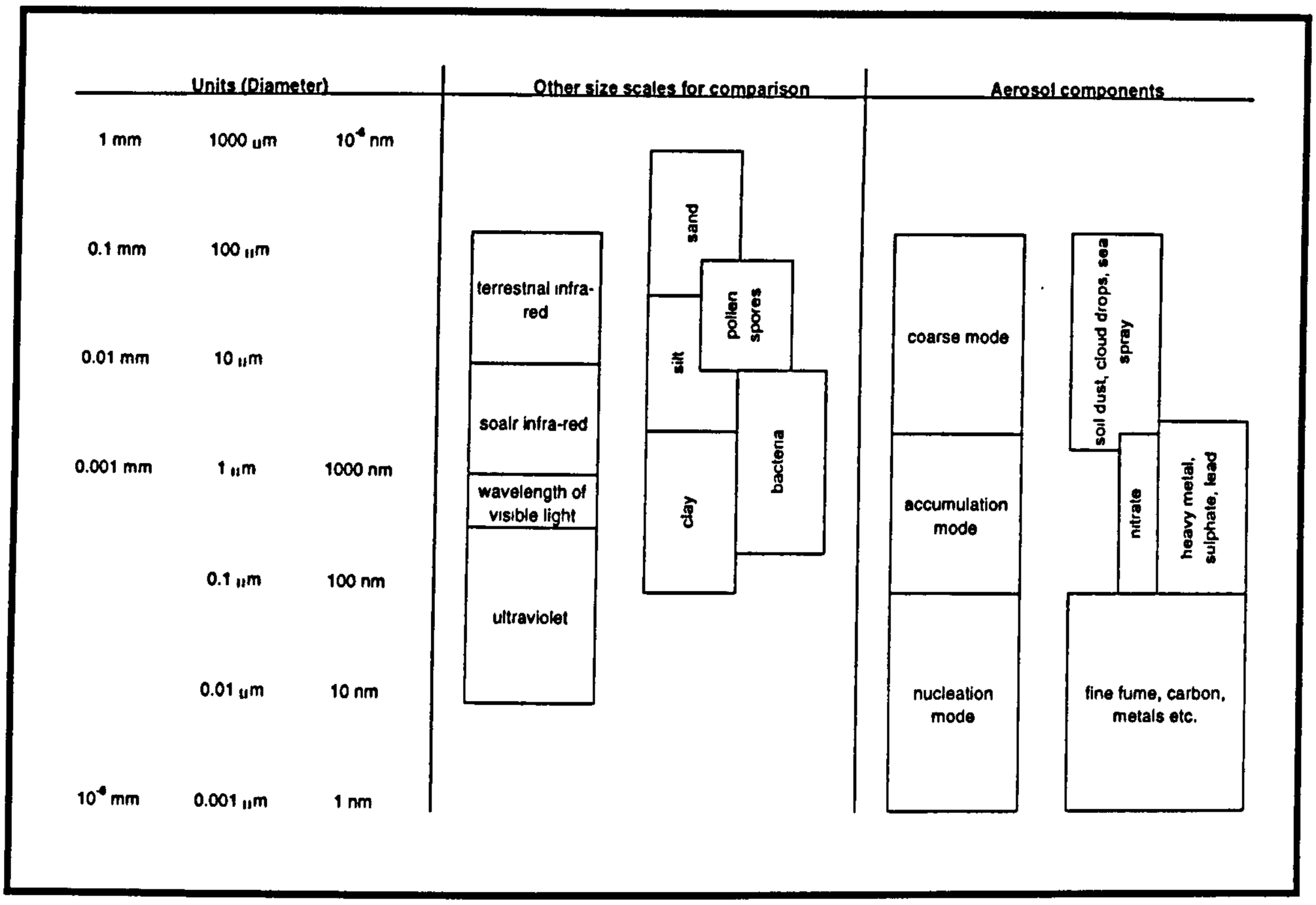

In urban areas the main source of particulates is road transport. Emissions from industrial or stationary combustion sources within London are not significant in comparison with road transport, which contributes 77% of the total PM_{10} emissions (APEG, 1999). Diesel vehicles emit much higher levels of particulates than petrol-powered vehicles and only diesel vehicles have to comply with limits for particulate matter.

Diesel and petrol cars with catalytic converters have a similar breakdown of the mass fraction of PM_{10} with 90% of the mass less than 2.5μm in size, 85% of the mass less than 1μm in size and 50% of the mass with a diameter less than 0.1μm. For petrol vehicles without catalytic converters 20% of the mass is from the 2.5-10μm size range (APEG, 1999; from the United States

Environmental Protection Agency and the Institute of Environmental Sciences, Energy Research and Process Innovation in the Netherlands).

1.5.1 Particle sources

The National Air Quality Strategy Consultation Document (AQS, 1999) describes atmospheric PM_{10} as comprising particles from three main sources:

Primary particles are those that are emitted directly by combustion processes including road transport, stationary combustion and industrial processes. These particles are generally less than 2.5 μm and often less than 1 μm in diameter and are mainly formed by homogeneous nucleation when the concentration of non-volatile particles is greater than the saturated vapour pressure in the atmosphere. Large numbers of very small particles around 1-10 nm in size can be produced. Growth of these particles through heterogeneous nucleation or agglomeration leads to formation of larger particles in the 'accumulation mode' (0.05-2 μm in diameter). Primary processes might also form coarse particles (see below).

Coarse particles are mostly formed by attrition and include particles generated by quarrying and the construction industry, resuspended road dust, tyre debris and natural sources such as wind blown dusts, soils, forest and other natural fires. These particles are likely to be greater than 5μm in size because a large amount of mechanical energy is required to break particles down further in size (APEG, 1999). Other particles that contribute to the coarse fraction are pollen (typically larger than 10μm) and spores (larger than 5μm). Fly ash is described by the Quality of Urban Air Review Group (QUARG, 1996) as a 'special case of comminution aerosol'. Comminution is a process that reduces fuel to small particles (in the case of coal) or droplets (in the case of oil). The particles are then further reduced through the loss of carbon and organic matter at high temperatures to leave involatile components (generally larger than 5μm (QUARG, 1996)). Smaller fly ash particles can also be a by-product of primary combustion (see above).

Secondary particles are formed in the atmosphere by chemical reactions between gases and are mostly less than 2.5μm in diameter. For example, SO_2 and NO_2 form sulphates and nitrates by homogeneous and heterogeneous nucleation in the atmosphere. The size of secondary particles may be affected by humidity but they are generally less than 2.5μm.

The relative contribution of each of the three source types (primary, secondary and coarse) to total PM_{10} varies on a daily basis depending on meteorological conditions and variation of emissions from mobile and stationary sources (AQS, 1999).

The biological component of the atmospheric particulate load is less well studied. In a seasonal study of individual particles collected using a Burkard Trap in London (Mackay, 1998) the contribution of biological particles such as pollen and spores comprised between 0.5% and 2.7% of the total numbers of particles counted. The contribution of bacteria and viruses to particle mass is not known.

1.6 Particle chemistry and source attribution

Composition of particulate pollution varies spatially and temporally and depends on the spatial distribution of particle sources, atmospheric chemical transformations, long range transport and removal processes. The chemical composition of particles can provide information about the particle source.

Receptor modelling has been developed as a method to apportion aerosol to sources, and includes a number of different techniques including chemical mass balance (CMB) and multivariate models (Henry et al., 1984).

CMB analysis requires detailed knowledge of source emissions (Watson and Chow, 2001) and is used to apportion pollution particles to sources based on their chemical characteristics (e.g. Javitz et al., 1988). The CMB approach has been used in combination with magnetic properties to identify sources of particles in Shanghai (Shu et al., 2001). Magnetic hysteresis parameters

were included with meteorological parameters and pollution data and showed that at one site there was a strong relationship between magnetic parameters and road transport derived combustion pollutants but not at another.

Multivariate methods have been used widely to relate particles to sources. For example, Sadasivan and Negi (1990) identified seven sources that contribute to aerosol mass in Bombay using instrumental neutron activation analysis (INAA) and energy dispersive X-ray fluorescence (EDXRF) on bulk aerosol samples and Moreno-Grau et al. (2000) related the Pb/Cd ratio of bulk aerosol samples to anthropogenic contributions from industrial areas. Other examples of multivariate methods include Boni et al., (1988); Maugeri et al., (1990); Harrison et al., (1997a); Prati et al. (2000); Hien et al. (2001) and Huang et al. (2001).

Other studies have focussed on the change in particle composition with particle size. Multivariate techniques were used by Chan et al. (2000) to identify source factors of size-fractionated PM_{10} bulk samples from Brisbane. The four source factors identified were soil, sea-salt, organics and vehicular exhaust. They found higher levels of contamination from fuel combustion products in the fine particle fractions. X-Ray diffraction analysis of size-fractionated particles from Cardiff showed an increase in concentrations of Ca, Si, Al and Fe with an increase in particle size (APEG, 1999).

The relationships between different size fractions of urban aerosol give an insight into contributions from different sources. Stedman et al. (2001) used an alternative method of receptor modelling to allocate PM_{10} collected in London to three source types; coarse particles, secondary particles and combustion generated particles. This method uses the contributions of measured PM_{10}, NO_x and particulate sulphate to estimate the total particle contributions from the three source types. However, these are broad source groups that contain a number of individual sources. For example, combustion generated particles derive mainly from road transport but also include emissions from power stations, industry and domestic combustion. In 1993 these sources contributed 48% of the PM_{10} emissions within the UK (QUARG,

1996). A study of five particle size fractions of street dust from Liverpool showed that there were significant correlations between the magnetic properties and size for some of the size fractions (Xie et al., 1999). Paciga and Jervis (1976) combined particle size fractions distributions and element ratios to determine the sources of some single elements from a number of competing sources. For example large particle sizes close to refineries were associated with Pb, As and Sb.

APEG (1999) states that analysis of the composition and morphology of individual particles is necessary to determine particle sources. Although it is also noted that it is quite difficult to use particle chemistry to distinguish local industrial particles (including coal-ash) from cement particles, limestone, gypsum and wind blown soils.

The composition of individual particles collected over the North Sea was determined by X-ray microanalysis and particles were classified using principle factor analysis into four sources of 'giant' aerosol particles (>1μm). The particle types were aluminosilicates, particles derived from combustion processes, particles from industrial sources and those from a marine source (van Malderen et al., 1992). Rojas and van Grieken (1992) examined the chemical composition of aerosols from different altitudes across the Southern Bight of the North Sea and found that almost 60% of the particles analysed were from combustion or energy related processes.

Long (1998) used a semi-quantitative approach to determine the concentration of selected elements heavier than Na in individual particulates collected in London. The effects of particle size were analysed and it was shown that the relative proportion of Ca in individual particles increased with particle size and that the highest concentrations of Fe were in the 2.5-5μm fraction. Both Si and Al were enriched in the fine and greater than 10 μm fractions and concentrations of Mg, Ti, Ni, Cu and Pb became a greater percentage of the total elemental composition as particle size decreased. Particle morphology and chemical composition were combined and analysed statistically to identify the following major source types: road traffic, power

stations, sea salt, road dust and industrial emissions. Industrial sources produce a complicated mix of particles and it was not possible to fully attribute industrial particles to their sources. In a similar study in London, Sitzmann et al. (1999) found that it was possible to use particle chemistry to identify individual particle types from transport microenvironments but they could only classify these particles into broad source groups. .

Analysis of specific types of particles that can be linked with individual source types can provide further information. For example, source attribution of lead particles is possible using lead isotope signatures (e.g. Deboudt et al., 1999). Vehicle sources have a different signature to those of industrial sources such as lead smelters and waste incineration plants. McCrone and Delly (1973) showed that the major elements in particles emitted by power stations are V, Fe, Si, S and Ca from oil-fired boilers and Fe, Ti, Si, S, K and Ca from coal-fired boilers. Ti and V had been traditionally used to separate emissions from the two fuel types. Rose et al. (1996a) differentiated between spheroidal carbonaceous particles (SCPs) from oil- and coal-fired power stations based on particle chemistry and particles from peat combustion were successfully separated from coal and oil. However Rose et al. showed that in some cases there might be an overlap in particle chemistry with some coal-derived SCPs containing V which is normally used to indicate oil. Hence the need for a multivariate approach to identify the SCP source fuel.

1.6.1 Relationships between particle size fractions

PM_{10} concentrations are derived from bulk particulate mass so a small increase in larger particles will have a significant effect on PM_{10}. Measurements of PM_{10} will vary as the impact from different sources varies and the degree of influence on PM_{10} will therefore depend on the size of particle produced by a particular source.

Simultaneous measurements of PM_{10} and $PM_{2.5}$ collected using a TEOM at a site in Birmingham are well correlated; in summer r=0.62 and in winter r=0.93 (Harrison et al., 1997b). The implications of these data are that changes in

the mass of $PM_{2.5}$ dominate changes in the mass of PM_{10} to a greater extent in winter than in summer. On some days in the winter almost all of the PM_{10} could be accounted for by $PM_{2.5}$. In the summer a significant component of PM_{10} was thought to be derived from wind-blown resuspended particles which have a larger particle size, therefore reducing the correlation coefficient.

The relationship between ultrafine particles and both PM_{10} and $PM_{2.5}$ was studied by Harrison et al. (1999b). It was found that the number of ultrafine particles in the atmosphere had a significant linear correlation with PM_{10} and $PM_{2.5}$ ($r^2 = 0.44$) and that ultrafine particles dominate the total particle count. However the relationship between ultrafines and PM_{10} was modified on days when the presence of larger particles increased particle mass but did not contribute greatly to particle number.

In London, the PM_{10} mass at roadside locations is dominated by fine particles less than 2.1 μm in diameter (Rickard et al. 1999). In contrast, counts of individual particles greater than 5μm collected using a Burkard Trap on the UCL Geography Department in Bloomsbury in July 1994 have a good relationship with PM_{10} concentrations from the Bloomsbury Russell Square monitor (r=0.71) (Battarbee et al., 1997). The fine fraction that comprised between 49.3% and 75.7% of the total particle count had a much poorer correlation with PM_{10} concentrations.

1.7 Fossil-fuel derived pollution

1.7.1 Particles emitted by high-temperature combustion of fossil-fuels

The need for efficient conversion from fossil fuel to electricity drives the combustion processes of power generation. Soot formation is essential for combustion of both oil and coal because it governs radiant heat transfer from the flame (Nettleton, 1979). In the furnace, pulverised coal particles are heated rapidly which leads to homogeneous and heterogeneous types of combustion. Homogeneous combustion of coal occurs when the volatiles evolve and ignite in a gas/gas reaction. Heterogeneous reaction of coal

happens when the coal particles reach ignition temperature and have not released a large enough volume of volatiles. This process is dependent on particle size with larger particles most likely to undergo heterogeneous combustion. In spite of the dependence on particle size, homogeneous combustion is the dominant mechanism for temperatures above 1100K (Morrison, 1986).

Two main groups of particles are produced by high-temperature fossil fuel combustion; inorganic ash spheres (IASs), which are formed by the fusing of inorganic minerals within the fuel (Raask, 1984) and SCPs, which are mainly comprised of elemental carbon (Goldberg, 1985). IAS are aluminosilicate spheres (Mamane et al., 1986) or cenospheres (Raask, 1968). Aluminosilicate spheres are mostly colourless or occasionally light brown, some are solid and some are hollow and they have a wide range of sizes (Ramsden and Shibaoka, 1982). Cenospheres are colourless and have a typical size range of 20-200 μm.

Figure 1.3: Classification of black carbon particles according to their shapes and surface texture (Goldberg, 1985)

MICROSOPIC SURFACE TEXTURE

SHAPE	SMOOTH 	ROUGH, IRREGULAR, PITTED or CELLULAR 	ETCHED, CONVOLUTED, LAYERED 
POROUS SPHERES 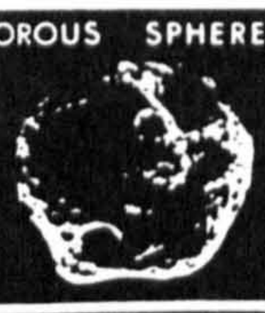	*COAL*	*COAL*	*OIL*
ELONGATE PRISMATIC 	*COAL* *WOOD*	*WOOD* *COAL*	——
IRREGULAR FRAGMENTS 	*COAL* *WOOD*	*COAL* *WOOD*	*OIL*

Large SCPs (>20μm) from fossil fuel and wood combustion have characteristic morphologies. These can be classified in terms of texture: smooth and homogeneous, rough and irregular with pits or cells or etched convoluted layer structures; and by shape: porous and spheroidal, elongated and prismatic or irregular fragments (Goldberg, 1985). Classification of carbonaceous particles is shown in Figure 1.3. However, it is not always possible to characterise SCPs solely by particle morphology. For example, Rose (1991) showed that particle surface chemistry is necessary to accurately discriminate between SCPs from oil- and coal-fired high-temperature combustion sources.

Since SCPs are produced only at high temperatures they are ideal tracers of emissions from power stations. Both oil- and coal-fired processes produce SCPs whereas IASs are produced only from combustion of coal in the UK. Boiler design, efficiency and capacity all affect the particle size range emitted (Goldberg, 1985). For example, SCPs are more abundant in the larger size fractions of coal-combustion stack samples (Griest and Harris, 1985).

All UK coal-fired power stations are equipped with electrostatic precipitators (ESPs) which remove an average of 99.5% of particulate emissions. Table 1.1 shows fuel use and particulate emissions data for coal-, oil- and gas-fired power stations in the UK. In spite of the use of ESPs, coal-fired power stations still emit 0.5% of TSP. This equates to 3240 tonnes of TSP emitted to the atmosphere by a small number of coal-fired power stations in the UK in one year (QUARG, 1996)

Table 1.1: Annual emissions of PM_{10} from UK power stations using data from National Power and PowerGen for 1994 and 1995 (from QUARG, 1996)

	Fuel burnt (kt)	Ash emitted (kt)	TSP emission factor (g kg^{-1})	%PM_{10}	PM_{10} emission factor (g kg^{-1})	PM_{10} emission (kt)	PM_{10} emission kg/MWh generated
Coal-fired	64090	66.8	1	80	0.6	38.45	0.267
Oil-fired	4330	4.8	1.1	20	0.2	0.962	0.116
Gas turbine	4556	-	-	-	0.02	0.093	0.004

1.7.2 Fossil-fuel derived particles in lake sediments

Lake sediments can provide a record of lake, catchment and atmospheric deposition history. SCPs are uniquely formed by high-temperature combustion processes and, therefore, records of SCPs in the environment only reflect emissions from these processes. SCPs are preserved in lake sediments (Renberg and Wik, 1984) and, provided the sediment is not disturbed, do not suffer from remobilisation or motion within the sediment. Particulates deposited onto the surface of lakes are incorporated into the sediment where they can potentially remain undisturbed for thousands of years.

The profiles of SCPs in cores of sediment from lakes in both polluted and 'pristine' environments can be related to historical records of fossil fuel burning (e.g. Griffin and Goldberg, 1979; Goldberg et al., 1981; Odgaard, 1993; Renberg and Wik, 1984, 1985; Wik et al., 1986; Wik and Renberg, 1991; Rose, 1995, Rose and Harlock, 1998). The onset of atmospheric contamination as indicated by SCPs and heavy metals in lake sediments shows good correlation with the lake acidification indicated by diatoms (Battarbee et al., 1995). The appearance of industrial and domestic combustion derived persistent magnetic spherules in lake sediments agreed well with the onset of human activity and its associated pollution (Nriagu and Bowser, 1969).

SCPs and IASs found in cores from Loch Tinker, Scotland have similar profiles and were used to infer the contribution of coal-derived pollution to the sediment (Rose, 1996). The IAS and SCP concentrations from levels of a dated sediment core taken from Hampstead Heath in London show similar profiles (Rose et al., 1994). The major difference between the two particle types is that SCPs are not present in the sediment prior to the Industrial Revolution. IASs, however, have a low, continuous background level that can be attributable to similar particles produced by other natural sources such as volcanic eruptions and meteoritic dust.

1.7.3 Pollution in London from fossil-fuel combustion

The contribution of fossil-fuel derived pollutants to London's environment is important even though there are few large combustion sources in the city. In particular SO_2 and volatile organic compound (VOC) emissions may cause exceedances of pollution standards during episodic plume grounding conditions (Laxen, 1996). Emissions from the power stations in the Thames Corridor, which is the area of land that lies along the sides of the Thames Estuary to the east of London, are responsible for increased concentrations of NO_2 both locally and in London (HMIP, 1996). As mentioned earlier, Rose et al. (1994) showed that SCPs and IASs from power stations are present in Hampstead Heath Men's Bathing Pond. Applestone (1997) and Long (1998) found SCPs and IASs on studies of individual particles collected using Burkard Traps. European emissions of PM_{10} were shown to have significant impacts on London (Malcolm and Manning, 2001) although the specific contribution of fossil-fuel combustion was not determined. In general the magnitude and extent of fossil-fuel derived particulate pollution in London is poorly understood.

1.8 Adverse impacts of air pollution

1.8.1 Materials

Metals, building stone, glass, wallpaper and paintings can all be affected by air pollution. Most of the damage is caused by the oxidation of sulphur dioxide to the secondary pollutant - sulphuric acid (e.g. Webb et al., 1992). Oil-fired carbonaceous particles have been found to exacerbate the decay of marble and limestone of historic buildings (e.g. del Monte et al., 1984; del Monte and Vittori, 1985; Sabbioni and Zappia, 1991, 1992) and the decay of high porosity natural rocks such as sandstone (Sabbioni and Zappia, 1992). Hamilton (1993) found coal- and oil-derived particles in black crusts on buildings in London and Vienna.

1.8.2 The natural environment

A study at Leeds University in 1906 examined the action of SO_2 and its acids on vegetation. Additionally, they looked at the effects of soot in cutting off sunlight and its deposition on plant leaves. The conclusions were that the atmosphere in and around industrial cities has a deleterious effect on plant growth and that pollution is deposited by rain falling through polluted air (Brimblecombe, 1988). During the 1970's the interest in power station-derived pollution was due to the impact of pollutants on distant sources as acid precipitation (Laxen, 1996). The Surface Waters Acidification Program (SWAP) was set up in 1983 (Battarbee and Renberg, 1990) to carry out palaeolimnological studies of lakes in areas of high and low acid deposition. SWAP used techniques including trace metal, sulphur, PAH chemistry, SCP analysis and mineral magnetic analyses to trace atmospheric contamination.

1.8.3 Health effects

Smogs and air pollution have always been associated with an increase in mortality and morbidity. It is more difficult to ascribe deaths to the effects of air pollution in the past since medical knowledge of the symptoms and causes of illnesses was less comprehensive. However, indoor air pollution from hut-fires in the dwellings of Anglo-Saxons is thought to have caused the sinusitis that was common in those times (Brimblecombe, 1988).

More recently particulate pollution has been associated with cardiovascular and respiratory disease in London (Anderson et al., 1996) and elsewhere (e.g. Seaton et al., 1995; Dockery et al., 1993).

The 'Great Smog' of 1952 was thought be responsible for a total of 12000 deaths. Official figures stated that only 4000 people died but these were the people that died before the cut-off date of December 30 in that year (Brimblecombe, 1988). A similar pollution disaster occurred in Donora, Pennsylvania in 1948 where 20 people died as a result of the effects of air pollution (http://www.eswp.com/donora.htm). These smog episodes were

evidence that air pollution can affect human health and by the 1970's a link was established between particulate and SO_2 pollution and respiratory disorders (Dockery and Pope, 1994).

SO_2 stimulates the nerves in the lining of the nose, throat and airways of the lung, which then causes these to constrict. Those suffering from asthma and lung disease are most sensitive to the effects of exposure. Relatively short exposures to SO_2 can cause a measurable restriction of the airways in sensitive people (Laxen, 1996). NO_2 causes inflammation of the airways at high concentrations and in sensitised individuals the response to allergens is enhanced. The Expert Panel on Air Quality Standards (EPAQS) concluded that, among those with pre-existing lung and heart disease, particulate air pollution episodes are responsible for causing extra deaths. Particulate air pollution is associated with asthma, increased levels of mortality and affects the respiratory and cardiovascular systems (AQS, 1999).

Dockery et al. (1993) showed in their study of 6 cities in the USA that, after adjusting for the effects of smoking and other risk factors, fine particulate air pollution contributes to excess mortality. Seaton et al. (1995) suggested that increases in lung disease and blood coaguability are caused in susceptible individuals by alveolar inflammation resulting from ultrafine particles in the urban environment. Increases in sulphur dioxide and particulate matter concentrations in European cities are associated with an increase in total mortality. Black smoke was found to have a stronger correlation with mortality than PM_{10} and as an explanation it was suggested that black smoke consists of finer particles than PM_{10} or that black smoke may consist of greater numbers of toxic particles from diesel sources (Katsouyanni et al., 1997). Air pollution levels experienced in London between 1987 and 1992 were found to have an adverse effect on daily mortality (Anderson et al., 1996).

Most particles larger than 5 μm deposit in the upper airways or the larger lower airways, particles smaller than 5 μm can travel to and be deposited in the smaller airways e.g. the bronchioles or the alveoli. $PM_{2.5}$ is defined as the

high-risk fraction of aerosol for children, the elderly and the infirm. The ultrafine fraction of particles below 0.1 μm is also of concern because these particles can penetrate deeply into the lung (Dockery and Pope, 1994).

There are three main mechanisms that remove particles from the lung (from Dockery and Pope, 1994):

1. larger particles deposited in the upper airways are moved along the mucociliary ladder to be coughed up or swallowed;

2. particles that penetrate further are cleared by lung macrophages that either push the particles onto the mucociliary ladder or into the lymphatic system or

3. the finest particles that penetrate beyond the terminal alveoli will be absorbed into the lymphatic system.

Particles provide a mechanism for transport of sulphuric acid to the lungs where damage occurs. Soot particles provide a surface for adsorption of water vapour and SO_2 and trace metals (e.g. V) catalyse the formation of sulphuric acid (Colls, 1997). Strokes may be caused by blood clots resulting from particulate pollution (Diociaiuti et al., 1999). Membrane damage was caused by the interaction of aerosil (silica in isotronic buffered solution) particles with human red blood corpuscles (erythrocytes), with greater concentrations of particles causing greater damage (Wordley et al., 1997). Dockery and Pope (1994) found that particles in the size range 2.5-30μm, which they defined as the coarse fraction, usually have a basic pH whereas fine particles (<2.5μm) are often acidic.

The biological mechanisms by which particulate matter may increase mortality are not well understood (Katsouyanni et al., 1997). Health studies are needed to look at the fine and ultrafine fractions of particles and to examine the effects of metals adsorbed onto particles. Toxicity of metals depends on their bioavailablity, which is affected by particle size. In addition,

agglomeration of particles will affect transport into the lung. For these studies knowledge of the composition of individual particles is essential.

The contribution of oil- and coal-power station derived particles to the reported health effects is not known. Generally it is assumed that fly ash particles are large and will not penetrate deeply into the lung. However, Schure et al. (1985) showed that the surfaces of small (<5 μm) non-porous fly ash particles were embedded with particles of porous carbon and these particles are within the respirable size range. Elements adsorbed onto the surface of these particles would then be available to interact with biological tissue. A study of coal fly ash particles between 0.5 μm and 5 μm in size showed that the concentration of trace elements increases with decreasing size (Cereda et al., 1995). Therefore, the particles that can penetrate furthest into the lung have the greatest concentration of potentially harmful elements. Heavy metals are associated with the surface of SCPs from power stations (e.g. Rose et al., 1996a) which means that it is feasible for SCPs to have an adverse effect on health. However, the contribution of SCPs to TSP and PM_{10} in ambient air is unknown and is therefore worthy of investigation.

The mixture of particle sources that impact on London, including primary particles from road transport and major power stations on the edge of the conurbation, make London an excellent environment in which to study SCPs and their contribution to particulate matter. A related fact is that a study of particles collected using a Burkard Trap in London by Long (1998) showed that on average 12.5% of particles were fly ash, which is derived from the same sources as SCPs.

1.9 Research objectives

In an urban area such as London it is difficult to determine the exact source of pollution and therefore equally difficult to specify the causes of pollution episodes. The complex cocktail of pollution emitted from stationary sources, road transport, high single point sources and low-lying area sources, combined with the contribution of transboundary movement of gases and

secondary particle formation, produces a complicated mixture of gases and aerosols.

Local authorities are required to declare Air Quality Management Areas (AQMAs) based on exceedances of pollution standards set out by the Expert Panel on Air Quality Standards (AQS, 1999). In order for each local authority to manage their pollution levels effectively they need to know the source of each pollutant so that reductions in emissions can be made. However, pollution concentrations as monitored by the LAQN cannot provide information about a specific pollution source when there are multiple sources for the same pollutant.

Regulation of pollution in London is especially difficult due to the transient nature of pollution and the close proximity of the London boroughs. Pollution originating in one London borough may cause the air quality standards to be regularly exceeded in another borough. In order to manage the problem of particulate air pollution, identification of particle sources is necessary and this cannot be done effectively through analysis of bulk samples.

The pollution problem in London is of concern to air quality specialists and health workers as well as to London's population. Particulate pollution is thought to be responsible for causing deaths in susceptible groups including those people that suffer from asthma or heart and respiratory disorders. The majority of particulate concentration data collected by the Government and London boroughs for monitoring purposes is bulk particle mass of PM_{10} and, in a few cases, $PM_{2.5}$. To understand the health effects of particulates information is needed about individual particles. PM_{10} does not provide information on particle number which is essential for identifying the health impacts of particles (Bérubé et al., 1999). $PM_{2.5}$ has a better relationship with particle number (Harrison, 1999b) but there are only a few sites where $PM_{2.5}$ is routinely monitored.

The contribution of power station derived particulates will be small when compared with particles emitted by road transport, however meteorological

conditions may produce episodes of high concentrations. Episodes of pollution resulting from increased emissions from industrial sources cause high values of SO_2 in London (SEIPH, 1996) and it is feasible that these episodes will be responsible for high concentrations of particles from the same sources. Since the impact in London of SCPs and IASs from power stations and other high-temperature fossil-fuel combustion sources is unknown, as are the precise health effects of SCP and IAS inhalation, it is vital to quantify this small contribution. Overall, this study aims to contribute to a better understanding of the transport and deposition of SCPs and IASs in London.

1.9.1 Aims

- To determine the footprint of pollution from high-temperature fossil-fuel combustion sources in and around London using lake sediments,
- To validate modelled deposition of SCPs,
- To assess short term variations of emissions from fossil-fuel combustion sources using Burkard Trap tapes;
- To determine spatial differences in deposition of SCPs and IASs using a transect of Burkard Traps across London; and
- To identify the meteorological conditions under which high concentrations of particles from high-temperature combustion sources impact on London.

1.9.2 Methodological approach

It is widely accepted that lake sediments can provide a historical record of both gaseous and particulate air pollution. The literature related to SCPs in lakes sediments is referred to in Chapter 4. Most studies involving SCPs as indicators of pollution have covered longer time periods, for example, to reconstruct the change in deposition prior to and following the oil crisis in 1973. Relatively little work has focussed on using sediments to reflect contemporaneous atmospheric deposition patterns which this study aims to do. However, the shortest time period that can be resolved using this approach is around 6-12 months .

Dispersion modelling is a widely used tool in the field of atmospheric science and is especially concerned with estimating the local impact of sources of pollution taking into account the effects of meteorology. This is discussed in detail in Chapter 3 but it is worthwhile to note that most dispersion models are used to predict the impact of pollution over periods of weeks to months. Real time monitoring of atmospheric concentrations, using approaches such as that of the Burkard Trap, provides information on a scale of hours.

It is important to emphasise that the approach of this study is original in that it brings together the three methodologies described above to evaluate the impact of SCP's on London. Within this study it has been necessary to assess the relationships between the methodologies and this has raised the need to also consider the relationships between the timescales of the measurements. There is an overall emphasis on the spatial distribution of SCPs deposited across London rather than any quantitative calculation of loadings, in order to determine the range of and area affected by SCPs.

1.9.3 Specific objectives

- Develop and validate a dispersion model for predicting deposition patterns of SCPs across London
- Examine the distribution of SCP concentrations in lakes and ponds across London.
- Examine the relationship between predicted and measured concentrations of SCPs
- Establish the frequency of SCP episodes across London using Burkard Traps
- Assess the impact of coal- and oil- fired power stations on London using Burkard Trap data
- Attempt to determine the relationship between meteorological variables and SCP and IAS pollution events using statistical analyses.

1.10 Thesis outline

The sites and methods are described in Chapter 2.

Chapter 3 identifies the footprint of SCPs emitted by fossil-fuel high-temperature combustion sources in and around London as derived from dispersion modelling.

The record of SCPs in the surface sediments of lakes and ponds is used to determine the spatial variation across London in Chapter 4. Modelled dispersion of pollution from Chapter 3 is then compared with the lake and pond pollution footprint. Confounding factors that influence the SCP record are considered and the particle size distribution of SCPs is also measured.

Records of SCPs and IASs on Burkard Trap tapes are analysed in Chapter 5.

Chapter 6 contains a statistical analysis of the meteorological data for each Burkard Trap IAS and SCP episode. Patterns in the SCP and IAS profiles for each episode identified in Chapter 5 are compared with meteorology.

Chapter 7 is a summary and conclusions with suggestions for further research.

CHAPTER 2: SITES AND METHODOLOGY

2.1 Lake and pond site selection

2.1.1 Lakes and ponds inventory

An inventory of lakes and ponds in the area within the M25 was created for the purpose of site selection. The name, size and four-figure grid reference of each lake or pond visible on 1:25000 Ordnance Survey maps was catalogued and entered onto a database. The size was measured directly from the map using a grid overlay and by counting the number of squares inside each lake or pond. At the edges of each site the portions inside the edge were added together to complete full squares. There are a total of 2873 lakes and ponds in London within the M25 including natural farmland ponds, artificial reservoirs, gravel pits and quarries, bathing ponds, ornamental ponds, fishing lakes and boating lakes. The location of all lakes and ponds in London within the M25 is shown in Figure 2.1. The size distribution is highly positively skewed with 86% of lakes and ponds in London covering an area of less than 0.5 ha. A further 4% are between 0.5 ha and 1 ha. Only 58 (2%) lakes are larger than 10 ha in size (Figure 2.2).

2.1.2 Site selection

Sites were chosen on the following basis:

1. The aim of the study is to identify the footprint of deposition of SCPs from high-temperature fossil-fuel combustion sources in London. Therefore it was necessary to choose a good spatial coverage of lakes and ponds across London.

2. To eliminate the effects of bias towards any particular type of lake or pond a random selection method was used.

Figure 2.1: Lakes and ponds in London within the M25 overlaid with a 10 x 10 km grid

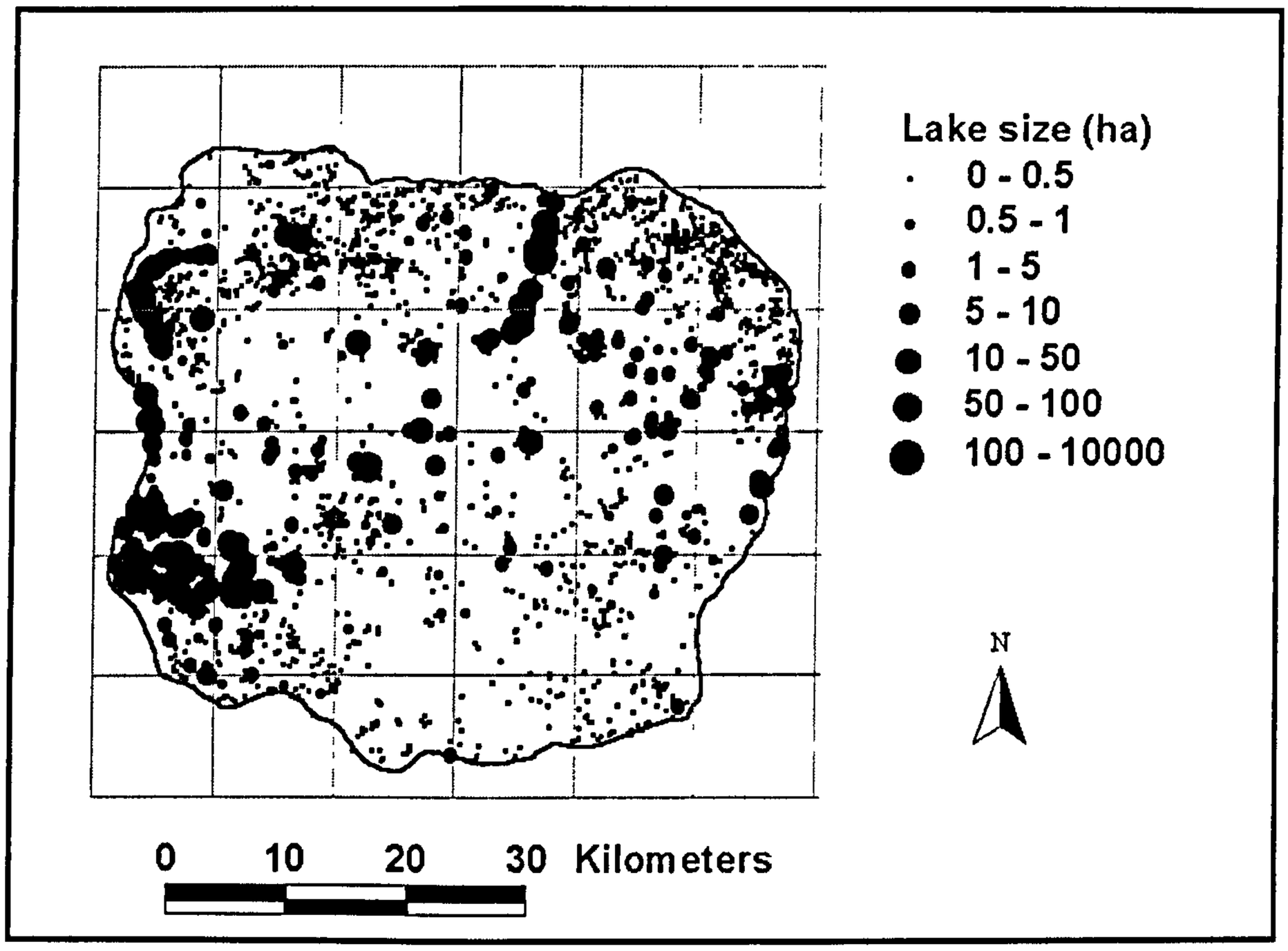

Figure 2.2: Size distribution of lakes and ponds (<10 ha) in London within the M25

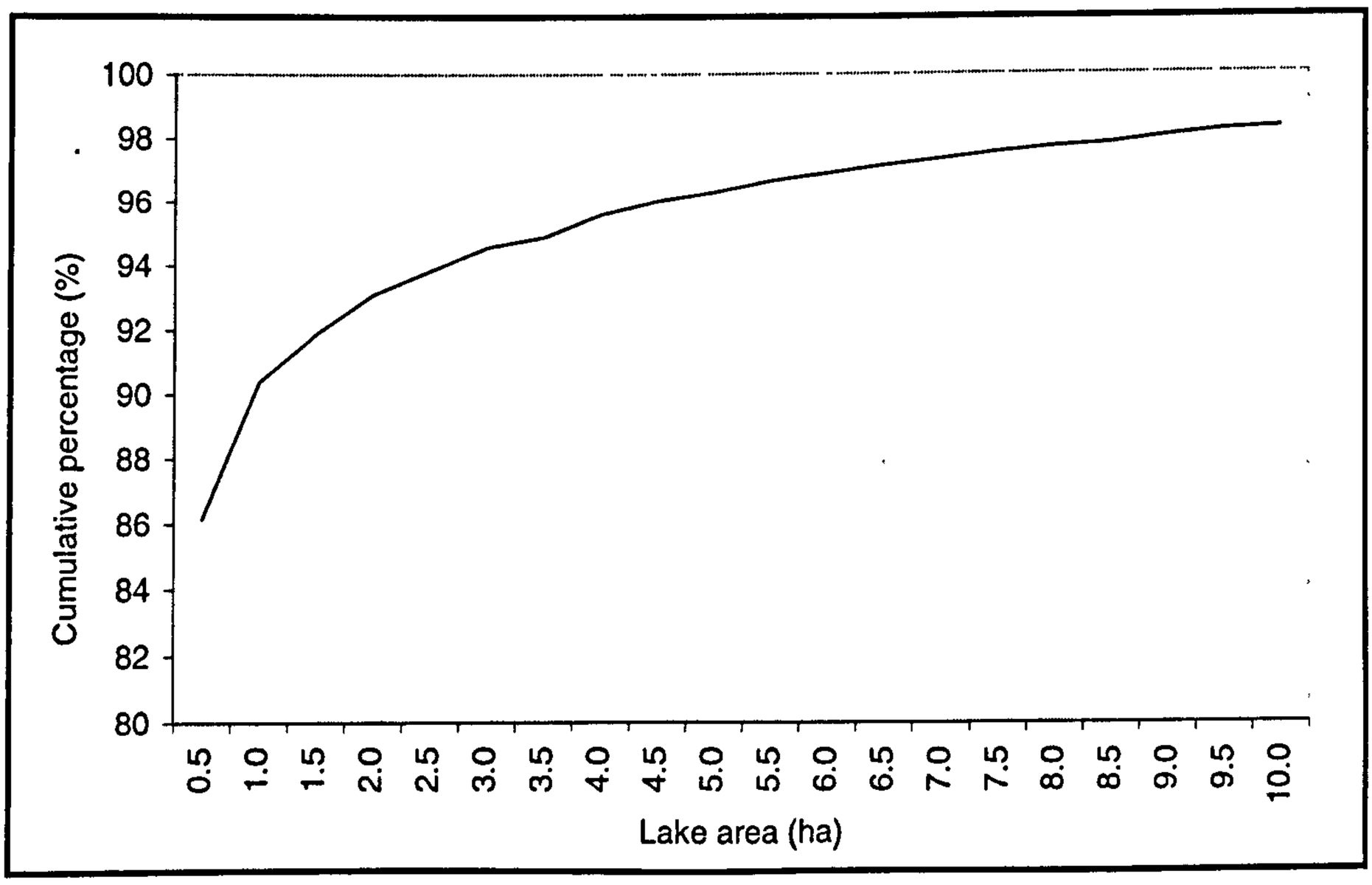

Figure 2.1: Lakes and ponds in London within the M25 overlaid with a 10 x 10 km grid

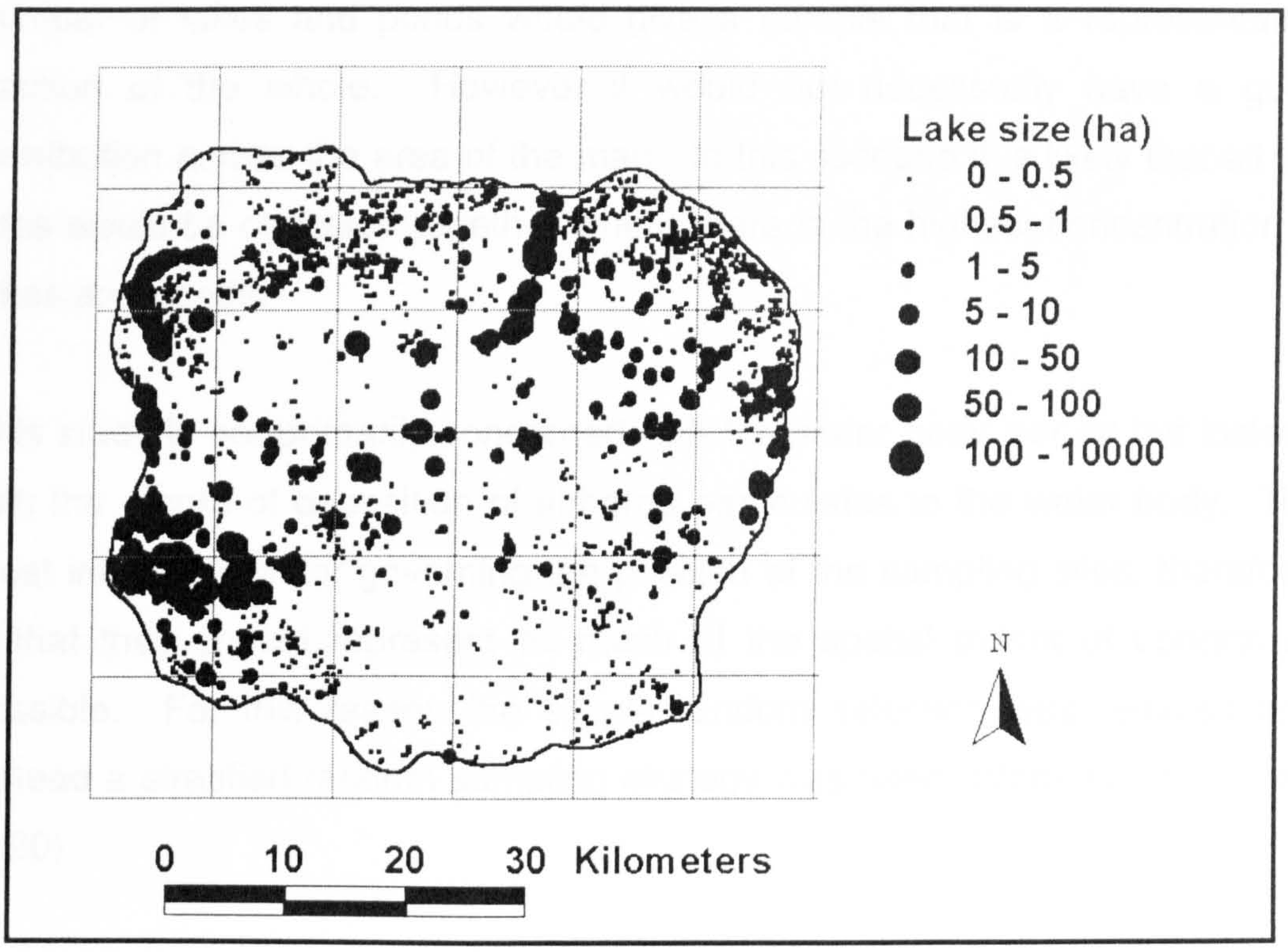

Figure 2.2: Size distribution of lakes and ponds (<10 ha) in London within the M25

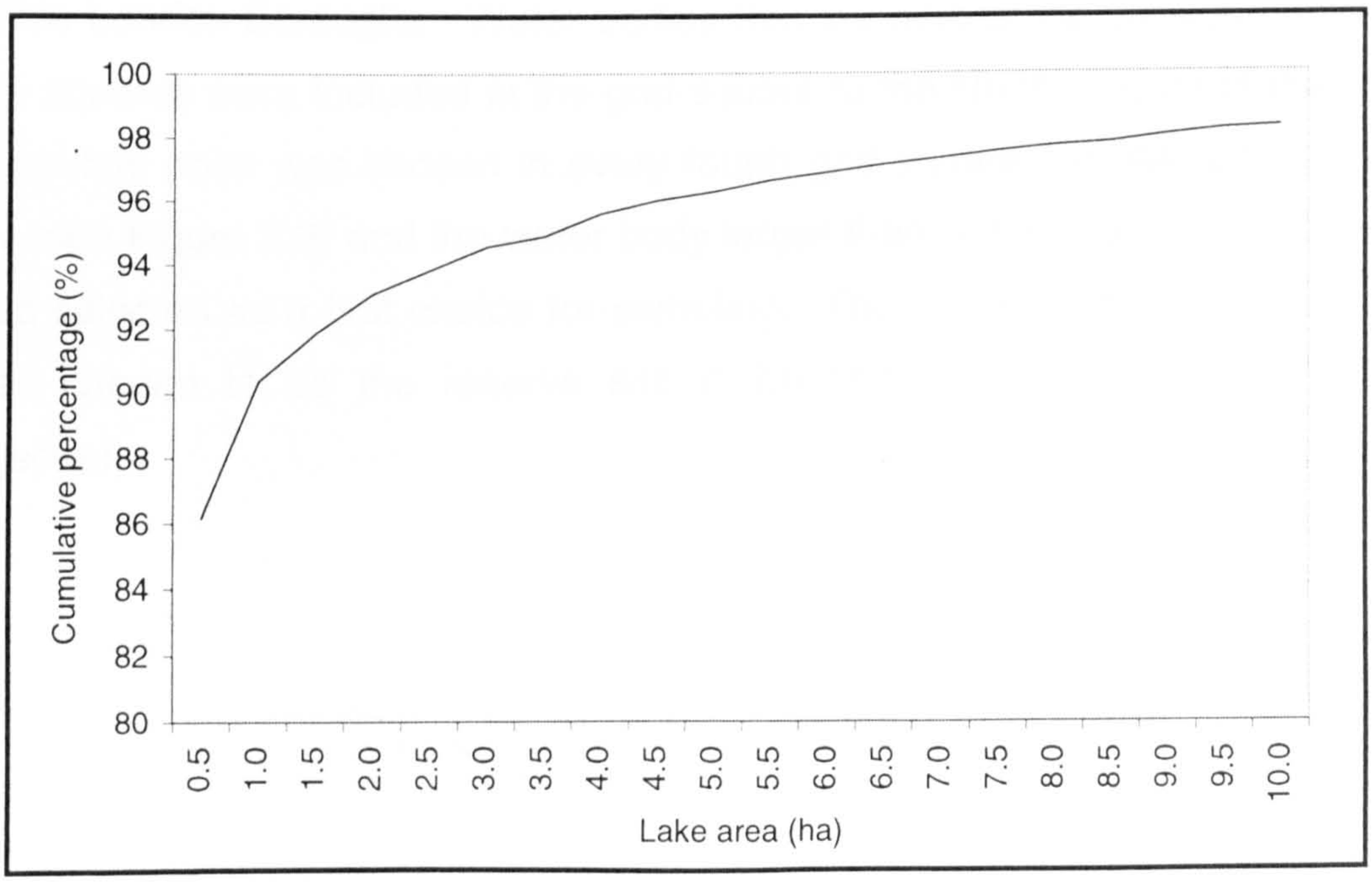

As can be seen in Figure 2.1 the spatial distribution of the water bodies is not uniform across London. A sample chosen simply at random from the total number of lakes and ponds would give a sample that is a representative fraction of the whole. However it would not necessarily have a good distribution across the area of the map. In this scenario it is likely that all the sites would be clustered together where there is the highest concentration of lakes and ponds.

This study is not primarily concerned with the water body *per se* but instead with the record of deposition of airborne particulates to the water body. The most important factor governing the position of the sampling sites, therefore, is that they should represent as much of the spatial extent of London as possible. For this reason the simple random selection was rejected and instead a stratified random sampling strategy was used (Webster and Oliver, 1990).

The area of London up to the boundary of the M25 was divided into 5km x 5km squares based on the Ordnance Survey national grid. For the purposes of this study the area within the M25 is referred to as London although the outskirts of the area surrounded by the M25 covers areas which do not lie within London Boroughs. Water bodies that lay across the division between two squares were included in the grid-square to the North or East of the line. A random point was chosen in every fourth grid square (i.e. A4, B4, C4, D4 etc. see Figure 2.3) and the water body larger than ¼ ha closest to that point was selected as a first choice for sampling. The second closest water body was chosen to be the reserve site if the first choice was subsequently rejected.

Figure 2.3: Site selection procedure

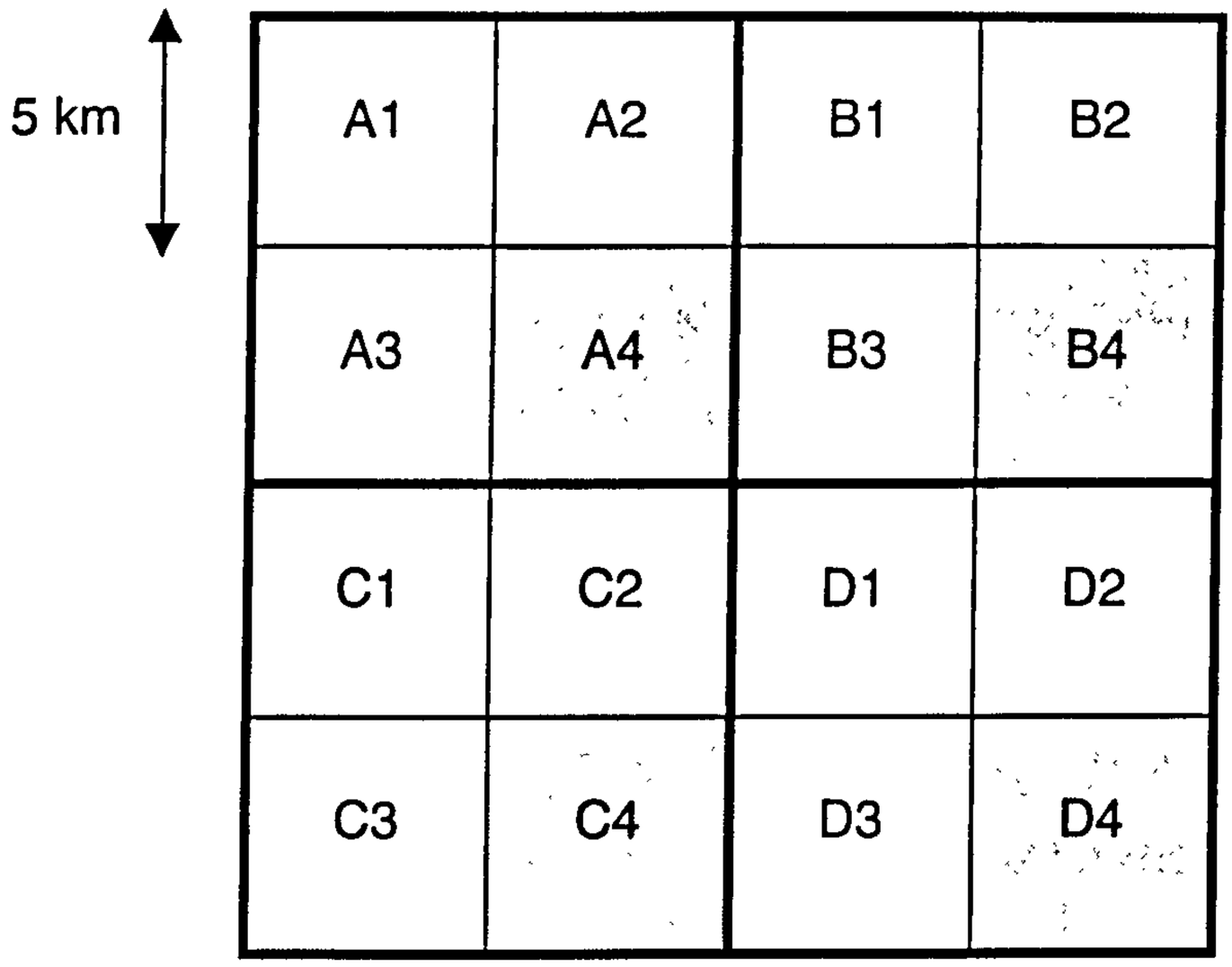

Figure 2.4: Lakes and ponds selected for SCP footprint study

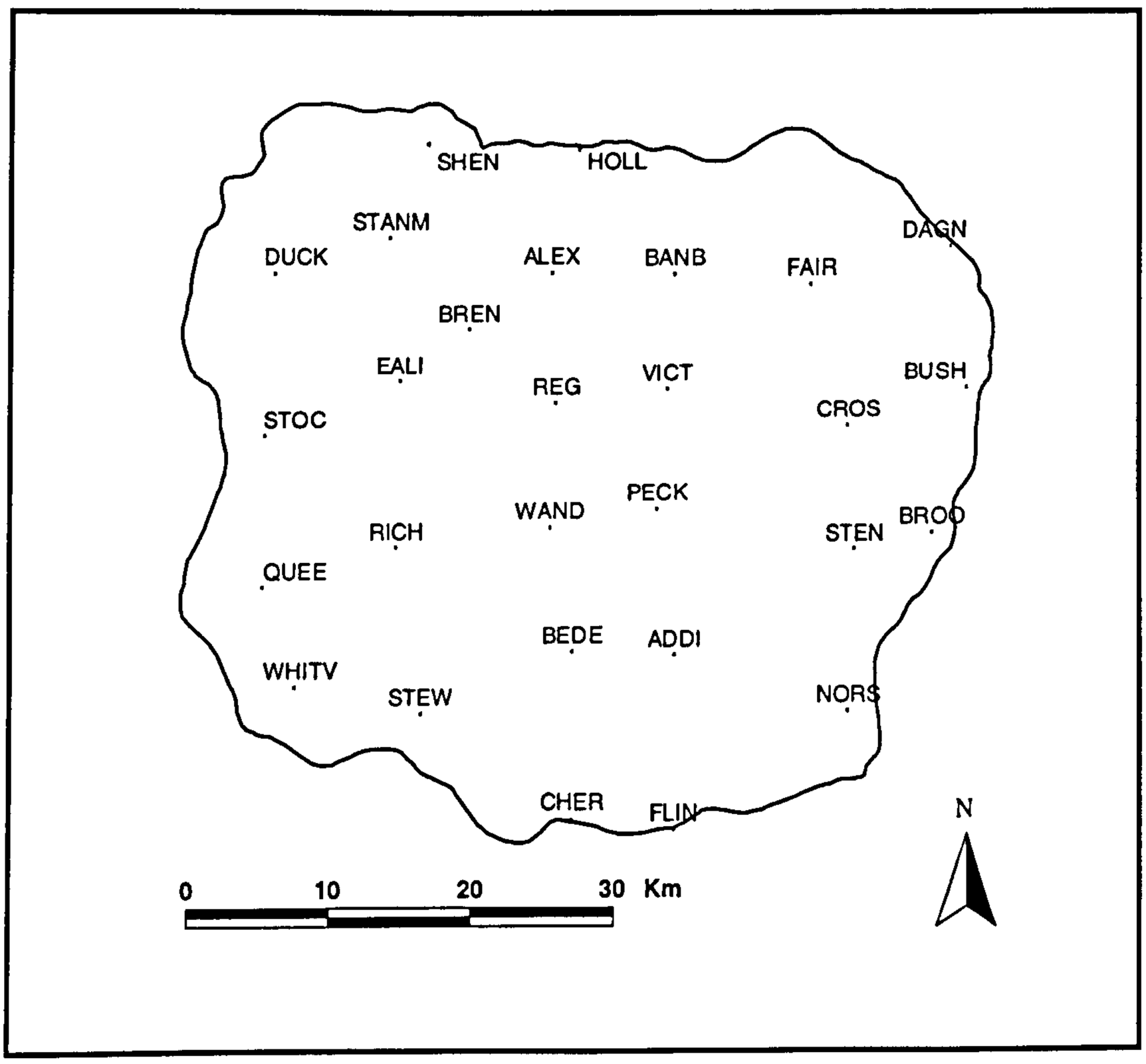

Evidence suggests that all ponds and lakes are equally likely to provide a suitable sedimentary record irrespective of size. Good sedimentary records can be found in lakes and ponds with a range of sizes; for example SCP profiles were obtained for sites in Scotland with sizes ranging between 2 ha and 60 ha (Rose, 1991). There is little existing information about the depths of lakes and ponds in London and so sites could not be pre-selected based on depth. During the first few field visits it was found that the smaller sites tended to be very shallow, and in some cases had dried out completely. Therefore, the sampling approach was arbitrarily refined to set a lower limit of 0.25 ha on pond size. This reduced the sample size from which a sub-sample could be selected to 398 sites. In practice the size criteria was used as a guideline rather than a rule since in a few grid squares there were no sites larger than 0.25 ha. In these cases, the largest site available was chosen.

This initial study targeted a sub-set of 27 lakes and ponds. One grid square had no suitable sites. A further core was taken as part of a separate study by Dr Nigel Cameron and was made available for inclusion in the pilot sample set taking the total to 28. These sites are listed in Table 2.1 and displayed graphically in Figure 2.4.

2.2 Coring Techniques

The Glew Gravity Corer (Glew, 1991) was used to take three cores of sediment from each site in June-August 1998. Given the limited time available at each site, the deepest point of each lake or pond was chosen to be representative of the historical record (Rose et al, 1998a) and was located by traversing the site with an echo-sounder.

Table 2.1: List of sites

No.	Site Name	Code	Grid Reference	Date Sampled
1	Addiscombe Scouts Lake	ADDI	5361 1648	12-Jun-98
2	Alexandra Park Conservation Pond	ALEX	5275 1916	17-Jul-98
3	Banbury Reservoir	BANB	5361 1914	30-Jul-98
4	Grange Park Lake	BEDE	5289 1651	09-Jun-98
5	Brent Reservoir	BREN	5217 1877	24-Jun-98
6	Brooklands Lake	BROO	5544 1731	15-Jul-98
7	Bush Farm	BUSH	5568 1833	19-Jun-98
8	Gatton Bottom Lake	CHER	5289 1537	17-Jul-98
9	Crosness Sewage Works Lake	CROS	5484 1807	05-Jun-98
10	Dagnam Park	DAGN	5557 1932	16-Jul-98
11	Riverside Club, Duck Lane	DUCK	5080 1916	11-Jun-98
12	Ealing Pond	EALI	5168 1841	03-Jul-98
13	Fairlop Waters	FAIR	5458 1907	19-Jun-98
14	Flint Hall Farm	FLIN	5361 1530	17-Jul-98
15	Holly Hill Farm	HOLL	5294 2001	17-Jul-98
16	Norstead Manor Farm Pond	NORS	5464 1609	21-May-98
17	Peckham Rye Park Lake	PECK	5349 1749	05-Jun-98
18	Queen Mary Reservoir	QUEE	5071 1697	17-Aug-98
19	Regents Park Lake	REG	5278 1825	09-Jun-98
20	Richmond Lake	RICH	5165 1724	03-Jul-98
21	Shenley Pond	SHEN	5188 2005	11-Jun-98
22	Stanmore Common Lake	STANM	5161 1940	11-Jun-98
23	Stenhil Lake	STEN	5489 1720	15-Jul-98
24	Stew Pond	STEW	5183 1609	14-Jul-98
25	Stockley Park Lake	STOC	5079 1804	03-Jul-98
26	Victoria Park Lake	VICT	5356 1834	05-Jun-98
27	Wandsworth Pond	WAND	5274 1737	09-Jun-98
28	Whitely Village Lake	WHITV	5094 1628	14-Jul-98

The samples taken were as follows:

- two replicate samples of the upper 0.5 cm of sediment were taken from separate cores and extruded in the boat. The samples were placed in small 'Whirlpak' bags and sealed whilst in the boat.

- one 'long' core of sediment. This core was sealed and taken back to the shore and was either extruded on site or taken back to the laboratory to be refrigerated and extruded as soon as possible. The upper 10 cm of sediment was sliced into 0.5 cm fractions. The sediment below 10 cm was sliced into 1 cm fractions. Each sample was placed in a small 'Whirlpak' bag and sealed. The sample was homogenised in the bag to ensure that the SCP distribution was constant throughout the whole slice. All samples were placed in a cool-box during the fieldwork and were stored in a cold-room prior to subsequent analyses.

2.3 Laboratory analyses of sediment samples

2.3.1 Dry weight and loss on ignition

A sub-sample of approximately 1g was taken from each 'Whirlpak' bag, placed in a pre-weighed crucible and heated overnight at 105°C until constant weight was achieved. Prior to weighing, the crucible was placed in a desiccator to prevent absorption of water from the atmosphere during cooling. Each sample was re-weighed, placed in a muffle furnace at a temperature of 550°C for 2 hours and then weighed again. Dry weight and loss on ignition ratios were calculated from weight loss after these two heating stages.

The remaining sediments were dried, either in a drying cabinet or using an Edwards Modulyo 4K freeze drier, until constant weight was achieved.

2.3.2 Spheroidal carbonaceous particle (SCP) digestion

The method used is a sequential extraction that removes organic, siliceous and carbonate fractions from the sediment. Laboratory procedure (from Rose 1994):

1) Weigh 0.1-0.15g of dried sediment into a 12ml polypropylene tube.

2) Add 1.5ml concentrated HNO_3 and leave overnight in a fume cupboard.

3) Add a further 1.5ml concentrated HNO_3 and heat in a water-bath for 2 hours at 80-90°C. At the end of this stage each tube is filled with distilled water and centrifuged at 1500 rpm for 5 minutes. (The centrifuge used was a Denley BS400). The supernatant is then carefully pipetted off and neutralised before being discarded.

4) Add 4ml 40% HF to each tube and return to the water-bath. Heat at 80-90°C for 3 hours. The residue is then washed, centrifuged and the supernatant pipetted off as before.

5) Add 3ml 6M HCl to each tube and return to the water-bath. Heat at 80-90°C for 2 hours. The residue is then washed and centrifuged as before at least twice before being transferred to pre-weighed and labelled 10ml glass vial with a snap-top lid.

To prevent contamination of the residue by SCPs in the laboratory atmosphere the tubes were covered whenever they were not in the fume cupboard.

2.3.3 Slide Preparation

A known fraction from each residue was pipetted onto a 19mm diameter cover-slip and then the cover-slip was mounted onto a slide using 'Naphrax' diatom mountant.

2.3.4 Counting

All SCPs on the cover-slip were counted at x400 under a light microscope. Most of the particles that survive the digestion are carbonaceous, however there will be some other mineral fractions present on the cover-slip. The non-carbonaceous material is different enough from the SCPs to enable accurate identification of the SCPs. The smallest SCP sizes that can be confidently identified at this magnification are around 2.5µm in diameter. Rarely, it is possible to identify a particle with a diameter less than 2.5µm.

The SCP concentration is calculated as the number of SCPs per gram dry mass of sediment (gDM^{-1}) with a 90% confidence interval. The confidence interval is a measure of the uncertainty associated with the number of particles counted and the amount of sediment used in the analysis. As the number of SCPs on a slide increases then the confidence interval decreases. Similarly, as the weight of sediment used increases then the confidence interval decreases.

2.3.5 Operator counting errors

Counts of carbonaceous particles were made on slides previously counted by Dr Neil Rose to ensure correct identification of SCPs (Table 2.2).

Table 2.2: Comparison of SCP counts

Site	Count (Rose)	Count (Berry)
Tinker	70	70
Burnmoor	90	118
Arr	7	6

The agreement is generally good with the largest discrepancy at Burnmoor. A study of fly ash across Europe involved comparisons of SCP counts from three analysts. Comparison of counts made on 15 slides circulated between the analysts showed that there was a great deal of variation between analysts (Rose et al., 1996b). Only one analyst counted SCPs in this current study and the results will be compared within the study rather than against other studies.

2.3.6 Particle size

Particle size measurements were made using a graticule on one of the eyepieces. The graticule was calibrated against a stage micrometer, which gave a measurement of 2.56 µm for each graticule unit and, therefore, the particle size was measured to the nearest 2.56 µm. Each particle was classed into a size range, 0-2.56 µm, 2.56-5.12 µm, 5.12-7.68 µm, and so on. SCPs at the upper limit of a size range were included in the lower range, for example, a SCP 5.12 µm in size was placed in the 2.56-5.12 µm size range.

2.3.7 Detection limit and repeatability

The theoretical detection limit for this method is 5-10 g DM^{-1}. To achieve the theoretical detection limit it is necessary to evaporate all the final sediment residue onto the cover-slip. Since only a fraction of the residue is used, the actual detection limit is in the range 50-80 g DM^{-1} (Rose, 1994)

The digestion method reduces 0.15g of sediment to less than 0.001g, thus reducing the unwanted fraction by 99.3%. The recovery rate of the method is 89%-103% with a mean recovery of 95.2% (Rose, 1994). Repeatability of this method was tested by Rose (1994) by digesting 5 replicate samples from 3 levels of a core. Triplicate counts were carried out for each replicate and standard deviations and confidence limits were given for each level. In general, the repeatability is good (around ± 3%, 95% confidence limits) at the top of the core. The error margin becomes larger with depth as SCP numbers become fewer (Rose, 1994).

2.4 Dating

In order to determine the time slice that the surface sediment represents it was necessary to date the sediment cores.

2.4.1 Radiometric dating

Radiometric dating using ^{210}Pb and artificial fallout radionuclides (^{137}Cs and ^{241}Am) (Appleby et al., 1986; Appleby and Oldfield, 1978) is ideal for dating recent sediments, but it is not practical or affordable for all sites within the context of this study. Radiometric dating was carried out on two cores (BANB and BREN) by the Liverpool University Environmental Radioactivity Unit using a well type co-axial, low background, intrinsic germanium detector fitted with a NaI(Tl) escape suppression shield.

2.4.2 Sediment accumulation rate dating method

At each site a measurement of the maximum depth of sediment was made so that the sediment accumulation rate could be estimated. The maximum depth of sediment was measured by pushing a long pole down through the sediment until it reached the base of the lake or pond. In most cases the sediment core covered the full extent of the sediment. If the age of the lake or pond is known then by assuming a constant sediment accumulation rate, it is possible to work out the accumulation rate.

$$\text{Accumulation rate (cm yr}^{-1}) = \frac{\text{Sediment depth (cm)}}{\text{Lake/pond age (yr)}}$$

Where the maximum depth of sediment is larger than the core length it is still possible to calculate the date of each level. However, this assumes that the accumulation rate is constant throughout the period of sediment deposition. The age of the sediment core is the age of the lake or pond multiplied by the fraction of core length divided by the maximum depth. This method is only suitable for artificial lakes and ponds that have a discrete bottom. In this

study there were twenty sites that could be classed as artificial, one site (BREN) is a flooded river basin and the remaining seven are uncertain.

2.4.3 Uncertainties of dating sediments

The success of any dating method is limited by other factors that include alteration of the shape or size of the lake or pond, sediment disturbance by dredging or by biological activity (e.g. Fisher et al., 1980; Davis, 1974), and core compression (Håkanson and Jansson, 1983). All these factors will influence the dating of cores taken in this study. Care was taken to avoid areas of the lakes and ponds where the shape had been altered or where regular dredging was undertaken. Sediment disturbance by biological activity and core compression are problems that affect all sedimentological work and were borne in mind when the cores were taken. During collection any cores that were disturbed or incomplete were discarded.

2.5 Site selection for the Burkard Spore Trap transect

The Burkard Volumetric Spore Trap (Figure 2.5) is based on a trap developed by Hirst (1952) and was developed in conjunction with the Burkard Manufacturing company in 1966. It is an inexpensive and effective method for collecting continuous high-resolution records of atmospheric particulates that can be archived for subsequent analysis using optical and scanning electron microscopy.

A Burkard Spore Trap was in operation at UCL between 1995 and 1999, immediately adjacent to the Geography Department in Bedford Way, Bloomsbury. Further traps were deployed between January and June 1999 along a transect joining UCL with Northfleet in the east Thames corridor (Figure 2.6). Three further traps were available and these were placed in Thamesmead at the Thamesmead Community College, in Dartford on top of a building at the Glaxo-Wellcome site and near Northfleet at Painters Ash Primary School, on top of the monitoring station run by Gravesham Borough Council (Figures 2.7a-d).

Figure 2.5: The Burkard Spore Trap

Reproduced from the Burkard Manufacturing Company trap operating manual

Table 2.3: Burkard Trap sites

Location	Grid reference	Start Date	Finish Date	Height above ground (m)
Bloomsbury	5299 1823	9/9/94	8/2/00	3.0
Thamesmead	5482 1796	10/2/99	9/6/99	5.0
Dartford	5545 1744	3/3/99	9/6/99	9.1
Painters Ash	5650 1708	24/2/99	9/6/99	2.0

Figure 2.6: Locations of Burkard Trap sites and air pollution monitoring stations used in this study

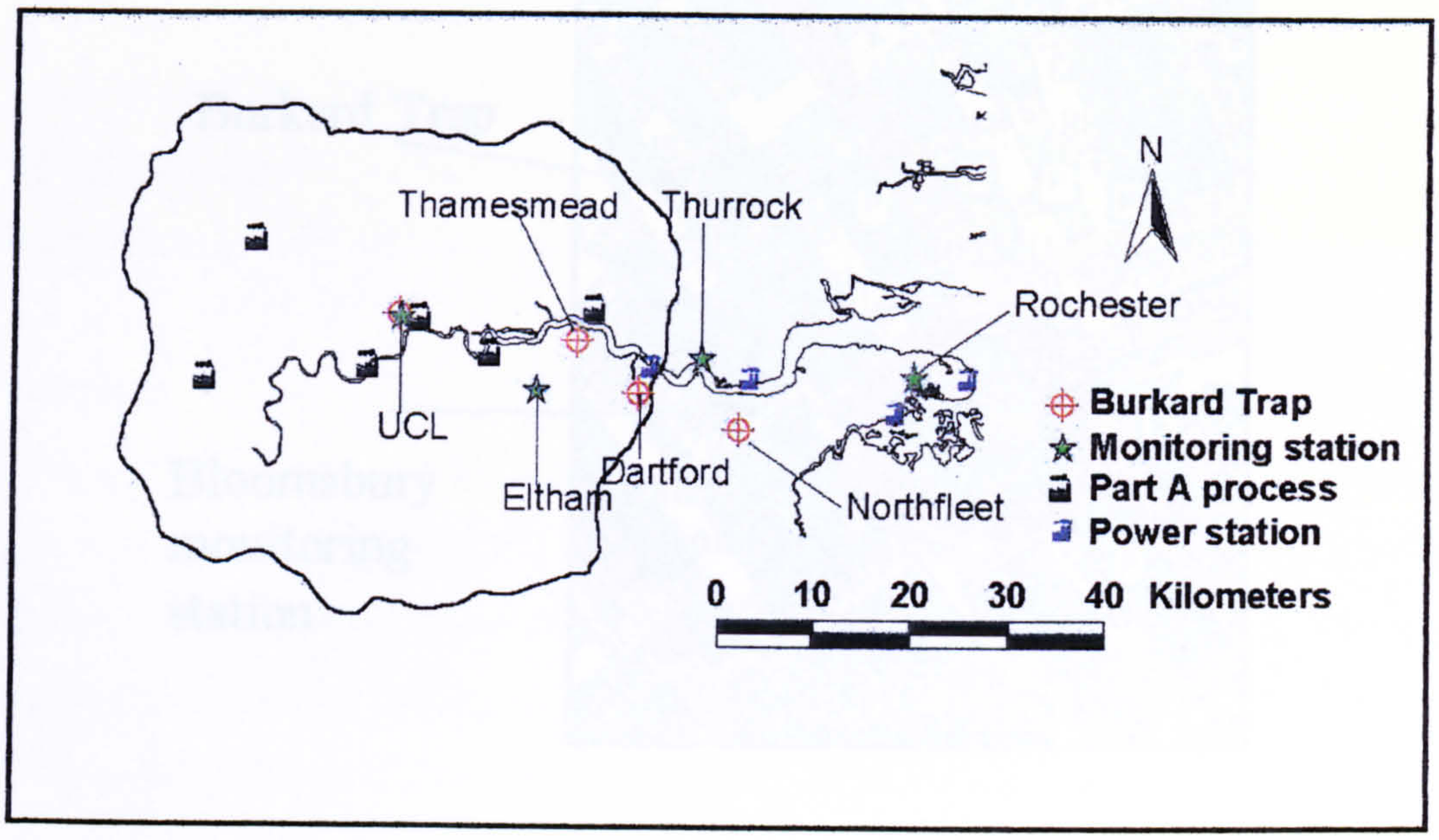

Sites were chosen so that the distance between the power stations in the Thames Gateway and central London would be split as evenly as possible. Table 2.3 shows the grid references, height above ground and the dates between which the traps were operational.

2.5.1 Description of Burkard Trap sites

Bloomsbury

The Burkard Trap was situated on a flat roof approximately 3m away from Gordon Square in Bloomsbury, central London (Figure 2.7a). The flat roof is within a canyon approximately 7m wide. One end of the canyon opens out onto the road and the other end opens out at the back of the UCL Geography Department building. This site would be classified as 'roadside' according to the First Report of the Urban Air Review Group (QUARG, 1993).

Figure 2.7a: Location of the UCL Burkard Trap

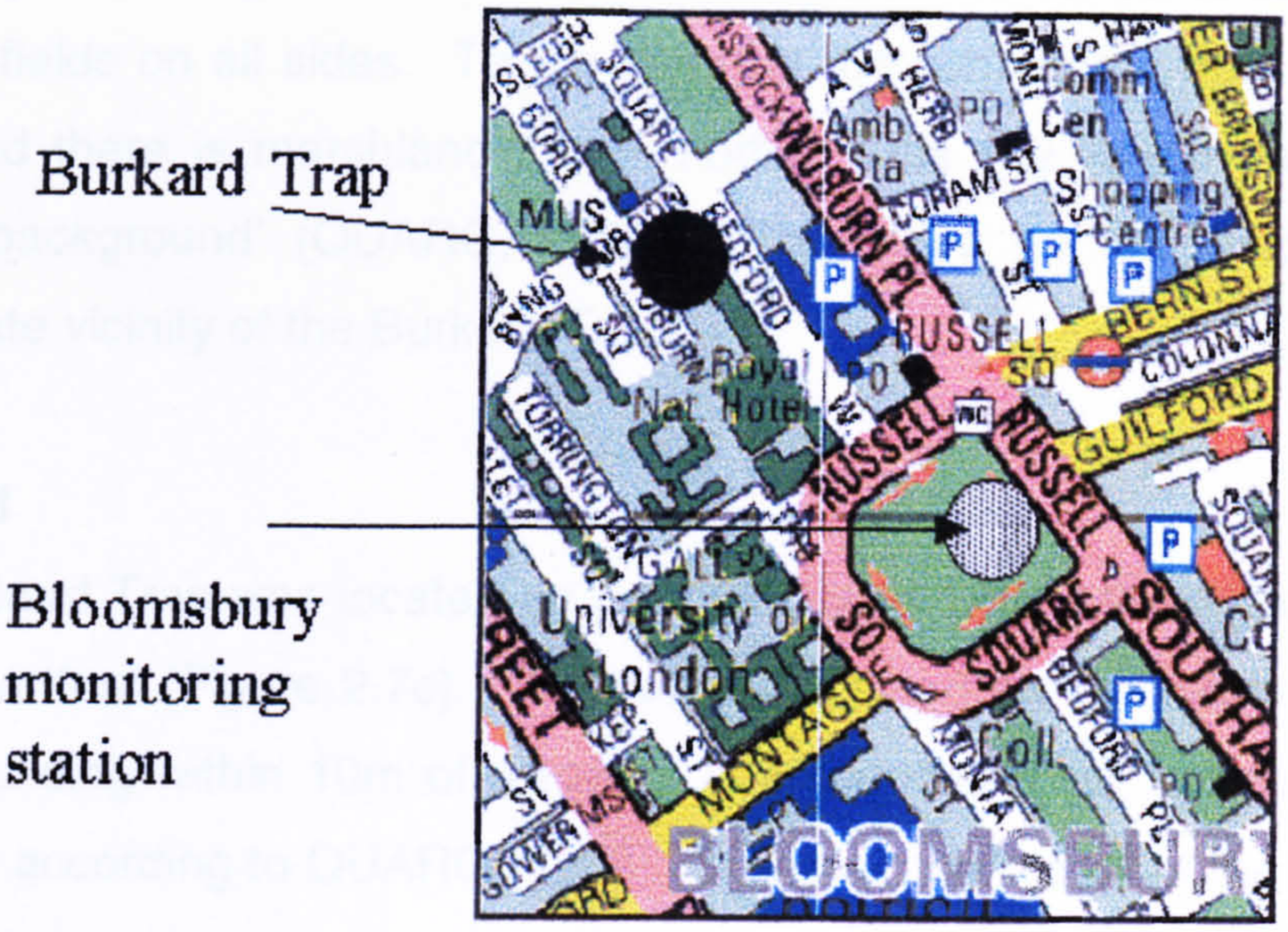

Reproduced from the Ordnance Survey maps by permission of Ordnance Survey on behalf of The Controller of Her Majesty's Stationery Office, © Crown Copyright NC/01/228

Figure 2.7b: Location of the Thamesmead Burkard Trap

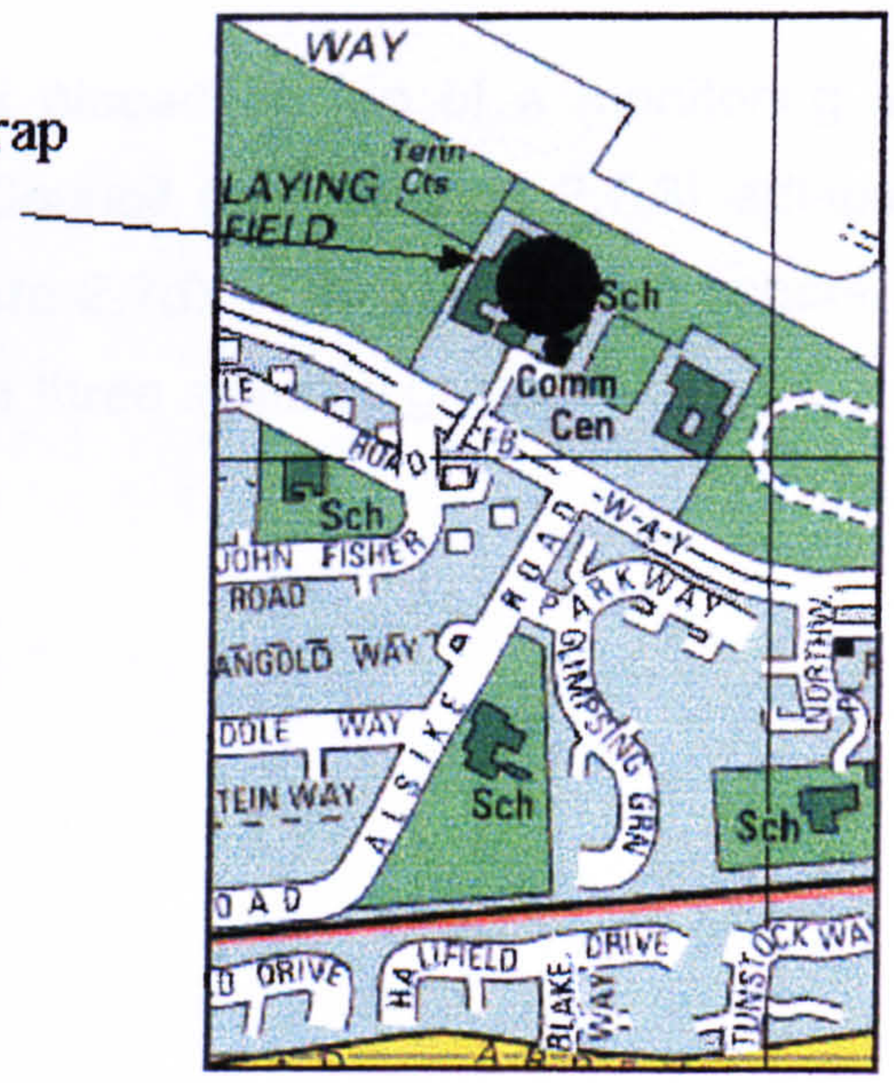

Reproduced from the Ordnance Survey maps by permission of Ordnance Survey on behalf of The Controller of Her Majesty's Stationery Office, © Crown Copyright NC/01/228

Thamesmead

The trap was positioned on top of a school building in Thamesmead (Figure 2.7b) approximately 70m from the closest road. The school is surrounded by playing fields on all sides. To the south of the school is a dual carriageway road and there is marshland to the north. This site would be classed as 'urban background' (QUARG, 1993). There are no tall buildings in the immediate vicinity of the Burkard Trap.

Dartford

The Burkard Trap was located on top of Building 150 at the Glaxo-Wellcome site in Dartford (Figure 2.7c). The trap was placed on the south-west corner of the building within 10m of a road. The site would fall into the 'roadside' category according to QUARG (1993). However the height of the building will reduce the amount of road transport generated particulates that impact on the Burkard Trap and, therefore, the site may be more representative of the urban background. There are a number of structures on top of Building 150, including the vents from the air conditioning system and the laboratory fume cupboards. The location on the roof was chosen to minimise the impact that any emissions from these vents might have on the Burkard Trap.

Northfleet

The Burkard Trap was placed on top of a monitoring station operated by Gravesham Borough Council (see Section 2.7.3) adjacent to the busy A2 road to the south (Figure 2.7d). The site is on a school playing field and is surrounded on the other three sides by grass.

Figure 2.7c: Location of the Dartford Burkard Trap

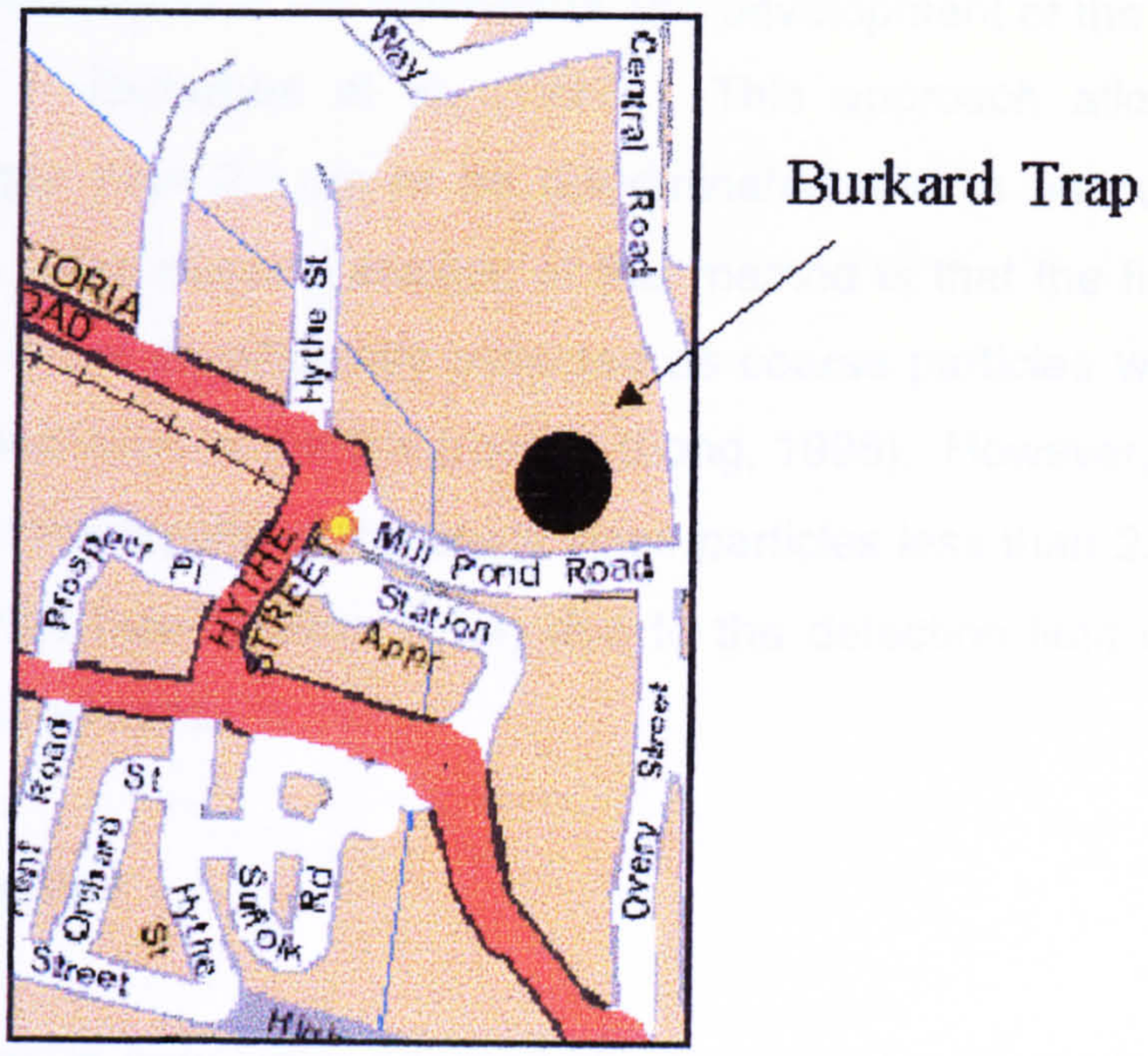

Figure 2.7d: Location of the Northfleet Burkard Trap

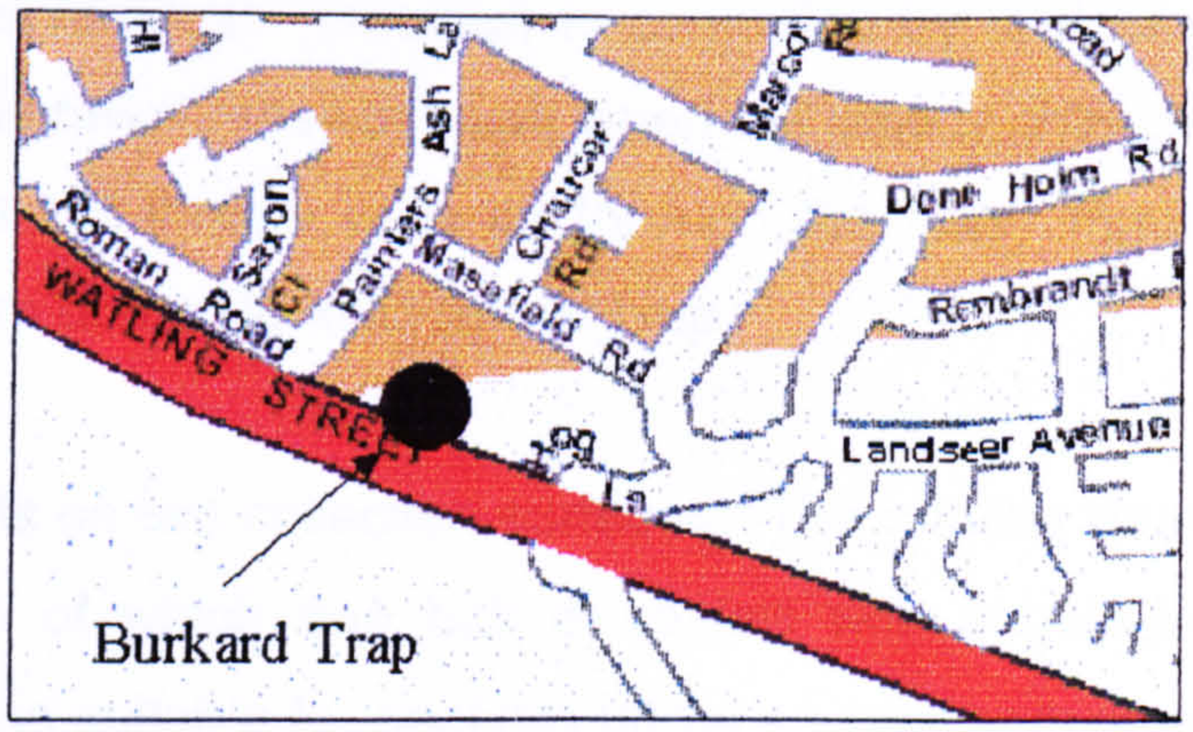

2.6 Spore trap operation

A detailed description of the mechanics and development of the Burkard Trap is included in Battarbee et al. (1997). This approach allows individual particles larger than 2.5 µm to be discriminated and to be counted on an hourly basis. The major drawback of this method is that the fine fraction of particulates is not so efficiently collected as coarse particles which leads to under-representation of the fine fraction (Long, 1998). However, this problem will not affect the results of this study since particles less than 2.5 µm are not easily identified (see Section 2.3.4) due to the detection limit of the optical counting method used.

2.6.1 Mechanics

The spore trap is constantly oriented into the wind by its wind vane (Figure 2.5). Air is drawn into the spore trap at a rate of 0.6 $m^3 hr^{-1}$ via an inlet orifice measuring 14 mm x 2 mm. The drum rotates at a rate of 2 mm hr^{-1}, therefore all particles deposited in one hour will be spread over a 4 mm wide band. The drum is 14 mm wide and the tape is 345 mm in length, which allows for the 336 mm length of the weekly record and a small amount of extra tape in case of a late removal. Rotation is controlled by a clockwork mechanism, which is simply rewound each week when the tape is changed. A small motor powered by a car battery pulls air through the trap. Figure 2.8 shows the impaction drum of the Burkard Spore Trap.

The air impacts on two collection surfaces. The rotating drum is covered by a 'Melanix' tape of which one half is coated with a gelatine/glycerol based mixture which is suitable for analysis under an optical microscope. The other half has a second layer of 'Scotch Magic' adhesive tape which can be examined under high vacuum, as in scanning electron microscopy. Long (1998) found a good correlation between particle number counts from both the gelatine-coated and 'Scotch Magic' adhesive surfaces. The rotating drum is removable thus allowing a new drum to be prepared in the laboratory and then quickly changed in the field.

Figure 2.8: The impaction drum of the Burkard Spore Trap

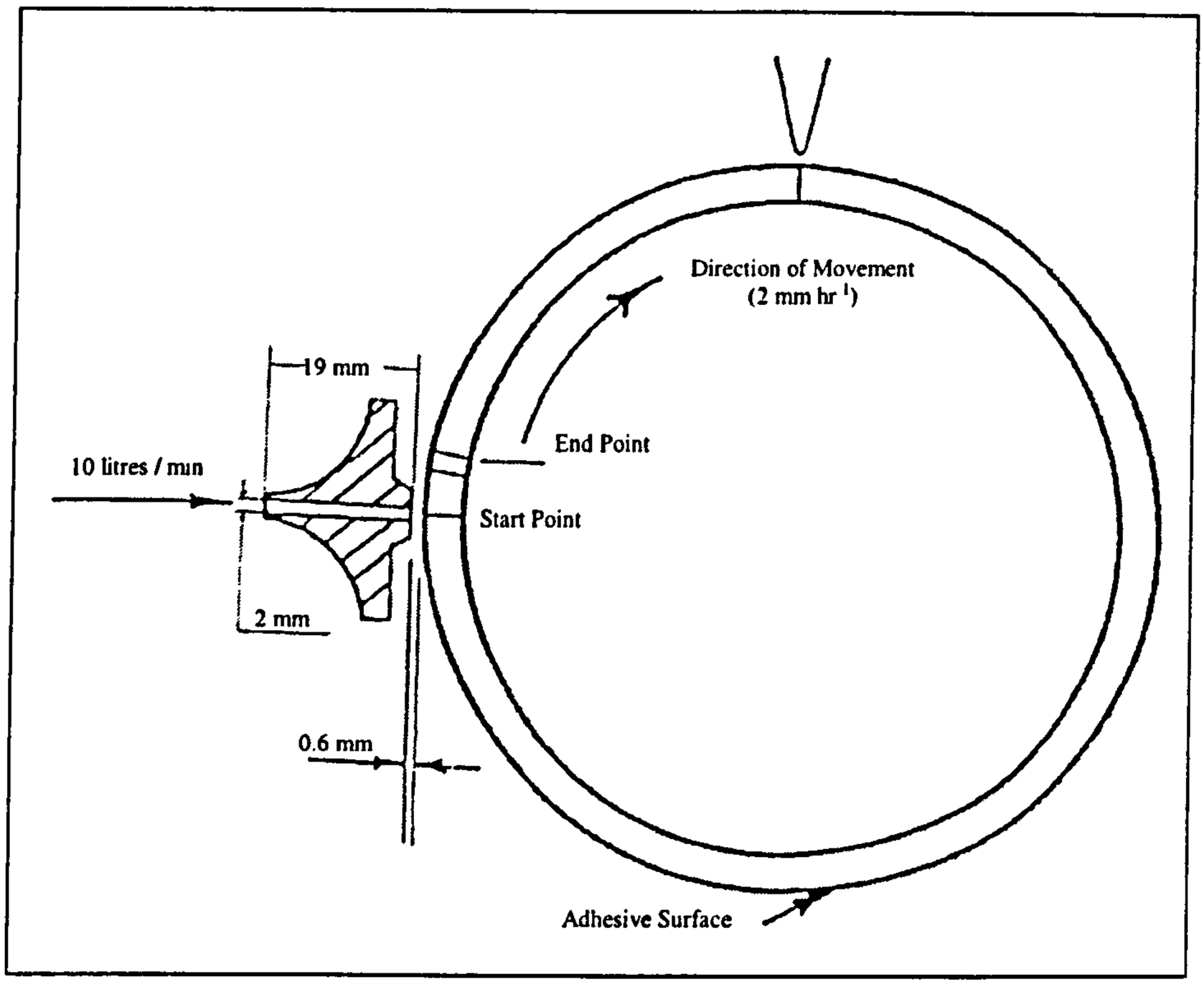

Reproduced from the Burkard Manufacturing Company trap operation manual

2.6.2 Tape preparation

The gelatine mix is prepared according to the following formula suggested by the Burkard Trap operation manual:

10g gelatine

54 cm^3 glycerol

60 cm^3 distilled water

The ingredients are added to a beaker and placed in a water bath. The mixture is heated at a low temperature until the solution is clear and fluid, making sure that the solution does not boil.

The 'Melanix' tape is attached to the rotating drum by strips of double-sided sticky tape. The 'Melanix' tape and the double-sided tape are both supplied by the Burkard Manufacturing Company. The 'Melanix' tape is then divided in

two around the circumference of the drum by placing a strip of 'Scotch Magic' tape' sticky side up over one half of the 'Melanix'. The exposed 'Melanix' is then painted with a thin layer of the gelatine mix.

Post collection, the strips were removed from the drum and stored in a cold store below 5°C to slow down bacterial and fungal growth. The tapes were made into slides for optical microscopy according to the following method (adapted from Burt, pers. comm.) Each week's length of 'Melanix' tape was cut up into 8 sections, each section corresponding to a calendar date. A glass slide was coated with a thin layer of distilled water and each tape was placed face up onto the thin layer of water. The water was to prevent the tape from slipping and to eliminate air bubbles between the tape and the slide. It was essential that the water did not leak onto the particle surface of the tape as this would result in particle movement. A thin layer of gelatine mixture was painted onto a 24 mm x 64 mm cover-slip which was then carefully placed on the tape. The gelatine mixture was warmed to a low temperature to reduce its viscosity. It was vital not to heat the mixture too much or, once the cover-slip was put onto the tape, its gelatine mixture would become fluid which would destroy the resolution of the particle record. Similarly, once the cover-slip was on top of the tape it was vital not to move it, otherwise the record may be affected.

2.6.3 Collection efficiency

The Burkard Trap is an inertial impactor. This means that particles with sufficient inertia will impact on the surface whilst those without sufficient inertia will follow the air stream. Impactor collection efficiency is based on particle size. For the Burkard Trap collection efficiency drops below 50% at a particle diameter of 2.8µm. Long (1998) found that the Scotch Magic tape is more efficient at collecting small particles (<2.5 µm) than the gelatine-coated tape. However, in this study, identification of particles smaller than 2.5 µm is limited by counting at x400 under a light microscope (see Section 2.3.6). A more detailed description of Burkard Trap efficiency is given in Long (1998).

2.6.4 Counting

SCPs and IASs were counted and sized as for the sediment samples, using an optical microscope at a magnification of x400. The number of SCPs and IASs were counted in each adjacent field of view along the tape. SCPs and IASs that fall on the edge of the field of view where more than half of the particle is visible are counted. Where less than half of the SCP or IAS is visible in the field of view it is excluded. The tape was moved length-wise beneath the microscope, each lateral movement representing an increment of time. The number of fields of view along the tape are then divided into the time period represented by the tape to get the number of fields of view per hour. The number of particles in each field of view in each hour were then combined to determine the number of particles per hour. The particle size of the SCPs was measured as for the sediment samples (Section 2.3.4)

2.6.5 Burkard trap tape counting errors

It is impossible to count a continuous line along the Burkard Trap tape. The method used looks at a continuous sequence of spots along the tape. The field of view examined at a magnification of x400 has a diameter of 250 μm and an area of 49087 μm^2. A square field of view would give an area of 62500 μm^2 therefore this method is missing out approximately 20% of the tape. The effect on the particle time-series will be small since the error is consistent for each field of view and will not cause a bias in the results.

2.7 Selection of pollution episodes

SCP and IAS counting is very time consuming and, therefore, it was necessary to reduce the number of Burkard Trap tapes available by selecting shorter periods of interest based on SO_2 concentrations.

2.7.1 Selection of SO_2 Episodes

SO_2 is produced in large quantities by high temperature combustion of fossil fuels. In Europe, in 1994, between 80% and 90% of the anthropogenic emissions of SO_2 were estimated to originate from the thousand largest point sources (Barratt and Protheroe, 1994). In the UK, in 1997, fossil-fuelled power stations accounted for 62% of the national total and there are significant emissions from other large industrial sources. Didcot and Kingsnorth, two of the power stations included in this study, are listed in the largest hundred SO_2 emitters in Europe (No. 61 and 72 respectively) (Barratt, 2000). Road transport emissions are thought to be relatively unimportant nationally, although, in urban areas, diesel powered road transport can make a significant contribution to background SO_2 levels (AQS, 1999).

In order to identify potential episodes of SCP and IAS on Burkard Trap tapes SO_2 concentrations were used as a surrogate for high-temperature point source derived pollution. Where there is a peak in the SO_2 profile or a SO_2 episode this is likely to be attributable to pollution from these sources, i.e. ones that also produce SCPs and, in some cases, IASs. NO_2 concentrations were also obtained for the same time periods to determine the potential contribution of road transport to an episode. If there is a coincidental peak in both SO_2 and NO_2 then the source is likely to be road transport rather power stations or industrial sources.

Pollution episodes were selected based on hourly average SO_2 concentrations exceeding 35 ppb at monitoring stations close to the Burkard Trap transect sites at London Bloomsbury, London Eltham, Thurrock and Rochester. The episodes chosen are shown in Table 2.4.

Table 2.4: SO_2 episodes selected for Burkard Trap tape analysis

Episode	Dates	Maximum SO_2 concentration (ppb)
1	4/3/99 – 9/3/99	46
2	15/4/99 – 17/4/99	51
3	13/3/96 - 14/3/96	98
4	11/3/97 – 13/3/97	84
5	19/12/99 – 22/12/97	57

2.7.3 Location of pollution monitoring stations

The locations of Burkard Trap sites and pollution monitoring stations are shown in Figure 2.6.

Bloomsbury

Bloomsbury monitoring station is used for comparison with the Burkard Trap at UCL. It is an urban centre site and is located in the south-east corner of Russell Square in central London (see Figure 2.7a). The square has many mature trees and grassy areas. The monitoring station is 35 m from the closest road; all four sides of the gardens are surrounded by busy roads.

Eltham

Eltham monitoring station is an urban background site in the grounds of an environmental education centre and is around 25 m from the nearest road. The concentrations from this station are compared with Thamesmead. The surrounding area consists of a variety of habitats that includes trees, areas of grass, ponds, a golf course and housing.

Thurrock

Thurrock is an urban background site 35 m from kerbside of the busy London Road and is in a generally open area surrounded by local light industry. The concentration data from Thurrock is compared with Dartford and Northfleet.

Rochester

Rochester is a rural site located at a primary school. The station is 80 m from a road with low traffic density. The local environment is generally open, although the site is close (within 6 km) to both Grain and Kingsnorth power stations. This site was principally chosen for comparison with Northfleet, however these two sites are several kilometres apart. Ideally the data from the monitoring station at Northfleet, where the Burkard Trap was co-located, would be used. Unfortunately it has not been possible to obtain these data.

The concentrations of SO_2 at this site are likely to be influenced by the busy A2 that runs alongside the monitoring station. The effect of the road transport emissions might partially mask emissions from industrial sources and it is therefore possible that elevated SO_2 levels might indicate a road transport derived pollution episode. However, comparison with the NO_2 data record will determine the pollution source.

2.8 Dispersion Modelling

Dispersion of particles emitted from power stations and other high-temperature point sources was modelled using ADMS 3, a PC-based dispersion modelling program developed by the Cambridge Environmental Research Consultancy.

2.9 Meteorology

The meteorological data were taken from the London Weather Centre (grid reference 530200, 180000, height 42 m) archive accessed through the British Atmospheric Data Centre (www.badc.rl.ac.uk).

2.9.1 Meteorology used in ADMS

Sequential data from 1996 were chosen, rather than ten-year statistical data, to reflect the weather of the year prior to the sampling. The particulates emitted by power stations in 1996 would be incorporated within the surface

sediments of the lakes and ponds samples by 1997. Long-term average data over ten years would not represent the dispersion of particulates for 1996 as accurately since meteorology varies from year to year.

Gatwick and Heathrow are the next two closest meteorological stations to London that have all the data necessary for modelling using ADMS 3. London Weather Centre was chosen for this study in preference to either Heathrow or Gatwick because it is the most central of the three and was felt to be most representative of the study site. Further details of the dispersion modelling procedure are included in Chapter 3.

2.10 Statistical methods

Statistical analyses including Pearson product-moment correlations, principle components analysis, stepwise multiple linear regression, redundancy analysis and general descriptive statistics were performed in Excel 97 for Windows, Canoco for Windows v. 4 and Statistica for Windows v. 5.1. Statistical analyses are dealt with in more detail in relevant chapters.

CHAPTER 3: DISPERSION MODELLING IN LONDON OF PARTICLES FROM HIGH-TEMPERATURE COMBUSTION SOURCES

3.1 Introduction

3.1.1 Pollution dispersion in the atmosphere

The troposphere is the region below the lowest 9-16 km (depending on latitude) of the earth's atmosphere, in which temperature decreases with height. Most weather is generated in the troposphere. It is relatively well mixed by the action of vertical convection and the vertical and horizontal advections of momentum, heat energy and moisture. The troposphere is separated from the stratosphere above by the tropopause which limits the movement of pollution (Arya, 1999).

The influence of the earth on the atmosphere is felt over a distance known as the atmospheric boundary layer. The boundary layer depth responds to the amount of incoming solar radiation (Figure 3.1). It varies depending on hour of day and time of year and can be up to 2.5 km above the earth. Atmospheric turbulence and cloud cover both affect the boundary layer depth. The boundary layer can be described as the region of the atmosphere that is characterised by turbulence generated by the frictional drag as the atmosphere moves across the earth's surface. (Oke, 1987). Pollution is dispersed within the boundary layer and its depth affects the vertical extent of pollution dispersion.

3.1.2 Effect of wind speed and direction on pollution dispersion

Insolation causes horizontal temperature variations in the atmosphere which form horizontal pressure differences and the result is motion of the air in the form of winds. The wind direction determines the path that pollutants follow and constantly varies with fluctuations that cover an arc of 30-45 degrees centred on the mean wind direction. These fluctuations give pollution plumes their characteristic cone shape. The magnitude of the horizontal pressure difference determines the speed of the wind. Pollution from a source is

diffused by turbulent transport in the across-wind direction and transported in the down-wind direction. As wind speed increases then more wind volume will pass the emission source in a given time and therefore the pollution emission is stretched along the direction of dispersion and thus is diluted.

Wind speed also affects the stability of the atmosphere due to internal shearing between air layers and the interaction of the wind with the surface of the earth. Turbulence generated in the atmosphere will diffuse pollution by mixing the plume with clean air. Wind speed also governs the distance that pollution will travel. Strong winds will cause a pollution plume to be transported a long way and also to be diffused effectively. Pollution problems occur when wind speeds are low and pollution diffusion is restricted both down-wind and cross-wind. Low wind speeds allow local circulation systems to develop (e.g. land and sea breezes, mountain and valley winds and urban circulations) and these have localised effects on pollution dispersion by preventing the pollutants mixing with clean air. For example, the air pollution problem in Mexico City is attributed to its location in a flat basin surrounded by mountains (e.g. Fast and Zhong, 1998; Raga et al., 1999).

Pollution dispersion is further complicated in the atmospheric boundary layer by the variation in wind speed and direction with height. Wind speed increases with height because the influence of the surface (drag) decreases with height. Wind direction changes with height and at the top of the atmospheric boundary layer is determined by the action of the Coriolis force. Wind speed decreases close to the surface where the influence of the surface roughness is greatest and the effect of the Coriolis force is reduced (Oke, 1987). Wind shear causes horizontal motion of the particles; as wind shear increases then the mean particle trajectory will touchdown closer to the source (Arya, 1999).

3.1.3 Atmospheric stability

Stability is a description of the relative tendency of an air parcel to move vertically and is driven by variations in temperature and specific humidity (Arya, 1999). There are three stability classes as follows (Arya, 1999):

Figure 3.1: The boundary layer (from Arya, 1999)

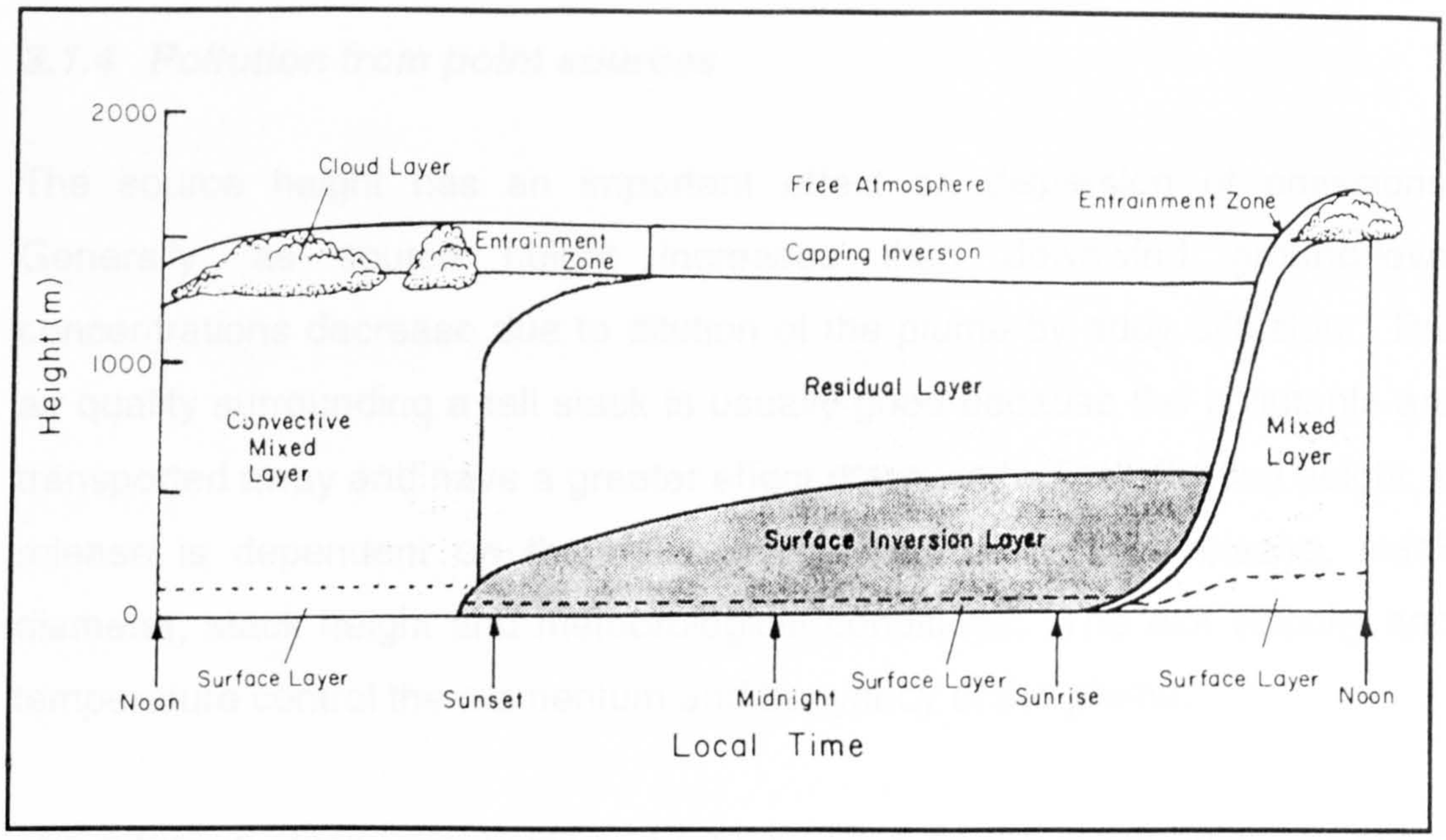

Stable

Stable conditions generally occur on calm, clear nights when there is strong cooling of the ground and lower layer of the atmosphere. Temperature inversions (increase of temperature with height) are common.

Neutral

Neutral conditions can occur either during the day or at night but are most common at dawn and dusk. A neutral atmosphere is characterised by cloudy conditions with medium to strong wind speeds that cause mixing of the lower atmosphere.

Unstable

Unstable conditions are also known as convective and they generally occur on hot, sunny days with light winds. Strong insolation causes warm thermals to rise from the ground, which cause boundary layer turbulence.

Both stability, due to its dependency on insolation, and boundary layer depth are dependent on the time of day, therefore pollution concentrations will also

vary on a diurnal time-scale. For a detailed description of stability and other atmospheric processes see Arya (1999).

3.1.4 Pollution from point sources

The source height has an important effect on dispersion of emissions. Generally, as source height increases then downwind ground-level concentrations decrease due to dilution of the plume by eddy diffusion. The air quality surrounding a tall stack is usually good because the pollutants are transported away and have a greater effect downwind. The effective height of release is dependent on the exit velocity, temperature of release, stack diameter, stack height and meteorological conditions. The exit velocity and temperature control the momentum and buoyancy of the plume.

The effective stack height (H_s) can be simplified as the stack height (h_s) plus the additional height due to the plume rise (Δh) as follows:

$$H_s = h_s + \Delta h$$

Plume rise due to both the momentum and buoyancy effects of release decreases with increasing wind speed and vice versa (Arya, 1999). Following emission, the plume characteristics are determined by the atmospheric stability (Oke, 1987).

Emissions from industrial sources have analogies in the natural environment. Dispersion from fires (Clark, 1988) are related to the height of the convection column. This provides energy and buoyancy much like the effect of the temperature and velocity of release from a stack.

The effect of meteorological conditions on emissions is dependent on the type of source. Pollution episodes caused by stack emissions occur generally in unstable and convective conditions (typical of a warm day), with low wind speeds, during mid-day and afternoon. Thermally induced circulations will cause the plume to move vertically and horizontally. A downward loop may

cause high concentrations at ground level quite close to the source. In contrast, low-level vehicular sources usually produce maximum ambient concentrations under stable atmospheric conditions in the winter (HMIP, 1996). Low wind speeds and low boundary heights prevent the dispersion of polluted air. Therefore the maximum contribution from industrial sources will not coincide with high pollution concentrations from road traffic. Pollution episodes can then be attributed to likely sources based on the specific meteorological conditions at that time.

The range over which pollutants in the plumes from stacks can be clearly detected is up to 50 km from the source. Beyond this the emissions blend into the background (Laxen, 1996). The impact that the pollutants within the plume have on people or the environment is dependent both on the meteorological conditions that exist at the time of the emission and later, as the pollution plume moves down-wind.

Figure 3.2 shows some typical plume patterns. *Looping* typically occurs during the daytime when there is strong instability. Transport in the atmosphere is dominated by large eddies that are wider than the emitted plume. The plume is then distorted by the movement of eddies and follows a vertically sinuous path. High pollution concentrations occur when the plume intersects with the ground.

Coning is characteristic of either windy or cloudy conditions or conditions that are both, with stability close to neutral. Vertical and lateral spreading of the plume are roughly equal and a cone is formed around the centreline of the plume. The plume will go to ground eventually but at a greater distance than during looping.

Fanning occurs during stable conditions, which possibly have an inversion. Turbulence is weak and buoyant mixing is suppressed so there is little vertical diffusion. Variations in wind direction horizontally may force the plume into a fan shape or, alternately, into a meandering ribbon. The plume can stay aloft

for many kilometres which means that ground level concentrations are negligible.

Figure 3.2: Characteristic plume patterns (from Arya, 1999; modified after Slade, 1968)

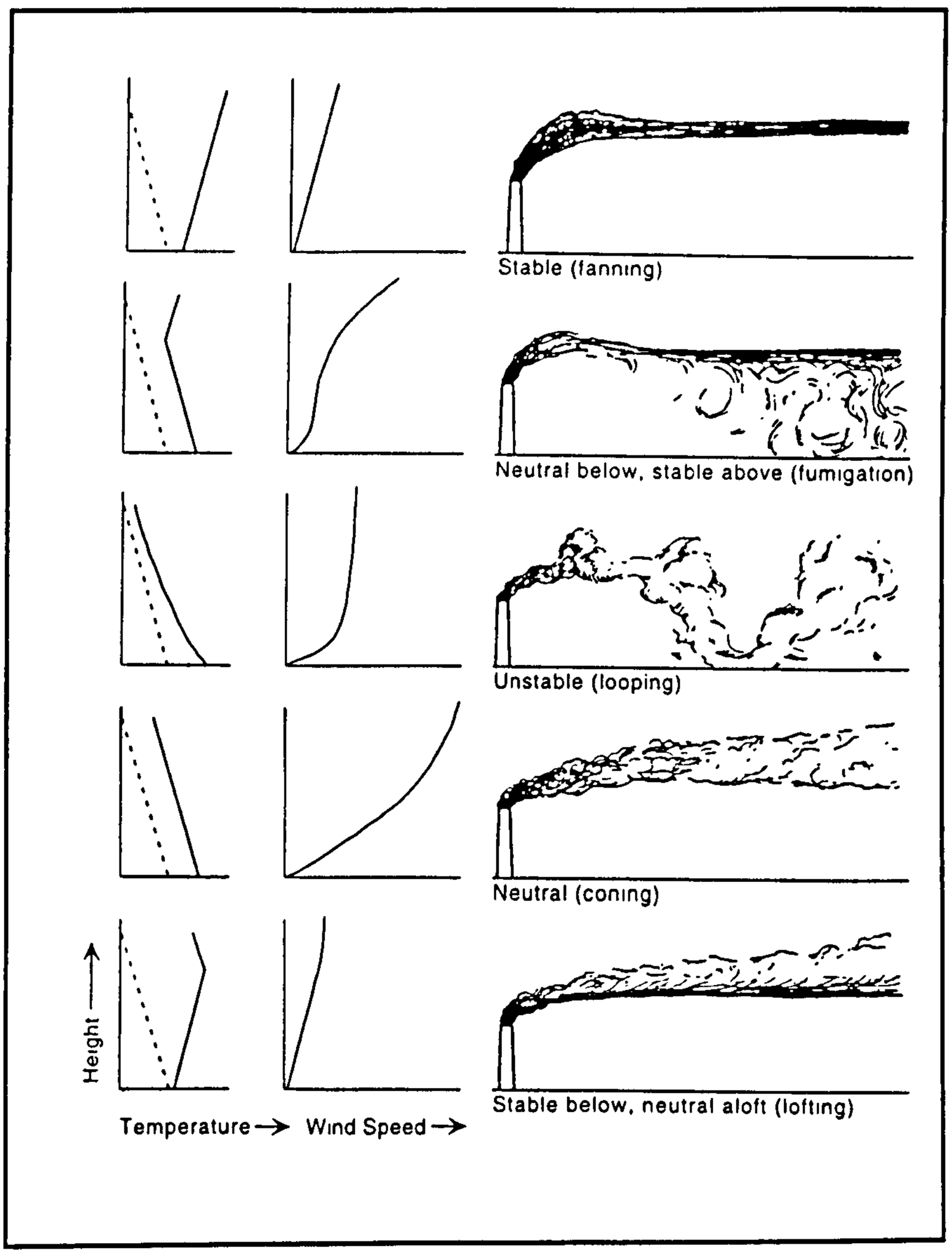

Lofting occurs during the early evening when the plume is emitted above a nocturnal inversion that builds up from the earth's surface. Pollution movement downwards is prevented by the stable layer beneath the plume, although once the nocturnal inversion grows higher than the effective stack height the plume changes to the fanning type.

Fumigation usually follows either lofting of fanning and causes the plume to be mixed downwards to ground level. This occurs shortly after sunrise through surface heating when the nocturnal inversion is replaced by an unstable layer that grows up to the top of the plume. Once the plume becomes part of the mixed layer it is drawn downwards by convective turbulence and the capping inversion forms a lid on the pollution preventing upward mixing. This condition only lasts a short time; once the mixing height grows well above the stack height the plume is spread over a greater volume.

Trapping can be caused when pollution is dispersed in an unstable or convective boundary layer until it occupies the whole layer. The pollution can disperse horizontally but is prevented from vertical dispersion by the capping inversion at the top of the boundary layer. Severe plume trapping occurs in steep valleys and gorges when the pollution is trapped horizontally, by the topographical features, as well as vertically.

3.1.5 Dispersion of aerosols in the atmosphere

An aerosol is a two-phase system that comprises solid or liquid particles and the gas that surrounds them. Particles are removed from the atmosphere by one of the following mechanisms: gravitational settling, dry deposition, precipitation scavenging.

The majority of particles emitted to the atmosphere with a diameter larger than 1 μm are removed by gravitational settling. Stokes' Law describes the settling behaviour of a particle in still air. The particle accelerates due to gravity until its terminal settling velocity is reached. At this point the drag force of the air is equal and opposite to the effect of gravity on the particle. Terminal settling velocity is proportional to the square of the particle diameter and thus increases rapidly with particle size.

As particle size approaches the mean free path of the gas (<1 μm) the particle settles faster in still air than predicted by Stokes' Law due to 'slip' at the particle surface (Hinds, 2000). However, in the atmosphere, turbulent diffusion will slow the descent of smaller particles and these may stay aloft

indefinitely. Dry deposition is the main mechanism by which most particles come to rest on the ground or another surface. Transfer of a particle from the air to a surface takes place in three stages. The first stage is transport to the immediate vicinity of the surface. This is followed by diffusion of the particle through the molecular sub-layer. The third stage is the substrate transfer component, in which material is absorbed by the surface. The amount of material that is absorbed depends on the solubility or absorptivity of the material at the surface (Arya, 1999). Dry deposition is a turbulent transfer process and affects those particles that do not undergo gravitational settling but instead are carried with the plume. As particles impinge on the surface there is a downward flux of matter and the underlying surface acts as a pollution sink. Dry deposition of particles is affected by their electrostatic and hygroscopic properties and is also affected by the nature of the underlying surface; for example in this study the receptor points are lakes and ponds and absorption over water is affected by the surface tension (Hinds, 2000).

Particle detachment, resuspension and bounce are all affected by particle size and surface characteristics. Detachment and resuspension become more difficult as particle size decreases because the adhesive force on small particles (<10 μm) is much greater than the other forces on the particle. The force required to resuspend a particle is less because it involves the particle sliding or being rolled first. Bounce depends on the velocity of the particle as well as adhesive forces but also decreases with particle size.

Wet deposition only occurs during precipitation and has the effect of removing particulate matter very quickly. Particles that pass through clouds may become nuclei for water or ice and these nuclei can then capture other particles. Once the droplet becomes large enough then it will be precipitated by rainout (or snowout). Washout of particles occurs below the cloud level, the efficiency and rate of which depends on the rainfall rate and the size and electrical charge of the particle. However, it has been suggested that particles in dust storms and possibly pollution particles in urban air will reduce rainout (Rosenfeldt and Rudich, 2001). Large particles that do not absorb

much water form a large number of nuclei that grow slowly. The available water is spread over a large number of nuclei and precipitation is suppressed.

Particle shape and density affect the rate that particles settle. Both can be incorporated into the concept of aerodynamic diameter in which particle characteristics are normalised to an equivalent spherical particle that has the same density as water. Particles with the same aerodynamic size will also have the same settling velocity. SCPs are spheroidal and for the purpose of modelling in this study are assumed to be spherical.

3.1.6 Dispersion modelling

While much is known about the bulk composition of atmospheric pollution particles it is not possible to use bulk properties to identify with certainty each pollution source (see Chapter 2), although the receptor modelling technique (e.g. Stedman et al., 2001; APEG, 1999) can be used to identify and quantify the contributions of major sources.

Emission inventories provide information about the emissions from individual sources but do not explain the distribution of pollutants in the atmosphere. For example, a comprehensive study on pollution emissions in London was used to develop the London Atmospheric Emissions Inventory (LRC, 1997). Sources of pollution in London within the M25 were identified and emissions were estimated for eight key and three additional pollutants. Direct monitoring of pollution concentrations shows actual pollution levels but it is expensive.

Dispersion modelling is used to predict the quantity and distribution of pollution in the atmosphere and deposited to the ground. Where there is a lack of monitored data, dispersion modelling uses the information in emissions inventories to predict impacts of pollution. Modelling can help to determine the causes of air quality exceedances in areas where there are many contributors to the air pollution levels, or to determine where exceedances will be in the future if the air quality guidelines change. If a new source is planned then its potential impacts can be modelled. Whereas

emission inventories show where the largest pollution emitters are located, dispersion modelling uses the effects of meteorology to determine the location of the greatest impact.

Table 3.1: List of dispersion modelling abbreviations

Abbreviation	Model name
ATDL	Atmospheric Turbulence and Dispersion Laboratory
AEOLIUS	Assessing the Environment Of Locations In Urban Streets
PAL	Point, Area and Line sources model
ISC	Industrial Source Complex model
CALINE	California Department of Transport Line Source model
ADMS	Atmospheric Dispersion Modelling System
AERMOD	American Meteorological Society / Environmental Protection Agency Regulatory Model Improvement Committee Model
NAME	Nuclear Accident Response Model

A number of dispersion models are available for modelling emissions from a range of different sources and these are described in detail in Middleton (1997) (see Table 3.1 for a list of abbreviations). Broadly, models can be divided into screening models e.g. ATDL; nomograms for estimating the air quality impact from a source e.g. AEOLIUS for street canyons; older style Gaussian plume models that can be used for multiple source modelling e.g. PAL, ISC and CALINE; and newer style models e.g. ADMS, Indic and AERMOD (Middleton, 1997). Long range transport of pollution can be predicted using models such as NAME, which was used in an investigation of an air pollution episode that occurred across central England in 1998 (EA, 2000). NAME was also used to model hourly concentrations of sulphate aerosol for two large PM_{10} episodes in the Midlands, UK. It was found that one episode was dominated by long-range transport from Europe and the other was attributed to a source within the UK (Malcolm et al., 2000). PM_{10} concentrations in the UK were also modelled by Abbott and Stedman (1999) using ADMS v2.2. Alternatively back trajectory modelling allows the pollution path to be modelled from deposition to likely source (e.g. Met-Office back trajectory model available via http://www.badc.rl.ac.uk).

There are many other models of varying degrees of complexity that have been developed by researchers for modelling pollution from a number of source types. These include Lagrangian particle models (e.g. Anfossi et al., 1998; Xia and Leung, 2001; Russell Bullock et al., 1998), pseudo-Lagrangian (Sofiev, 2000), hybrid models (e.g. Nimko et al., 1999), regression-mapping techniques (e.g. Briggs et al., 2000), stochastic particle models (e.g. Haan, 1999) and neural network modelling (e.g. Gardner and Dorling, 1999; Perez et al, 2000, Kolehmainen et al., 2001).

Dispersion of particles from industrial sources have also been modelled; for example, dispersion of radionuclides from the Chernobyl accident have been modelled successfully (Hatano et al., 1998). Oza et al. (2001) simulated the effects of sea breezes on dispersion of ^{41}Ar particles from a 100 m stack in Kalpakkan, India. Modelling in the UK indicates that releases of primary particles from large industrial stacks in the UK are unlikely to lead to breaches of the 1997 Strategy Objective (AQS, 1999).

3.1.7 Long-range transport

Many studies have shown that there is long distance transport of large particles. For example carbon and fly ash particles with a range of sizes from 2 μm to over 23 μm were collected on meshes on the bows of ships in the North Sea, although the larger particles were collected closer to the coast. The largest particle found in the open sea was 6 μm (Parkin et al., 1970). Charcoal particles in the size range 5-20 μm emitted from fires in lake catchments are more likely to travel thousands of kilometres rather than to be deposited locally (Clark, 1988).

Natural particles such as Saharan dust can be transported many kilometres from source, for example to Spain (Rodríguez et al., 2001). Large but irregularly-shaped particles, suggested to be wind blown soil dust particles with a mean diameter of 15 μm, were collected above the southern bight of the North Sea (Van Malderen et al., 1992). Particles from high-temperature

combustion sources with a mean diameter of 4 μm were also collected in the same study.

3.1.8 Transport of pollution to London

Long range transport of particulate matter to London is possible given the right meteorological conditions. The impact on London of long-range transport was shown by Barnes and Eggleton (1977) who found evidence of particles transported from eastern Europe to eastern England. Based on 1992 emissions data, annual average concentrations of 1.9 μg m^{-3} of PM_{10}, 1.6 μg m^{-3} of $PM_{2.5}$ and 0.27 μg m^{-3} of $PM_{0.1}$ were modelled as originating from major emissions sources in Europe (APEG, 1999). Slightly lower concentrations were found in Edinburgh using the same model. In both cases the smallest particle size fraction had the lowest concentrations.

Modelled NO_x concentrations from proposed new sources in the East Thames Corridor are predicted to only have a small effect on the 98th percentile of hourly means for NO_2 and are not expected to lead to a breach of the statutory European Commission (EC) Limit value for NO_2. Modelling of the plumes from two power stations with 200 m stacks using ADMS 2.2 was carried out to determine whether changes in the plume composition would increase the chance of exceeding various pollution standards (EA, 1996).

Other studies that model pollution concentrations within London have focussed on processes within London and their impact on pollution concentrations. For example, Gardner and Dorling (1999) used neural network modelling to predict concentrations of NO_x and NO_2 in London from meteorological data. Seika et al. (1998) developed a Gaussian dispersion model called ABM (ambient background model) and applied it to a number of pollutants in London including PM_{10}. The purpose of this ABM model was to predict annual mean background concentrations from both point and area sources.

Current knowledge of dispersion and deposition of combustion derived particles to London from the major point sources in south-east England is limited. Although the detrimental impacts of fly ash on building stone are well understood (see Section 1.8.1), the precise health effects of SCP and IAS inhalation are not known. Given the capacity for IAS and SCP to adsorb trace elements (Schure, 1985), those within the inhalable size fraction may constitute a threat to human health (see Section 1.8.3). Therefore it is vital to extend the current knowledge of the impact of particles from high temperature combustion sources, especially to areas that have high populations.

3.1.9 Aims

This chapter describes the use of ADMS 3 to model emissions of SCPs from coal- and oil-fired Part A processes in and around London. The aims of this chapter are:

1. to use dispersion modelling to predict the pattern of deposition of different sizes of SCPs deposited in London; and
2. to test the hypothesis that SCP deposition to London is related to distance from the power stations in the east Thames Corridor and decreases from the east to the west of London.

The main focus of this study is on deposition of pollution to receptor points in London (Figure 2.4). The receptor points correspond to lake and pond sites where sediment samples have been taken (see Section 2.1.2). The distribution pattern of particles deposited in London is plotted. An assessment is made of the sensitivity of the model to different meteorological parameters. The output from this chapter is compared with the concentration of SCPs in surface sediments of lakes and ponds in London detailed in Chapter 4.

3.2 Dispersion modelling of particles from power stations and other Part A processes in London

3.2.1 Modelling software

ADMS version 3 is the most recent version of a PC-based atmospheric dispersion model developed by the Meteorological Office and Cambridge Environmental Research Consultants. ADMS 3 has a great deal of flexibility in the model options. The effects of coastline, buildings and topography can be taken into account. The model can be customised to reflect variations in the roughness length (see Section 3.5) between the meteorological site and the receptor site. Long- and short-term concentrations and deposition (both wet and dry) can be calculated. Meteorological data can be specified and edited as necessary. ADMS 3 was chosen for this project because it is suitable for modelling particle deposition from either single point sources or from multiple point sources in combination. ADMS 3 is capable of generating deposition data for a spatial output grid or at predefined receptor points.

In ADMS the boundary layer is characterised by the boundary layer height *h* and the Monin-Obukov length (M-O) as opposed to the older approach that describes the atmosphere in terms of the Pasqill-Gifford stability class. The M-O length is the buoyancy length scale and describes the depth of the near-surface layer in which shear effects are likely to be significant under any stability condition. The Pasquill-Gifford stability class is defined by a classification scheme (from A to F) that refers to simplified atmospheric stability derived from routinely available meteorological variables. For example, Class A is extremely unstable and relates to low wind speeds with moderate to strong incoming radiation (Arya, 1999). The advantage of using the M-O length is that it more accurately represents the state of the boundary layer. A detailed description of calculations and parameterisations used in ADMS 3 are included in the technical summary of the model User Guide (CERC, 1999).

Figure 3.3: Location of power stations and other high-temperature combustion Part A processes in and around London

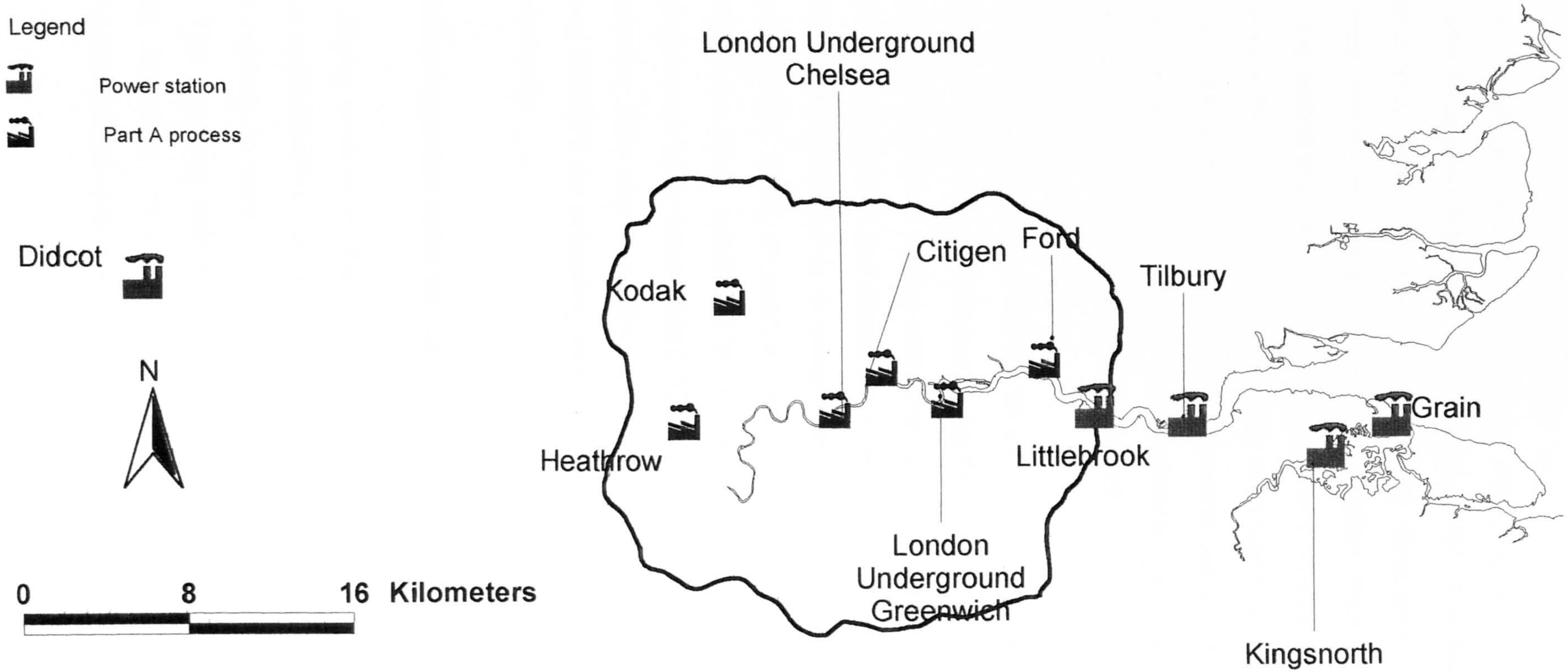

ADMS 3 includes a plume rise module that takes into account the effect of plume buoyancy and momentum in calculating the plume rise. ADMS 3 is conceptually similar to Gaussian models (e.g. NRPB – R91 (National Radiological Protection Board model number R91), US EPA (United States Environmental Protection Agency) models such as ISC (Middleton, 1997)) in that a continuous plume is assumed to travel downwind under steady meteorological conditions. However, ADMS 3 differs from older Gaussian models during convective conditions especially for elevated plumes. Under these conditions the plume spread parameters are used in a skewed plume to take account of the strong updrafts and weak downdrafts and the effect these have on the plume. In stable and neutral conditions the spread parameters are described by a Gaussian plume (Middleton, 1997).

A comparison of ADMS with the AERMOD and ISC Dispersion models was carried out (Hall et al., 2000a) which found significant differences between the three models. There are many concerns about atmospheric dispersion models, and some of these are discussed in Hall et al., (2000b). However, ADMS 3 has been validated in a number of studies over flat terrain (e.g. Bennett and Hunter, 1997), in wind tunnel studies to simulate the building module (Carruthers et al., 1999) and the fluctuation, chemistry and line, area and volume sources have been tested (CERC, 1999). There are strengths and weaknesses with any modelling system and to a certain extent the usefulness of ADMS 3 for modelling dispersion of particles in London will be tested in this study.

3.2.2 Pollution sources selected for inclusion in the modelling study

There are many sources in the UK and in Europe that will contribute to background concentrations of SCPs but the deposition pattern from these sources is unlikely to vary spatially over a relatively small area such as London. The sources selected for inclusion in the model are high-temperature fossil-fuel combustion sources in London and south-east England and are described below.

Power stations

The power stations included were Grain, Kingsnorth, Tilbury and Littlebrook power stations to the East of London and Didcot power station to the West (Figure 3.3). Pollution from the four main power stations in the east Thames Corridor (Grain, Kingsnorth, Tilbury and Littlebrook) will contribute to London's pollution load during episodic weather conditions (HMIP, 1996). Didcot is further away from London and lies in almost the opposite direction to the east Thames Corridor sources.

Other power stations in south-east England that use fossil fuels are Richborough and Fawley. Fawley is part of an oil refinery and lies approximately 115 km distant from London. Fawley was not selected because it is a relatively minor source, in 1997 it generated only 214 GWh of electricity. Although Littlebrook only produced 332 GWh in that year, it is much closer to the lakes and pond receptor sites (it is the only power station located inside the M25) and therefore will have a much greater impact on London. Richborough lies to the east of London (approximately 105 km away) and was closed in 1996. Although Richborough was in operation for part of 1996 it is not included in the study as it was fuelled by orimulsion which produces particles that have a very different morphology to SCPs (Watt pers. comm.)

Other non-power station Part A processes

Part A processes are those that are most likely to cause serious pollution. All power stations fall within the Part A1 process category. There are around 6 000 Part A1 and A2 processes in England and Wales. Part A1 processes fall under the jurisdiction of the Environment Agency (LRC, 1997) whereas Part A2 processes are controlled by local authorities (Pollution Prevention and Control Act, 1999). Where a Part A process is wholly or partly responsible for a breach of the UK air quality objective it is required to use the best available techniques (BAT, see Section 1.2) to correct the problem. Particulate emissions from Part A processes are included in the Pollution Inventory (http://216.31.193.171/asp/pi_about.asp?language=English, Sep, 2001) and, prior to 1998, were incorporated in the Chemical Release

Inventory (LRC, 1997). Part A processes within London that burn either coal or oil at high temperatures and therefore produce SCPs have been selected for inclusion in the model (Figure 3.3). These are the combustion plants at Ford in Dagenham, London Underground in Chelsea, London Underground in Greenwich, Kodak in Harrow and Heathrow Airport. Other non-power station Part A processes outside London were excluded. It was assumed that these processes would not have a significant impact on London. These non-power station processes have lower stack heights and much lower emissions than the power stations that are situated outside the M25 but are included in the model.

Part B processes

Part B processes are those industries that operate under local authority authorisation. There are 644 Part B processes in London of which only 14% are combustion processes. There is no legal requirement for Part B processes to declare emissions (LRC, 1997) and so it would be difficult to obtain the necessary information in order to run the model. In addition, emissions from oil- and coal- fired combustion Part B processes are likely to be small in comparison with Part A processes and deposition of particles from Part B processes will be more localised than all types of Part A processes due to lower emissions and stack heights. For these reasons Part B processes have not been included in this study.

3.3 Source parameters

ADMS 3 has options to model line, area, volume, jet or point sources. Each of the power stations and other Part A processes in this study was modelled as a point source. The model requires information about the particles emitted and both physical and operational parameters for each source. Either terminal velocity or deposition velocity is needed by ADMS 3 in order to calculate particle settling rate. In this case neither are known for SCPs and so the settling rate is calculated by the model from particle size and density.

3.3.1 Particulate emissions

Particle emission data were taken from the PowerGen plc Environmental Performance Report 1996 (PowerGen, 1996) for Grain, Richborough and Kingsnorth and from the National Power Environmental Performance Review 1997 (National Power, 1997) for Didcot 'A', Littlebrook and Tilbury. PowerGen data represents the 1996 calendar year whereas data from National Power covers the period from April 1996 to March 1997 inclusive.

Littlebrook and Grain are oil-fired and do not use coal, which means that all the particulates emitted can be attributed to oil combustion. Kingsnorth, Tilbury and Didcot are powered by coal but are fired up using oil and so the particles produced are from both oil and coal combustion.

To split the total mass of particulates emitted into a coal-derived and oil-derived component it was necessary to make a calculation based on the quantities of each fuel used. The total suspended particle (TSP) emissions were calculated for each coal-fired process based on the mass of coal and oil used in the study year and the emission factors from QUARG (1996). These factors are 1.0 g of TSP for each kilogram of coal and 1.1 g for each kilogram of oil used and were based on 1995 data from PowerGen and 1994 data from National Power.

The ratio of coal-derived to oil-derived particulates was then applied to the published emissions to produce oil and coal components of actual emissions data (Table 3.2).

Table 3.2: Conversion of particulate emissions into coal- and oil- derived fractions

Power Station	Coal used (Kt yr-1)	Oil used (Kt yr-1)	Particles from coal (Kt yr-1)	Particles from oil (Kt yr-1)	Total particles (Kt yr-1)	Published particulate emissions (Kt yr-1)
Kingsnorth	2460	120	2.460	0.1320	2.5920	3.360
Didcot A	1152	42	1.152	0.0462	1.1982	1.021
Tilbury	1243	41	1.243	0.0451	1.2881	0.190

The sum of the oil- and coal-derived particles is shown in the total particles column and the published particulate emissions weights are also shown for comparison. The calculated total and the published emissions are of the same order for Kingsnorth and Didcot. Differences between the two figures are small and are likely to be due to errors in the measurement of particle emissions or to rounding errors in the published data. All three sources are equipped with electrostatic precipitators (ESPs) but the ESPs at Kingsnorth were due for refitting in 1996 (Johnson, 2000 pers. comm.), which might explain slightly higher emissions than expected.

The published emissions are considerably smaller than the calculated emissions from Tilbury and the reasons for this are unclear. The TSP factors used in this study are based on 1994/1995 data. If different fuels were used in 1996 a different amount of ash might be produced thus causing the TSP factor to be inaccurate. Alternatively, if the fuel usage statistics are correct then the difference in ash produced may be due to electrostatic precipitator efficiency (ESP). Didcot and Tilbury use a similar amount of fuel but Didcot produces over five times more ash. If the ESP at Didcot is less efficient or not working correctly then this may account for the difference in ash emitted. Another explanation might be that there is an error in the published emission data. However, the published data were assumed to be correct and for each source the published data were used in the model.

3.3.2 Particle characteristics

SCPs are uniquely emitted by high-temperature combustion sources and have a characteristic morphology that is easy to identify using optical microscopy. Oil- and coal-derived SCPs are black and spheroidal often with a porous structure (Rose, 1991). It has been suggested that oil and coal particles can be separated visually by the presence of surface contouring around the pores of oil-derived particles although Rose et al. (1996a) showed that this contour effect may also be present on coal-derived particles. SCPs in coal fly ash only account for around 5% of the particulate matter by mass (Raask, 1984; BEI, 1991) because the majority of coal-derived emissions are denser particles formed from mineral inclusions in coal. Mineral matter only

accounts for 0.1% of fuel oil (Goldstein and Sigmund, 1976) and so for the purpose of this study it has been assumed that SCPs comprise all of the fly ash produced by oil-fired processes.

SCP bulk density was determined by Rose (1998, pers. comm.) using fly ash from oil- and coal-fired power stations. The densities are 0.467 g cm^{-3} for oil fly ash and 1.020 g cm^{-3} for coal fly ash. The density of the coal fly ash includes the particle fraction that is formed from mineral matter, which means that the density is unlikely to reflect the true density of the coal-derived SCPs. Since oil- and coal-derived SCPs are similar in terms of morphology and structure an assumption was made for modelling purposes that the density of coal-derived SCPs is the same as the density of oil-derived SCPs. To reflect the actual emissions of SCPs the deposition output from the model was scaled down to 5%.

3.3.3 Size range of SCPs emitted by power stations and other Part A processes

A typical grading for coal-derived fly ash shows that the majority of the ash (52%) is in the size fraction less than 20 μm (BEI, 1991). All coal boilers emit particles in two distinct phases, a sub-micron mode and a large particle (>1 μm) mode and the distribution profile of these phases is dependent on boiler design (McElroy et al., 1982). Oil-derived fly ash has a smaller average size fraction than coal; most of the particles have a diameter less than 5 μm (Raeymaekers et al., 1988).

Particles in pulverised fly ash (pfa) do not have the same particle size distribution as the fly ash that escapes from the stack. Each of the power stations modelled in this study has an electrostatic precipitator (ESP). ESPs are most efficient at collecting larger particles and have an efficiency that is typically between 99.3% and 99.7%. Particle size measured after the aerosol has passed through the ESP typically has a smaller average size with 50% of oil-fired particles less than 0.38 μm compared with 50% of coal fired particles smaller than 4.9 μm (Shen et al., 1976).

All the measurements referred to in this section were made on particles emitted from boilers of different sizes and different operating conditions. The size of SCPs emitted from combustion processes will be affected by many factors including the type of fuel, combustion chamber operation efficiency, maintenance of particle arrestment equipment and sulphur content of the coal (for coal-fired processes). The particle size mass distribution of fly ash from a coal combustion source was altered during an experiment to reduce emissions of NO_x (Griest and Harris, 1985). Lower NO_x was associated with a production of larger fly ash particles. The properties of fuel oil such as specific gravity, viscosity, volatility, ash content and heat values are also important in terms of particle production.

Agglomeration of particles will also affect the size distribution for dispersion. Oil combustion typically produces a higher H_2O/CO_2 ratio compared with coal combustion and this will increase agglomeration of particles in the flue gases (Shen et al., 1976).

Since the size distribution of SCPs emitted by combustion sources is not known in detail, no attempt has been made here to fit deposition to a particle size distribution. In order to model the deposition of a range of particle sizes, different particles sizes were input as separate pollutant species in the emissions data entry screen of ADMS 3. It is not possible in ADMS 3 to model a continuous size range because it can only model deposition for discrete particle sizes. For example, if a particle size of 10 μm is modelled then the output is for a particle of exactly 10 μm diameter. The data do not include particles that are smaller or larger. The particle sizes modelled increased in increments of 10 μm between a minimum of 10 μm and a maximum of 100 μm.

It is possible to use a mass fraction factor for each particle size to correct emissions for each size according to the particle size distribution. The resulting output is total deposition for the whole of the emissions and does not discriminate between particle sizes. Since the object of this study was to

assess the deposition patterns of particle sizes and not the magnitude then the mass fraction factor was not used.

3.3.4 Operational parameters

Operational parameters for the power stations and other Part A processes modelled in the study are shown in Tables 3.3 and 3.4.

Table 3.3: Part A Process release characteristics – input data for model

Process	Stack number	Efflux exit velocity (m s^{-1})	Flue gas exit temperature (°C)	Emission of oil-derived particles (g s^{-1})
Citigen	1	32.3	157	0.539
	2	32.3	157	0.539
Heathrow	1	6.7	250	0.381
	2	15.0	250	0.054
	3	15.0	250	0.092
Kodak	1	7.5	160	0.507
	2	13.3	106	0.152
	3	13.3	106	0.184
Ford	1	8.2	141	0.800
	2	10.1	139	1.200
	3	10.8	146	0.720
	4	10.0	149	0.720
London Underground Greenwich	1	14.0	250	0.026
	2	14.0	250	0.026
	3	14.0	250	0.026
	4	14.0	250	0.013
London Underground Chelsea	1	10.0	149	1.268
	2	10.0	149	1.046

Data supplied by the London Research Centre (Sadler, 1998, pers. comm.).

Table 3.4: Power station process release characteristics - input data for model.

Power Station	Flue gas exit temperature (°C)	Efflux exit velocity (m s^{-1})	Coal-derived particles (g s^{-1})	Oil-derived particles (g s^{-1})
Grain	130	24.7	-	15.221
Kingsnorth	130	25	101.119	5.426
Didcot 'A'	115	28	31.127	1.248
Littlebrook	140	31	-	1.300
Tilbury	130	17	5.814	0.211

Data supplied by the Environment Agency (Powesland, 1998, pers. comm.).

3.3.5 Physical parameters

The physical parameters are stack height and stack effective diameter (Tables 3.5 and 3.6). Where a power station has multiple flues (several chimneys within one stack) an equivalent radius has been calculated as if the emissions were emitted via a single orifice which has the same effective area as the total orifice area of the individual chimneys. Some of the Part A processes have been treated slightly differently. Where there are multiple flues the parameters for each individual flue were input separately and then combined in the model to make up the emissions from the source. Power station data were supplied by the Environment Agency (Powesland, pers. comm.) and Part A Process data were supplied by the London Research Centre (Sadler pers. comm.).

Table 3.5: Physical parameters of the power stations

Power Station	Easting	Northing	Stack Height (m)	Effective Stack Diameter (m)
Grain	588500	175500	244	13.4
Kingsnorth	581150	172050	198	12.2
Didcot 'A'	451000	191300	199	12.0
Littlebrook	555700	176500	215	11.3
Tilbury	566000	175500	164	8.9

Table 3.6: Physical parameters of the other Part A Processes

Source	Easting	Northing	Stack Number	Stack Height (m)	Stack Diameter (m)
Citigen	531630	181740	1	42	1.28
			2	42	1.28
Heathrow	506470	174410	1	39.4	1.13
	507420	175760	2	29.0	0.5
	509520	175720	3	36.6	0.5
Kodak	514640	189670	1	50.0	1.26
	514660	189680	2	64.0	1.35
			3	64.0	1.35
Ford	549900	181900	1	80	1.5
			2	80	1.5
			3	80	1.5
			4	80	1.5
London Underground Greenwich	538800	178100	1	61.8	3.9
			2	61.8	3.9
			3	61.8	3.9
			4	61.8	3.9
London Underground Chelsea	526400	177000	1	83.8	1.5
			2	83.8	1.5

3.4 Model Options

3.4.1 Topography

Local terrain can have an effect on airflow that will in turn affect plume dispersion. Generally, if the terrain varies by more than a slope of 1:10 then the effects of topography should be included in the model (Robinson, 2000 pers. comm.). The study area for this project is relatively flat - most of the Thames corridor is less than 50 m above sea level (Figure 3.4) - so in this case the topography module was not used.

Figure 3.4: Topography of the Thames Corridor

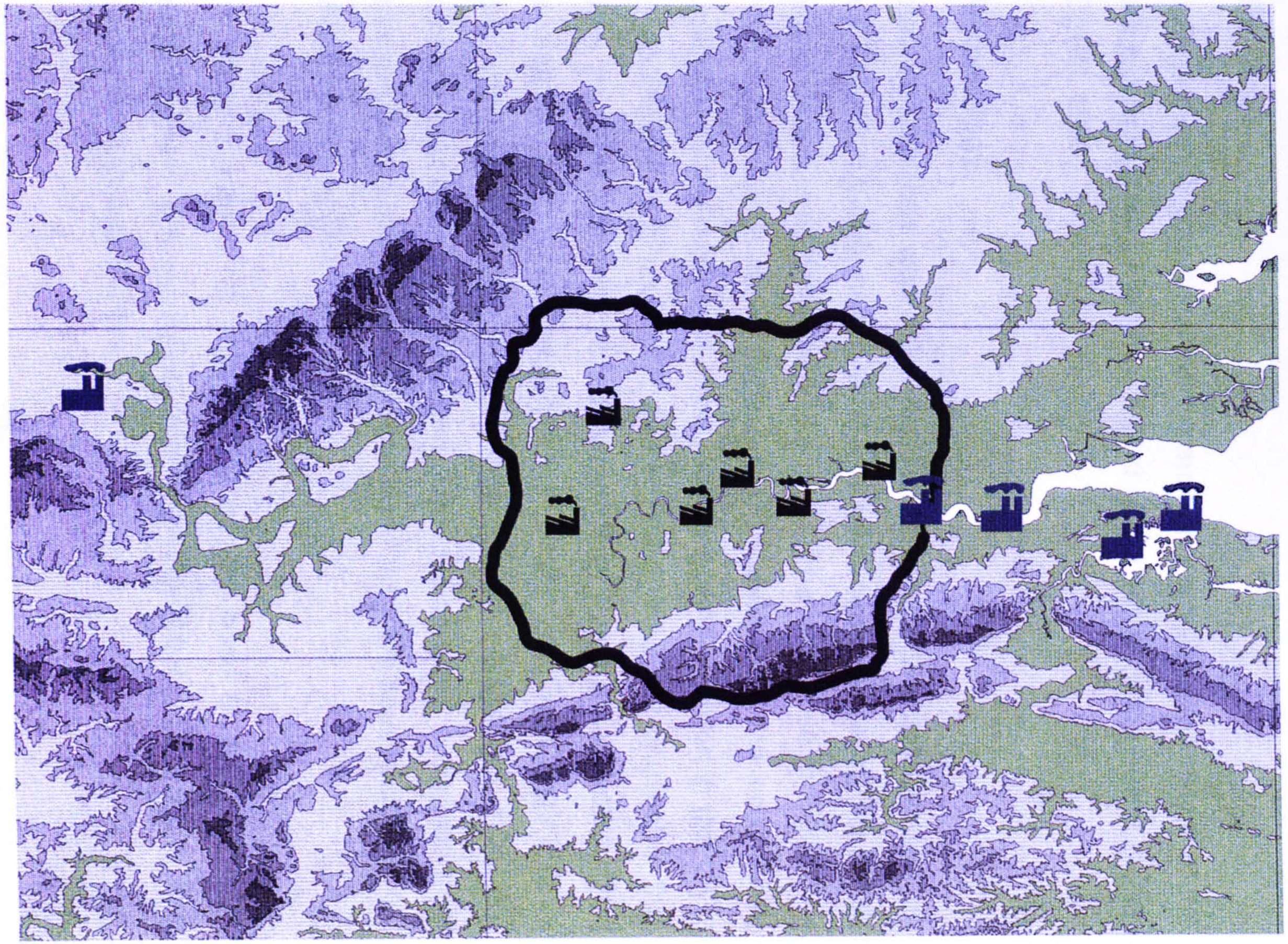

3.4.2 Coastline

The coastline module takes into account the effect of coast and sea breezes on dispersion. It was not used even though it may have been appropriate for modelling emissions from Grain and Richborough, which are located close to the coast. The coastline module will only work under specific meteorological conditions and the model will stall if these conditions are not met (Robinson, 2000, pers. comm.). To run successfully it would have been necessary to edit the meteorology file to only include lines of data that meet these conditions. It was not feasible to model the long-term pattern of deposition in London using this option.

3.4.3 Buildings

The buildings module was not used because in each case the height of the surrounding buildings was less than a third of the height of the power station stack (CERC, 1999).

3.5 Meteorology

The meteorological data were taken from the London Weather Centre (grid reference 530200, 180000, height 42m) archive accessed through the British Atmospheric Data Centre (www.badc.rl.ac.uk). The wind rose in Figure 3.5 shows that hourly winds most frequently originated from the south-west, closely followed by the north-east. The prevailing wind direction in the UK is from the south-west (Stirling, 1997) and so 1996 is slightly unusual in that winds from the north-east are more frequent than would be expected. The average speed for each wind direction at the London Weather Centre (Figure 3.6) does not vary much. The strongest winds originated from 60° (approximately east-north-east) and from 230° (south-west) but winds from the north were also relatively strong. The winds from the south-east had the lowest average wind speed.

ADMS 3 offers a number of options that can be used to alter the input parameters to more closely reflect real meteorological conditions. Two scenarios were created as follows:

Figure 3.5: Number of occurences of wind from each direction at the London Weather Centre in 1996

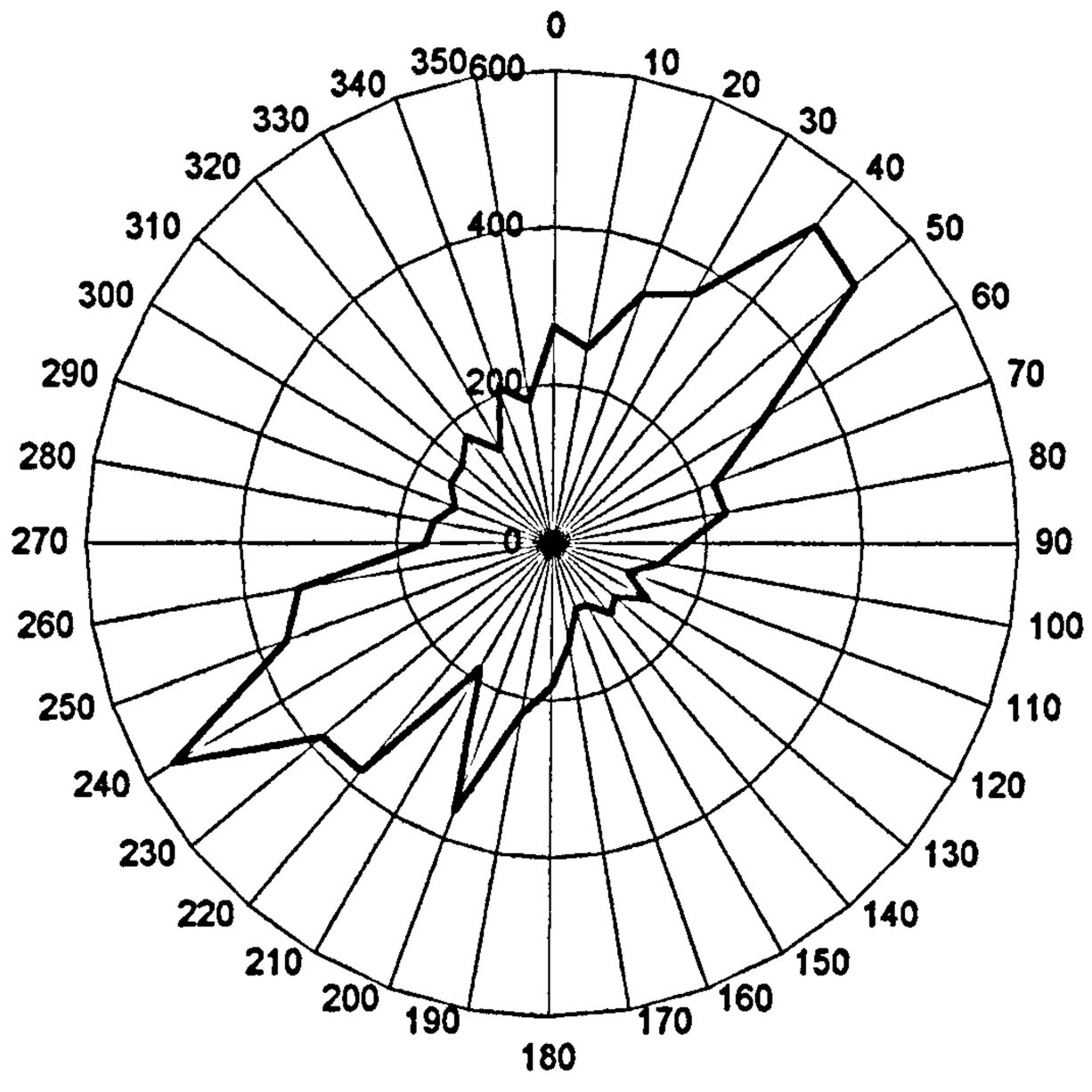

Figure 3.6: Average wind speed and direction at the London Weather Centre in 1996 (speed is in knots (0.515 m s^{-1}) and direction is in degrees)

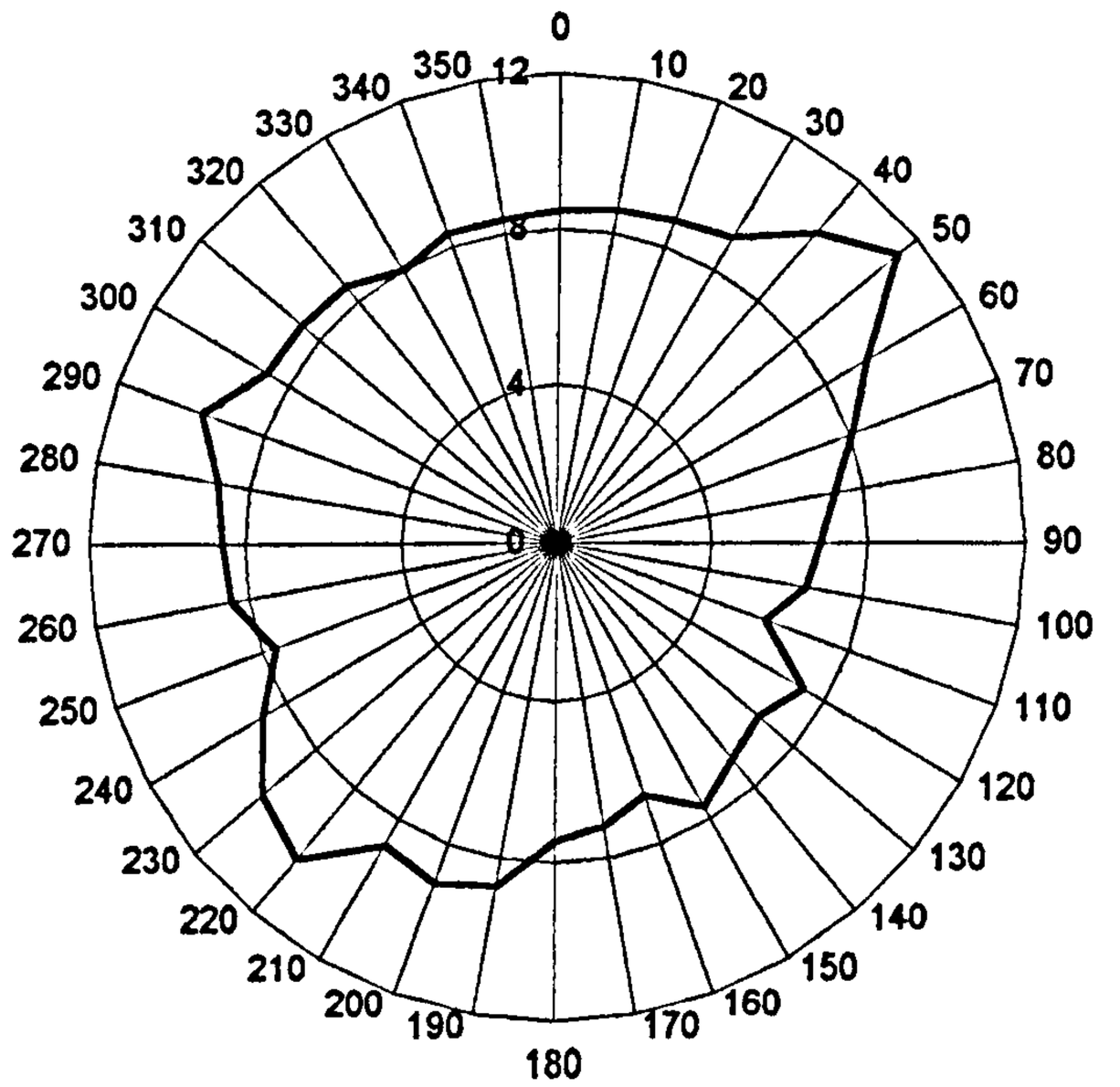

Base 1: emissions outside London (power stations in the east Thames corridor and Didcot)

Base 2: emissions within London (Part A processes and Littlebrook)

The input parameters for Base1 and Base 2 are shown in Table 3.7.

Table 3.7: Meteorological input parameters

	Base 1	Base 2
Roughness length (m)	0.2	1.5
Minimum Monin-Obukov length (m)	No minimum	30

The roughness length is a measure of the friction of the surface of the earth. The height of the top of the boundary layer increases with surface roughness (Oke, 1987). Roughness length affects turbulence and is one of the driving forces behind the creation of the urban heat island effect. Some typical roughness lengths are shown in Table 3.8

In Base 1 the meteorological data are specified as unrepresentative of the source site and so a different roughness length is used for each site. The roughness length of the meteorological site was set to 1.5 m to reflect the urban and suburban environment. The source environment is flat and featureless agricultural land interspersed with pockets of industry therefore the roughness length was set to 0.2 m. The roughness length for Base 2 was specified to be representative of the source site since all of the Part A processes and Littlebrook power station are within the extended built up area of London and its satellite towns. A roughness length of 1.5 m was used for both.

Table 3.8: Roughness lengths of artificial and natural surfaces (modified from Oke, 1987)

Surface	Roughness Length
Water – open sea	$0.1 - 10.0 \times 10^{-5}$
Ice	0.1×10^{-4}
Soils	0.001 – 0.01
Grass (0.02 – 0.1m)	0.003 – 0.01
Grass (0.25 – 1.0m)	0.4 – 0.1
Agricultural crops	0.04 - 0.2
Forests (deciduous or coniferous)	1.0 – 6.0
Scattered settlement	0.2 - 0.6
Suburban	0.4 – 1.8
Urban	1.5 – 10

The Monin-Obukov (M-O) length is a measure of the stability of the atmosphere. Its length is the distance that convective thermals take to accelerate to be capable of generating significant turbulence (Middleton, 1997). The M-O length is one of the most important parameters in ADMS 3 as it is used with boundary layer height to determine atmospheric stability. ADMS 3 allows the user to specify a minimum M-O length so that any factor that might affect atmospheric stability, but is not represented by the meteorological data, can be taken into account. For example, heat production in cities will cause warming of the atmosphere and cause an unstable atmosphere. This is one of the causes of the urban heat island effect. In Base 1 no minimum M-O length was set because the pollution plumes mostly travel across flat agricultural land. In Base 2 the effect of changing M-O length and roughness length on deposition is shown in Section 3.8.

The other meteorological parameters that it is possible to alter are the default albedo value and the Priestly-Taylor value. Albedo is the ratio of the amount of incident solar radiation reflected by a body to the amount incident upon it and it has a value between 0 and 1. Low numbers show that most of the radiation is absorbed and high numbers show that most is reflected. Fresh

snow has an albedo of 0.95. Albedo is likely to vary across the study area due to the change in surface properties from agricultural land to the urban area. Soil has an albedo of between 0.05 and 0.40 whereas agricultural crops range between 0.18 and 0.25. The materials that make up the urban environment range from 0.05 to 0.20 for asphalt roads, between 0.10 and 0.35 for concrete and 0.08 to 0.52 for glass depending on its angle. Albedo is another variable that is important in determining the urban heat island effect. The albedo is likely to vary across the study site and so the default value (0.23) was used.

The Priestly-Taylor parameter represents the surface moisture available for evaporation. This parameter is likely to change spatially across the study area, like albedo, but there is no single value that can be specified to represent the whole area, and therefore, the default parameter (1.0) was used.

3.6 Results

Total deposition from power stations, other non-power station Part A processes and all sources are plotted in Figures 3.7 - 3.9 for SCP sizes ranging between 10 μm and 100 μm. However, predicted deposition is based on the assumption that all the SCPs emitted were of that particular size fraction i.e. for the 10 μm graph all the emissions were modelled as if they had a diameter of 10 μm, and likewise for the all the other size fractions (see Section 3.3.3). This approach does not attempt to predict the size distribution of SCPs once emitted from a power station stack but instead focuses on the spatial distribution of SCPs of a certain size. The results will show the distance that one size of SCPs will travel relative to other sizes.

The broad line surrounding the study area in each graph is the M25. The size fraction in microns refers to emissions that have an aerodynamic diameter of that size.

3.6.1 Total deposition from all power stations

Figure 3.7 shows total deposition from Tilbury, Grain, Kingsnorth, Didcot A and Littlebrook to lake and pond receptor sites in London.

Deposition is highest in the east and south-east of London for all particle sizes with the maximum deposition occurring at BROO for all sizes (approximately 20 mg m^{-2} yr^{-1} and 34 mg m^{-2} yr^{-1} for 10 μm and 100 μm respectively). This pattern is consistent with deposition expected from power stations located to the east of London. Didcot is the only source to the west of London and its impact is likely to be much less because it is further away than most of the sources in the east Thames corridor. This is borne out by the deposition patterns that do not suggest a significant western source. The pattern of deposition is similar for both small and large particles and the mass of deposition increases as particle size increases showing that larger SCPs particles are deposited in London from the same sources as the smaller SCPs.

3.6.2 Total deposition of SCPs from all other Part A Processes

For other Part A processes the overall pattern of deposition also varies very little with particle size (Figure 3.8). The highest deposition is in the centre of London with VICT (almost 90 mg m^{-2} yr^{-1} for 10 μm diameter SCPs) and WAND (just over 104 mg m^{-2} yr^{-1} for 10 μm diameter SCPs) having the highest levels of deposition for each particle size. These sites are close to Citigen and London Underground Chelsea. There are hotspots of higher levels of deposition close to all of the modelled sources. Variations in the pattern at some sites can be linked to the location of sources, for example deposition to EALI is higher for deposition of sizes 10-80 μm than for 90-100 μm. This can be explained by the impact from a source that is close enough to deposit smaller particles but too far away to contribute to the largest size fractions. Away from the source locations deposition is low and consistent regardless of SCP diameter. The distance of influence of other Part A processes is less than the distance of influence of power stations.

Figure 3.7: Modelled total deposition of power station derived SCPs with diameters ranging from 10 to 100 microns

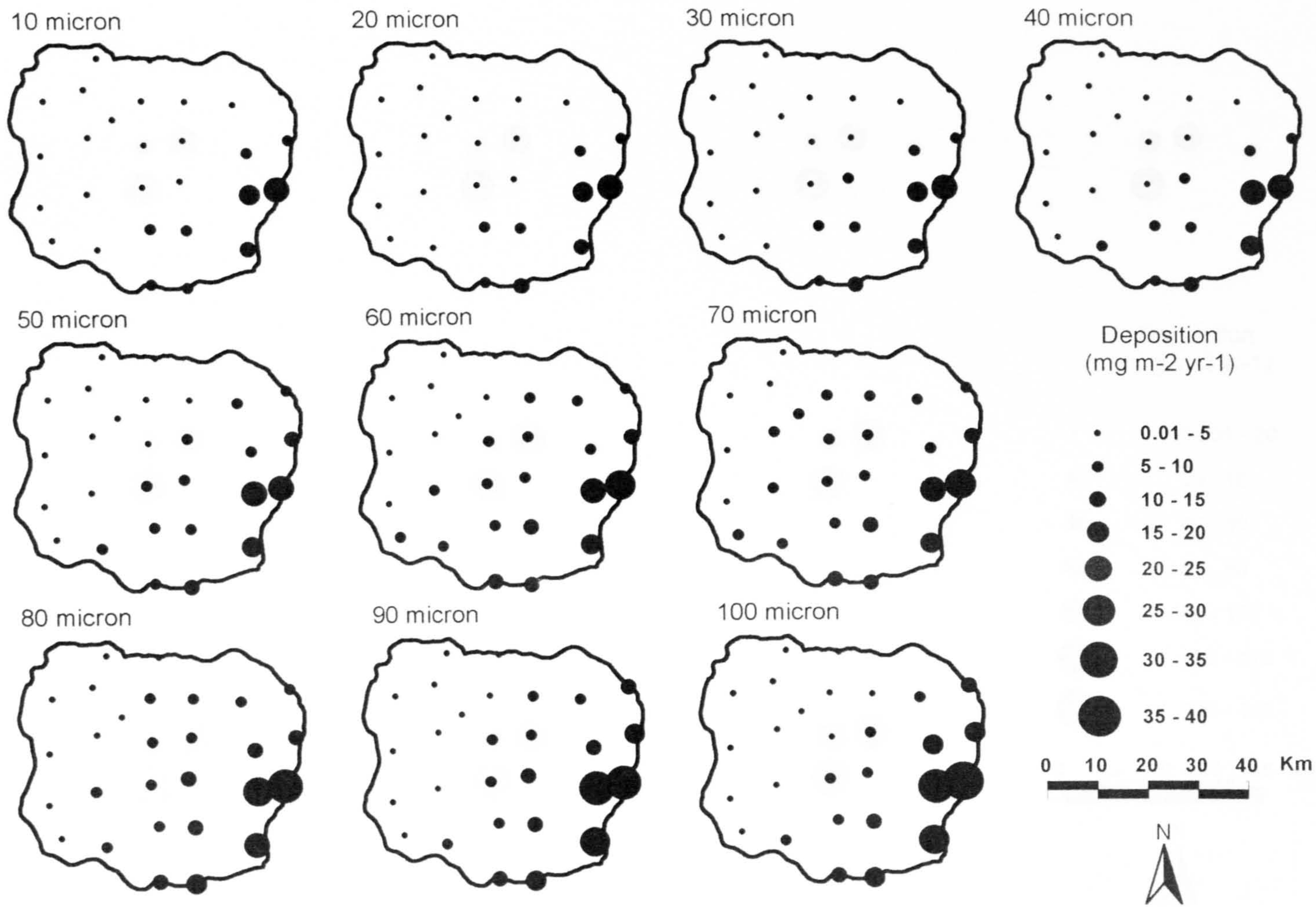

Figure 3.8: Modelled total deposition of non-power station Part A process derived SCPs with diameters ranging from 10 to 100 microns

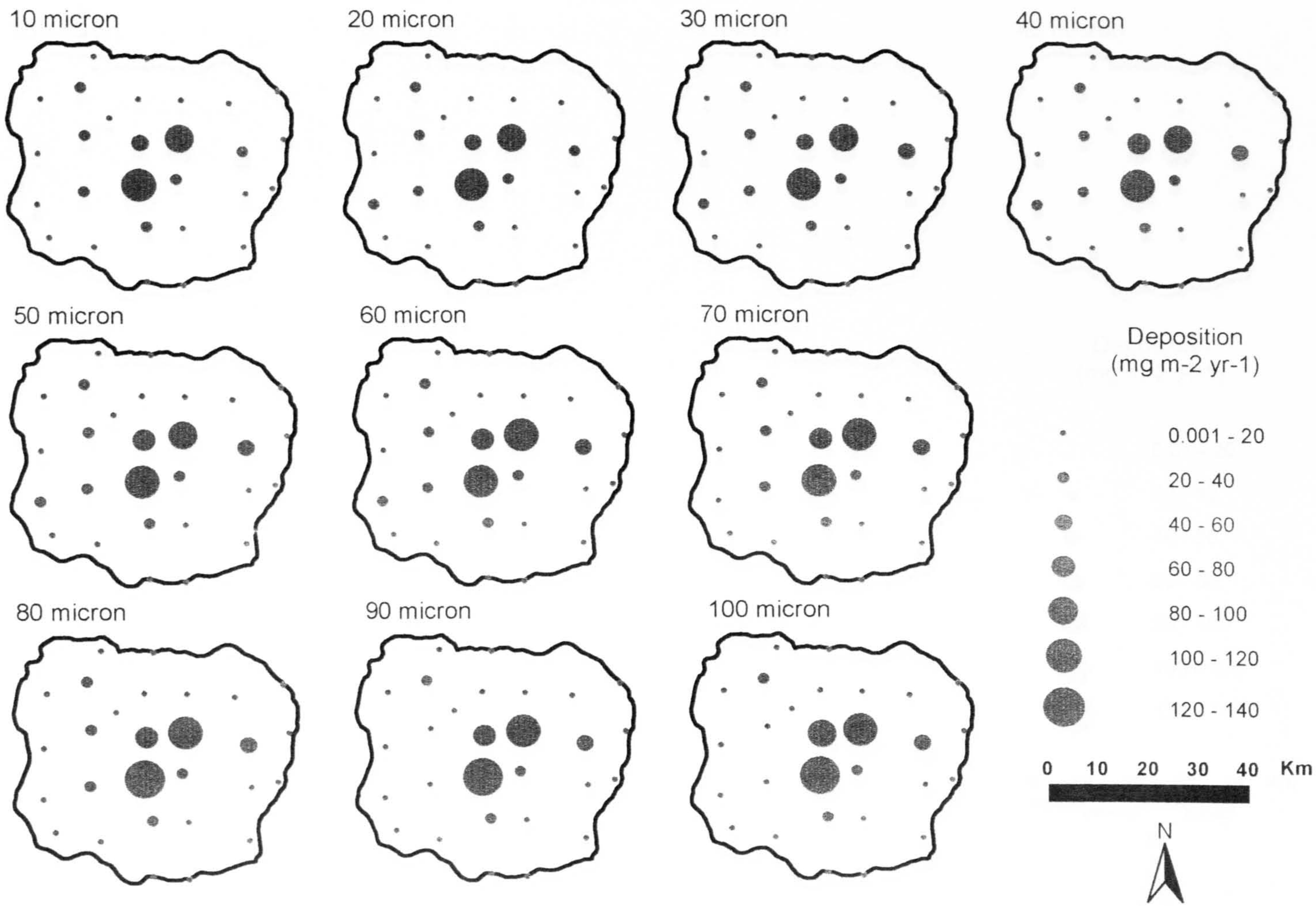

Figure 3.9: Modelled total deposition of SCPs from power stations and other Part A processes with diameters ranging from 10 to 100 microns

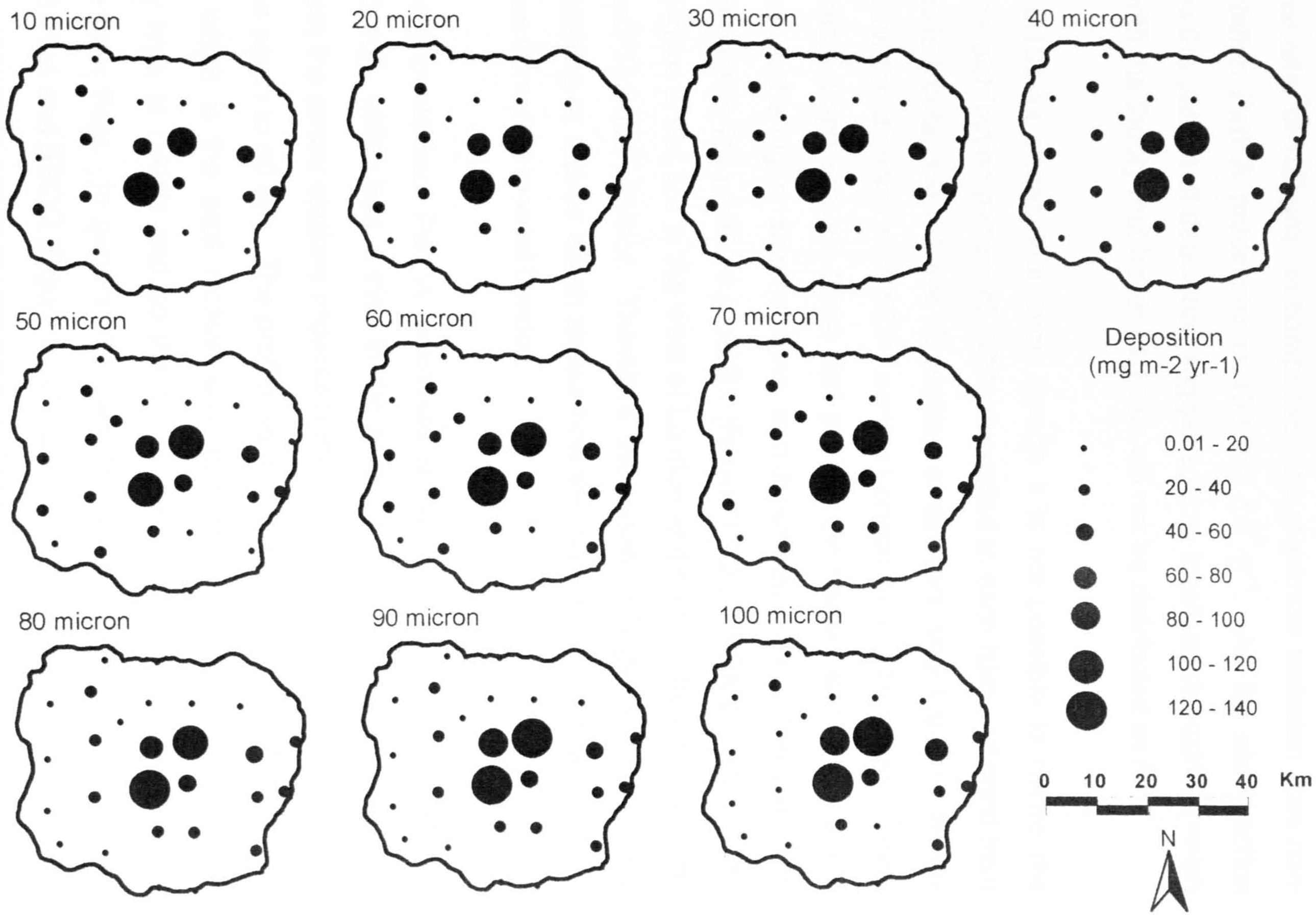

3.6.3 Total deposition from all sources

The pattern of deposition from all sources in combination is dominated by the non-power station Part A processes (Figure 3.9). Deposition from the power stations is much lower with a maximum deposition of 39 mg m^{-2} yr^{-1} for SCPs with a diameter of 100 µm. In comparison the maximum emission from non-power station Part A processes is 130 mg m^{-2} yr^{-1}. As the size fraction increases the pattern of deposition suggests more localised deposition, which agrees with the theory that larger particles will not be distributed as far.

Figures 3.10a-aa shows that even though it is not possible to derive the actual size distribution pattern of SCPs deposited to each lake and pond from the modelled data, the relative deposition of different size fractions shows much about the dispersion of SCPs across London from all sources. There are two main graph shapes, those that peak in the middle size fractions and drop down at the higher size fractions, and those that peak at 100 µm. The ones that peak in the middle e.g. ALEX (Figure 3.10b), BREN (Figure 3.10e), QUEE (Figure 3.10r) are in the west of London and furthest from the sources in the east Thames corridor. Therefore deposition of larger SCPs to these sites is starting to reduce which shows how the impact of the power stations diminishes from east to west London.

Localised impacts from Part A processes show up at sites such as DAGN (Figure 3.10j), which has a kink in the graph profile. Deposition of larger SCPs from the power stations reduces from 100 µm down to 70 µm but then increases again to 60 µm. The profile would be reduced as at FAIR (Figure 3.10m), which is the next closest site, however deposition from Ford is relatively high at DAGN and so the SCPs larger than 70 µm are likely to originate from Ford. In general the sites that peak at 100 µm (e.g. BUSH (Figure 3.10g) and BROO (Figure 3.10f)) are those to the east of London that are close enough to power station sources to receive deposition of the largest particles.

Figure 3.10a-i: Modelled total deposition of SCPs from power stations and Part A processes with diameters ranging from 10-100 μm

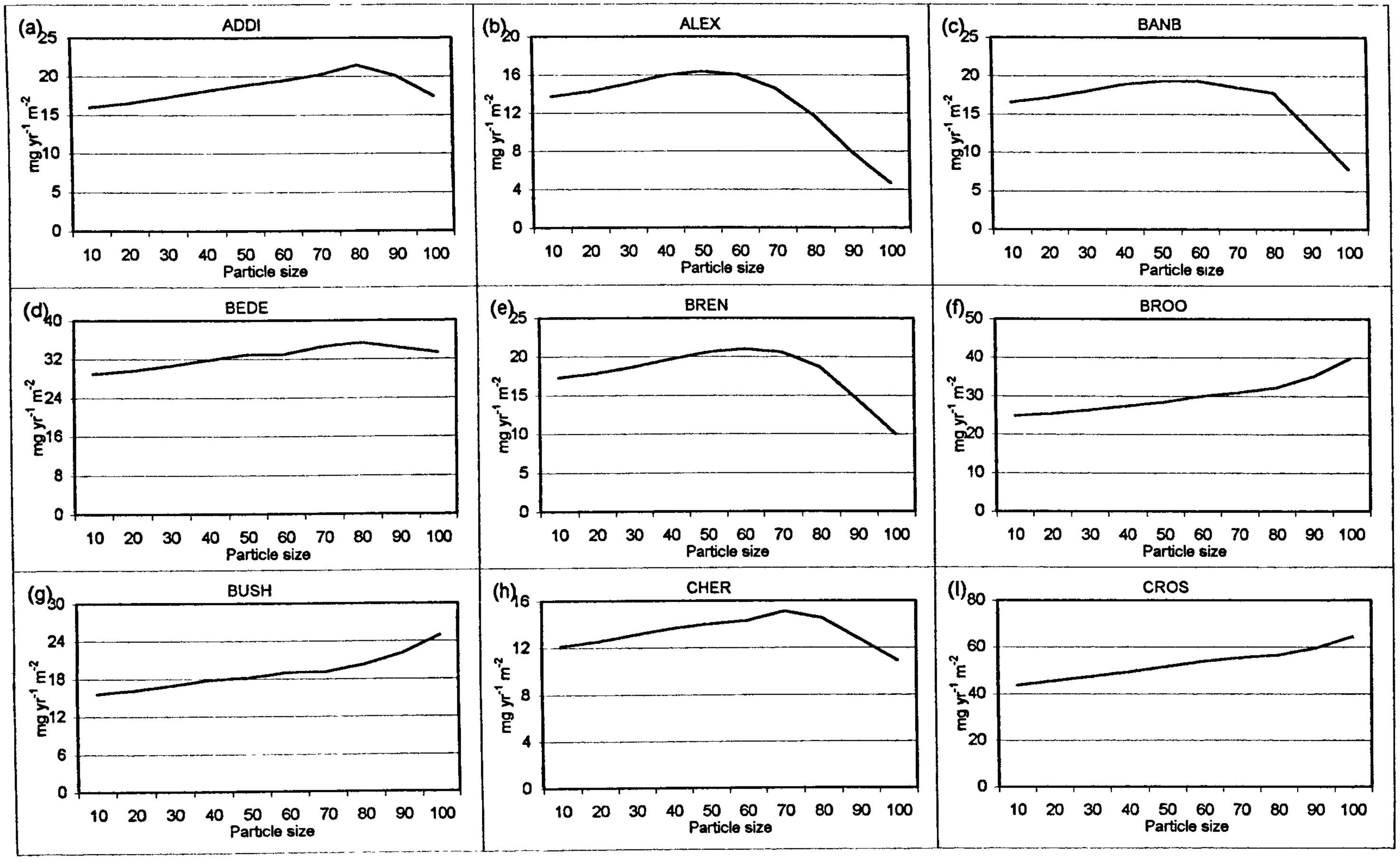

Figure 3.10j-r: Modelled total deposition of SCPs from power stations and Part A processes with diameters ranging from 10-100 μm

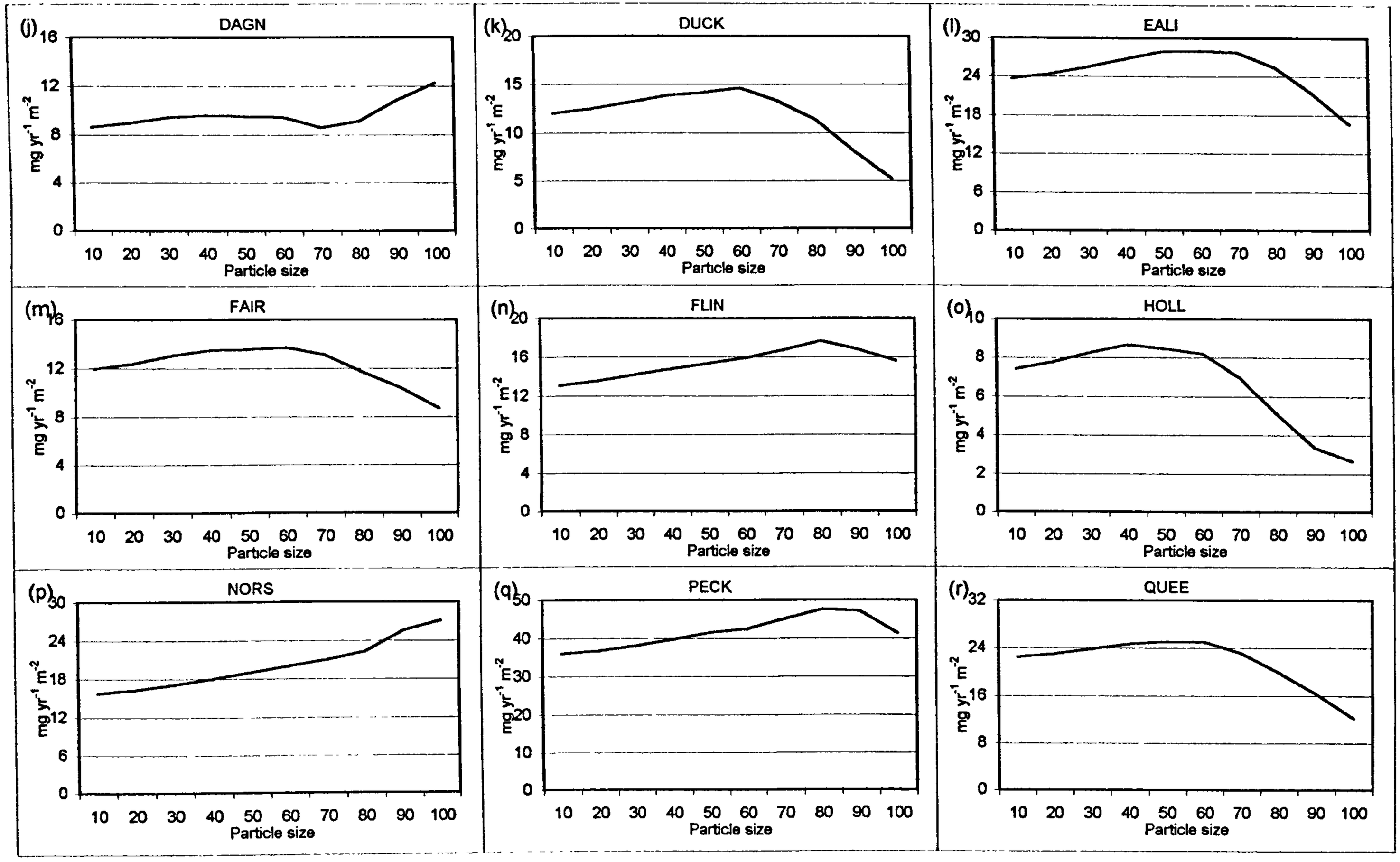

Figure 3.10s-aa: Modelled total deposition of SCPs from power stations and Part A processes with diameters ranging from 10-100 μm

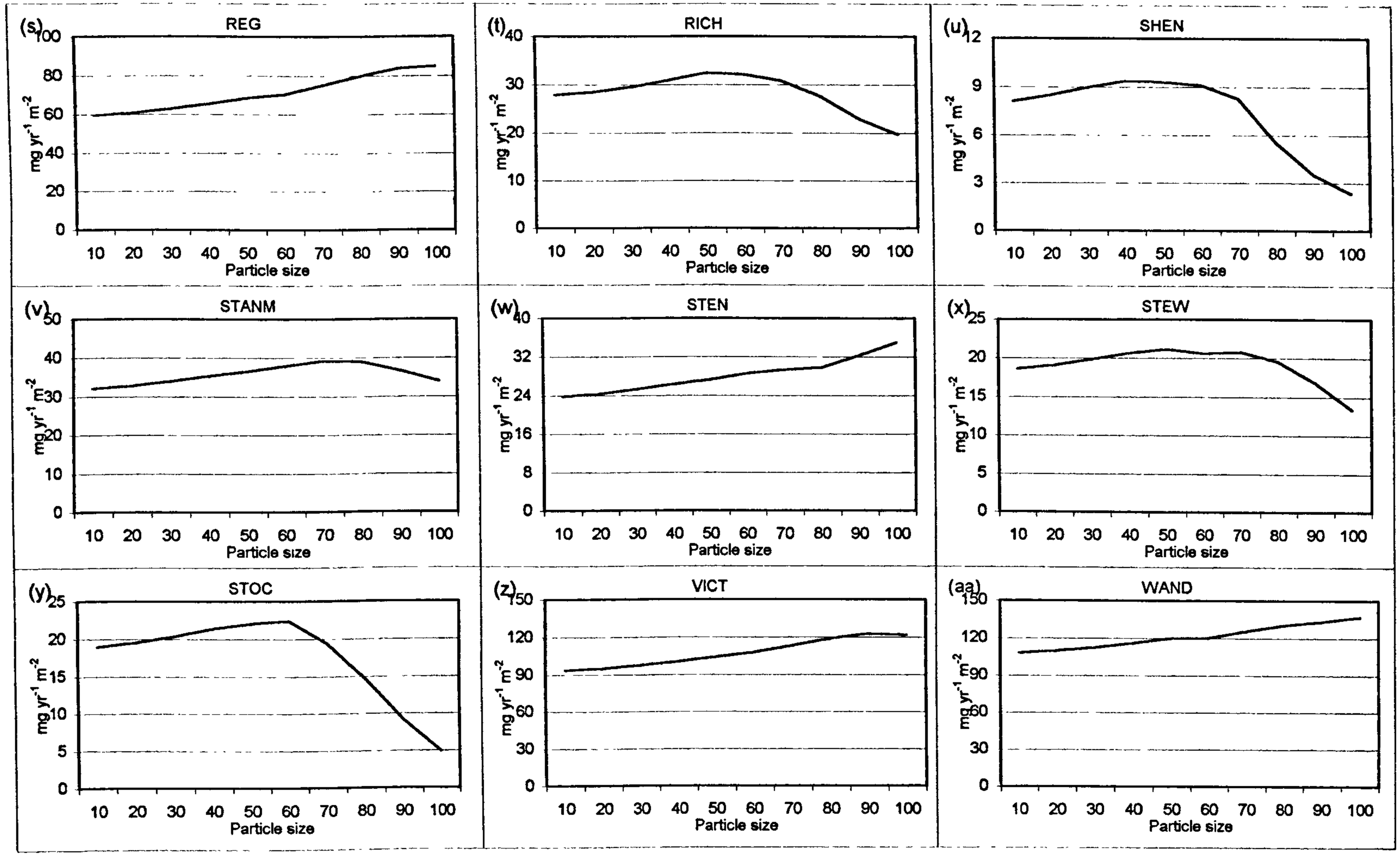

Figure 3.11: Modelled deposition of SCPs from power stations from east to west London

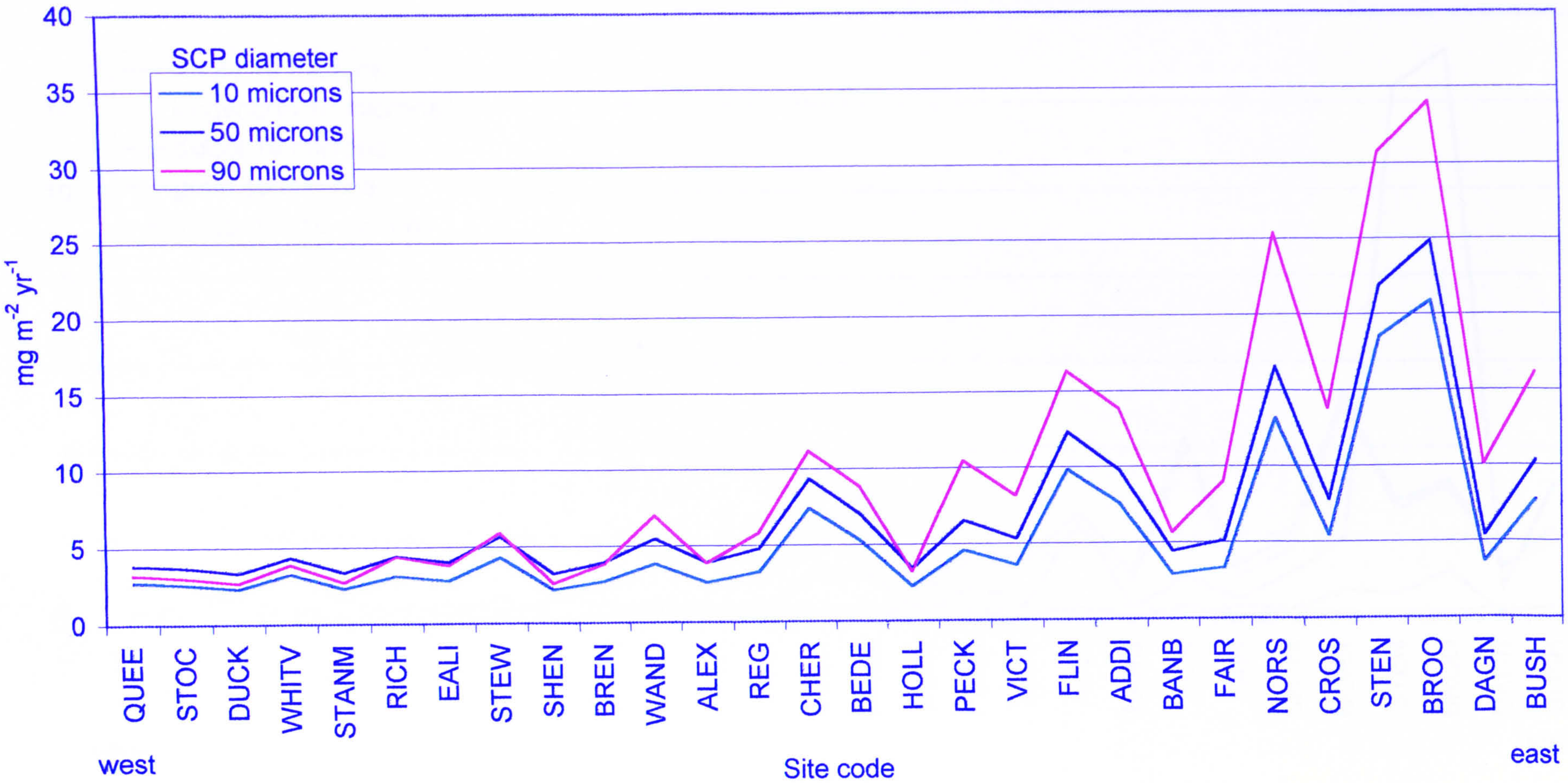

Figure 3.12: East-west deposition from individual power stations for SCPs 10 μm in diameter

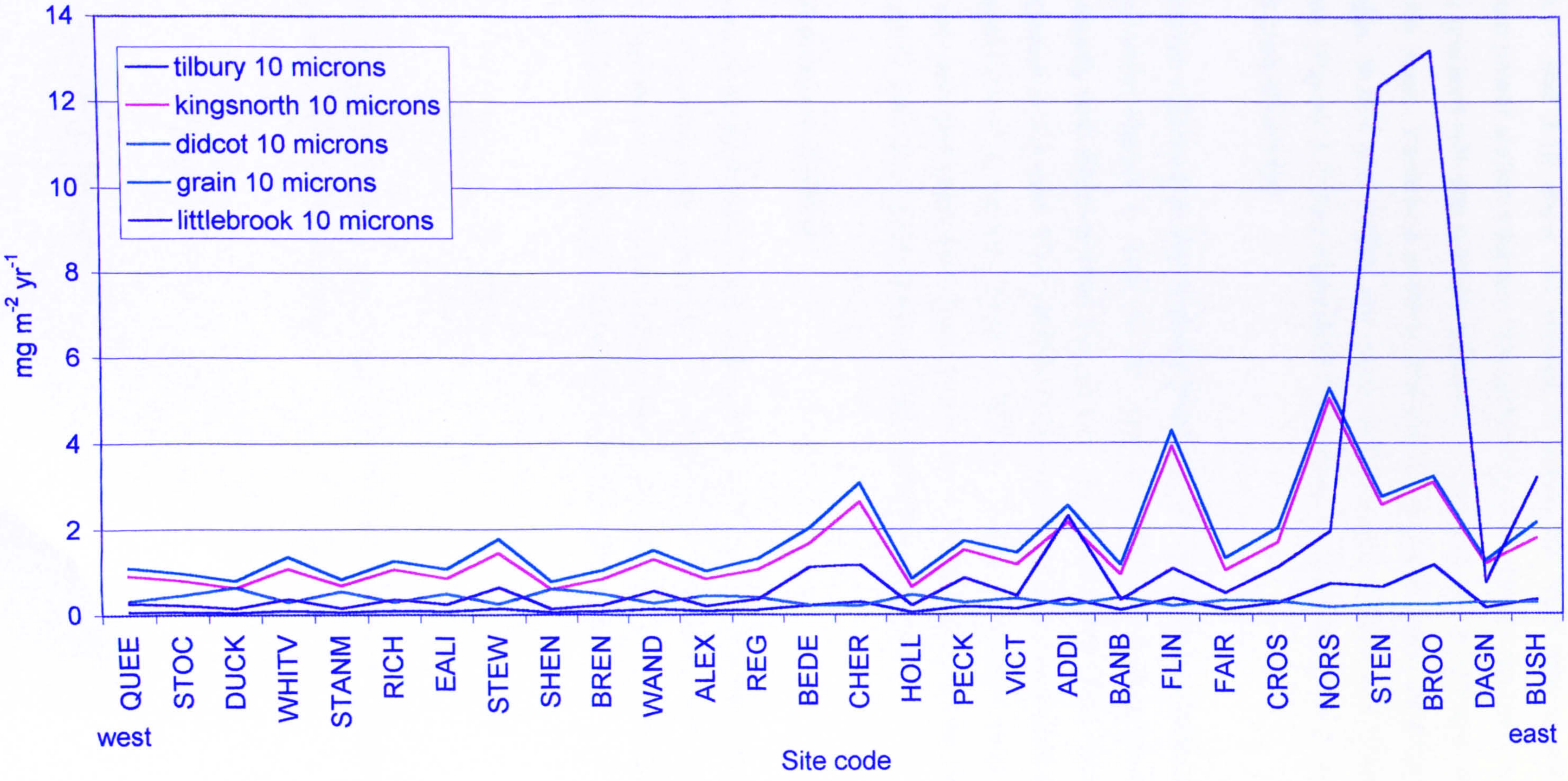

3.6.4 East-west variation

Figures 3.11 and 3.12 show the change in deposition from east to west London from power station sources. The general pattern shows that there is a deposition gradient with the highest deposition in the east of London and the lowest in the west. Variations in the profile are due to north-south variations. For example, BUSH and DAGN are more northerly than BROO and it has been shown (Figure 3.7) that deposition from power stations is higher in the south-east area of London.

Deposition from individual power stations (Figure 3.12) shows that Littlebrook has the greatest impact at sites in the east of London and that levels decrease rapidly with distance from this source. Kingsnorth and Grain have lower deposition in the east than Littlebrook but in the west are responsible for the deposition of a greater mass of SCPs. Tilbury deposition peaks slightly in the east and deposition from Didcot tends to increase towards the west of London, with very slight peaks at SHEN, STANM and DUCK.

3.6.5 SCP mass vs. number

Particle mass does not have a linear relationship with particle number which means that if particle size increases and mass stays the same then the number of particles in that mass decreases according to some function. Mass is proportional to volume as shown by the following equation:

$$Density = \frac{Mass}{Volume}$$

And as the particle diameter increases then the volume of the particle increases according to the relationship:

$$Volume = \frac{4}{3}\pi\left(\frac{d}{2}\right)^3$$

Where *d* is the particle diameter.

Therefore, particle mass is proportional to diameter according to the following:

$$Mass \quad \propto \left(\frac{d}{2} \right)^3$$

For example, the model predicts the deposition of 15.8 mg m^{-2} yr^{-1} at NORS if all the SCPs emitted had a diameter of 10 µm. This mass of SCPs is equivalent to 64 000 000 particles using the density of 0.467 g cm^{-3} from Section 3.3.2. If all of these particles were emitted with a diameter of 100 µm then the particle number would have been just 64 000 particles. The model actually predicts deposition of 27.2 mg m^{-2} yr^{-1} of 100 µm SCPs, which corresponds to 111 000 particles m^{-2} yr^{-1}. The mass of 100 µm SCPs is almost double the mass of 10 µm SCPs, but the number of 100 µm particles is less than 0.2 % of the number of 10 µm SCPs.

Particle mass and number will have very different patterns for different particle sizes, however the spatial pattern across London for each particle size will be the same whether particle number or size is used.

3.7 Sensitivity analysis

3.7.1 Relative contributions of individual power stations to total deposition

Figures 3.13 and 3.14 show the levels of deposition from each of the power stations and their relative contributions to each of the lake and pond sites respectively for SCPs with a diameter of 10 µm. The 10 µm size fraction was chosen arbitrarily as dispersion of particles of this size is most relevant in terms of the health impact of PM_{10}.

Figure 3.13: 10 micron sized SCPs deposited from individual power stations across London

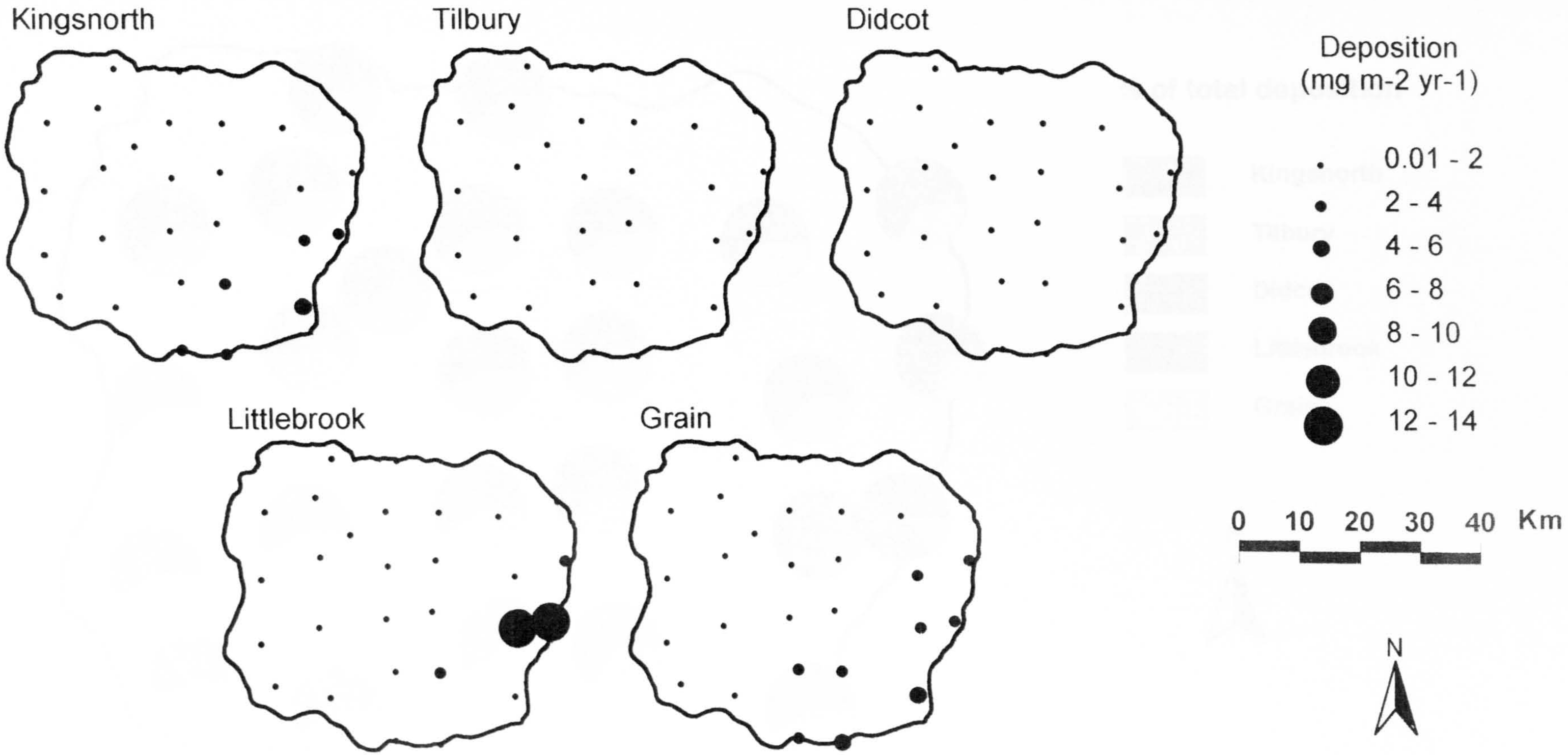

Figure 3.14: Relative deposition of SCPs with a diameter of 10 microns at each receptor site from power stations

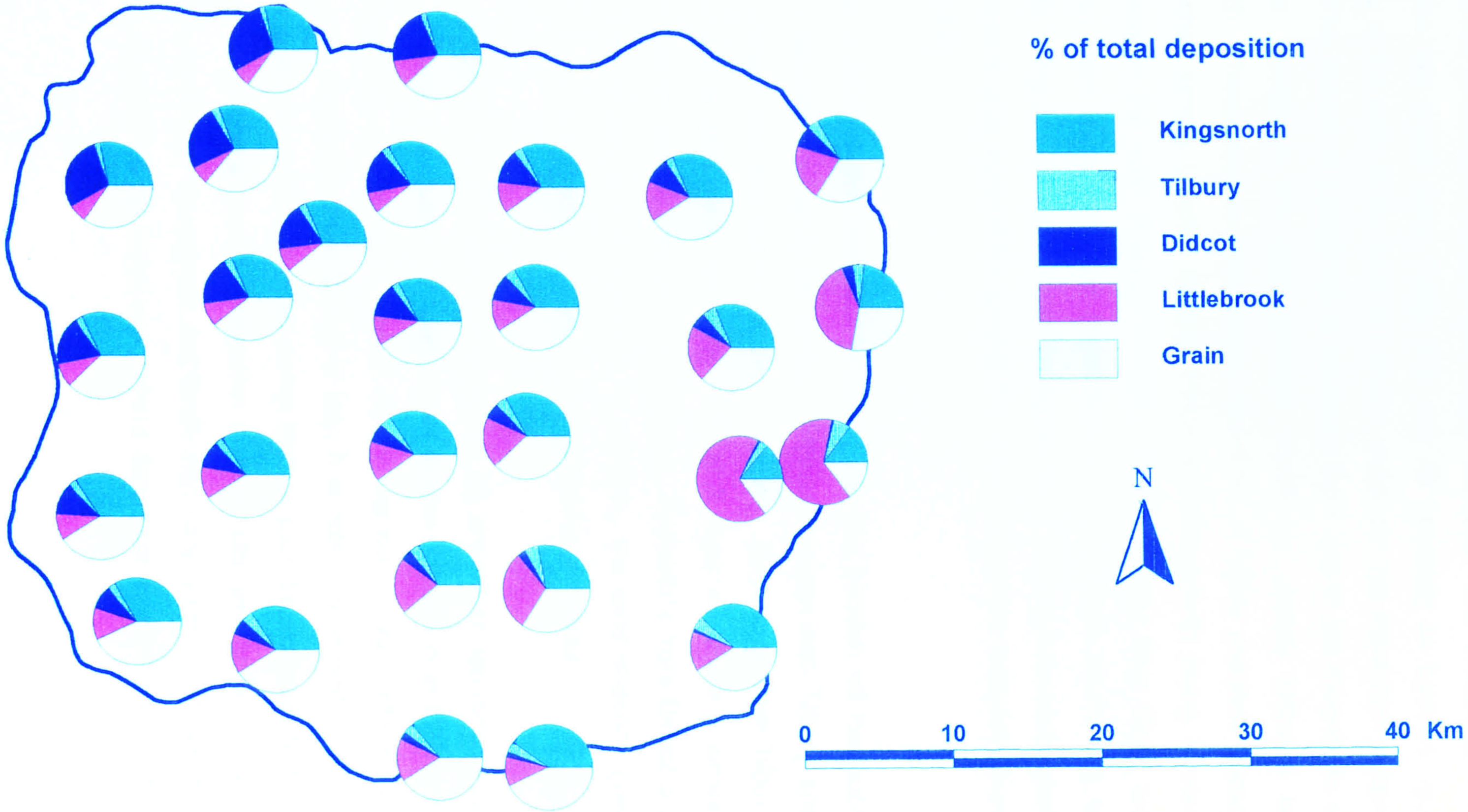

The greatest contribution to deposition is from Littlebrook which is the closest power station to London, situated just inside the M25. The emissions from this source are small (see Table 3.3) but its proximity to London, and especially to the sites in the east of London, produces the deposition pattern shown. The impact of Littlebrook is relatively local due to the magnitude of emissions. Grain is the next greatest contributor closely followed by Kingsnorth. These sources emit greater quantities of SCPs and their impact is felt further across London despite Grain and Kingsnorth being located further away in the east Thames corridor. The emissions from Grain are lower than from Kingsnorth but deposition is higher from Grain due to Kingsnorth being coal-fired and Grain being oil-fired. SCPs produced by coal-fired processes only account for around 5% of the particulate emissions (see Section 3.3.2).

Deposition of SCPs from Grain and Kingsnorth across London will be much lower than deposition close to the source. Deposition from both Tilbury and Didcot is uniform and low but for different reasons. Emissions from Tilbury are low and it is sufficiently far away so that it does not have a similar distribution pattern across London to Littlebrook. Emissions from Didcot are higher but the source is further away. In addition, the wind direction (see Figure 3.6) is less favourable for transport of pollutants to London.

The relative contributions at each site (Figure 3.14) show that deposition from Didcot forms almost a quarter of total power station deposition in the north-west whereas the contribution is almost zero in the south-east. This shows that, although deposition from Didcot is low, it is relatively important in the west of London compared with other power station sources. Deposition from Tilbury has roughly the same contribution to each site and makes up only around 3% of the total. Kingsnorth and Grain also have a similar contribution to each site except close to Littlebrook, where deposition is dominated by that source.

3.7.2 Relative contributions of individual non-power station Part A processes to total deposition

Spatially, the relative contribution from each non-power station Part A process source varies considerably (Figures 3.15 and 3.16). Each source, with the exception of London Underground Greenwich has localised high levels of deposition that fall off rapidly with a distance from source. The highest deposition across London from all sites is to WAND from London Underground Chelsea with levels just over 90 mg m^{-2} yr^{-1} (Figure 3.15). Citigen produces the next highest levels of deposition with the maximum deposition from this source to VICT (approximately 75 mg m^{-2} yr^{-1}). London Underground Greenwich does not appear to have a significant contribution to any lake or pond site in London, however this is due to its relatively low emissions of SCPs (see Table 3.4)

Relatively, the contribution from Part A processes to each lake or pond (Figure 3.16) is very complex. Kodak is the greatest source of SCPs in the north-west of London whereas deposition from London Underground Chelsea dominates the south and south-east of London. Heathrow and Ford have very localised impact and Citigen makes a strong contribution to central London and the north-east. Deposition to all sites from London Underground Greenwich is virtually negligible in comparison with deposition from any of the other sources. Deposition from each source corresponds well to the magnitude of emissions. Emissions from Ford are higher than the deposition levels suggest because it is a coal-fired process and deposition is only modelled for SCPs (see Section 3.3.2).

Figure 3.15: 10 micron sized SCPs deposited from individual Part A processes across London

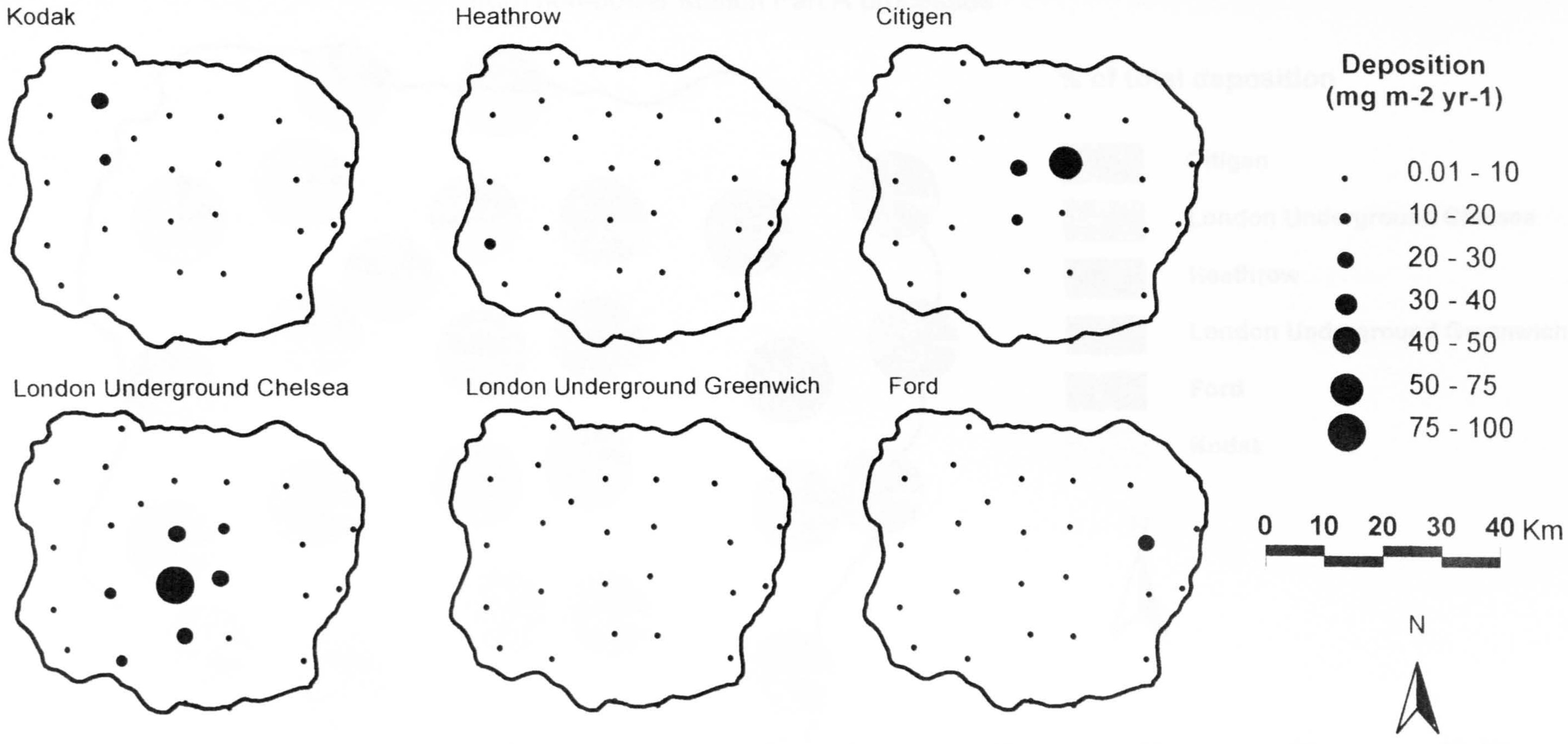

Figure 3.16: Relative deposition of SCPs with a diameter of 10 microns at each receptor site from non-power station Part A processes

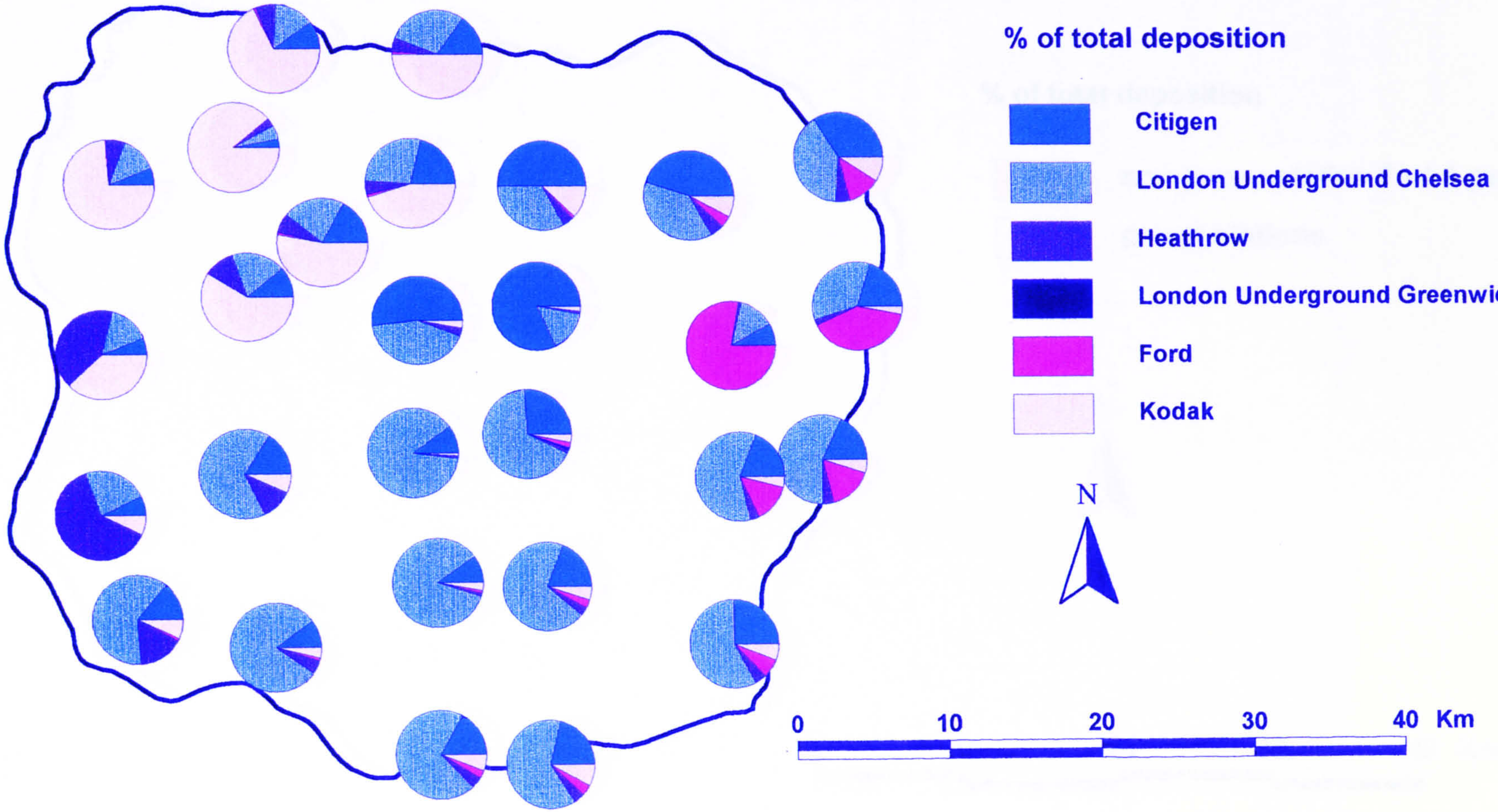

Figure 3.17: Relative deposition of SCPs with a diameter of 10 microns at each receptor site from non-power station Part A processes compared with power stations

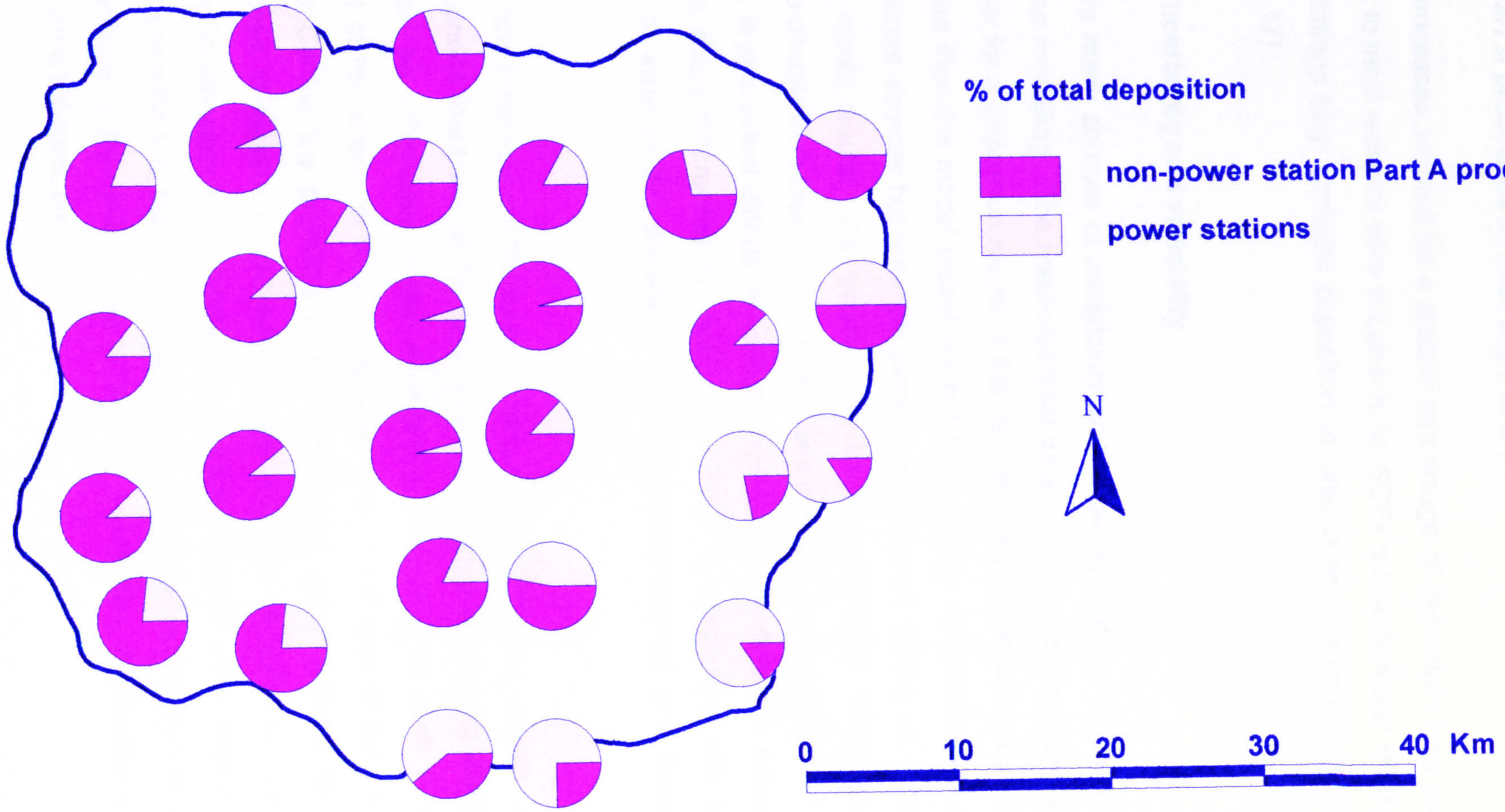

3.7.3 Relative contributions of power stations and non-power station Part A processes to total deposition

Part A processes account for a greater percentage of deposition than power stations, to most receptor sites in London, for SCPs with a diameter of 10 μm. Power stations only dominate deposition to sites in south-east London (see Figure 3.17).

3.8 Uncertainty and variability

There are many sources of uncertainty and variability that are inherent with dispersion modelling. The meteorological data are the most important input parameter for a dispersion model. If the data do not accurately represent the study area then the model output will not be accurate. Meteorological data from different sources but from the same meteorological station will produce different model results. For example the UK Meteorological Office data is available directly from them or via Trinity Consultants in the United States and the data is processed differently by both organisations before it is released. However, these differences are likely to be small in comparison with other sources of error in the dispersion modelling process (Hall and Spanton, 1999).

Gatwick and Heathrow are the next two closest meteorological stations to the City of London that have all the data necessary for modelling using ADMS 3. There will be differences in the meteorology measured at each location because of the effects of local topography and, in the case of the London Weather Centre, the presence of the urban heat island that will be less pronounced at Heathrow and will possibly not exist at Gatwick. London Weather Centre was chosen for this study in preference to either Heathrow or Gatwick because it is the most central of the three and was felt to be most representative of the meteorology of London. In addition, the meteorological records were the most complete.

The sensitivity of particulate deposition to variations in roughness length and minimum M-O length was considered by running scenarios with changes to

model parameters. Each of the scenarios is described in Table 3.9. To reduce processing time the model was simplified to compare deposition of oil combustion-derived SCPs with a diameter of 10 μm from Kingsnorth and Littlebrook power stations. All other model parameters were the same as for Base 1.

Table 3.9: Input data for analysis of dependence of deposition on roughness length and minimum Monin-Obukov length

Run number	Roughness length	Minimum Monin-Obukov Length
1	0.2	100m
2	0.2	30m
3	0.2	No minimum
4	0.5	No minimum
5	1.0	No minimum
6	1.5	No minimum

In general, deposition increases with increasing roughness length, particularly for sites close to source. The sites adjacent to Littlebrook power station show the greatest differences in deposition for changes in roughness length (Figure 3.18a). There are fewer differences for deposition to sites further from source for emissions from both Littlebrook and Kingsnorth (Figures 3.18a and 3.18b). Deposition from Kingsnorth is dependent on roughness length but the changes in the spatial deposition pattern will be relatively small. These results show that the influence of roughness length on deposition is most important for deposition close to source. Changing the minimum M-O length has virtually no effect on deposition of 10 μm sized particles (Figures 3.19a and 3.19b). The effect on other size classes is unknown.

Figure 3.18a:: Effect of changing roughness length on modelled deposition of SCPs from Littlebrook power station

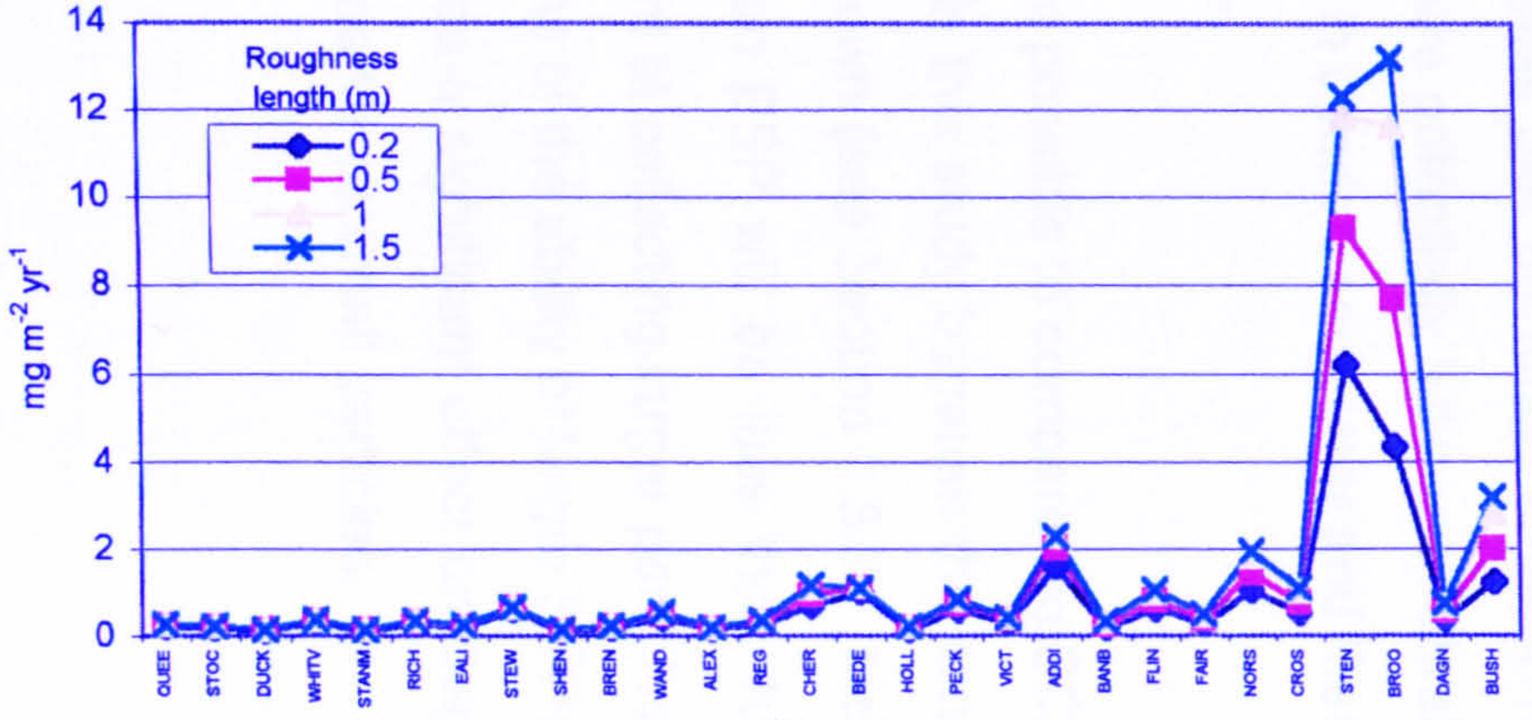

Figure 3.19a:: Effect of changing the minimum Monin-Obukov length on modelled deposition of SCPs from Littlebrook power station

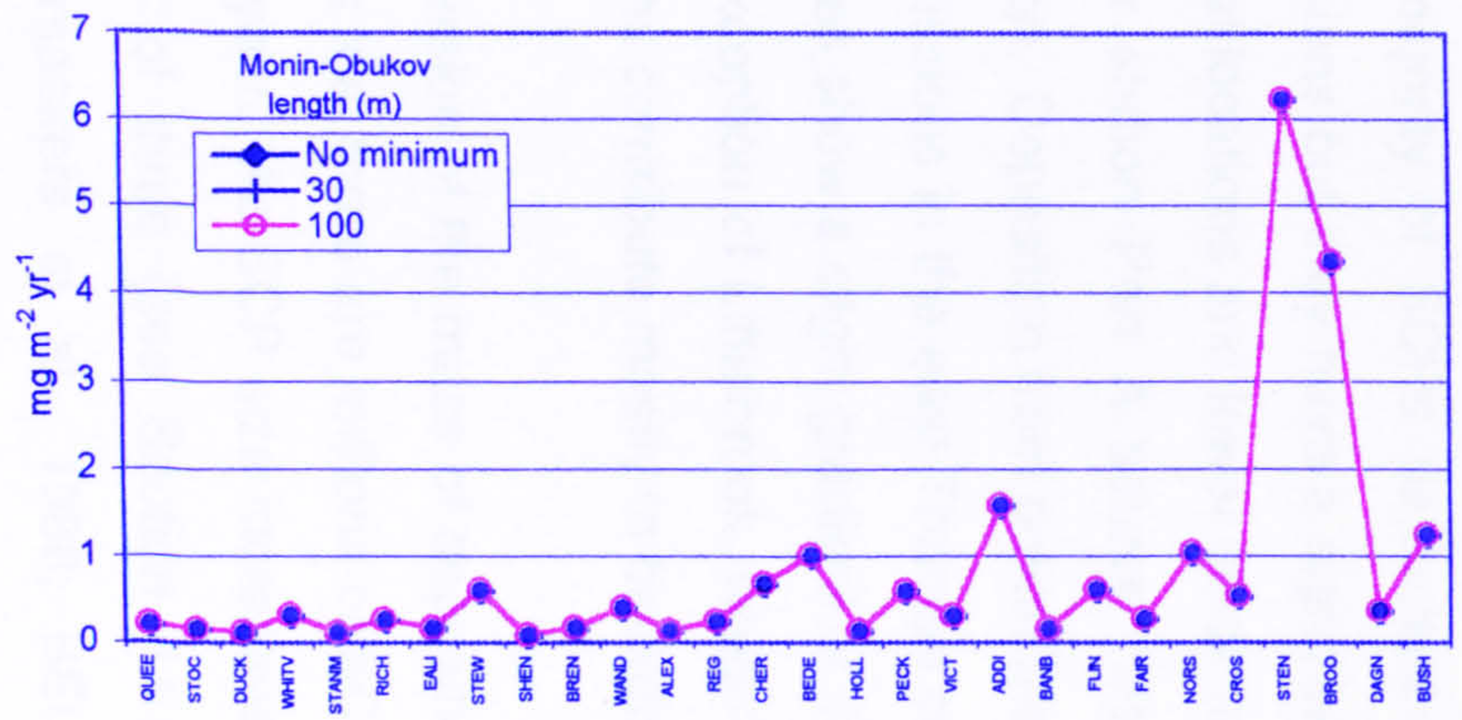

Figure 3.18b:: Effect of changing roughness length on modelled deposition of SCPs from Kingsnorth power station

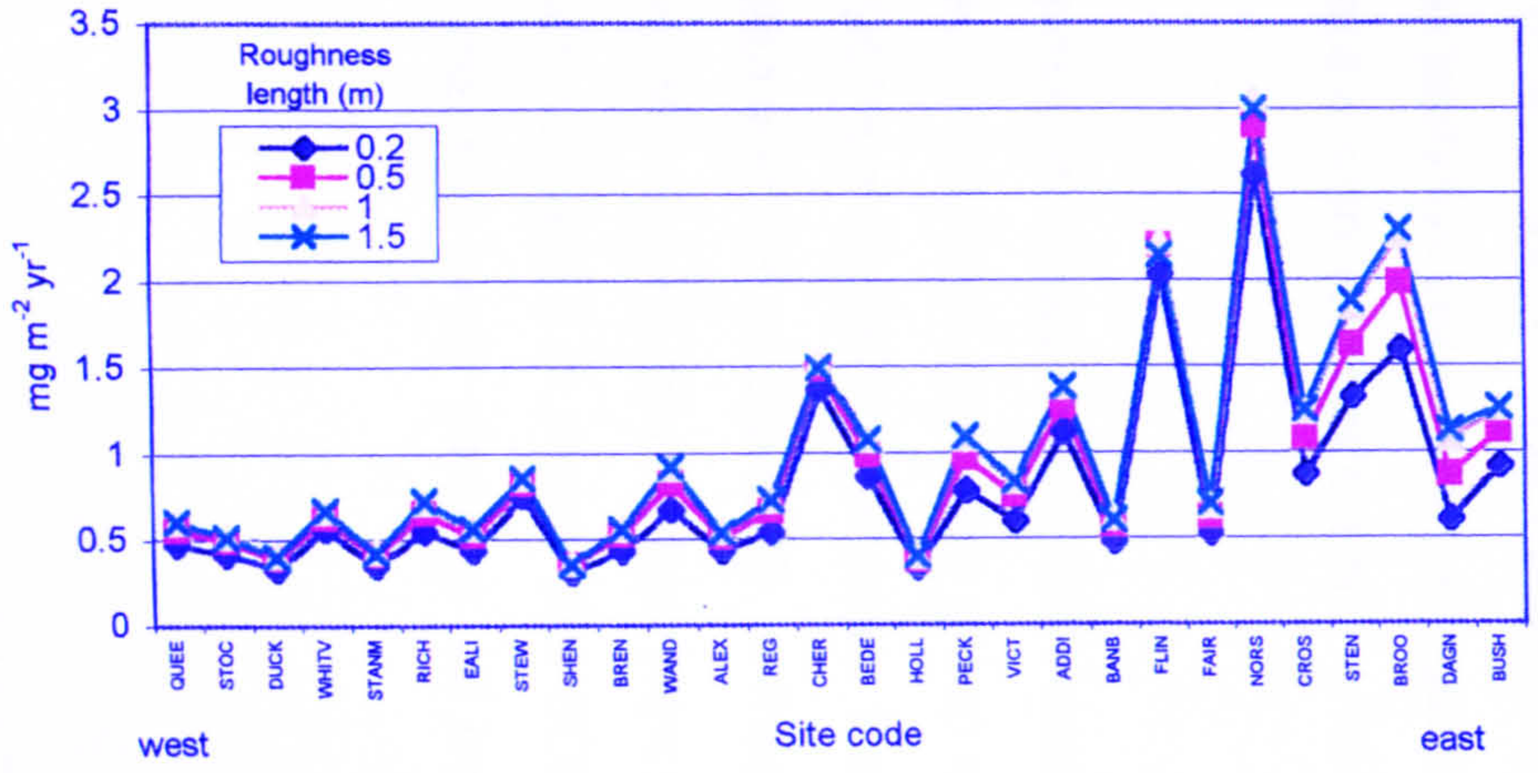

Figure 3.19b : Effect of changing the minimum Monin-Obukov length on modelled deposition of SCPs from Kingsnorth power station

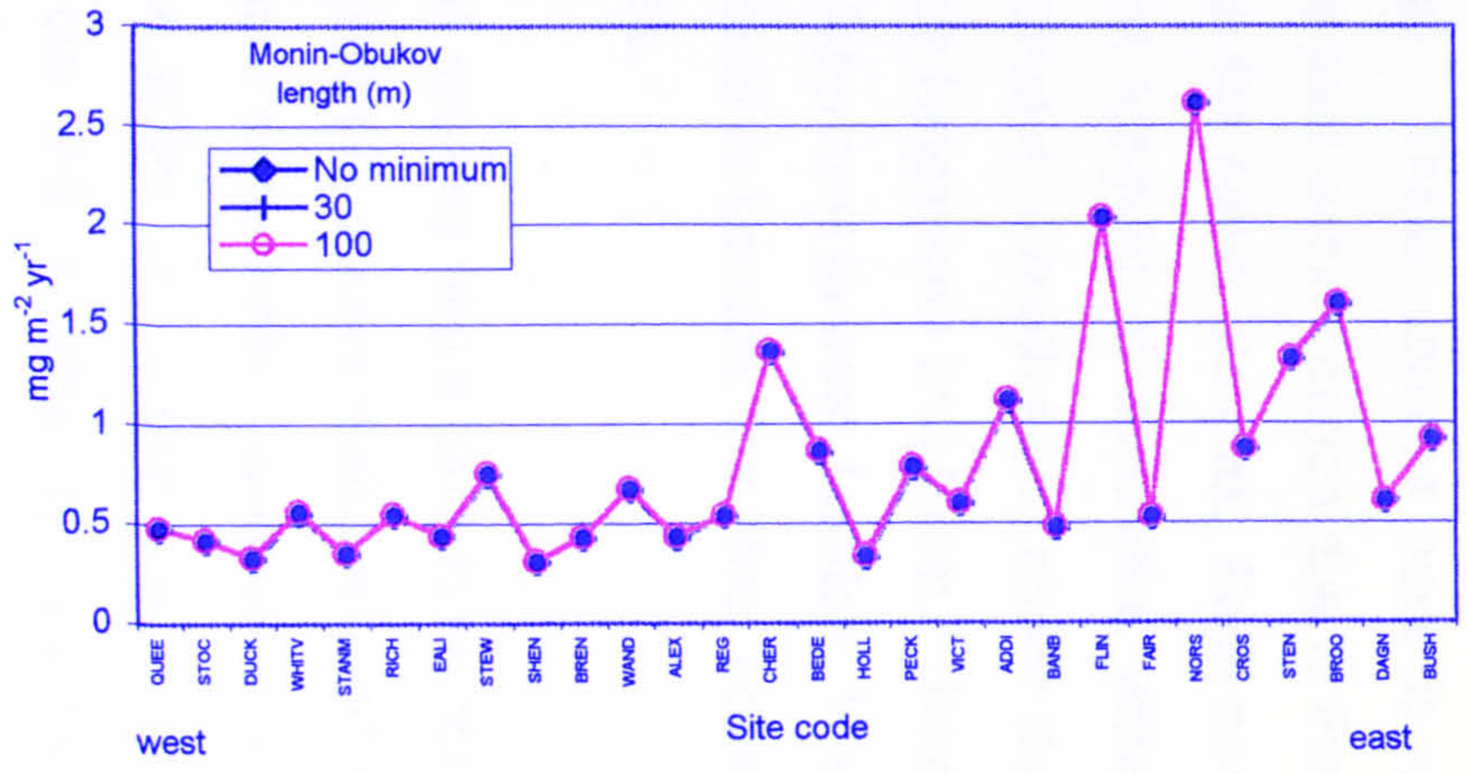

3.9 Discussion

The results show that non-power station Part A processes are responsible for the majority of SCPs deposited in London. These sources have lower emissions but they have a significant local impact within London due to their central locations and lower stack heights than the power stations. Each non-power station Part A source has a distinct footprint of deposition within London. Deposition from power stations dominates in south east London due to emissions in the east Thames corridor from Kingsnorth and Grain. These sources show a slight gradient of deposition from east to west. London. With the exception of Littlebrook, which is more local to London, the other power stations contribute mostly to background levels.

Conversion of the mass of deposition from all sources into a particle number shows that there are millions of SCPs deposited per square metre in London each year. As SCP size increases the number of particles increases to the power of three (see Section 3.6.5). Most SCPs are larger than 5 µm (Raeymaekers et al., 1988; BEI, 1991) but IAS emitted by coal-fired processes can be much smaller (McElroy, et al., 1982). This means that there are potentially billions of ultrafine fly ash particles deposited per square metre in London each year and these may have a significant effect on human health.

It is not possible to compare the SCP size deposition values directly with each other in this study because the actual quantity of SCPs in each size group is not known (see Section 3.3.3). Most of the SCPs emitted by processes that have an ESP will be less than 10 µm in diameter since the ESP is most efficient at collecting larger particles. However, the results can be interpreted in terms of the ability of larger SCPs to be dispersed and it is shown that SCP size has a significant effect on dispersion in that the larger particles will not travel as far as small particles.

3.9.1 Comparison of model results with SCP deposition data

All types of modelling require a number of assumptions to be made about sources, meteorology and the environment.

Sources

It was assumed that each source was operating under the same conditions continuously throughout the whole of the study. However, usually a process will operate in a number of different modes including start-up, shut-down, stand-by load, operation with back-up fuels and operation with pollution control equipment off-line in addition to normal (EA, 1998). Operating conditions will affect the release of different types and rates of pollution. The physical and chemical properties, and particle size of coal-derived fly ash are related to coal type, burner geometry, combustion parameters and particle abatement technology (Marcazzan et al., 1990). Oil and coal combustion particles emitted from a power station during conditions other than normal will have different morphologies and sizes (BEI, 1991).

The emissions from power stations respond to the demands for electricity from the National Grid and are not constant throughout the year. Since 1990, the National Grid has worked on a day-ahead bidding process that allows each power generator to bid to supply electricity for each half-hour of the day. The National Grid predicts the demand for each half-hour and then generates a pool market price that will be paid to the generating company. The National Grid then undertakes a technical assessment of its system and determines which power stations will be switched on. The system is very complex and the implication for this modelling study is that the power stations will not be switched on all the time. However, in this study it was necessary to assume that the emissions were constant and also that all the chimneys in the stack were in operation.

The problems with this approach occur during extreme meteorological events. Supposing that the power station was switched off during a temperature inversion, the typical conditions for pollution events, there would be an absence of a pollution plume and therefore no pollution episode. The model

does not know that the power station was not in operation and it produces a deposition based on that set of meteorological parameters. Alternatively, if the power station is only switched on during those conditions then the effect of this approach will exaggerate the real impact of the power station. Unfortunately it was not possible to get detailed information about the amount of time that each of the power stations or other Part A processes was operational. It is possible to use ADMS to model time-dependent emission for short periods but not for a whole year. The best results will be obtained when the model is run over short time scales with as much detailed information as possible. Even so, assumptions will always need to be made and must be acknowledged accordingly.

Meteorology

The effect of the urban heat island (Oke, 1987) on plume dispersion has not been considered in this study. Urban areas have a boundary layer with a specific climate caused by the presence of a city on the earth's surface. There is increased absorption of short-wave radiation due to the increased surface area and multiple reflection caused by urban canyon geometry. Absorption of and re-emission of energy by air pollutants causes an increase in long-wave radiation. The sensible heat storage capacity of materials such as concrete is larger and so it takes longer for concrete to warm up during the day than natural materials and longer for concrete to cool down at night. Therefore there will be heat storage in the urban area that will modify the diurnal climate. Energy production by buildings and road transport will also artificially heat the atmosphere. There is decreased evapotranspiration due to the waterproofing nature of construction materials

Buildings in the city are often tall, rigid and have sharp edges which results in large roughness lengths ranging from 1.5 to 10m. Wind speeds in the city will be lower than in the surrounding areas for equivalent heights due to increased drag and turbulence. This will cause a deeper zone of frictional influence that in turn causes the air to converge over the city. The build up of air is relieved by uplift and movement of air from the urban area to outside the city. One effect of this is that the urban area has its own pollution plume.

The difference between urban and rural temperatures is greatest at night and depends on wind speed and cloud cover. Sharan et al. (2000) modelled the effects of the urban heat island on the Bhopal gas accident and found a temperature gradient of six degrees between the rural and urban areas and that a low geostrophic wind results in the formation of a distinct heat island urban circulation. The intensity of the heat island is related to the size of the urban area and the difference in temperature between the urban and rural area is proportional to the log of the population (Oke, 1987). However, in Prague the urban heat island temperature difference increased through time (1922-1995) while the population in the centre of Prague decreased (Brazdil and Budikova, 1999). They suggested that the urban heat island intensification through time was caused by the expansion of the built up area and by population movement to the outer city.

The effect of the urban heat island is to create an urban boundary layer that is higher than that of the surrounding rural area. Plumes emitted in rural areas will impinge on this boundary layer and, depending on its magnitude, will be modified in some way. For example, fumigation may occur when a pollution plume impacts on a boundary layer when there are clear skies and light winds. The power stations in the east Thames corridor and Didcot are in rural areas and, dependent on the meteorology, plumes from these sources may fumigate when they reach London, thus causing particles to be deposited and for there to be a greater pollution impact than the model suggests. The urban heat island will have a complex spatial structure that is modified by the spatial pattern of different surfaces and topographies within the urban area. The presence of cooler areas that are more natural such as open spaces and lakes, will cause temperature troughs in the urban heat island. In London the presence of the Thames is likely to provide a low temperature barrier between north and south London. This may provide a favourable route for pollution dispersion from power stations in the east Thames corridor.

In the summer the urban heat island is formed through increased absorption of short wave radiation and increased sensible heat storage whereas in winter the anthropogenic heat source is the dominant process for heating the

atmosphere. Therefore the effect of the heat island is likely to be important at all times during the year.

The impact of the urban heat island on modelled deposition from the power stations around London is not clear. It is not possible to incorporate it fully as a factor that affects dispersion in ADMS, especially since the meteorological data chosen are representative of the within-urban heat island climate, but not the climate outside the city. Emissions from the sources within London will be more accurately modelled by ADMS 3 because the meteorological conditions are more accurately represented.

3.9.2 Effects of the local environment

Sensitivity of dispersion and deposition to the characteristics of the receptor points has not been addressed. The urban canopy layer and local terrain surrounding the lake and pond receptor points will affect localised dispersion patterns because of the increased amount of turbulence. The complex patterns of dispersion in street canyons has been studied (e.g. Scaperdas and Coalville, 1999) but is not likely to affect deposition to lakes and ponds, which are more likely to be situated within the urban area in open spaces. As mentioned above (Section 3.9.1), the presence of lakes and open spaces can cause temperature troughs in the urban heat island which would also affect atmospheric turbulence. The influence of the local environment on deposition of SCPs is discussed in Chapter 4.

CHAPTER 4: PARTICLE SIZE DISTRIBUTION OF SCPS IN SURFACE SEDIMENTS OF LAKES AND PONDS IN LONDON

4.1 Introduction

Profiles of SCPs concentrations in lake sediments have been shown to reflect fossil-fuel burning history on a regional scale (e.g. Griffin and Goldberg, 1981, Renberg and Wik, 1984, Rose, 1995; Odgaard, 1993). Comparison of historical records of high temperature fossil-fuel combustion and SCP profiles has enabled SCP counting to be developed as a dating method for sediments deposited after the Industrial Revolution (e.g. Renberg and Wik, 1984; Rose, 1995).

The presence of SCPs in sediments from remote lakes on Svalbard and remote mountain lakes across Europe and Asia, i.e. where there are no local sources, implies that there is a background level of SCPs across the northern hemisphere (Rose, 1995). Distributions of SCPs in surface sediments have been used to assess the contemporary spatial impact of fossil-fuel derived pollution across Europe (Wik and Natkanski, 1990; Rose et al., 1998c, 1999a) and across the UK (Rose and Harlock, 1998). On a more regional scale, surface sediments were taken from sixty-six lakes in south-western Sweden around Gothenberg (Renberg and Wik, 1985). Lakes close to Gothenberg contained more than 200,000 'soot' spheres per gram of hydrogen peroxide soluble dry sediment whereas lakes further away (50-100 km distant) contained just 10,000-20,000 spheres. Regional and local emissions of SCPs are reflected in the sediments of Lake Baikal (Rose et al., 1998b) where the spatial distribution of SCPs in the upper sediments is related to the locations of industry around the lake.

SCP concentration data in London are limited to a few sites, Hampstead Heath Men's Bathing Pond (e.g. Rose, 1996) and Banbury Reservoir (BANB) (Yang, 2000). Hampstead Heath was incorporated into a spatial study of SCPs in the UK but there has not been a similar study that focuses just on London.

SCP concentration in surface sediments is dependent on the internal lake and pond processes that affect the sediment together with the input to the lake or pond from atmospheric deposition. SCPs are chemically robust and do not suffer from chemical remobilisation, which can be a problem when using sediment chemistry to determine pollution impacts. In addition there are background levels of chemical pollutants whereas SCPs fall to a pre-industrial revolution background of zero. However, SCPs are still vulnerable to mechanical processes such as bioturbation or disturbance (e.g. through dredging or wind stress).

This study focuses on twenty-eight lakes and ponds to assess the spatial footprint of high-temperature derived fossil-fuel combustion. All the lakes and ponds are in London, within the boundary of the M25 motorway. The results of dispersion modelling (Chapter 3) predict a complex deposition pattern from high-temperature fossil-fuel combustion sources. The hypothesis that modelled deposition of SCPs will decrease across London from east to west was disproved for all sources in combination and non-power station Part A processes were highlighted as the most significant contribution to SCP deposition in London. This Chapter further tests the hypothesis against actual concentrations of SCPs in sediments and, additionally, compares actual concentration to predicted deposition described in Chapter 3. Statistical analyses are carried out to extract the main variables that affect the concentration of SCPs deposited.

A second aim of this Chapter is to examine the SCP size distribution at each lake or pond and then to compare it with predicted deposition of SCP sizes. The particle size distribution of SCPs in a sediment sample will be independent of SCP concentration and within-site processes. Instead, the proximity of the source to the lake or pond and the characteristics of both the source and emission (see Chapter 3) will affect the size of SCPs that are physically able to reach the lake or pond. For example, if the profile is dominated by large particles then the sources of the particles will be local whereas, if the distribution of particles is dominated by finer particles then the most significant sources are likely to be further away.

4.2 Spatial distribution of SCP size fractions in lakes and ponds in London

SCP concentrations and upper and lower 90% confidence limits from twenty-eight sites in London are listed in Table 4.1. The spatial distribution of these data is shown Figure 4.1. The highest concentrations are found in the sediments of REG and VICT (152,578 gDM^{-1} and 152,374 gDM^{-1} respectively) (Table 4.1) in central London. The SCP concentrations at VICT and REG are nearly double the next highest SCP concentrations at other localised hotspots found in north-west London at STANM (81,707 gDM^{-1}), in north London at HOLL (65,508 gDM^{-1}) and in the south-west at WHITV (49,916 gDM^{-1}).

Figure 4.1: Spatial distribution of total SCPs in the surface sediments of twenty-seven lakes and ponds across London

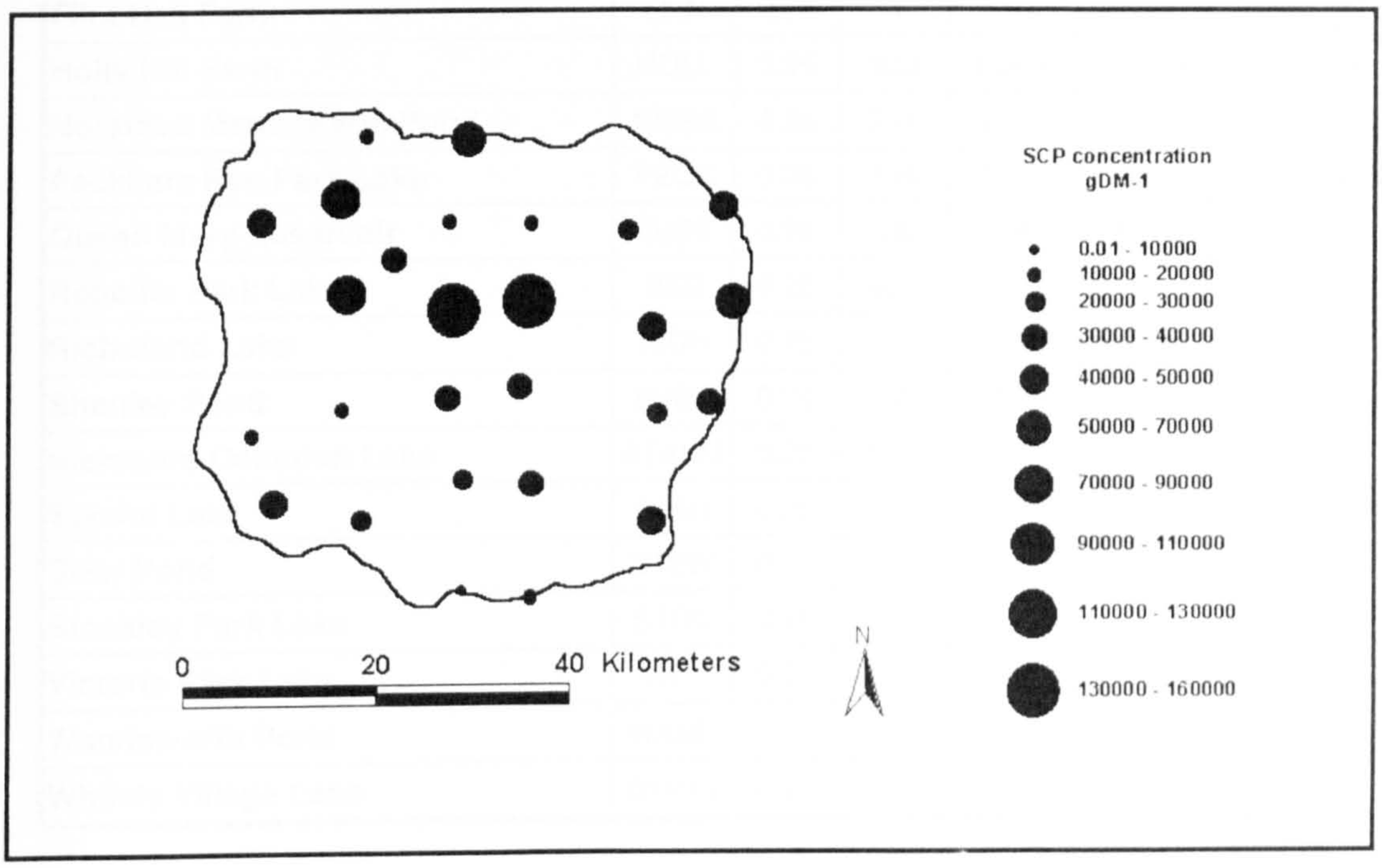

Table 4.1: Concentration of SCPs in surface sediments from twenty-eight lakes and ponds in London

Name	Core	Mean depth	Count	Conc^{n}	Upper 90% conf.	Lower 90% conf.
Addiscombe Scouts Lake	ADDI	0.25	215	38057	40601	35514
Alexandra Park Conservation Pond	ALEX	0.25	62	12479	14033	10926
Banbury Reservoir	BANB	0.25	97	18778	20646	16910
Grange Park Lake	BEDE	0.25	61	25212	28376	22049
Brent Reservoir	BREN	0.25	76	31688	35250	28126
Brooklands Lake	BROO	0.25	244	39334	41802	36867
Bush Farm	BUSH	0.25	332	54057	56965	51150
Gatton Bottom Lake	CHER	0.25	12	4592	5891	3292
Crosness Sewage Works Lake	CROS	0.25	187	40557	43464	37651
Dagnam Park Lake	DAGN	0.25	240	43085	45810	40359
Riverside Club, Duck Lane	DUCK	0.25	321	41630	43907	39353
Ealing Pond	EALI	0.25	350	78764	82889	74638
Fairlop Waters	FAIR	0.25	159	25922	27937	23907
Flint Hall Farm	FLIN	0.25	46	8532	9765	7299
Holly Hill Farm	HOLL	0.25	330	65508	69036	61979
Norstead Manor Farm Pond	NORS	0.25	331	43012	45328	40695
Peckham Rye Park Lake	PECK	0.25	194	32923	35239	30607
Queen Mary Reservoir	QUEE	0.25	28	3540	4195	2884
Regents Park Lake	REG	0.25	632	152578	158525	146629
Richmond Lake	RICH	0.25	74	18285	20368	16202
Shenley Pond	SHEN	0.25	62	17797	20012	15582
Stanmore Common Lake	STANM	0.25	585	81707	85018	78396
Stenhil Lake	STEN	0.25	143	22979	24862	21096
Stew Pond	STEW	0.25	96	20617	22679	18555
Stockley Park Lake	STOC	0.25	0	0	0	0
Victoria Park Lake	VICT	0.25	618	152374	158376	146372
Wandsworth Pond	WAND	0.25	283	31922	33781	30062
Whitely Village Lake	WHITV	0.25	309	49916	52699	47133

Figure 4.2a-l: Spatial distribution of SCP size fractions in the surface sediments of twenty-seven lakes and ponds across London

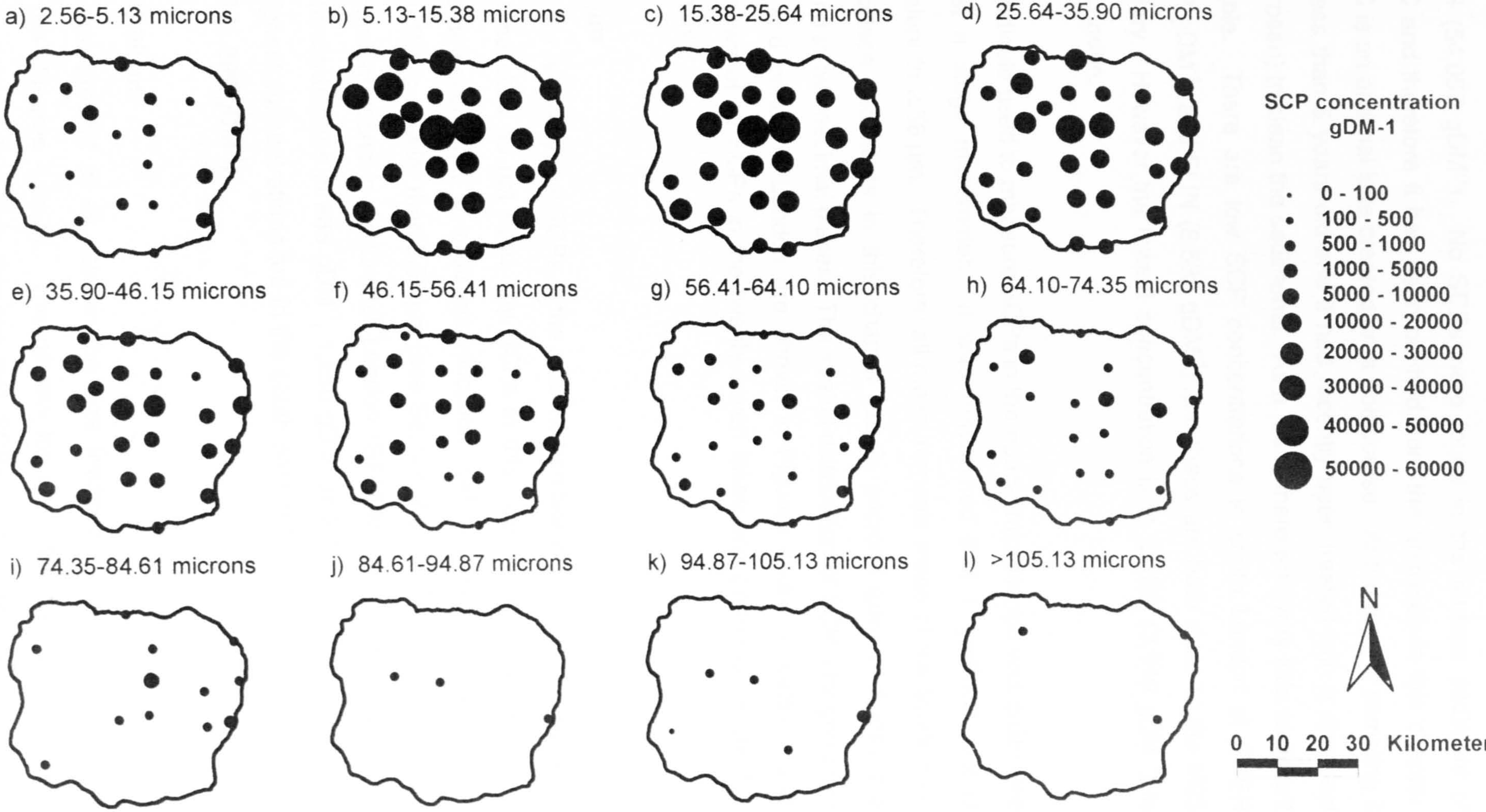

Concentrations are elevated along the eastern edge of the M25, especially at BUSH (54,057 gDM^{-1}). No SCPs were found in the surface sediment of STOC and therefore it has been omitted from the analyses in this chapter. STOC is an artificial lake created on a golf course. At the time of sampling it was less than 5 years old and it had recently been treated with a chemical (Clearosan) to clean the sediments. As a result there was very little sediment available. There are low SCP concentrations in south London at CHER (4,592 gDM^{-1}) and FLIN (8,532 gDM^{-1}) and these are both close to the M25 boundary. However the lowest concentration is in QUEE (3,540 gDM^{-1}) in west London.

The graticule used to measure SCPs in the optical microscope was calibrated against a stage micrometer. It was determined that 1 graticule unit is equivalent to 2.56 µm. Therefore, all measurements made of the SCPs from the surface sediments in this chapter are in microns (µm) and they are reported to two decimal places. The spatial distribution of SCP size groups in lakes and ponds in London are shown in Figures 4.2a-l. A detailed size breakdown of all SCPs in the twenty-seven lakes and ponds is included in Appendix 2.

<5.13 µm

There are relatively few SCPs in the size fraction below 5.13 µm (Figure 4.2a) and some sites do not have any SCPs in this size range. 2.56 µm is the visible detection limit at x400 magnification and it is difficult to accurately identify SCPs smaller than 2.56 µm (see Section 2.3.4). There is a cluster of high concentrations in north-west London (STANM, BREN and EALI have SCP concentrations of 838 gDM^{-1}, 1,250 $gDM^{-1}$and 675 gDM^{-1} respectively). The highest concentrations are in the south-east at STEN (1,285 gDM^{-1}) and NORS (1,299 gDM^{-1}).

5.13-35.90 µm

SCPs are present at all sites in the size fractions between 5.13 µm and 35.90 µm (Figures 4.2e-h). The pattern for each size range shows less spatial variation therefore showing that SCPs in this size range are well

distributed across London. The sites in the centre of London have the highest concentrations of SCPs (e.g. REG contains 53,112 gDM^{-1} and VICT contains 43,888 gDM^{-1} in the fraction 5.13-15.38 µm). The cluster of sites in north-west London that had high concentrations of SCPs in the 0-5.13 µm fraction, also have high concentrations of SCPs in the range 5.13-35.90 µm, in comparison with most of the other sites across London.

35.90-86.61 µm

There is a gradual transition in the distribution pattern between 35.90 µm and 86.61 µm. The pattern of distribution for SCP sizes 35.90 µm to 46.15 µm is similar to the lower fraction (25.6-35.90 µm) except that SCPs are absent at CHER. Between 35.90 µm and 86.61 µm the number of sites without SCPs increases as the size fraction increases. SCPs larger than 74.35 µm are present in only a few sites and at very low concentrations. The maximum concentration in the fraction 35.90-46.15 µm is at VICT (18,245 gDM^{-1}) and this site has the highest concentrations for all SCP sizes up to the fraction 74.35-84.61 µm (1,479 gDM^{-1}). As SCP size increases the higher concentrations are focussed in the east of London and appear to follow the course of the Thames (see Figure 3.4). Although one exception in the 64.10-74.35 µm fraction is STANM in north-west London which has a high concentration of SCPs (1,117 gDM^{-1}), in comparison with 1,084 gDM^{-1} at CROS and 1,725 gDM^{-1} at VICT along the Thames Corridor.

>86.61 µm

SCPs larger than 86.61 µm are present in the sediments at only a few sites (Figures 4.2j-l). In the 86.61-94.87 µm fraction there are only three sites (EALI, REG and BROO) which all have low concentrations of SCPs (225 gDM^{-1}, 484 gDM^{-1} and 483 gDM^{-1} respectively). These three sites lie along the Thames Corridor and also have SCPs in the 94.87-105.13 µm fraction. However, there are two other sites (QUEE and ADDI) that have SCPs of this size but do not lie along the Thames. The largest size fraction includes all SCPs larger than 105.13 up to a maximum of 125.64 µm, the largest SCP

was found at STEN in the size fraction 123.08-125.64 μm. There are only small numbers of SCPs in the largest size fractions.

4.3 Particle size distribution patterns for each of twenty-seven lakes and ponds across London

The particle size distributions of SCPs for each site are shown in Figures 4.3.a-aa. In total 6507 particles were counted and sized. The number of particles counted on each slide (n) is displayed on each graph. Each graph shows the number of particles counted in each size fraction (histogram) and, so that the sites can be compared with each other, the number in each size fraction has been converted to a percentage of the total (red line). The blue line represents the moving average of the percentage data.

The moving average smoothes fluctuations in the data, thus aiding in the interpretation of profiles that are highly variable. The moving average is a sequence of averages calculated from parts of the data series. In this case, a two point moving average is used which is calculated by taking the average of each data point and the preceding data point. In some of the size classes the number of SCPs present is small and, therefore, the effects of any size misclassification will be large.

The summary statistics for each site are shown in Tables 4.3a-c. Each particle was measured against the graticule and put into a size range. The upper size limit was used as the SCP size (see Chapter 2 for details) and the mid-point of the size class was used for further statistical calculations. For example, a SCP that lies between 4 and 5 units (10.24 μm and 12.80 μm in size) is allocated to the 12.80 μm size class but for calculating summary statistics the mid-point of 11.52 μm is used. With the exceptions of CHER and SHEN, all distributions display positive kurtosis; i.e. the size distribution is relatively peaked compared to a normal distribution. Many sites have a polymodal distribution profile and the shape of the profile appears to consist of a number of separate distributions. The particle size distribution profiles and statistics for each of the individual sites are described below.

Figures 4.3a-d: Size distribution of SCPs in the surface sediments of twenty-seven lakes and ponds in London

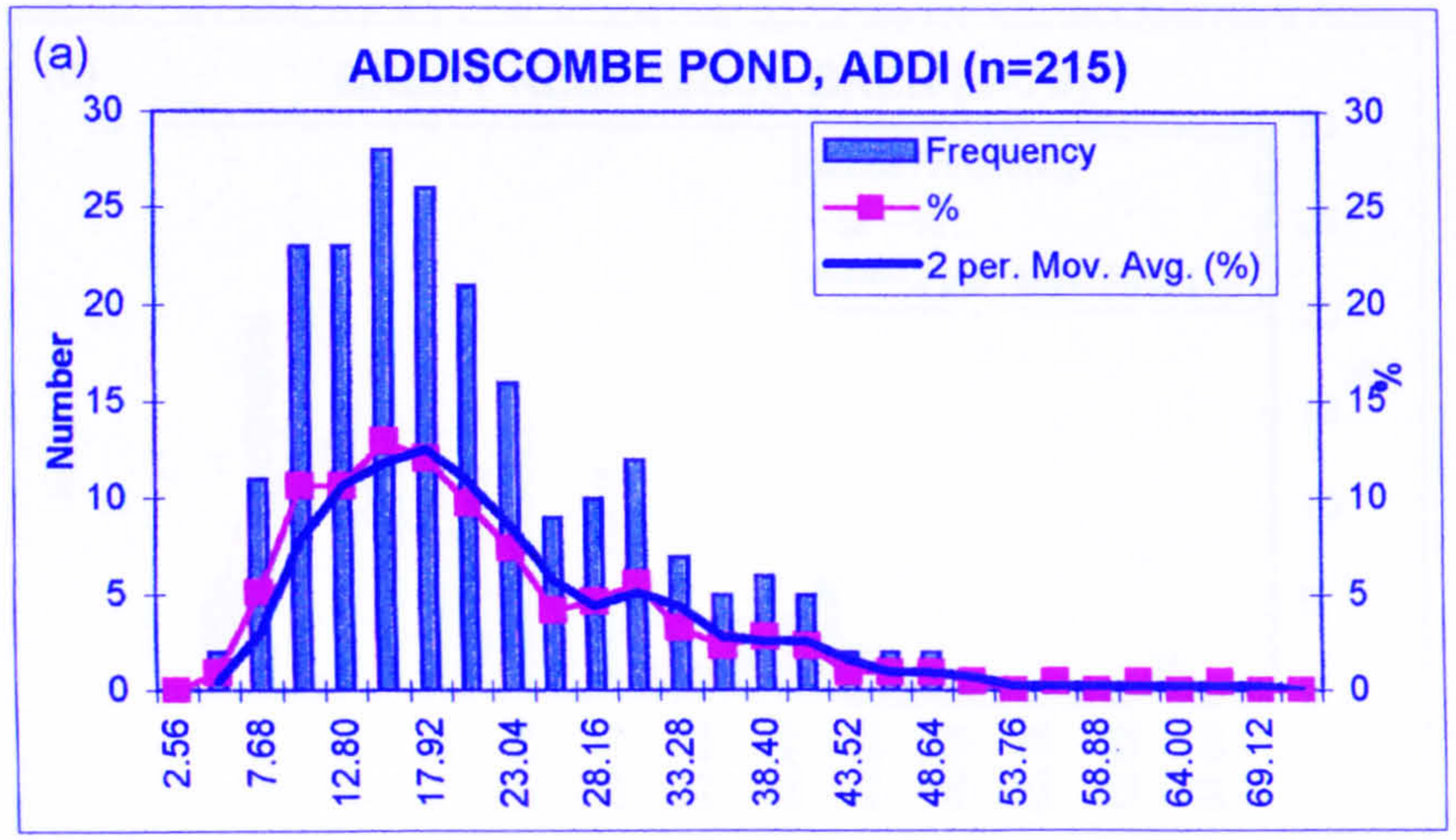

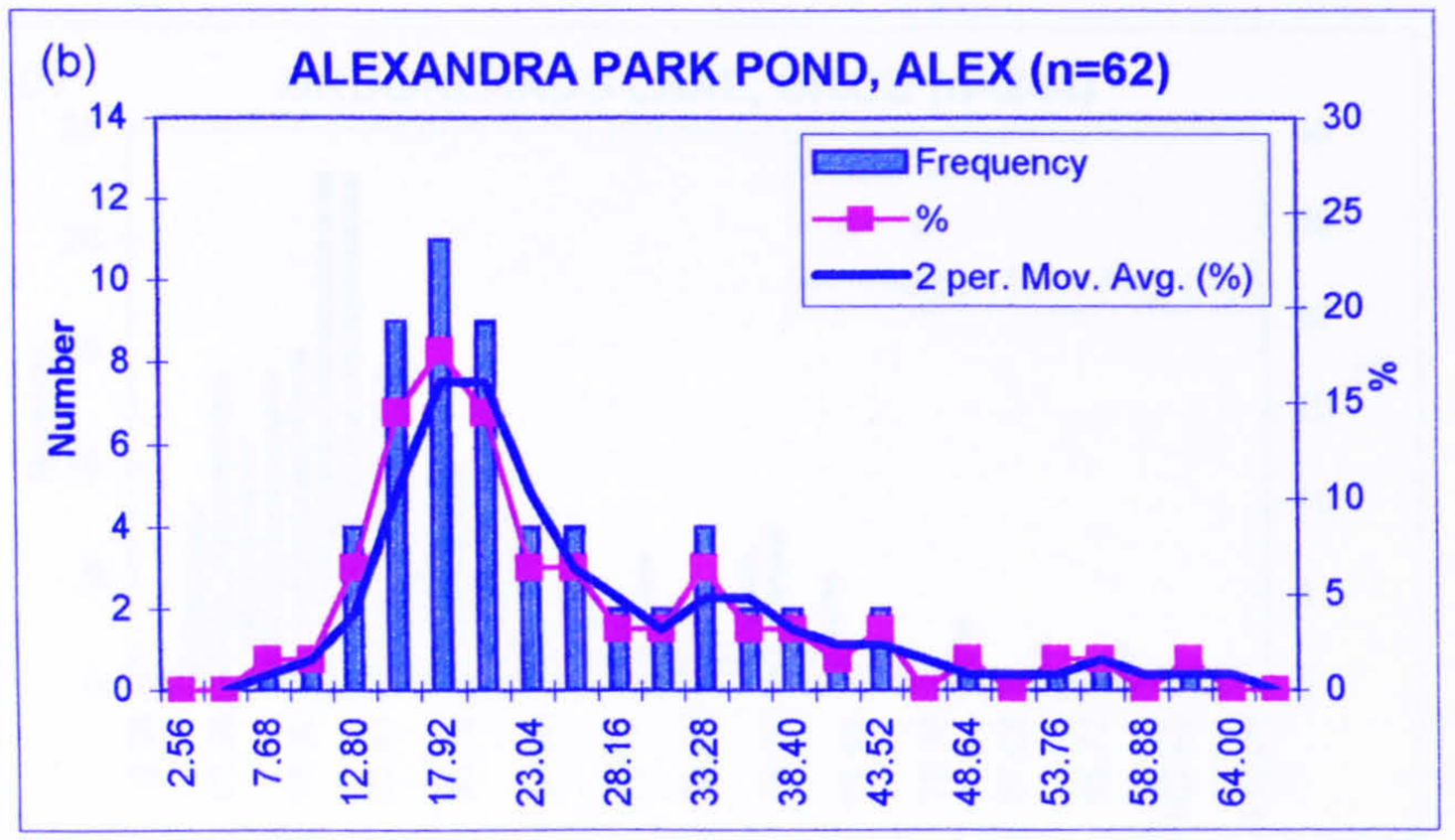

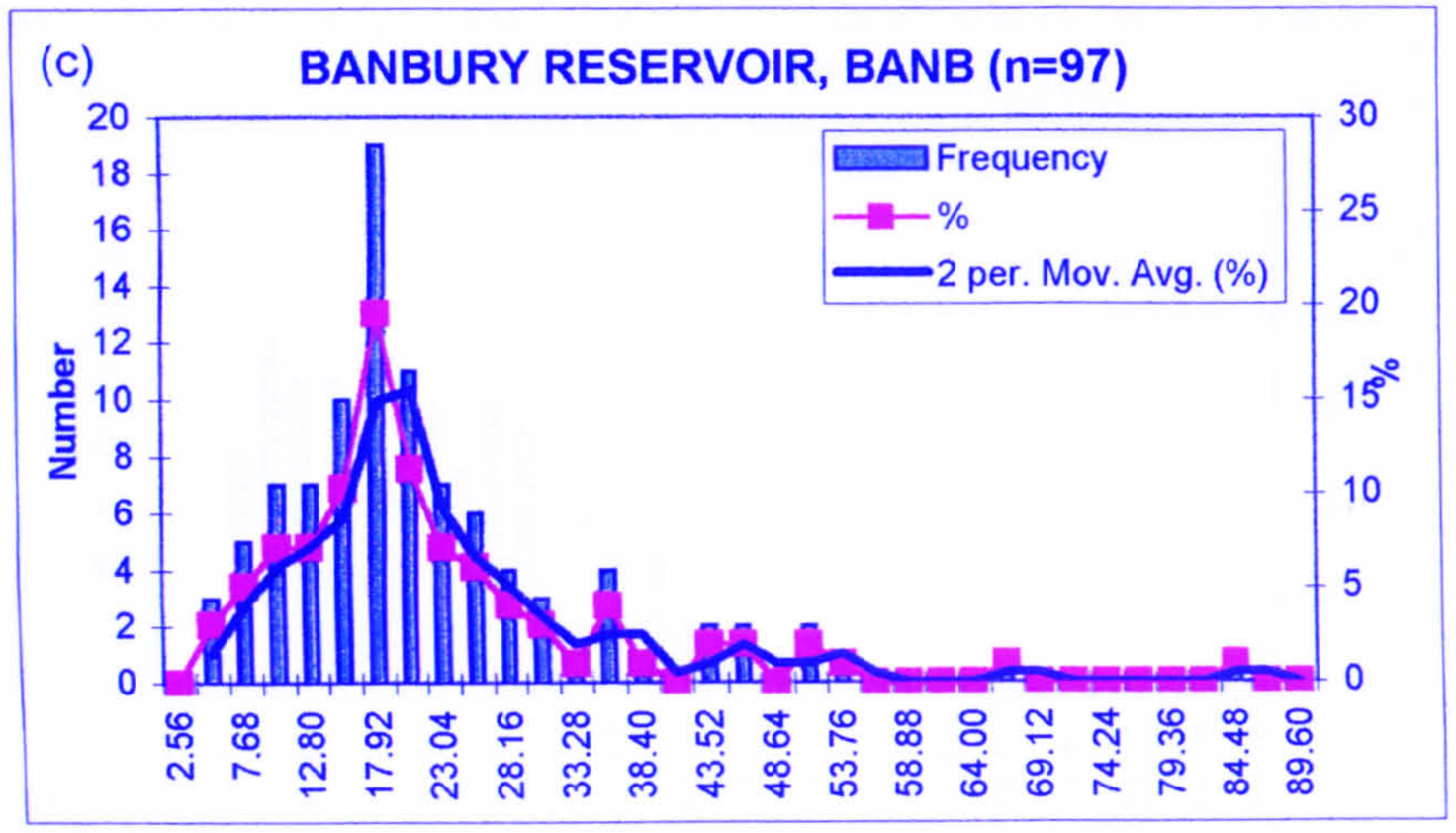

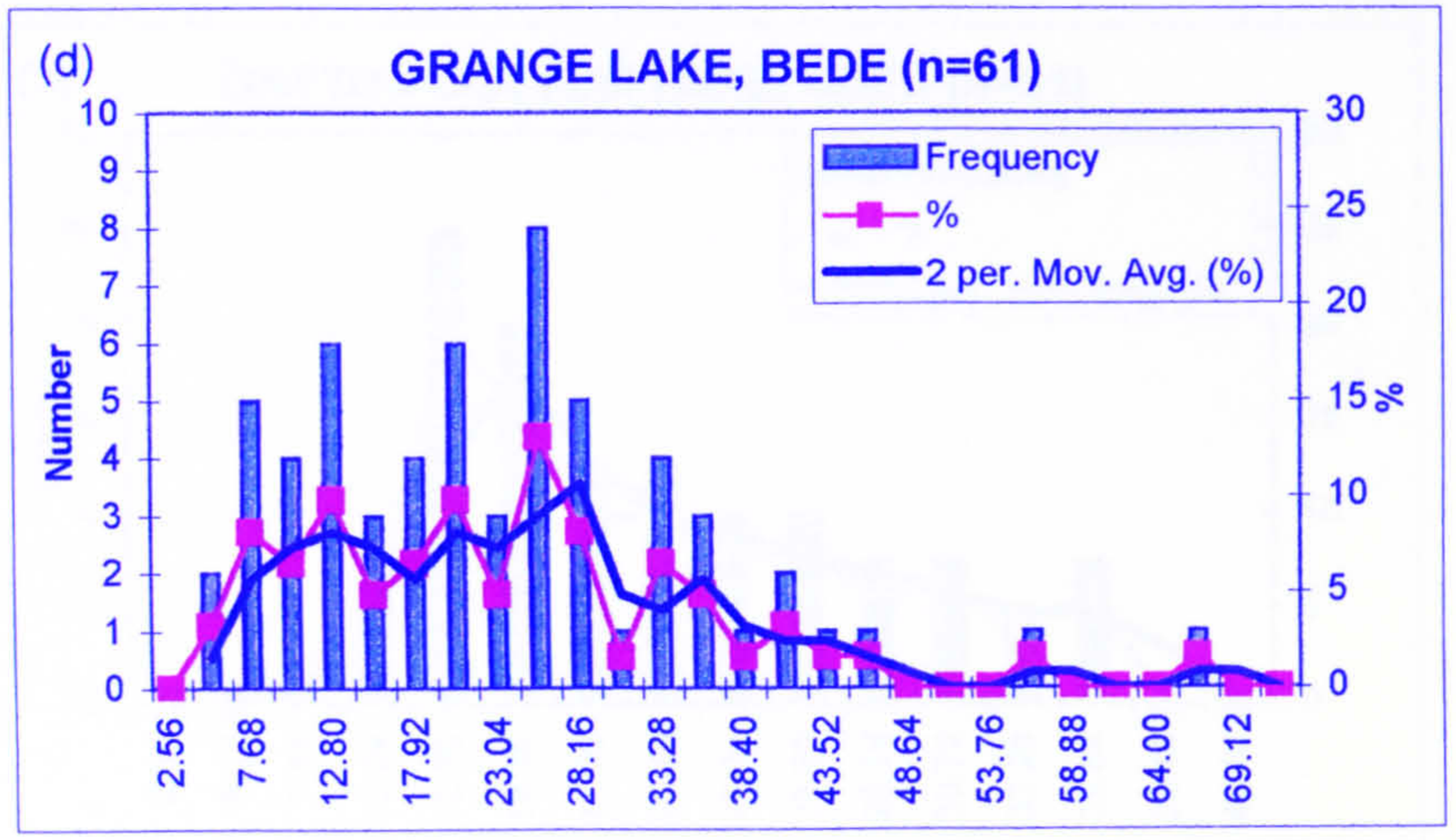

Figures 4.3e-h: Size distribution of SCPs in the surface sediments of twenty-seven lakes and ponds in London

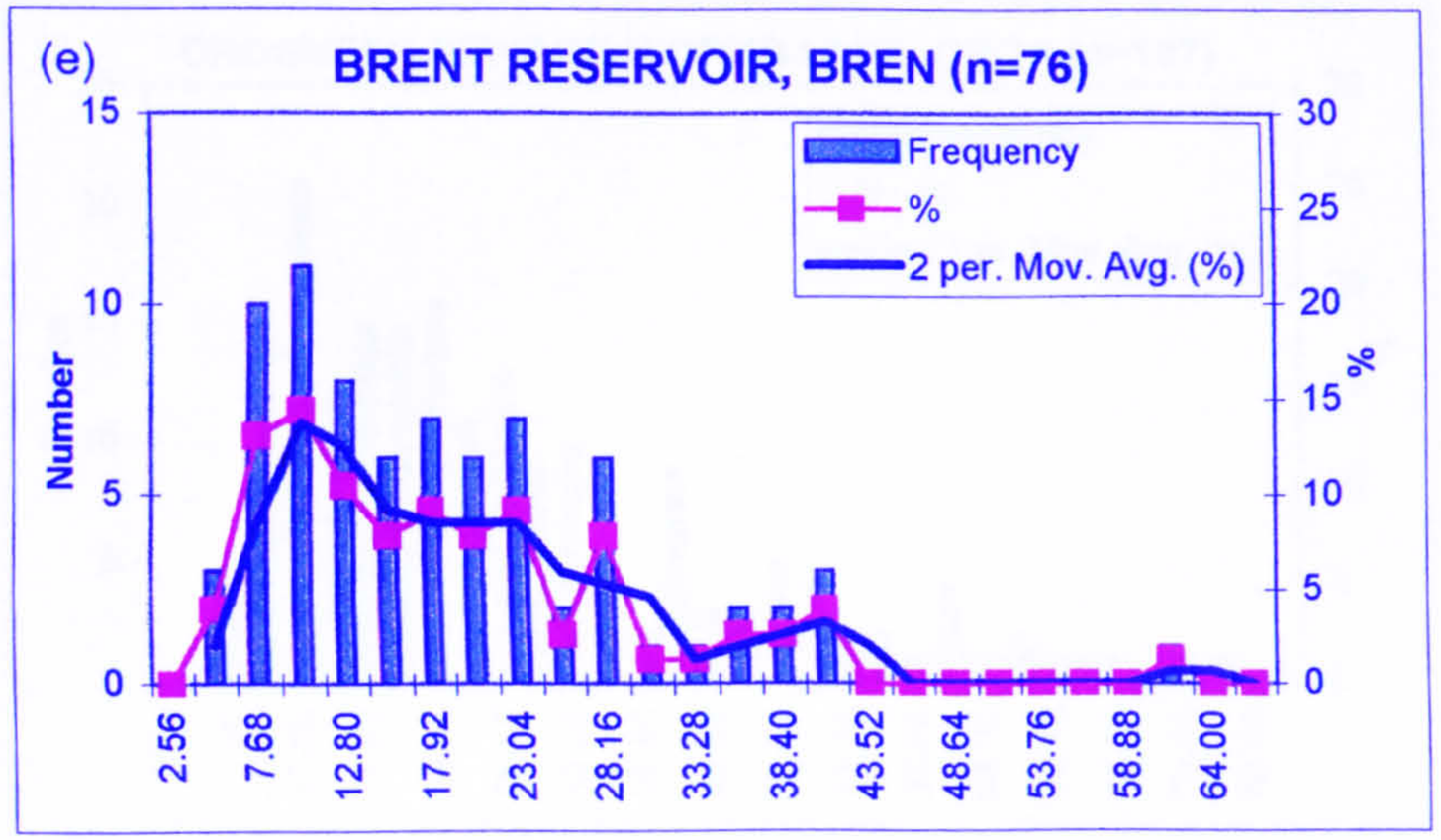

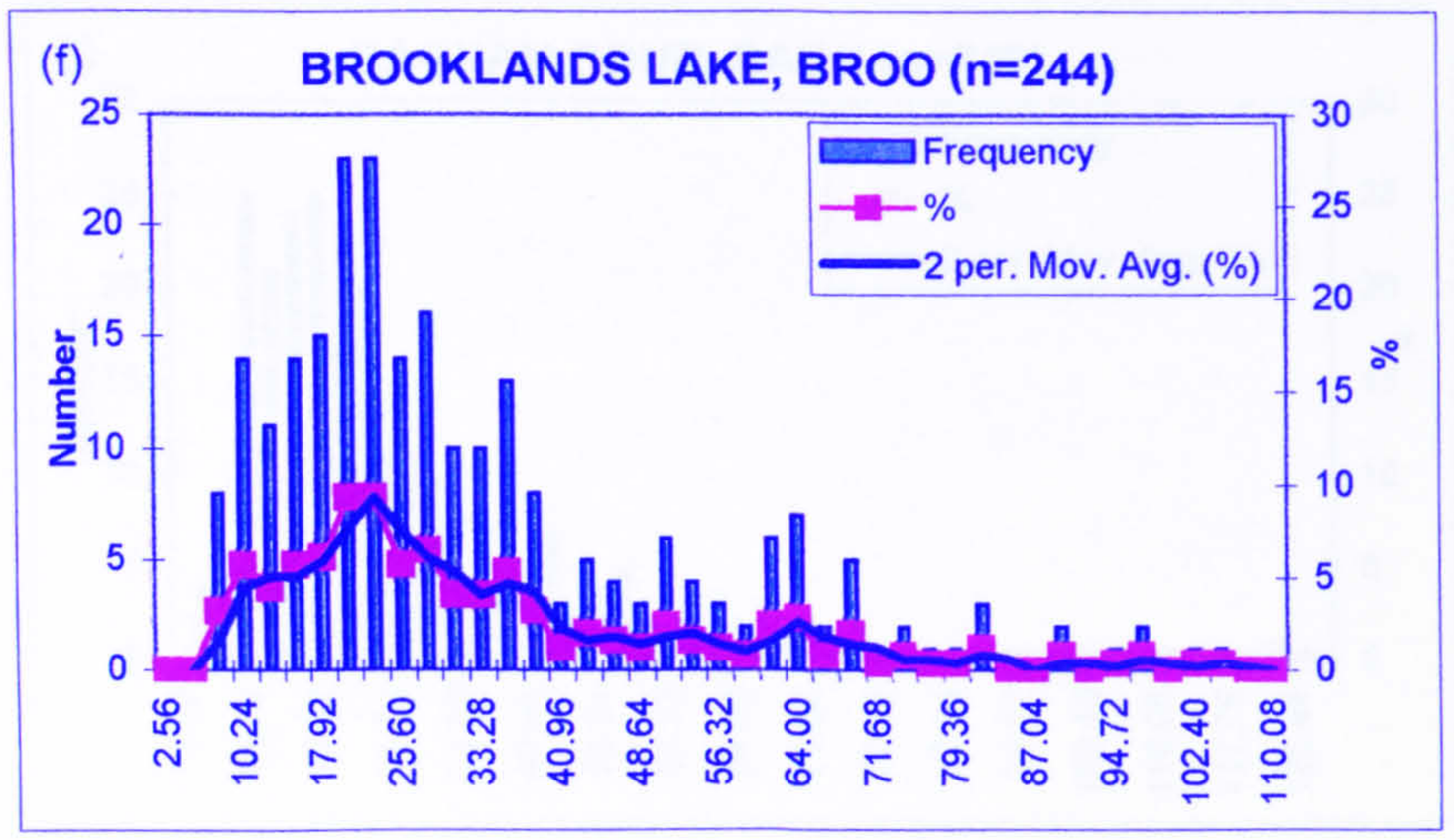

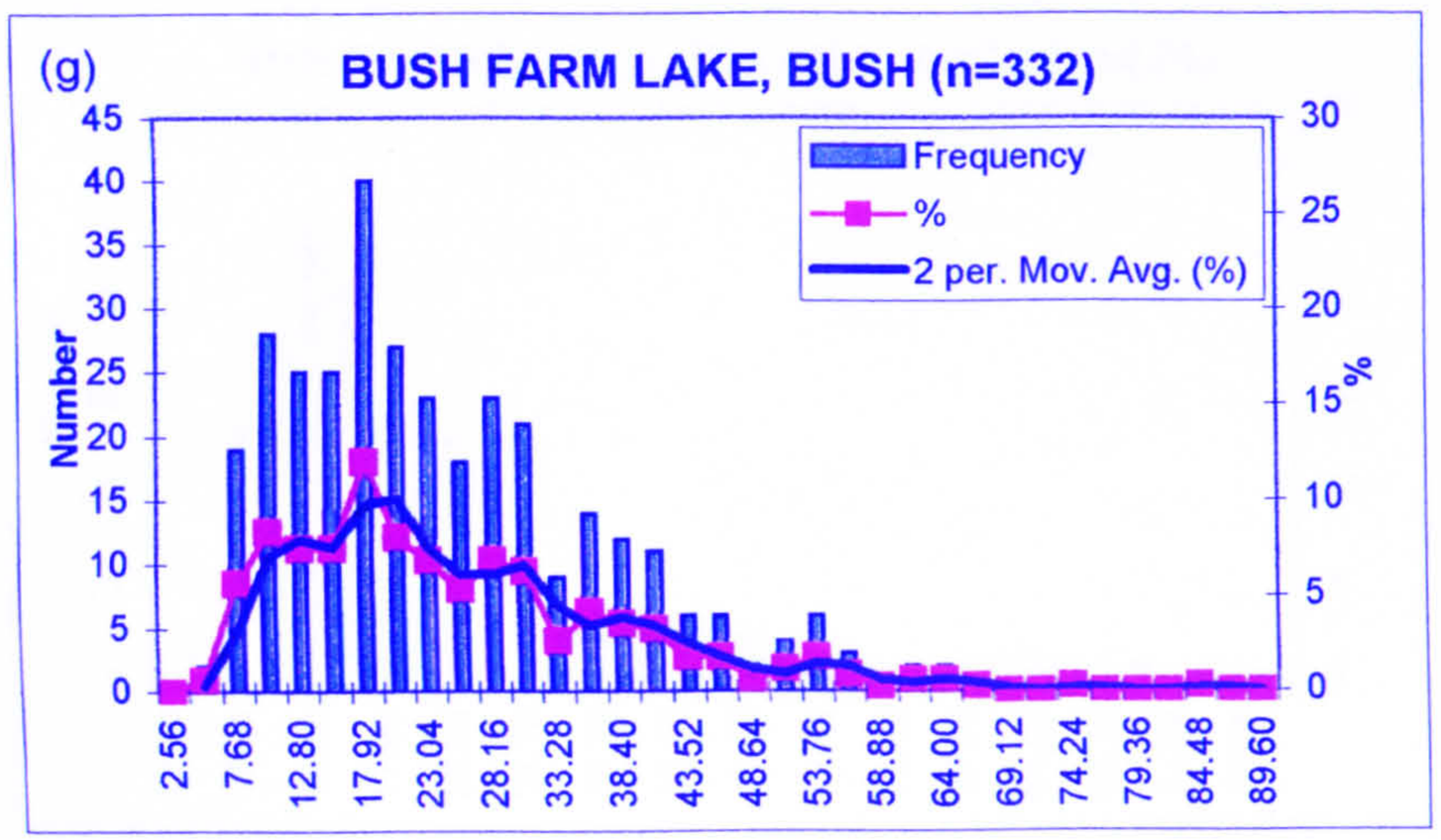

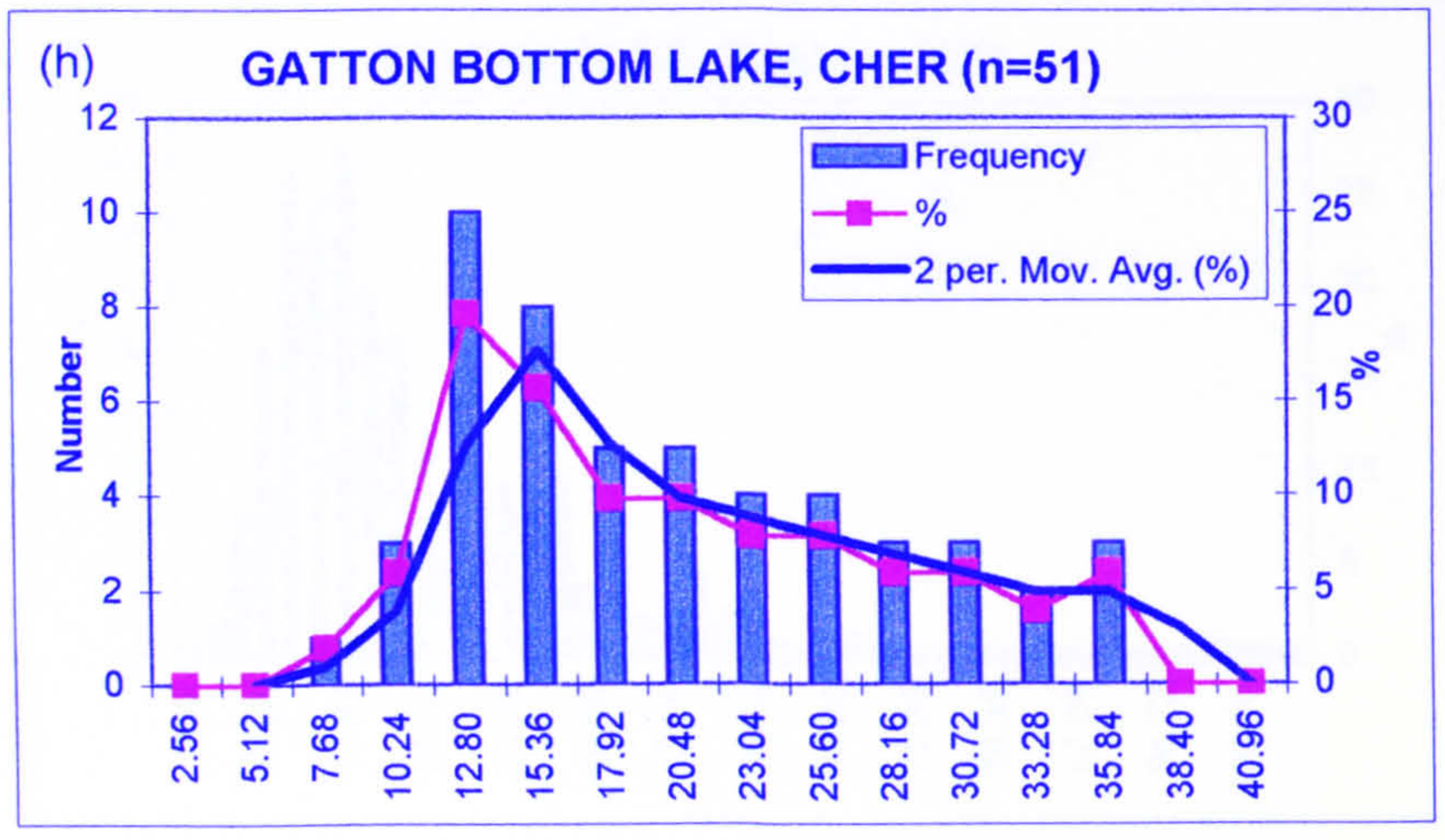

Figures 4.3i-l: Size distribution of SCPs in the surface sediments of twenty-seven lakes and ponds in London

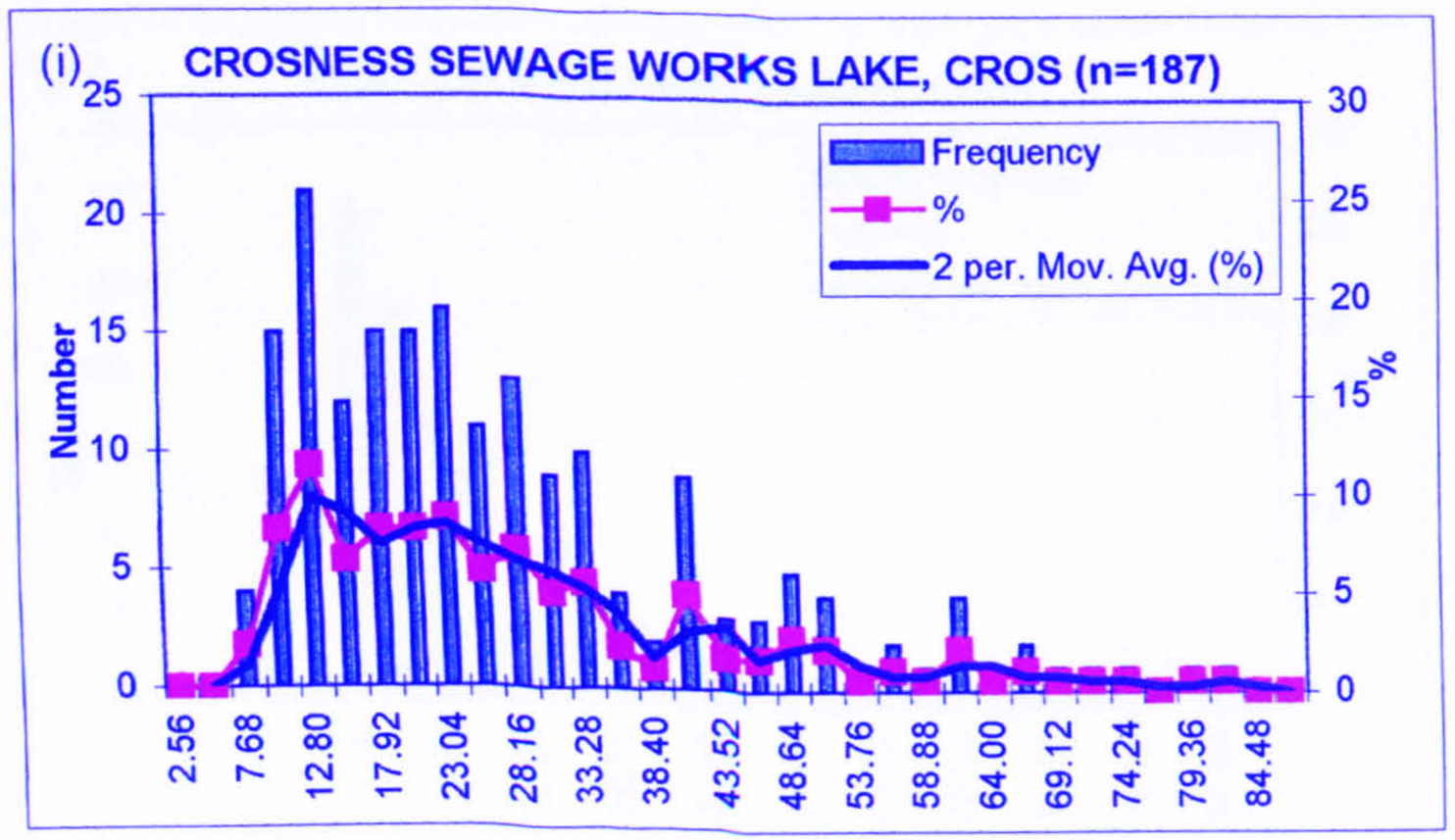

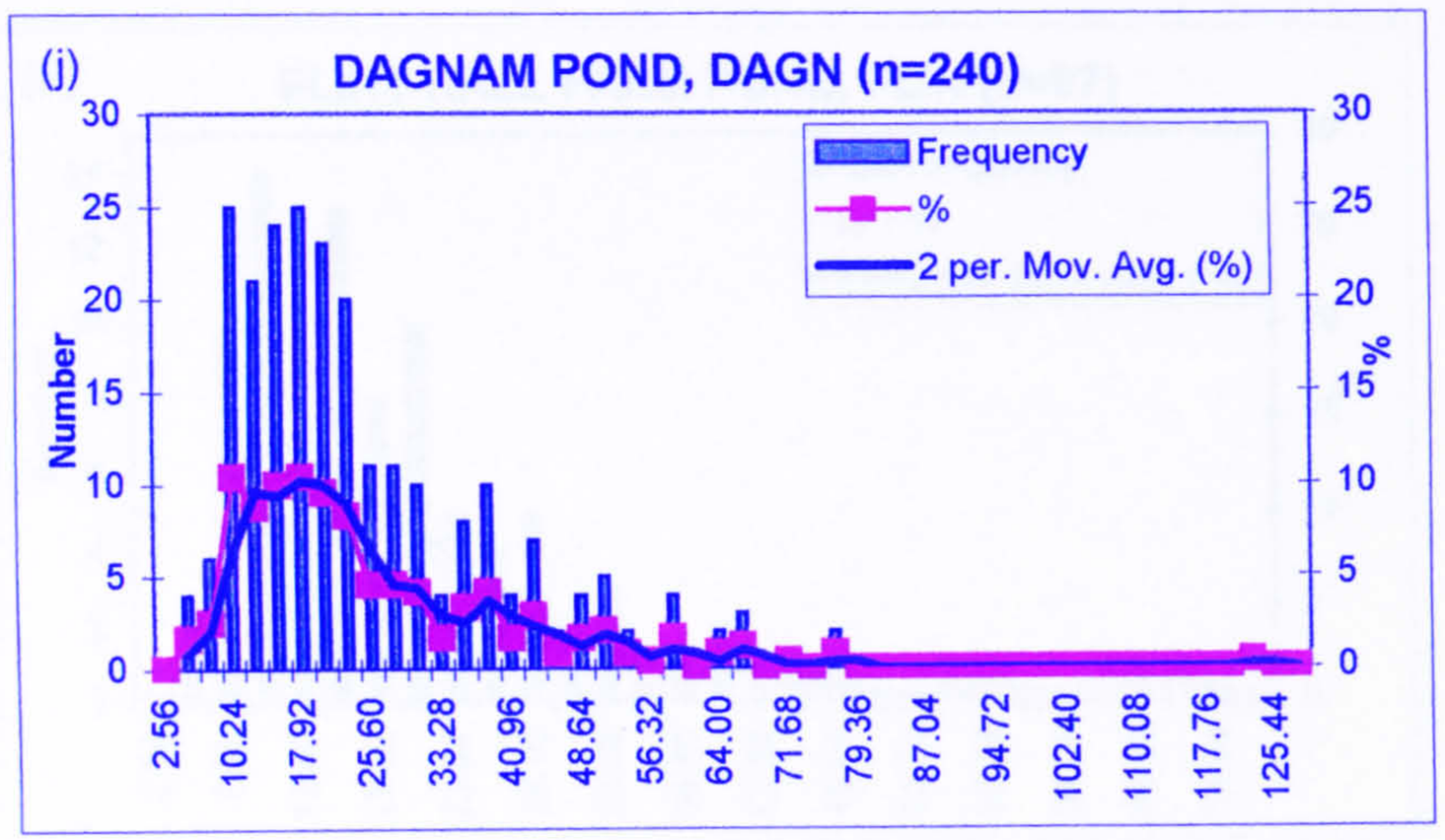

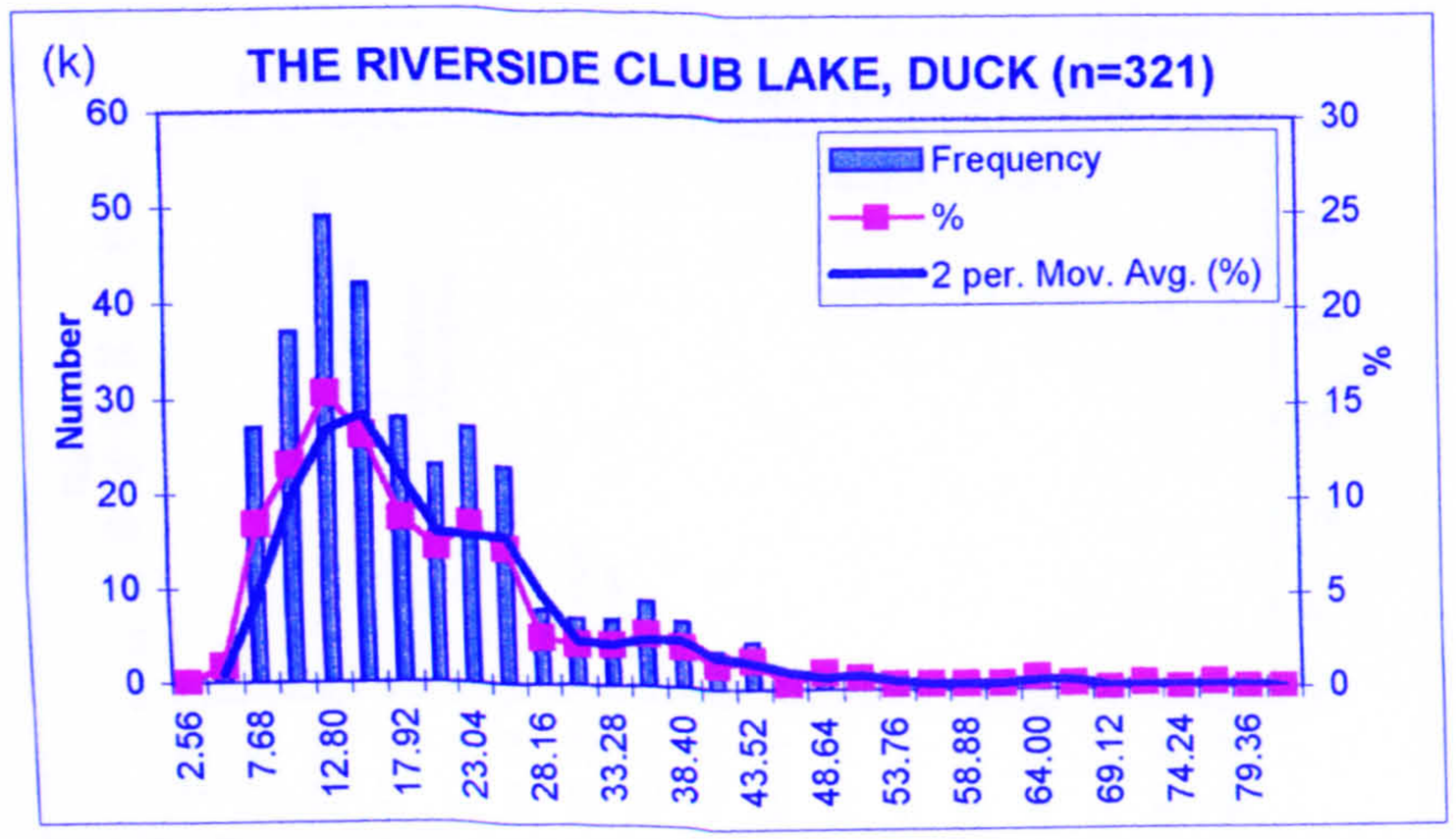

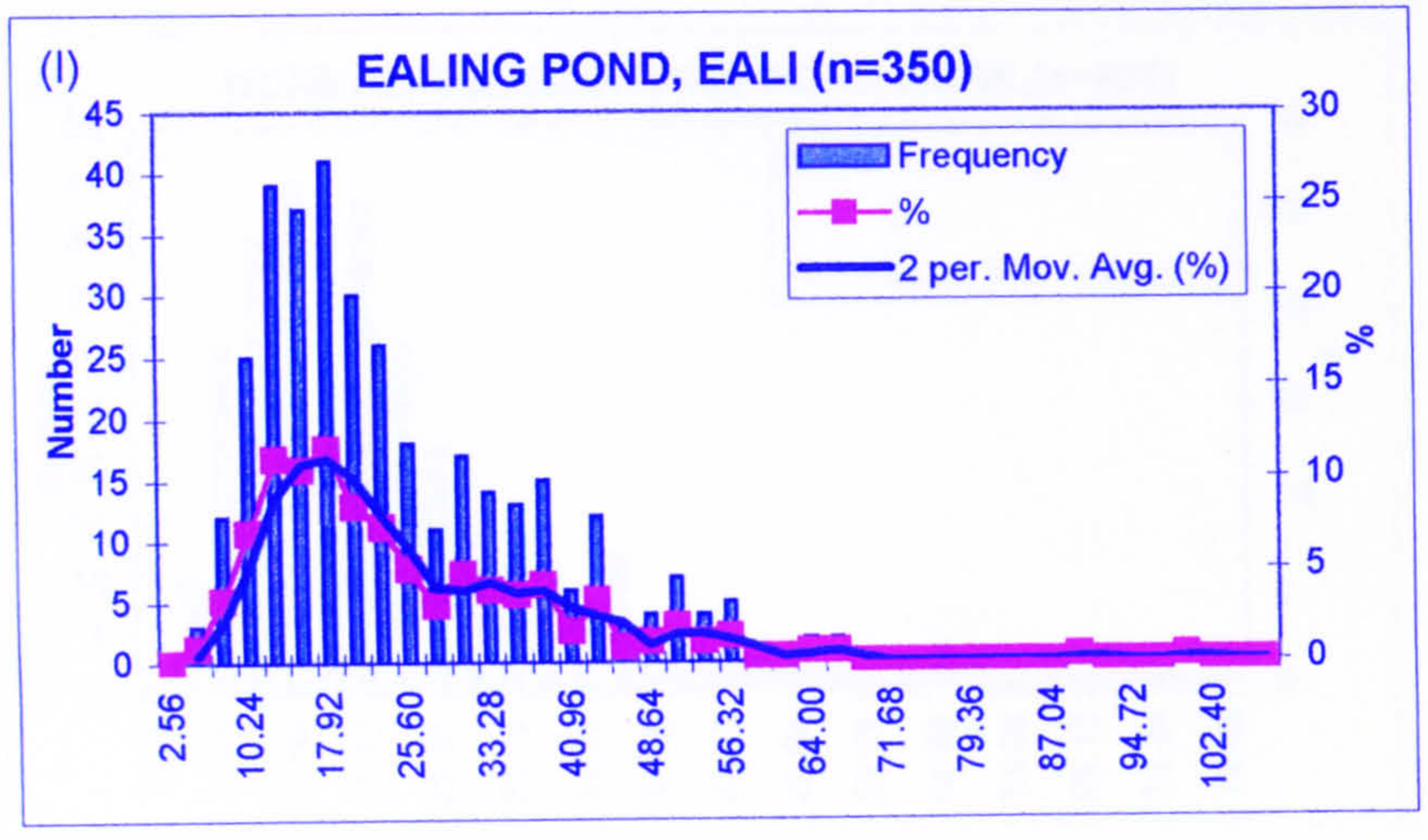

Figures 4.3m-p: Size distribution of SCPs in the surface sediments of twenty-seven lakes and ponds in London

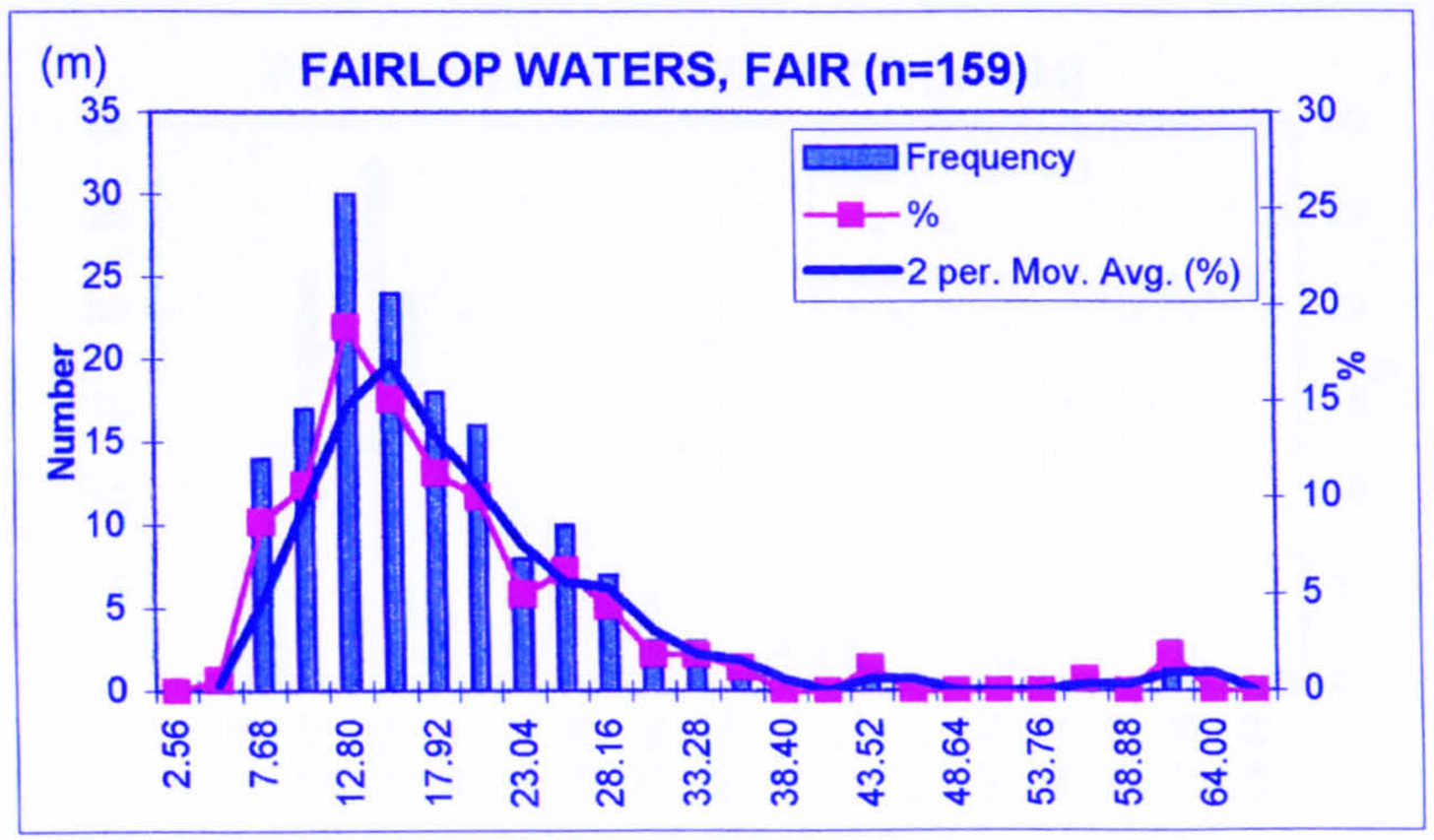

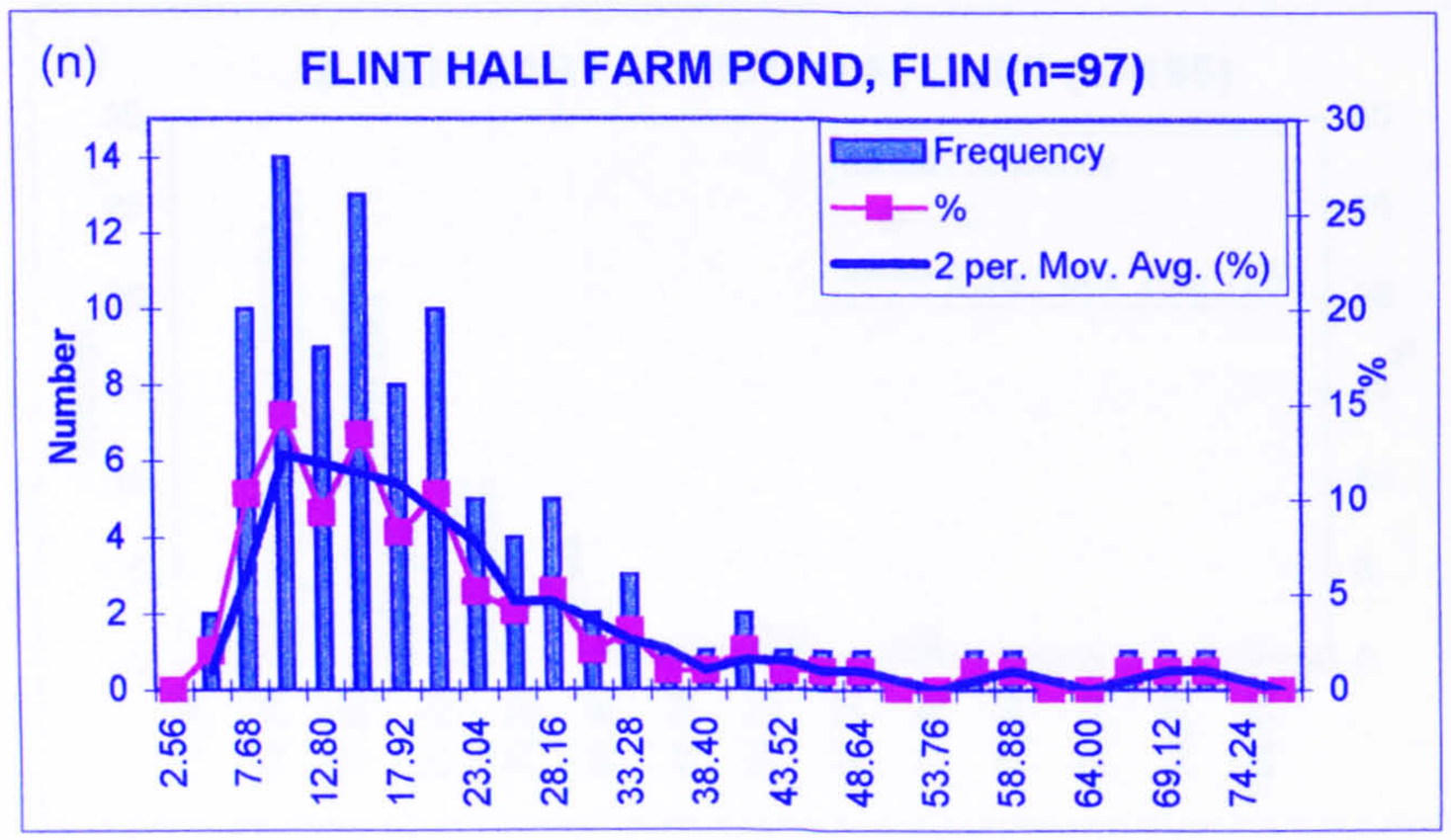

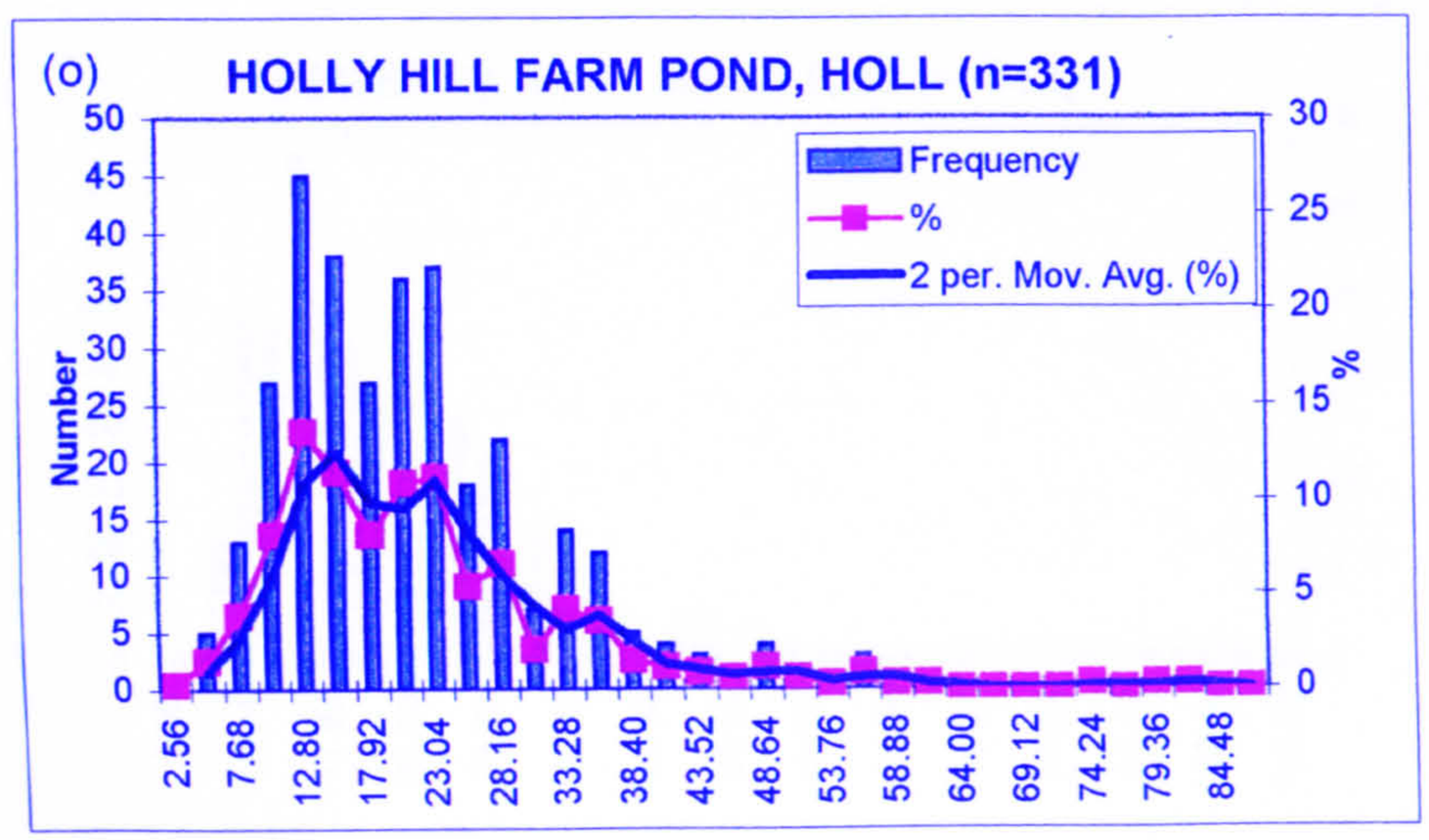

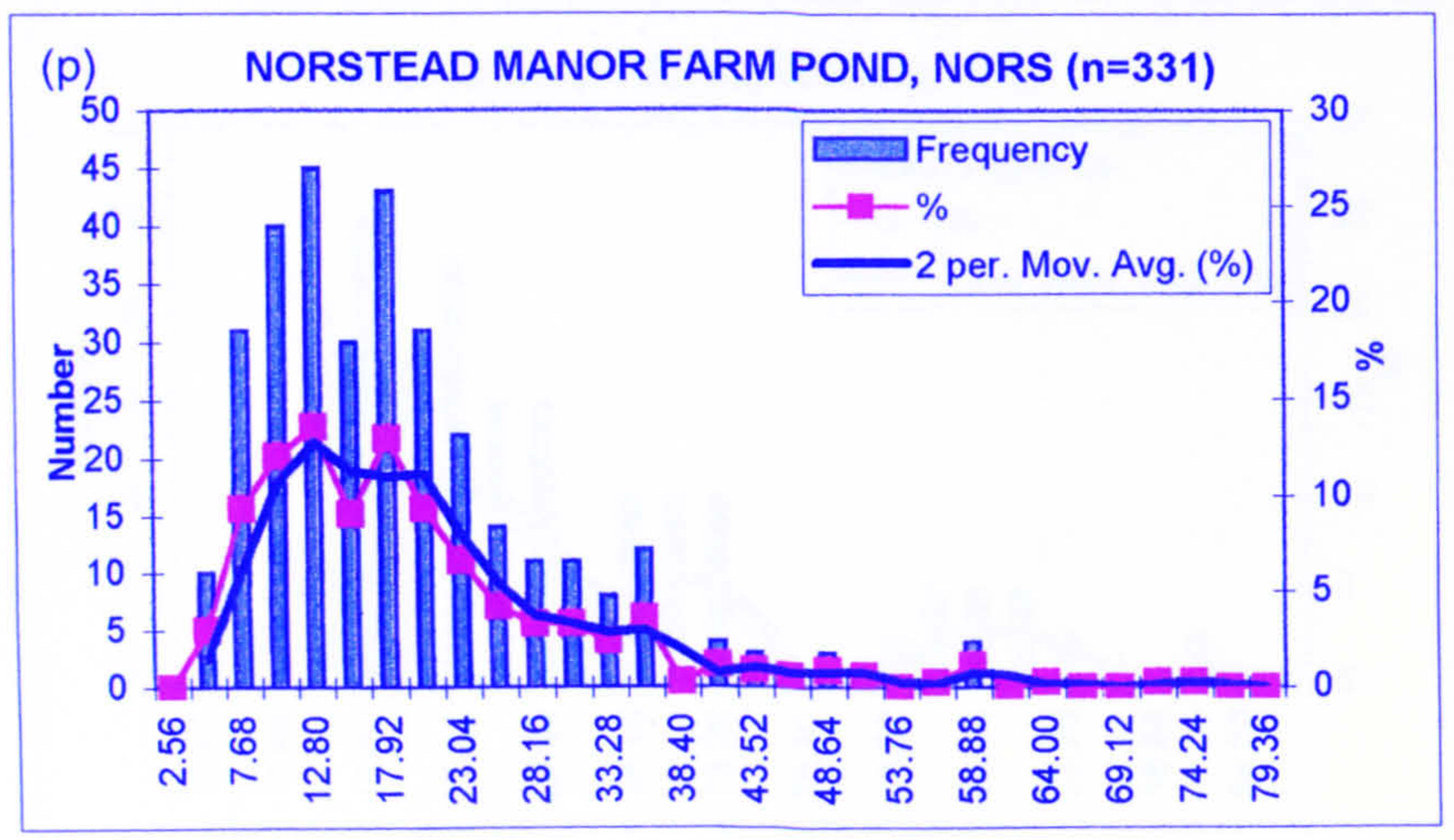

Figures 4.3q-t: Size distribution of SCPs in the surface sediments of twenty-seven lakes and ponds in London

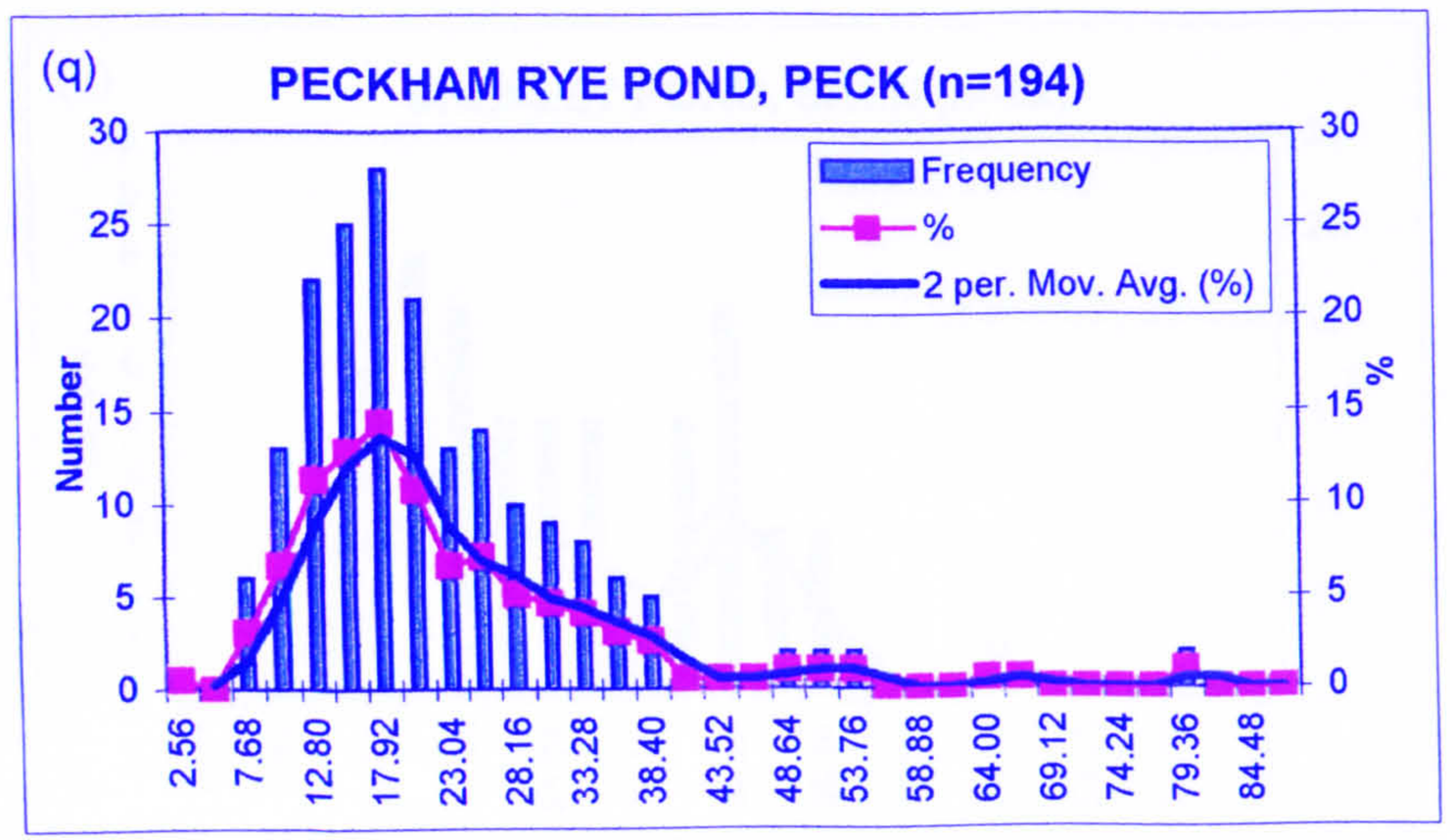

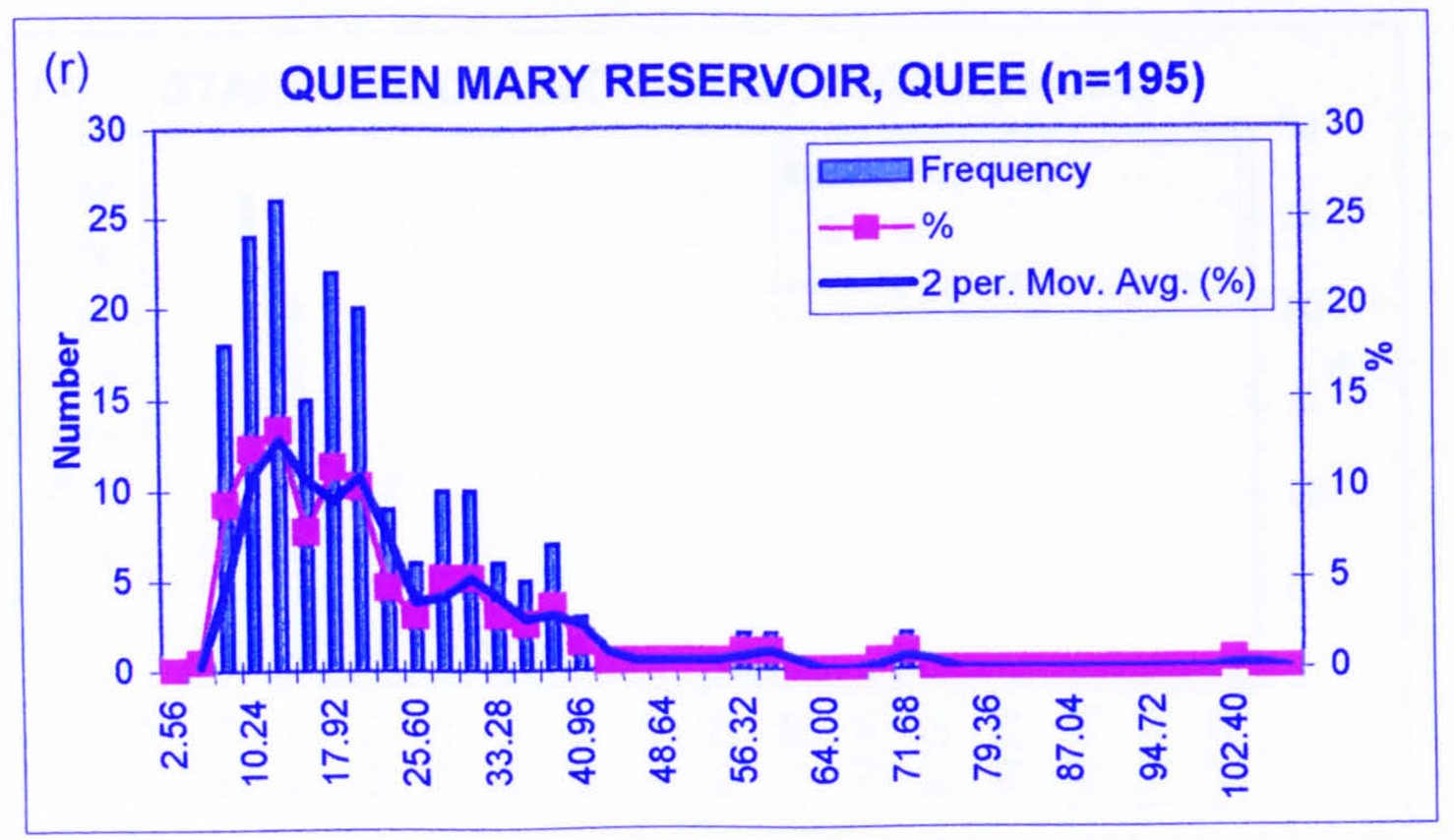

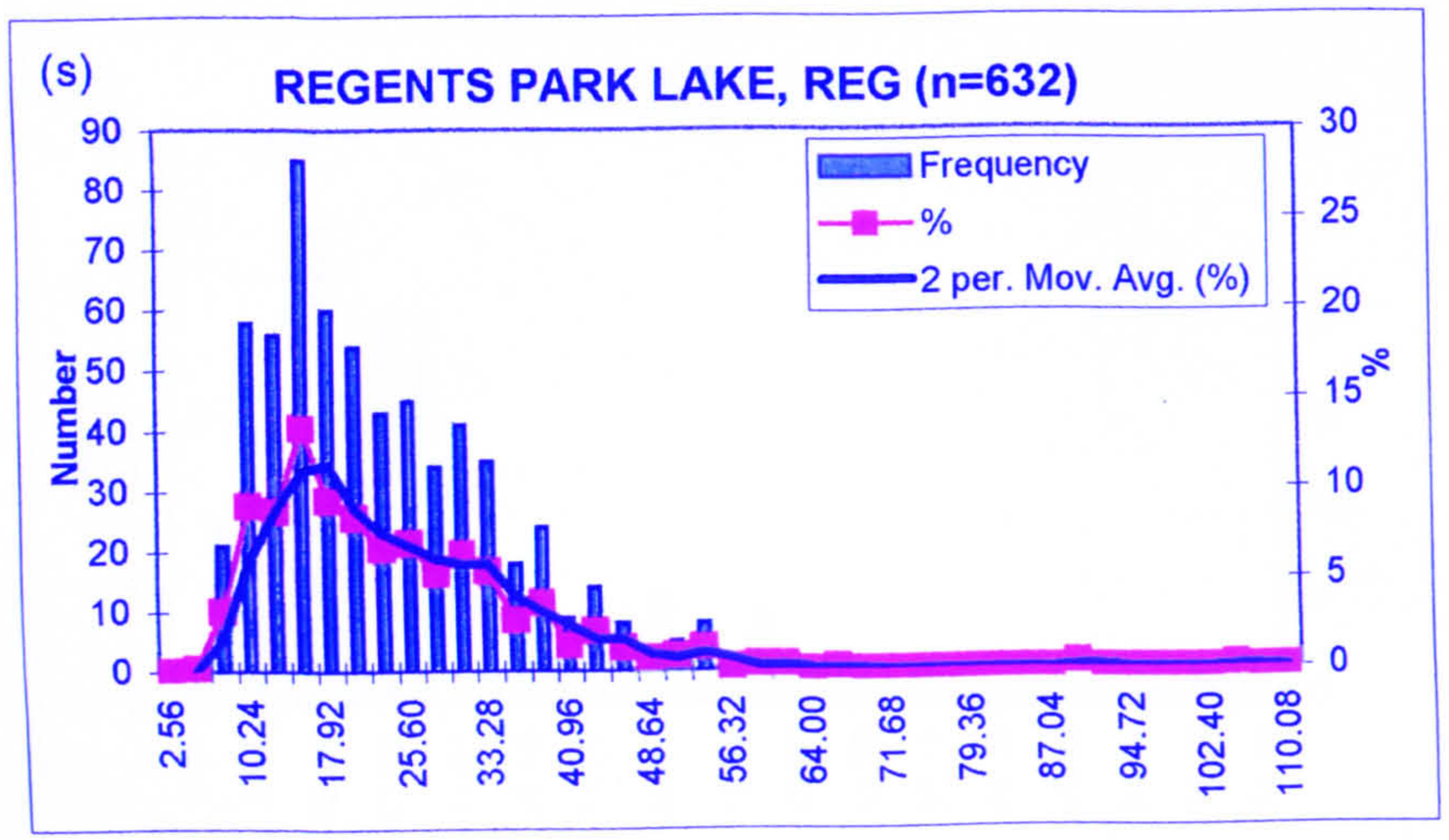

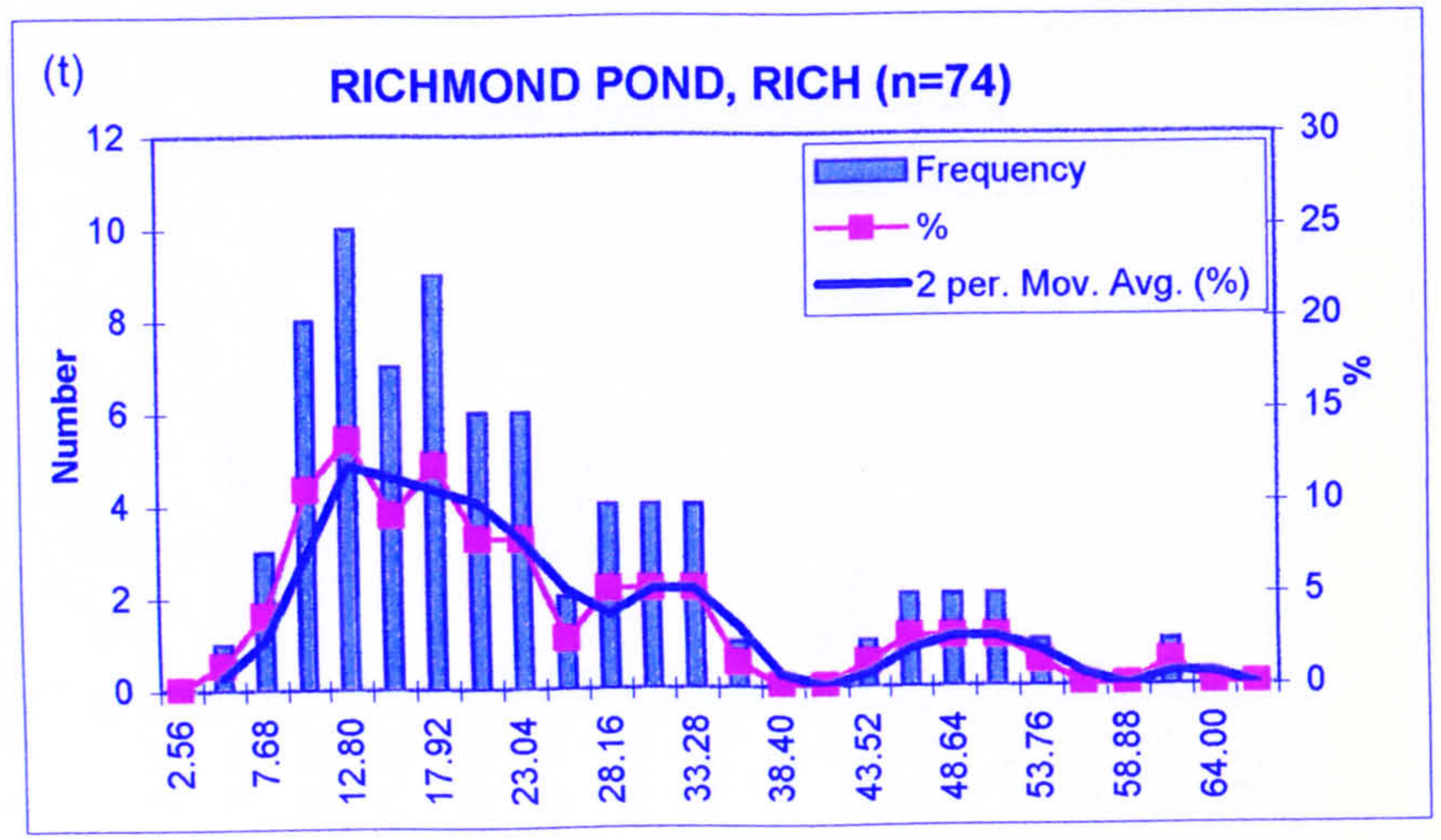

Figures 4.3u-x: Size distribution of SCPs in the surface sediments of twenty-seven lakes and ponds in London

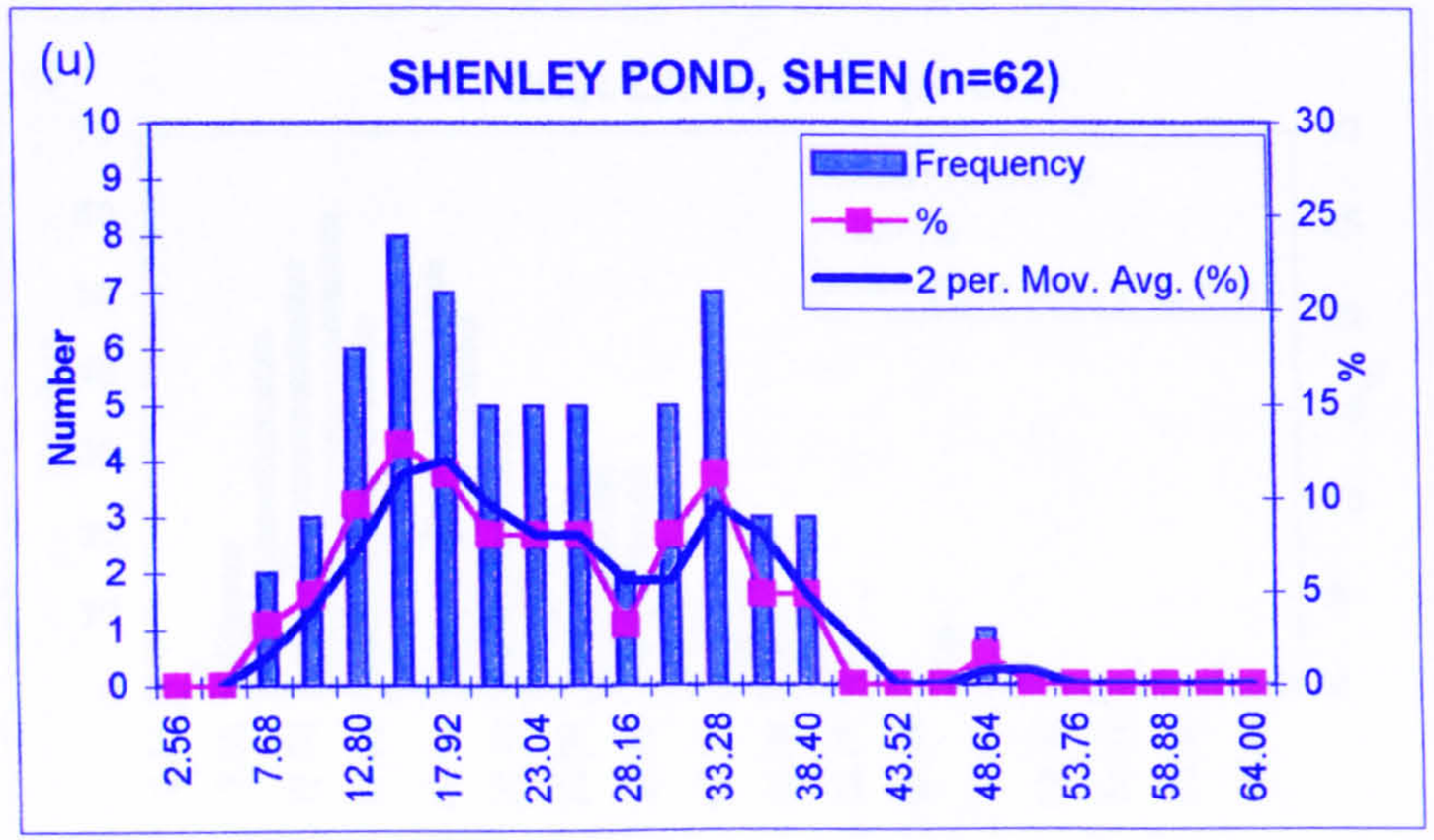

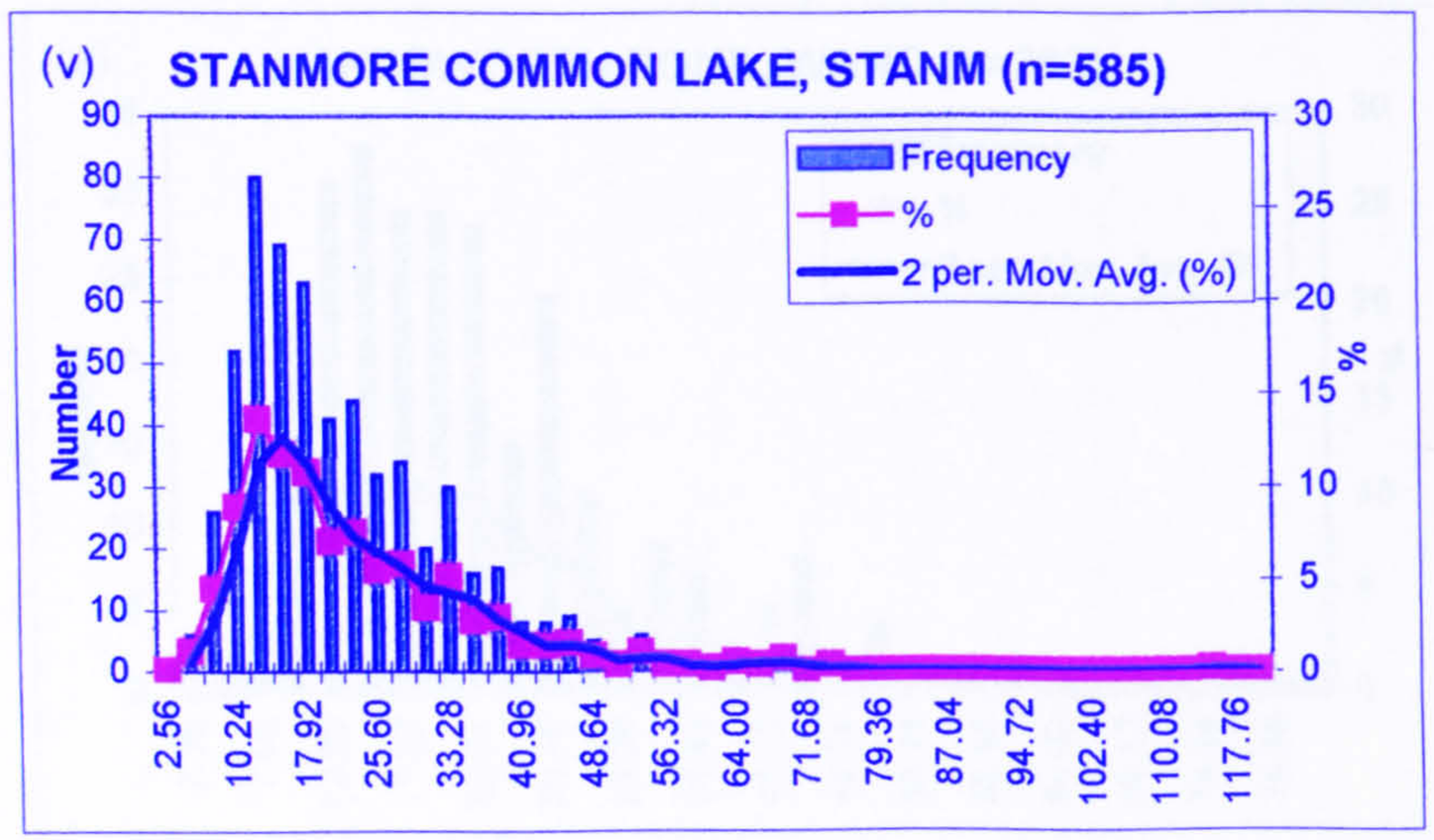

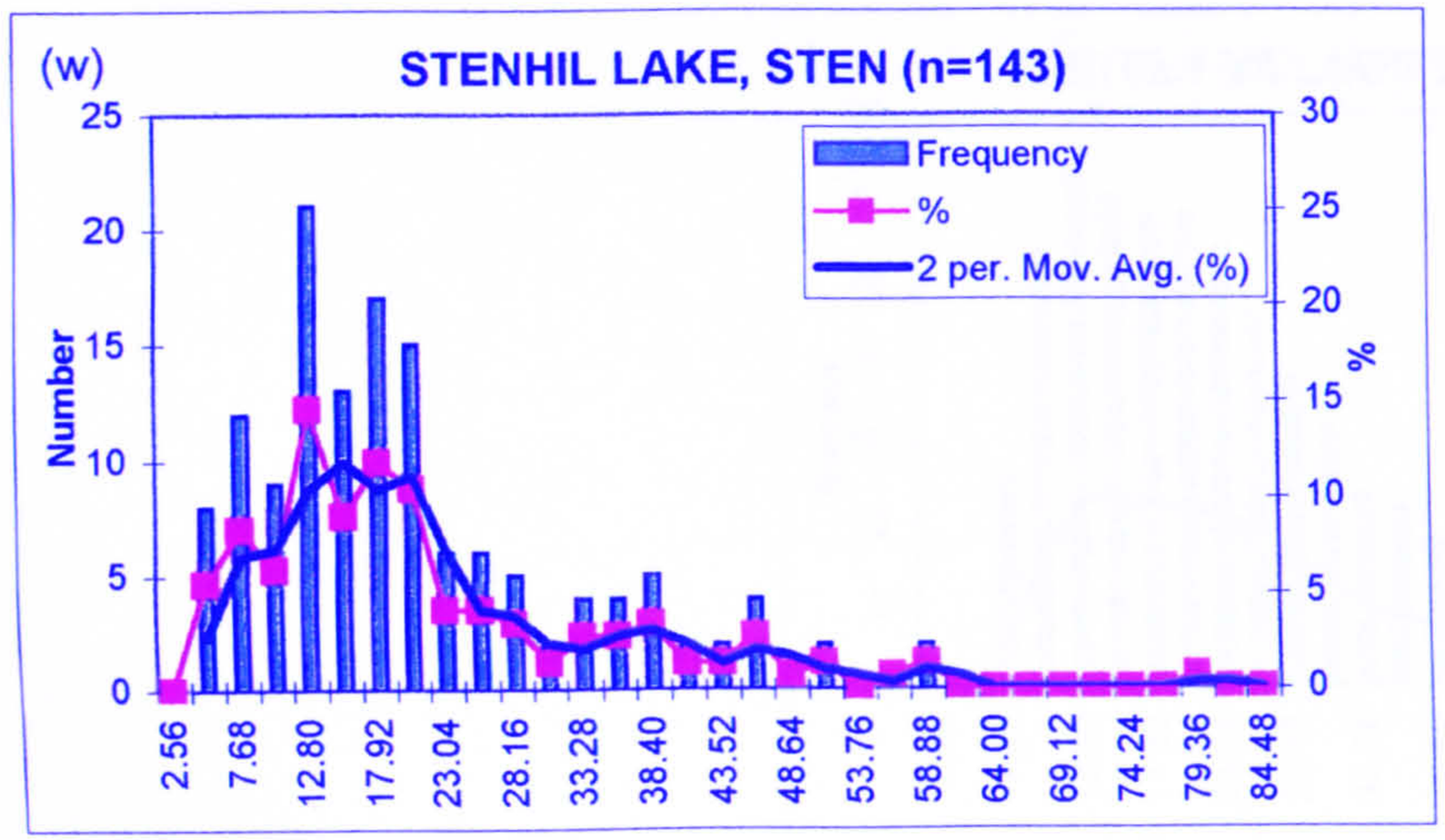

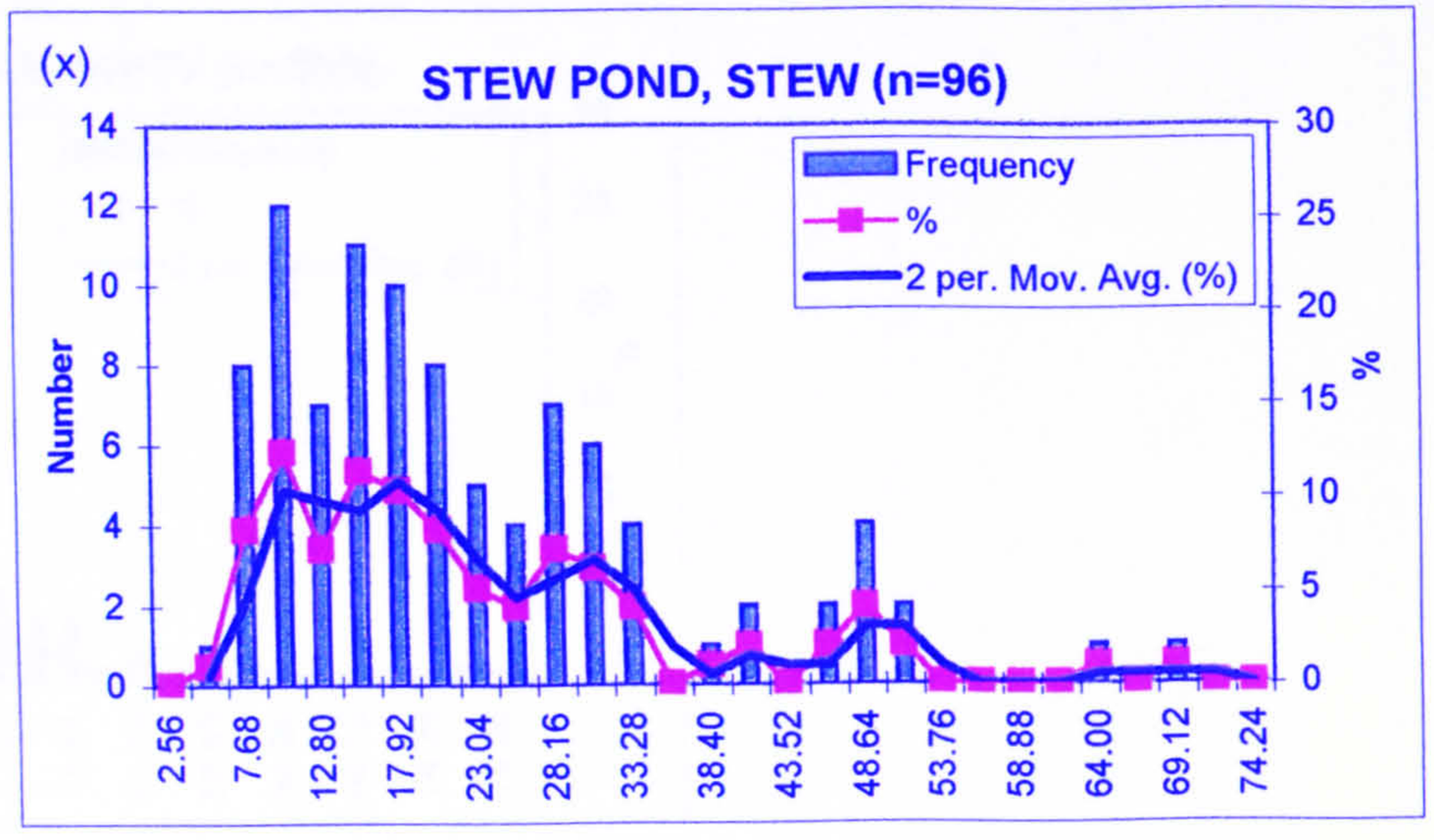

Figures 4.3y-aa: Size distribution of SCPs in the surface sediments of twenty-seven lakes and ponds in London

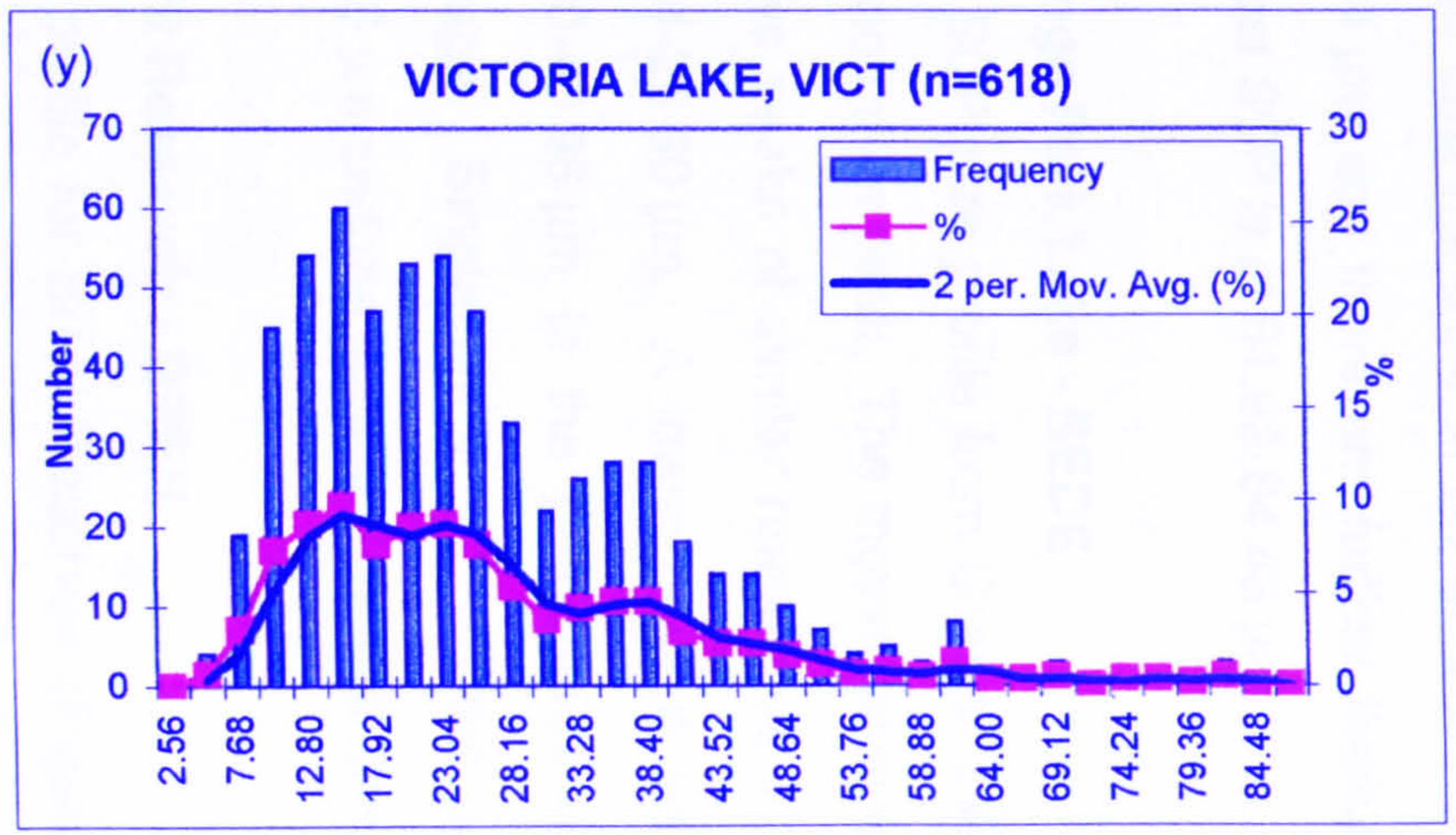

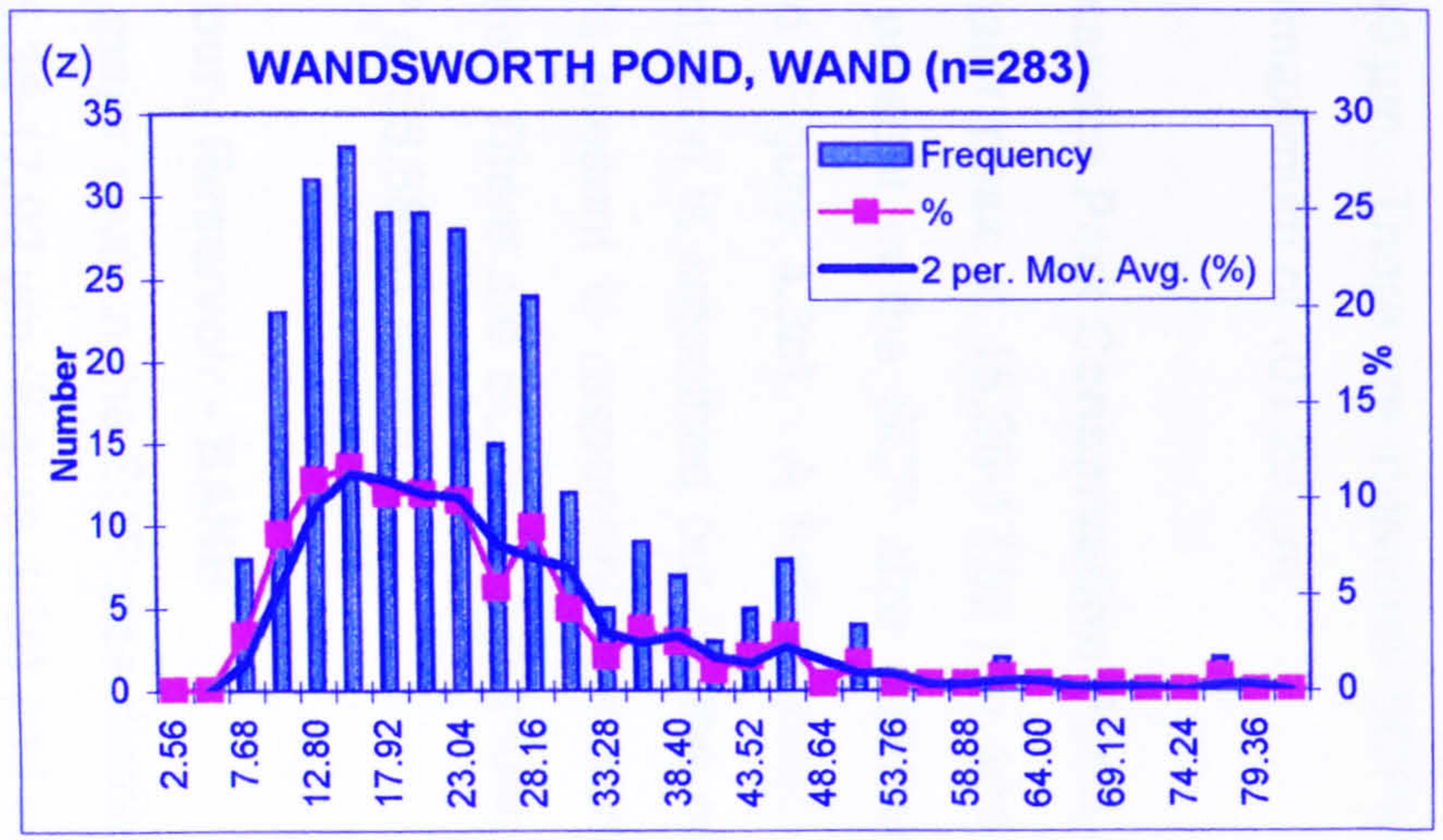

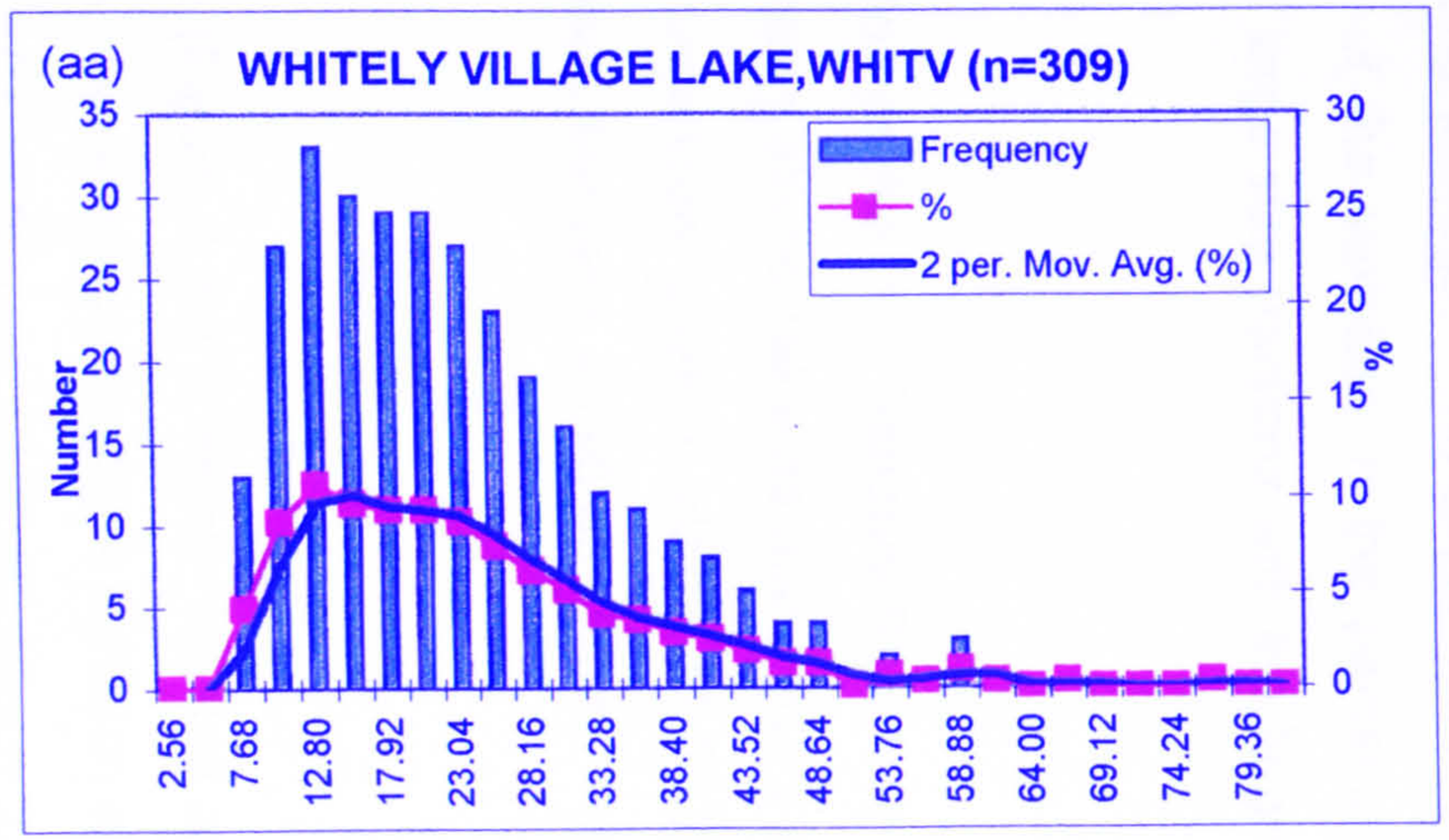

Addiscombe Pond - ADDI

The SCP size distribution for Addiscombe Pond (Figure 4.3a) shows a major peak at 12.80-15.36 µm and secondary peaks at 28.16-30.72 µm and 35.84-38.40 µm. There are individual SCPs in some of the higher size fractions up to a maximum of 101.28 µm.

Alexandra Park Conservation Pond - ALEX

A major peak at 15.36-17.92 µm and a secondary peak at 30.72-33.28 µm are present in the SCP size distribution for Alexandra Park Conservation Pond (Figure 4.3b). A further peak at 40.96-43.52 µm in the percentage distribution is smoothed out by the moving average. The small number of SCPs present is responsible for some of the variation in the percentage profile. There are SCPs in a number of large size fractions with the largest SCP at 58.88-61.44 µm

Banbury Reservoir - BANB

The major peak in the SCP size distribution profile from Banbury Reservoir is at 15.36-17.92 µm (Figure 4.3c) and contains almost twice as many SCPs as in the size fractions at either side. A secondary peak is visible at 33.28-35.84 µm and there are further fluctuations between 40.96-53.76 µm. The largest SCP is at 81.92-84.48 µm.

Grange Park Lake - BEDE

The SCP size profile from Grange Lake (Figure 4.3d) is highly variable and has no major peak. The moving average smoothes some of the variation and shows peaks of similar magnitude at 10.24-12.80 µm, 17.92-20.48 µm and 23.04-25.60 µm. A lower peak is visible at 30.72-33.28 µm. The peak at 38.40-40.96 µm in the percentage data is smoothed out by the moving average. Single large SCPs were counted at 53.76-56.32 µm and 64.00-66.56 µm and the largest SCP is in this fraction.

Brent Reservoir - BREN

The profile for Brent Reservoir (Figure 4.3e) also shows a large amount of variation that is smoothed by the moving average. It has an initial peak

between 5.12 µm and 10.24 µm which then drops to a plateau between 12.80-23.04 µm. At higher SCP size fractions peaks are present at 25.60-28.16 µm and 38.4-40.96 µm with one SCP in the maximum size fraction of 58.88-61.44 µm.

Brooklands Lake - BROO

A major peak at 17.92-23.04 µm dominates the profile from Brooklands Lake (Figure 4.3f). There are two shoulders to the main peak at 7.68-10.24 µm and 33.28-35.84 µm. At higher SCP sizes the profile is more variable with low peaks at 48.64-51.20 µm and 61.44-64.00 µm. There are a number of SCPs present at higher size fractions with the largest SCP at 102.4-104.96 µm.

Bush Farm Lake - BUSH

The smoothed profile for this site (Figure 4.3g) is similar to that of Brooklands Lake but with a lower initial peak. The major peak at this site is at 15.36-17.92 µm with minor peaks at 7.68-10.24 µm, 25.60-28.16 µm, 33.28-35.84 µm and 51.20-53.76 µm. Compared with Brooklands Lake there is an absence of SCPs in higher size groups. The maximum SCP size at this site is 81.92-84.48 µm.

Gatton Bottom Lake - CHER

The SCP distribution profile from Gatton Bottom Lake (Figure 4.3h) has the smallest range of SCP sizes of all the sites in this study, and the smallest number of SCPs counted, with all the SCPs contained between 5.12 µm and 35.84 µm. An initial peak is present at 10.24-12.80 µm with an elongated shoulder from 15.36-35.84 µm that may be disguising secondary or tertiary peaks.

Crossness Sewage Works Lake - CROS

The major SCP peak occurs at 10.24-12.80 µm (Figure 4.3i). There is a second, more broad peak at 20.48-23.04 µm. Further peaks are present in the profile at 38.40-40.96 µm, 46.08-48.64 µm and 58.88-61.44 µm. The

between 5.12 µm and 10.24 µm which then drops to a plateau between 12.80-23.04 µm. At higher SCP size fractions peaks are present at 25.60-28.16 µm and 38.4-40.96 µm with one SCP in the maximum size fraction of 58.88-61.44 µm.

Brooklands Lake - BROO

A major peak at 17.92-23.04 µm dominates the profile from Brooklands Lake (Figure 4.3f). There are two shoulders to the main peak at 7.68-10.24 µm and 33.28-35.84 µm. At higher SCP sizes the profile is more variable with low peaks at 48.64-51.20 µm and 61.44-64.00 µm. There are a number of SCPs present at higher size fractions with the largest SCP at 102.4-104.96 µm.

Bush Farm Lake - BUSH

The smoothed profile for this site (Figure 4.3g) is similar to that of Brooklands Lake but with a lower initial peak. The major peak at this site is at 15.36-17.92 µm with minor peaks at 7.68-10.24 µm, 25.60-28.16 µm, 33.28-35.84 µm and 51.20-53.76 µm. Compared with Brooklands Lake there is an absence of SCPs in higher size groups. The maximum SCP size at this site is 81.92-84.48 µm.

Gatton Bottom Lake - CHER

The SCP distribution profile from Gatton Bottom Lake (Figure 4.3h) has the smallest range of SCP sizes of all the sites in this study, and the smallest number of SCPs counted, with all the SCPs contained between 5.12 µm and 35.84 µm. An initial peak is present at 10.24-12.80 µm with an elongated shoulder from 15.36-35.84 µm that may be disguising secondary or tertiary peaks.

Crossness Sewage Works Lake - CROS

The major SCP peak occurs at 10.24-12.80 µm (Figure 4.3i). There is a second, more broad peak at 20.48-23.04 µm. Further peaks are present in the profile at 38.40-40.96 µm, 46.08-48.64 µm and 58.88-61.44 µm. The

effect of smoothing reduces the number of peaks considerably by removing the peaks and troughs between 23.04 µm and 33.28 µm. The resulting smoothed profile suggests that there are two or more contributions to the distribution below 35.84 µm. The maximum SCP size is in the fraction 79.36-81.92 µm.

Dagnam Pond - DAGN

The main peak region for this site (Figure 4.3j) is centred at 12.80-17.92 µm. The SCP counts drop by more than half at 23.04-25.6 µm. There is the suggestion of a peak in the shoulder at 25.60-28.16 µm and there are five other minor peaks at 35.84-38.40 µm, 40.96-43.52 µm, 48.64-51.20 µm, 56.32-58.88 µm and 64.00-66.56 µm. The peaks in the three highest size fractions consist of relatively few SCPs. There is one very large SCP at 120.32-122.88 µm.

Riverside Club Lake - DUCK

There are three peaks in the relatively simple profile from the Riverside Club (Figure 4.3k) with the major peak at 10.24-12.80 µm and the minor peaks at 20.48-23.04 µm and 33.28-35.84 µm. A large number of SCPs were counted and the profile is very smooth, appearing to be trimodal. The maximum SCP size is low compared with many of the other sites, at just 74.24-76.80 µm.

Ealing Pond - EALI

The SCP size distribution from Ealing Pond (Figure 4.3l) has one major peak at 15.36-17.92 µm and two minor peaks at 28.16-30.72 µm and 48.64-51.20 µm. The counts below 23.04 µm are high compared with those above 23.04 µm. Individual SCPs are scattered along the profile in the largest size fractions up to a maximum of 97.28-99.84 µm.

Fairlop Waters - FAIR

The smoothed profile of Fairlop Waters (Figure 4.3m) has a major peak at 10.24-12.80 µm and then minor peaks at 40.96-43.52 µm and 58.88-61.44 µm. The distribution has a sharper peak than those of other sites. A

minor peak in the percentage size distribution at 23.04-25.60 µm is almost smoothed out. The maximum SCP size is 58.88-61.44 µm and contains three SCPs.

Flint Hall Farm Pond - FLIN

The profile for Flint Hall Farm Pond (Figure 4.3n) is highly variable, due to the smaller numbers of SCPs counted, with most of the SCPs in size classes below 20.48 µm. The moving average line smoothes the peaks and troughs and suggests that there is a primary peak at around 7.68-12.80 µm and secondary peaks forming the shoulder of the distribution at 17.92-20.48 µm and at 25.60-28.16 µm. There are individual SCPs at higher size fractions up to a maximum of 69.12-71.68 µm.

Holly Hill Farm Pond - HOLL

Both the smoothed and the percentage distributions show similar profiles with two major peaks of similar magnitude at 10.24-12.80 µm and 20.48-23.04 µm (Figure 4.3o). There is a minor peak at 30.72-33.28 µm with possible further peaks in the 46.08-48.64 µm and 53.76-56.32 µm size fractions. Single SCPs are present in higher size fractions with the maximum SCP size at 79.36-81.92 µm.

Norstead Manor Farm Pond - NORS

The profile at this site (Figure 4.3p) has two peaks of similar magnitude at 10.24-12.80 µm and 15.36-17.92 µm suggesting that there is a bimodal size distribution. A minor peak is present at 33.28-35.84 µm which contributes to the shoulder of the main peak. At 56.32-58.88 µm there is evidence of a small peak caused by relatively few SCPs. The maximum SCP size is 71.68-74.24 µm.

Peckham Rye Lake - PECK

The distribution profile from Peckham Rye Lake (Figure 4.3q) is very smooth with a major peak at 15.36-17.92 µm. The profile appears bimodal with a second peak at around 23.04-25.60 µm. This peak has been smoothed out in

the running average profile and just appears as a shoulder of the main distribution. Between 46.08 µm and 53.76 µm there is a minor peak caused by low SCP numbers. There are two SCPs in the maximum SCP size fraction of 76.80-79.36 µm.

Queen Mary Reservoir - QUEE

The profile from Queen Mary Reservoir (Figure 4.3r) is similar to that from Norstead Manor Farm Pond in that it has two major peaks close together and of similar magnitude. These peaks are at 10.24-12.80 µm and 15.36-17.92 µm. Further peaks are evident at 25.60-30.72 µm and 35.84-38.40 µm. There are several groups of small numbers of SCPs at higher sizes with the largest SCP at 99.84-102.40 µm.

Regents Park Lake - REG

The profile from Regents Park Lake (Figure 4.3s) appears to comprise a number of distributions with a main peak in the distribution at around 12.80-15.36 µm. A second peak is present at 28.16-30.72 µm. There are further peaks in the percentage profile at 35.84-38.40 µm and 40.96-43.52 µm although the effects of these are smoothed out by the running average. A low-level peak caused by a few SCPs is present at 51.20-53.76 µm. The maximum SCP size is 102.40-104.96 µm.

Richmond Pond - RICH

The distribution profile from Richmond Pond (Figure 4.3t) has a smaller range than most of the other sites with a maximum SCP size of 58.88-61.44 µm. The main peak in the profile is at 10.24-12.80 µm although it may have a contribution from a smaller distribution at 15.36-17.92 µm that is masked by the major peak. There are other peaks between 25.60 µm and 30.72 µm and one comprising only a few SCPs between 43.52 µm and 51.20 µm.

Shenley Pond - SHEN

The distribution profile from this site (Figure 4.3u) is one of only two in the group that has a negative kurtosis. The major peak is at 12.80-15.36 µm

followed by a secondary peak of similar magnitude at 30.72-33.28 µm. An isolated SCP at 46.08-48.64 µm is the largest SCP found at this site.

Stanmore Common Lake - STANM

The smoothed profile from Stanmore Common Lake (Figure 4.3v) shows a major peak at 10.24-12.80 µm, whereas the percentage profile displays more variation in spite of the total SCPs counted being large. There is a minor peak at 30.72-33.28 µm that forms the shoulder of the smoothed profile. Other distributions may be part of the profile but these are incorporated into the major peak. The maximum SCP size is 112.64-115.20 µm.

Stenhil Lake - STEN

There are many peaks and troughs in the percentage distribution profile for Stenhil Lake that are smoothed by the moving average profile (Figure 4.3w). In spite of the effect of smoothing there is still a large amount of variation showing a major peak at 10.24-12.80 µm and a secondary, slightly lower peak at 15.36-17.92 µm. There are other peaks at 5.12-7.68 µm, 35.84-38.40 µm, 43.52-46.08 µm and 56.32-58.88 µm. The largest SCP is at 122.88-125.44 µm.

Stew Pond - STEW

The smoothed line follows a similar profile to the percentage line showing two major peaks of similar magnitude at 7.68-10.24 µm and 12.80-15.36 µm (Figure 4.3x). A slightly lower but distinct peak is present at 25.60-28.16 µm) followed by further peaks at 38.40-40.96 µm and 46.08-48.64 µm. The largest SCP is at 66.56-69.12 µm.

Victoria Lake - VICT

A large number of SCPs counted in the sediment of Victoria Lake (Figure 4.3y) means that the effects of smoothing the profile are small. The main peaks in the size distribution are close together at 12.80-15.36 µm and 20.48-23.04 µm and are of similar magnitude. A further large peak is present at

33.28-35.84 µm and a minor peak at 58.88-61.44 µm. The largest SCP is 79.36-81.92 µm in size.

Wandsworth Pond - WAND

There is a cluster of similar SCP counts between 10.24 µm and 23.04 µm, which form the major peak in the distribution at Wandsworth Pond (Figure 4.3z). A secondary peak at 25.60-28.16 µm is evident in the percentage profile but is smoothed to form a shoulder of the main peak in the running average profile. Further peaks can be seen at 33.28-35.84 µm and 43.52-46.08 µm. Individual SCPs are present in higher size fractions with the largest SCP at 74.24-76.80 µm.

Whitely Village Lake - WHITV

This site (Figure 4.3aa) has a very smooth profile with a major peak at 10.24-12.80 µm. The extended shoulder in the higher size fractions suggests that there may be a number of smaller secondary peaks present that cannot be distinguished from the main peak. Small numbers of SCPs at 51.20-53.76 and 56.32-58.88 µm may be part of another distribution. There is one large SCP at the maximum size class of 74.24-76.80 µm.

The variation in the distribution profile is caused by low SCP counts. The standard deviation of a distribution is dependent on the population size (*n*) and the range of the SCP sizes. It is not possible to alter the range of the distribution since it is one of the properties of the SCP count of interest. However, as *n* increases then the standard deviation is reduced. It follows that as *n* increases the confidence in each of the counts in each of the size classes also increases.

Ideally a large number of SCPs should be counted to get a smooth distribution. One answer to this problem is to make slides with extra digested suspension (see Section 2.3.2). However, each sediment suspension contains varying amounts of residual materials that also survive the digestion process. If too much suspension is used to make a slide then it might not be possible to see through the slide well enough to count the SCPs present.

Therefore a balance between too much post-digestion material and too few SCPs is achieved by trial and error.

A lower limit of 50 SCPs was chosen as a reasonable number from which a SCP size distribution could be produced. New slides were prepared for counting where the number of SCPs on the original slide was less than 50. In the case of Gatton Bottom Pond the number of SCPs was once again less than 50 on the second slide. In combination the number of SCPs totalled 51 so for this site the two counts were combined. However, it must be borne in mind that the errors on the SCP count due to physically making a slide will be compounded by counting two slides (see Section 2.3.7).

4.3.1 Correlations between SCP concentration size fractions

The correlation matrix for sediment SCP size fractions (Table 4.2) produces high, positive and significant ($p<0.05$) values of r (0.77-0.98) for the size fractions between 15.38-25.64 μm and 56.41-64.10 μm. Adjacent pairs of concentration size fractions are also well correlated (e.g. 5.13-15.38 μm and 15.38-24.64 μm, r = 0.96; 64.10-74.35 μm and 74.35-84.61 μm, r = 0.77). Most concentration size fractions, with the exception of 0-5.13 μm and those larger than 94.87 μm where there are only a few SCPs, are significantly correlated ($p<0.05$) with the total concentration of all size fractions in the sediments. The highest values of r between total concentration of SCPs and size fractions are for the fractions 5.13-15.38 μm (r=0.97), 15.38-25.64 μm (r=1.00), 25.64-35.90 μm (r=0.98), 35.90-46.15 μm (r=0.95) and 46.15-56.41 μm (0.88). Above 56.41 μm the correlation decreases quickly as size increases. This shows that the overall pattern of SCPs in lakes and ponds in London is driven by the concentration of SCPs in the smaller size fractions.

4.4 Summary statistics for SCP size distributions from twenty-seven lakes and ponds in London

Table 4.3 shows the summary statistics for SCPs in the surface sediments of each lake and pond used in this project.

4.4.1 Mean, median and mode

The mean varies from 17.10 µm at FAIR to 32.07 µm at BROO with a wide range of values in between. The median is more consistent with twelve sites having a median value of 16.67 µm and eight sites having a median value of 19.23 µm. The range of median values is from 14.10 µm at FAIR to 25.64 µm at BROO, the same sites at either extreme of the mean values. The modal value is the most frequently deposited size of SCP and thus must be from the dominant SCP source. The modal range is from 9.97 µm at three sites, FLIN, DAGN and STEW to a maximum of 24.36 µm at BEDE. The modal value at eleven of the sites is 11.54 µm and is 14.10 µm at five sites. The mean values vary more than either median or mode because they are not constrained by SCP size groups. Distributions with large average or modal values might have a more local source of particles.

4.4.2 Minimum, Maximum and Range

The smallest SCP in the sediments is 1.28 µm (size group 0-2.56 µm, see Section 4.1) at two sites. 1.28 µm is smaller than the minimum particle that can be detected (2.56 µm), however this is an artefact of taking the mid-point of the size range for the statistical analyses. The largest SCP is 124.36 µm at STEN which also has the largest SCP size range of 120.51 µm. A site containing very large SCPs would need a close source. Figure 4.4 shows a plot of maximum SCP size against the distance from the closest Part A process. Although the direction of the Part A process relative to the lake or pond has not been taken into account, the general trend is for SCP size to increase if there is a local Part A process. However, there is a large amount of variation in these data, indicated by the poor regression coefficient (R^2=0.12), and, therefore these results should be interpreted with caution.

Table 4.2: Correlation matrix of size fractions of SCP concentrations in lake and pond sediments

			SCP in surface sediments (μm)											
		Total	0-5.13	5.13-15.38	15.38-25.64	25.64-35.90	35.90-44.15	46.15-56.41	56.41-64.10	64.10-74.35	74.31-84.61	84.61-94.87	94.87-105.13	> 105.13
SCP in surface sediments (μm)	Total	1.00												
	0-5.13	0.28	1.00											
	5.13-15.38	0.97	0.34	1.00										
	15.38-25.64	1.00	0.28	0.96	1.00									
	25.64-35.90	0.98	0.17	0.93	0.98	1.00								
	35.90-44.15	0.95	0.22	0.87	0.95	0.94	1.00							
	46.15-56.41	0.88	0.16	0.77	0.88	0.87	0.92	1.00						
	56.41-64.10	0.67	0.12	0.54	0.66	0.64	0.75	0.81	1.00					
	64.10-74.35	0.51	0.10	0.38	0.49	0.49	0.58	0.68	0.88	1.00				
	74.31-84.61	0.50	0.13	0.33	0.51	0.47	0.60	0.65	0.86	0.77	1.00			
	84.61-94.87	0.46	-0.17	0.41	0.44	0.52	0.40	0.48	0.43	0.34	0.16	1.00		
	94.97-105.13	0.22	-0.20	0.14	0.20	0.26	0.21	0.34	0.46	0.44	0.24	0.88	1.00	
	> 105.13	0.04	0.39	0.07	0.02	-0.01	0.05	0.03	0.07	0.17	0.01	-0.12	-0.13	1.00

Shaded correlations are significant at $p \leq 0.05$

Table 4.3: Summary statistics of SCP counts (in μm)

	ADDI	ALEX	BANB	BEDE	BREN	BROO	BUSH	CHER	CROS
Mean	20.44	23.45	20.98	22.13	17.51	32.07	23.69	18.88	26.51
Standard Error	0.83	1.48	1.33	1.61	1.24	1.34	0.74	1.08	1.17
Median	16.67	19.23	16.67	21.79	15.38	25.64	20.51	16.67	21.79
Mode	14.10	16.67	16.67	24.36	8.97	21.79	16.67	11.54	11.54
Standard Deviation	12.22	11.67	13.15	12.54	10.80	20.90	13.54	7.71	16.01
Sample Variance	149.42	136.26	172.80	157.24	116.66	437.01	183.21	59.44	256.31
Kurtosis	9.13	1.37	5.61	1.48	2.17	1.10	1.41	-0.73	1.01
Skewness	2.18	1.31	1.98	0.98	1.27	1.24	1.12	0.56	1.19
Range	97.44	53.85	79.49	61.54	56.41	97.44	79.49	28.21	74.36
Minimum	3.85	6.41	3.85	3.85	3.85	6.41	3.85	6.41	6.41
Maximum	101.28	60.26	83.33	65.38	60.26	103.85	83.33	34.62	80.77
Sum	4393.59	1453.85	2034.62	1350.00	1330.77	7825.64	7866.67	962.82	4957.69
Count	215	62	97	61	76	244	332	51	187
Confidence Level(95.0%)	1.63	2.91	2.62	3.15	2.43	2.62	1.46	2.12	2.29

Table 4.3 (contd.): Summary statistics of SCP counts (in μm)

	DAGN	DUCK	EALI	FAIR	FLIN	HOLL	NORS	PECK	QUEE
Mean	24.29	19.22	23.63	17.10	19.68	20.76	18.46	21.41	20.62
Standard Error	1.04	0.68	0.75	0.79	1.43	0.66	0.65	0.87	1.01
Median	19.23	16.67	19.23	14.10	16.67	19.23	16.67	19.23	16.67
Mode	8.97	11.54	16.67	11.54	8.97	11.54	11.54	16.67	11.54
Standard Deviation	16.12	12.16	14.09	9.92	14.04	11.94	11.74	12.16	14.16
Sample Variance	259.90	147.95	198.54	98.39	197.10	142.52	137.94	147.87	200.57
Kurtosis	5.70	3.67	3.11	6.54	3.37	4.47	3.66	5.25	6.46
Skewness	1.85	1.74	1.45	2.18	1.79	1.70	1.69	1.91	2.07
Range	117.95	71.79	94.87	56.41	66.67	79.49	69.23	76.92	97.44
Minimum	3.85	3.85	3.85	3.85	3.85	1.28	3.85	1.28	3.85
Maximum	121.79	75.64	98.72	60.26	70.51	80.77	73.08	78.21	101.28
Sum	5830.77	6170.51	8271.79	2719.23	1908.97	6870.51	6111.54	4153.85	4021.79
Count	240	321	350	159	97	331	331	194	195
Confidence Level(95.0%)	2.04	1.33	1.48	1.54	2.79	1.29	1.27	1.71	1.99

Table 4.3 (contd.): Summary statistics of SCP counts (in μm)

	REG	RICH	SHEN	STANM	STEN	STEW	VICT	WAND	WHITV
Mean	22.38	21.38	21.84	21.59	20.79	21.31	25.07	22.38	22.26
Standard Error	0.49	1.48	1.18	0.55	1.33	1.36	0.58	0.74	0.68
Median	19.23	16.67	20.51	16.67	16.67	16.67	21.79	19.23	19.23
Mode	14.10	11.54	14.10	11.54	11.54	8.97	14.10	14.10	11.54
Standard Deviation	12.26	12.73	9.29	13.21	15.94	13.31	14.42	12.48	11.88
Sample Variance	150.24	162.12	86.33	174.41	254.10	177.21	208.05	155.79	141.10
Kurtosis	5.26	0.81	-0.56	5.53	12.54	1.46	1.58	2.80	1.75
Skewness	1.61	1.18	0.40	1.80	2.70	1.26	1.21	1.51	1.18
Range	100.00	56.41	41.03	110.26	120.51	64.10	76.92	69.23	69.23
Minimum	3.85	3.85	6.41	3.85	3.85	3.85	3.85	6.41	6.41
Maximum	103.85	60.26	47.44	114.10	124.36	67.95	80.77	75.64	75.64
Sum	14143.59	1582.05	1353.85	12632.05	2973.08	2046.15	15494.87	6334.62	6878.21
Count	632	74	62	585	143	96	618	283	309
Confidence Level(95.0%)	0.96	2.90	2.31	1.07	2.61	2.66	1.14	1.45	1.32

Figure 4.4: Plot of maximum SCP size against distance from the closest Part A process

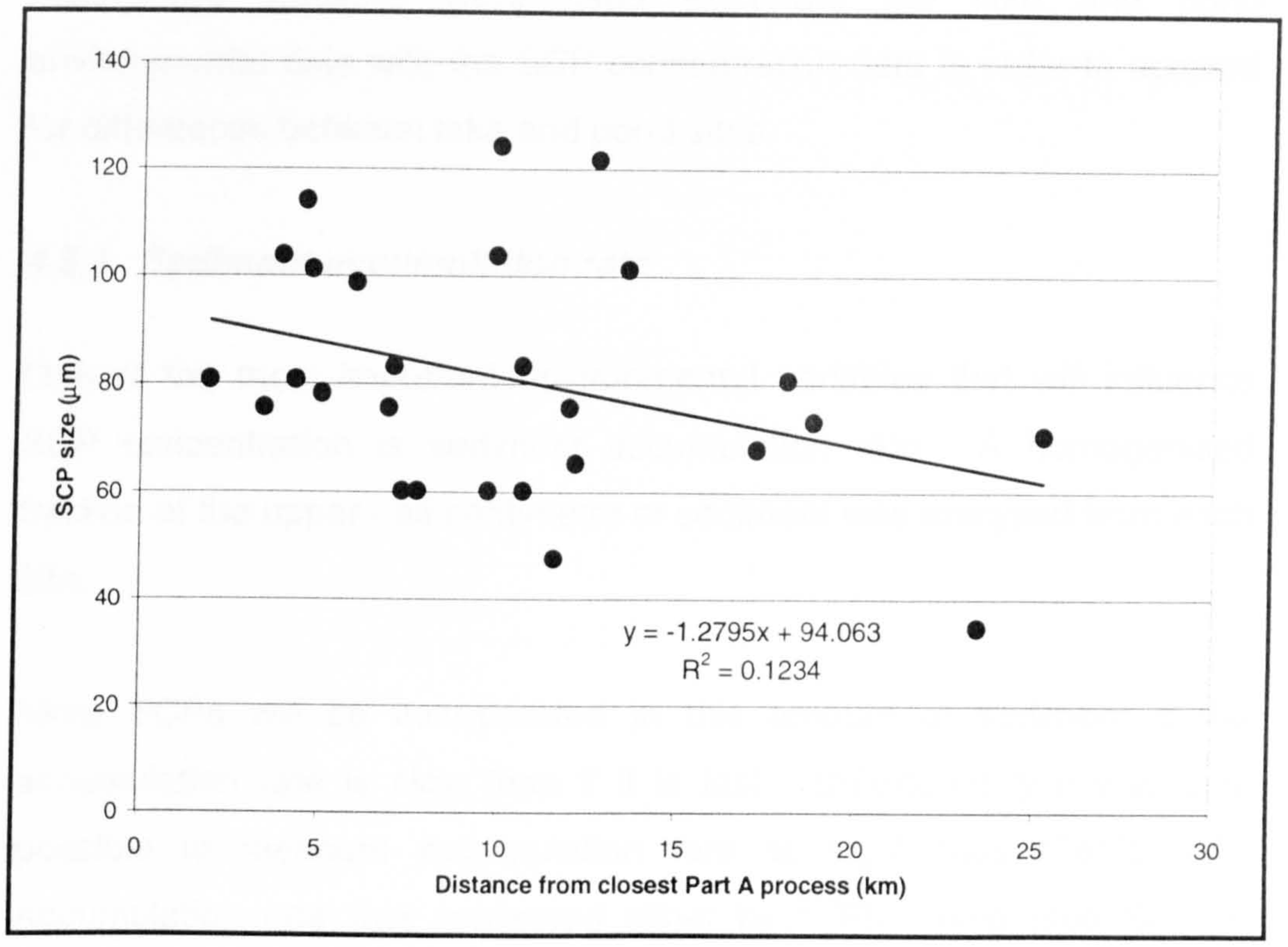

4.4.3 Kurtosis and Skewness

Kurtosis is a measure of the peak of a distribution compared with the normal distribution. All but two sites (CHER and SHEN) have positive kurtosis that means that the distributions are peaked with respect to the normal distribution (Table 4.3). Skewness is a second measure of deviation from the normal distribution. Distributions are either positively skewed which indicates that the distribution has more than half of its weight below the mean, for example as shown by a lognormal distribution; or negatively skewed where majority of the weight is above the mean. The distributions from all the sites are positively skewed showing that in each case the distribution tends towards a lognormal profile

4.5 Effect of lake and pond characteristics on SCP concentration

Multivariate statistics were used to relate the lake and pond environmental data with the SCP concentration data in order to account for differences between lake and pond sites.

4.5.1 Sediment accumulation rate

One of the most important environmental variables that will influence SCP concentration is sediment accumulation rate. A homogenised fraction of the upper half centimetre of sediment was analysed from each site.

More SCPs will be incorporated in this amount of sediment if the accumulation rate is slow than if it is fast. Unfortunately it was only possible to measure accumulation rate at eight sites (Table 4.4). Accumulation rate was measured either by ^{210}Pb dating (see Section 2.4.1) (at BREN and BANB only) or by physical measurement of the maximum depth of sediment and relating this depth to the time it took for that sediment to be deposited (see Section 2.4.2).

Since SCP concentrations will be affected by accumulation rates, it would be useful to compare SCP loadings from one site to another. This was not undertaken explicitly but instead was incorporated into a multivariate statistical analysis so that accumulation rate could be considered in combination with other environmental variables that might influence SCP concentration.

To this end an environmental data set was created that contained only those sites that had accumulation rate data. The other environmental variables available at those sites were lake area, percentage dry weight (%DW) and percentage loss on ignition (%LOI) (see Section 2.3.1), and these were also included in the analysis. The dependent variable is total

SCP concentration and so a similar data set was created for the same sites but containing just total SCP concentration.

Table 4.4: Sediment accumulation rate for eight lakes and ponds

Site	Accumulation Rate (mm yr^{-1})
BANB	3.16
BREN	2.90
BUSH	13.64
CROS	8.82
QUEE	10.96
RICH	28.75
STEN	34.88
WHITV	15.87

A step-wise multiple regression was performed using Canoco for Windows version 4 (ter Braak and Smilauer, 1998). The scaling was focussed on correlations between the SCP concentration data and the data were log transformed. The data were centred on SCP concentration and the SCP concentration scores were divided by the standard deviation, which gives each line of SCP concentration data equal weight in the analysis. Unrestricted Monte Carlo permutation tests were used to test the statistical significance ($p \leq 0.05$) of variables during forward selection. The objective of step-wise multiple regression is to attempt to create a model that will explain SCP concentration in the lakes and ponds that were sampled in London.

Table 4.5: Significant environmental variable selected by the step-wise multiple regression for eight lakes and ponds with SCP concentration as the dependent variable

Variable	Coefficient	Standard deviation	*p*-value	r^2
Area	56.57	114.80	0.005	0.48

The output of the forward selection showed that accumulation rate did not have a statistically significant relationship with SCP concentration at these sites, although it must be borne in mind that the data set is very small. The only significant variable ($p \leq 0.05$, 199 permutations) was lake area (Table 4.5), which on its own explained 48.0% of a total of 68.2% variation in the SCP data. The model is significant at $p \leq 0.05$ (199 permutations). This result suggests that other factors (in this case, lake area) are more important than accumulation rate for determining SCP concentrations in lakes and ponds across London.

4.5.2 Other environmental variables

Since accumulation rate is not a significant predictor of SCP concentration at sites where accumulation rate is known (Section 4.5.1) the analysis was extended to determine the impact of environmental variables on SCP accumulation at sites where accumulation rate is not known. Exploratory data analysis was carried out using environmental variables of lake area, maximum depth, core depth, %DW and %LOI and these data exist at twenty-four sites. BREN, DAGN, EALI are omitted from the analysis because maximum depth data were absent and it was felt that it may be an important explanatory variable.

Core depth and maximum depth were used to create the ratio core depth to maximum depth (C:M). The most accurate representation of the record of atmospherically deposited pollutants was shown to be usually found in cores taken from the deepest areas of a lake (Rose, 1999b). The C:M ratio will indicate whether there is a difference in concentration for cores taken at the deepest part of the lake or pond compared with those that were not. Lake area to maximum depth ratio (A:M) was calculated and will determine whether the effect of wind and wave action on the surface sediments will affect SCP concentration. If the area of the lake is large relative to its depth then A:M will also be large. Resuspension in lakes with a 'comparatively large' area relative to mean depth will be dominated by wind and wave action (Håkanson and

Jansson, 1983). %LOI and %DW will take into account the effects of dilution of the sediment by organic matter and water content respectively.

The correlations shown in Table 4.6 show that there are no significant relationships between SCP concentration and environmental variables. %DW and %LOI are negatively correlated with each other (r=-0.66, $p \leq 0.05$) suggesting that wetter samples contain a larger amount of organic material than drier samples.

Lake area is correlated with maximum lake depth (r=0.78, $p \leq 0.05$) showing that as the lake size increases then so does the lake depth. The depth that the core was taken from at most sites is the same as the maximum depth, which explains the correlation (r=0.72, $p \leq 0.05$) between core depth and lake area.

Table 4.6: Correlations between environmental variables and SCP concentration

	%LOI	%DW	Area	Max depth	Core depth	A:M	C:M	SCP conc^n
%LOI	1							
%DW	-0.66	1						
Area	-0.34	0.15	1					
Max depth	-0.34	0.14	0.78	1				
Core depth	-0.34	0.14	0.72	0.99	1			
A:M	-0.37	0.17	0.99	0.76	0.70	1		
C:M	-0.25	0.18	-0.18	0.02	0.08	-0.19	1	
SCP conc^n	0.20	-0.14	-0.18	-0.17	-0.17	-0.06	-0.05	1

Table shows values of r

Shaded correlations are significant at $p \leq 0.05$

The other significant relationships are between the A:M ratio and lake area, maximum lake depth and core depth.

4.5.3 *Principal components analysis (PCA) of SCP concentration and environmental data at twenty-four sites*

The object of a PCA is to find the combination of a number of variables to produce indices that are uncorrelated. The PCA technique combines these SCP size fractions and produces new indices that maximise the variation in the original variables. The original data are then plotted against the new indices that take the form of principal component axes. The first axis represents the maximum variance and therefore is the most important of all the components for representing the variance in the data. The second axis explains less variance and is not correlated with the first axis. This means that whatever mechanism is driving the variation in the first axis is unrelated to the mechanism driving the second axis, the same rules apply to further axes.

PCA is widely used to explain patterns in data. For example, PCA is used in the creation of temporal synoptic indices for the synoptic classification of meteorological variables (e.g. Kalkstein et al., 1987; Cheng and Lam, 2000). Long (1998) used PCA to determine the chemical signatures of particles in urban aerosol. More specifically, Rose (1991) used PCA to characterise the chemical characteristics of coal- and oil derived SCPs in order to devise a classification based on fuel type.

Figure 4.5 shows a PCA biplot of SCP concentration and environmental variables. As before (Section 4.5.1), the scaling was focussed on correlations between environmental variables and a log transformation was carried out on the environmental data. The data were centred on total SCP concentration and the total SCP concentration scores were divided by the standard deviation. There are several methods that can be used to determine the number of axes that should be retained to explain the data. For example, the axes retained should explain between about 70% and 90% of the variation in the data. In this case the 1st axis explains 76.7% of the variance and so fulfils this criterion

alone. The 2nd axis explains 15.8% and the 3rd and 4th axes in combination only contribute an additional 9.1%. This makes a total of 99.8% of the variation, although some of the explanation is spurious due to correlations between variables. An alternative method for selecting axes is the broken stick method (BSTICK, Jackson (1993)) which divides the total variance (variance = 1 for PCA) randomly between the axes. If the eigenvalue of the axis is greater than that predicted by BSTICK then that axis is significant. It was found in this analysis that, once again, only the 1st axis is significant.

Figure 4.5: PCA biplot of SCP concentration and environmental variables

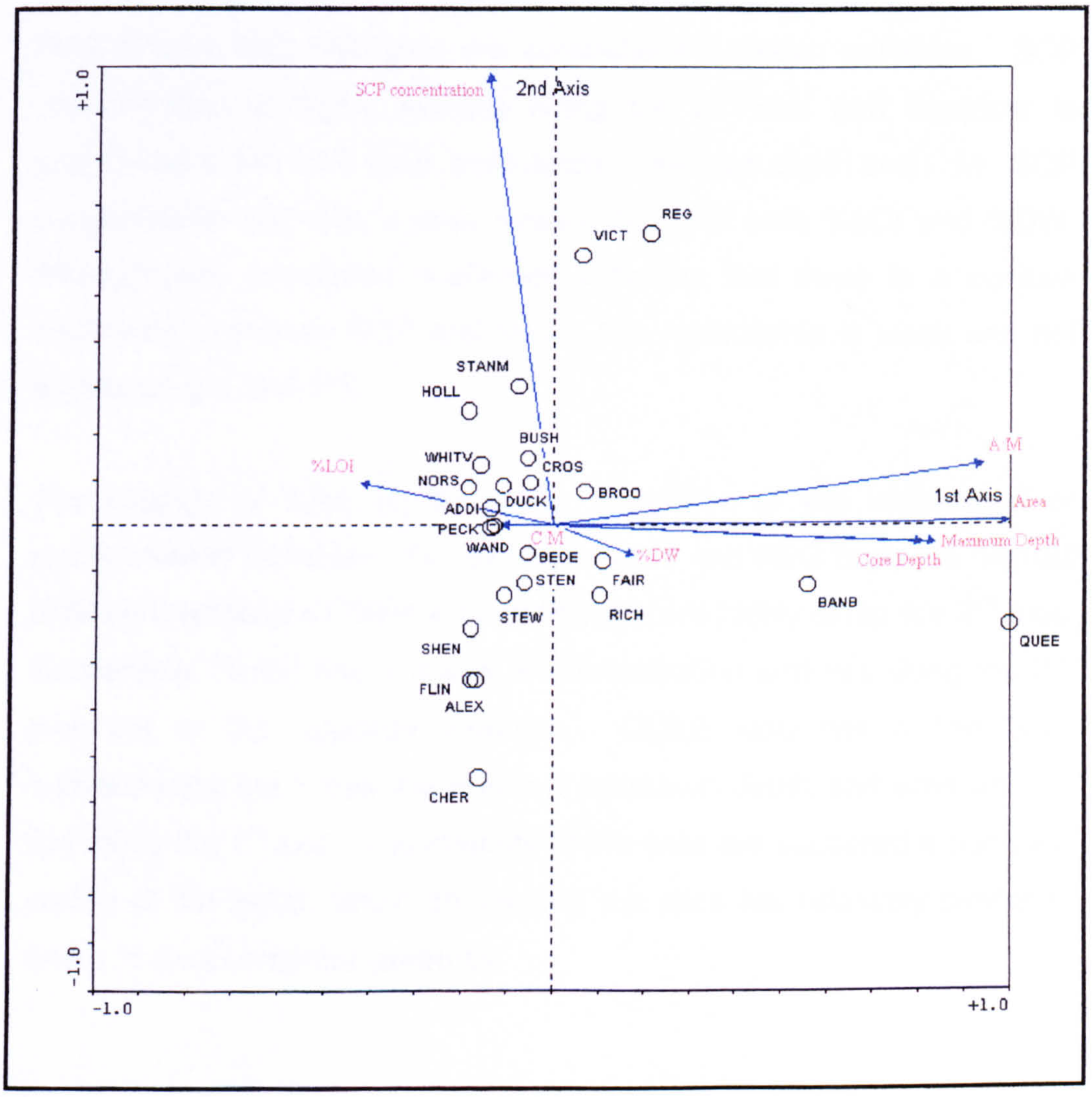

A:M, area, core depth and maximum depth are all highly variable along the 1st axis. The length of the arrow indicates the amount of variation in that variable. Variables that have arrows in a similar direction are correlated and information on the biplot agrees with the correlation data in Table 4.5. These variables are negatively correlated with C:M although only the correlation coefficients for C:M with area or A:M are negative (r=-0.18 and -0.19 respectively). The correlation coefficients for C:M with maximum depth or core depth are small and positive (r=0.02 and 0.08 respectively). None of these correlation coefficients are significant ($p \leq 0.05$) and so these relationships must be interpreted with caution.

Although the 2nd axis is not significant in this analysis, examination of the PCA (Figure 4.5) highlights the correlations between variables. SCP concentration is highly variable along the 2nd axis and therefore is uncorrelated with A:M, area, core depth, maximum depth and C:M. SCP concentration also has a poor relationship with both %LOI and %DW. Although the correlation coefficient indicates that there is a positive relationship between SCP and %LOI, this relationship is weak and not significant (i.e. $p>0.05$).

The location of sites on the biplot is related to the importance of environmental variables. For example, VICT and REG have the highest SCP concentrations (Table 4.1) and they score highly along the 2nd axis. Conversely, CHER has a low SCP concentration and lies along the 2nd axis but in the opposite direction. QUEE also has a low SCP concentration but it has the greatest maximum depth and area and so lies along the 1st axis. The majority of the sites are scattered around the centre of the biplot, which shows that the sites are relatively similar in terms of environmental variables.

4.5.4 Multiple linear regression of SCP concentration and environmental data at twenty-four sites

The multiple linear regression approach in Section 4.5.1 was extended to include those sites that do not have accumulation rate data. SCP concentration once again was the dependent variable. None of the environmental variables showed a significant ($p \leq 0.05$) relationship with SCP concentration. If the multiple regression was performed without forward selection to test the significance of each environmental variable then all the environmental variables in combination account for only 44.8% of the variation in SCP concentration.

4.6 Principal components analysis of SCP size fractions in lakes and ponds in London

The SCP size distribution data described in Section 4.3.1 is complex and therefore difficult to interpret. Some of the sites appear to have similar distributions and some of the SCP size groups are highly correlated (Table 4.2). There is a major peak at most of the sites at a number of similar SCP sizes and there are few SCPs at higher sizes at any of the sites. However, upon closer examination there are many differences between sites and there are therefore no clear patterns that can be brought out by visual examination alone. The data were examined by PCA to determine any inter-lake and pond relationships in the size distribution data. The variables for each lake and pond are the SCP sizes and the number of SCPs in each size fraction varies from site to site.

The SCP size fractions have been combined to reduce the number of variables from 50 to 25. The size fraction 0-5.12 μm is represented by n1; 5.12-10.24 μm is n2 and so on (see Table 4.7). This will have the effect of comparing the moving average data (Section 4.3) and will smooth out some of the incongruities caused by the counting method. The data have been standardised by using percentage count data to remove the effect that SCP concentration will have on the PCA. This

prevents the sites that have larger SCP concentrations from having extra weight in the analysis. Usually, percentage data are avoided in PCA because the variables will not be independent, however in this case, it is the distribution of the size data that is important and this will not be affected by converting concentrations into percentages (Birks pers. comm.). Each SCP size fraction is treated as if it is a species where the presence or absence of a value (in this case percentage) of SCPs is a variable.

Figure 4.6: PCA biplot of the SCP size fractions in the surface sediments of twenty-seven lakes and ponds in London

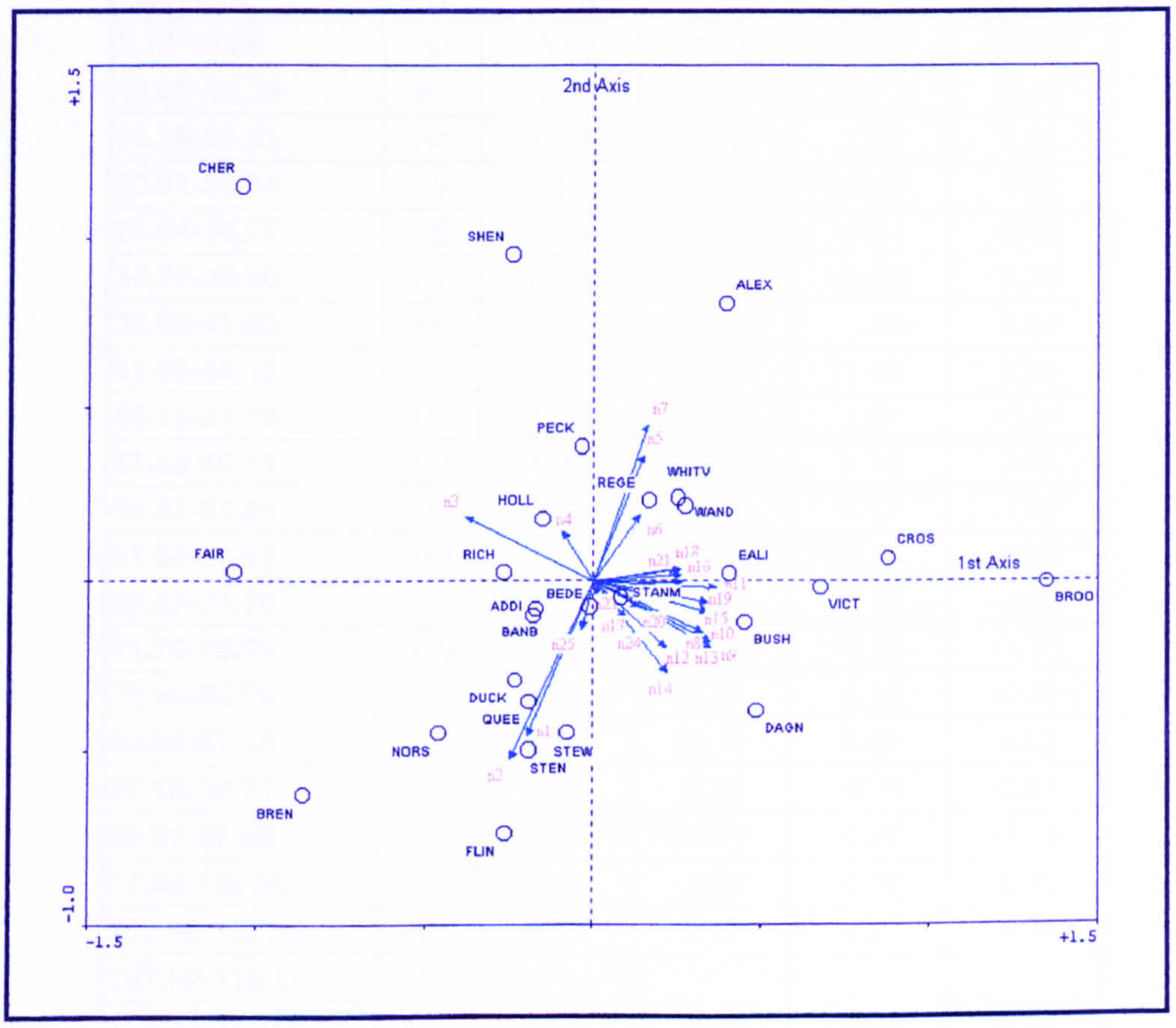

Scaling was based on inter-sample distances, which preserves the Euclidian distance between sites. This means that the distance between sites on the PCA biplot approximates the distance between sites in m-dimensional space (Jongman et al., 1995). The data were square root transformed to give less weight to dominant species. The 1st and 2nd

axes represent 28.1% and 19.2% respectively of the total variance in the original data set. The 3rd and 4th axes explain a further 20.5% of the variance. The first four axes that are the output from Canoco for Windows were shown to be statistically significant using the broken stick model as before. The variable loadings for the first four principle components are shown in Table 4.7. Figure 4.6 shows the PCA biplot of the first two axes of SCP percentage counts in the surface sediments.

Table 4.7: Variable loadings for the 1st, 2nd, 3rd and 4th principle components from the PCA of the SCP size data

Size (μm)	Code	1st Axis	2nd Axis	3rd Axis	4th Axis
Total		0.28	0.19	0.11	0.09
0.00-5.13	n1	-0.70	-1.61	0.38	1.52
5.13-10.26	n2	-0.89	-1.85	-0.60	-0.60
10.26-15.38	n3	-1.36	0.68	0.71	-0.62
15.38-20.51	n4	-0.34	0.52	1.66	1.36
20.51-25.64	n5	0.52	1.30	-0.82	0.33
25.64-30.77	n6	0.49	0.68	-1.14	-0.92
30.77-35.90	n7	0.58	1.60	-0.89	0.76
35.90-41.03	n8	1.15	-0.53	-1.66	1.23
41.03-46.15	n9	1.25	-0.63	1.63	0.60
46.15-51.28	n10	1.20	-0.32	1.07	-0.58
51.28-56.41	n11	1.30	-0.08	1.12	0.70
56.41-61.54	n12	0.77	-0.70	0.57	-1.07
61.54-66.67	n13	1.24	-0.68	-0.26	-0.30
66.67-71.79	n14	0.78	-0.95	-0.43	-2.02
71.79-76.92	n15	1.20	-0.23	-0.18	-1.15
76.92-82.05	n16	0.93	0.07	0.10	-0.41
82.05-87.18	n17	0.04	-0.16	0.82	1.13
87.18-92.31	n18	0.93	0.12	-0.11	-0.51
92.31-97.44	n19	0.94	-0.01	-0.20	-1.18
97.44-102.56	n20	0.48	-0.26	-0.36	-0.45
102.56-107.69	n21	0.88	0.12	-0.27	-0.90
107.69-112.82	n22	-	-	-	-
112.82-117.95	n23	0.06	-0.05	-0.10	-0.07
117.95-123.08	n24	0.34	-0.39	0.17	0.04
123.08-128.21	n25	-0.13	-0.51	0.67	1.06

The size fractions that have a high loading on the first principle component will be responsible for the majority of the variance in the

data. The location of a site along the axes and along the lines represented by the size fractions shows the score of that site.

The size fractions between 35.90 µm and 107.69 µm (n8-n21 respectively) and 117.95-123.08 (n24) are grouped together with similar directions and variances. These groups contribute the greatest amount to the variance of the 1st axis, showing that these size fractions contain the greatest amount of variance in the data set. As the size fraction increases the arrows become shorter indicating a decrease in variation. The direction of the arrows gradually changes to point along the 2nd axis as the fraction reaches 112.82-117.95 µm (n23) and 123.08-128.21 µm (n25). The highest fraction 123.08-128.31 µm (n25) follows the 2nd axis, in a similar direction to n1 and n2, but shows much less variation than these smaller fractions. This shows that these size fractions are correlated and suggests that, at sites where the smallest size fractions dominate, deposition of the large size fractions is also important.

Negatively correlated with the n8-n21 are 10.26-15.30 µm (n3) and 15.38-20.51 µm (n4). Negative correlation indicates that a large percentage in one of the size fractions is associated with a low percentage in the negatively correlated size fraction and vice versa. The 2nd axis is dominated by size fractions 0-10.26 µm (n1-n2) and, in the opposite direction, 20.51-35.90 µm (n5-n7). These size fractions have no relationship to the size fractions n3-n4 and n8-n21, suggesting that these size fractions are controlled by different source processes.

The location of sites on this biplot shows the importance of particular size fractions at each site. Sites that are close together in Figure 4.6 will have similarities in their SCP size distributions (Figure 4.3). BROO, CROS, VICT, BUSH and EALI all lie along the 1st axis indicating that these sites have the highest percentages for n8-n21 and n24. High percentages in large size fractions would suggest that there is a local SCP source. FAIR and CHER lie in the opposite direction along the 1st

axis and have relatively low percentages in these fractions. Correspondingly CHER and FAIR score highly along the directions of the n3 and n4 arrows, which shows that their distribution patterns have greater percentages in the 10.26-20.51 µm size fraction. CHER also scores highly along the 2nd axis, which is caused by the lack of SCPs at CHER in size fractions greater than 38.40 µm (Figure 4.3h).

REG, WHITV and WAND are close together on the biplot and lie along the line indicated by n6 (25.64-30.77 µm). Comparison with the SCP distribution profiles shows that WHITV and REG have similar profiles (Figures 4.3aa and 4.3s respectively) that appear to be made up of a single distribution. The distribution pattern at WAND varies more and appears to have two distribution components. ALEX lies in a similar direction to REG, WHITV and WAND but has a very different distribution profile, the only similarities being the dominance of n5-n7 size fractions.

4.7 Relationship between sedimentary SCP size and modelled SCP deposition from power stations and other Part A processes

In this section the particle size breakdown of the SCPs found in lake and pond sediments is compared with modelled deposition of a range of sizes of SCPs (see Chapter 3) to those lake and pond sites. Table 4.8 shows the correlation matrix between modelled deposition of a range of SCP sizes and the size fractions of SCPs in the surface sediments. The correlation used in this study is the Pearson product-moment correlation.

4.7.1 Correlations between size fractions of modelled SCPs and size fractions of SCPs in sediments

Significant correlations (shaded boxes, Table 4.8) between the total concentration of SCPs and predicted deposition in all size fractions are positive and range between 0.52 and 0.56. The highest correlations are between the SCP concentration size fraction of 35.90-46.15 µm and deposition of SCPs with a diameter of 90 µm (r=0.62). However, for

each concentration size range the effect of changing the size of deposited SCPs has very little effect on value of r. For example, the concentration size fraction 35.90-46.15 µm has a range of r between 0.59 and 0.62.

The range of r for some of the other concentration size fractions is wider, e.g. 56.41-64.10 µm has r ranging between 0.47 and 0.54. These results show that variation in the pattern of predicted emissions due to SCP size is very small compared with the actual concentrations found in lakes and ponds. This is confirmed by the presence of high values of r (all greater than 0.97) in the inter-variable correlation matrix of size fractions of predicted deposition (Table 4.9).

Although the variation in r is small for the relationships between SCP deposition and each of the concentration size fractions (Table 4.8) there is a gradient in the correlation matrix from top to bottom, i.e. for each SCP concentration fraction there is little change in r with increasing deposition size. For SCP concentrations smaller than 46.15 µm the highest value of r occurs with deposition of 90 µm sized SCPs, whereas concentrations above 56.41 µm the best relationship is with 100 µm deposition. This shows that, generally, the relationship between predicted and actual improves slightly as the modelled SCP size increases. The reasons for this relationship are unclear. Since there is very little variation in the correlation coefficient between SCP deposition and concentration for changes in concentration size then the improvement in relationship with an increase in deposition size is unimportant. The value of r is not significant when the concentration of SCPs in the range 64.10-74.35 µm is compared with modelled deposition of SCPs smaller than 50 µm, whereas the relationship becomes significant (r = 0.39-0.44) for deposition of SCPs larger than 60 µm.

Table 4.8: Correlation matrix of deposition from power stations and other Part A processes with concentration of size fractions of SCPs in surface sediments

		SCP in surface sediments (μm)												
		Total	0-5.13	5.13-15.38	15.38-25.64	25.64-35.90	35.90-46.15	46.15-56.41	56.41-64.10	64.10-74.35	74.31-84.61	84.61-94.87	94.87-105.13	> 105.13
Deposition of SCPs from all power stations (μm)	5	0.52	-0.05	0.44	0.52	0.54	0.59	0.50	0.47	0.37	0.50	0.17	0.04	-0.09
	10	0.52	-0.05	0.44	0.52	0.54	0.59	0.50	0.48	0.37	0.50	0.17	0.04	-0.09
	20	0.52	-0.05	0.44	0.52	0.54	0.59	0.50	0.48	0.37	0.50	0.17	0.04	-0.09
	30	0.52	-0.05	0.44	0.52	0.54	0.59	0.50	0.48	0.37	0.50	0.17	0.04	-0.10
	40	0.52	-0.05	0.44	0.52	0.54	0.59	0.50	0.48	0.37	0.50	0.17	0.04	-0.10
	50	0.52	-0.05	0.44	0.52	0.54	0.59	0.51	0.48	0.37	0.50	0.18	0.05	-0.10
	60	0.53	-0.04	0.45	0.53	0.55	0.60	0.52	0.49	0.39	0.51	0.18	0.05	-0.09
	70	0.54	-0.04	0.46	0.54	0.56	0.60	0.52	0.49	0.39	0.51	0.19	0.06	-0.09
	80	0.55	-0.03	0.47	0.55	0.57	0.61	0.53	0.50	0.41	0.52	0.20	0.07	-0.08
	90	0.56	-0.02	0.48	0.56	0.58	0.62	0.54	0.53	0.43	0.53	0.22	0.09	-0.06
	100	0.55	-0.02	0.47	0.55	0.58	0.61	0.54	0.54	0.44	0.54	0.24	0.11	-0.04

Table shows values of r

Shaded correlations are significant at $p \leq 0.05$

Table 4.9: Correlation matrix of deposition of size fractions of SCPs from power stations and other Part A processes

		Modelled deposition of SCPs from all sources (μm)										
		5	10	20	30	40	50	60	70	80	90	100
Modelled deposition of SCPs from all sources (μm)	5	1.00										
	10	1.00	1.00									
	20	1.00	1.00	1.00								
	30	1.00	1.00	1.00	1.00							
	40	1.00	1.00	1.00	1.00	1.00						
	50	1.00	1.00	1.00	1.00	1.00	1.00					
	60	1.00	1.00	1.00	1.00	1.00	1.00	1.00				
	70	1.00	1.00	1.00	1.00	1.00	1.00	1.00	1.00			
	80	0.99	0.99	0.99	0.99	0.99	1.00	1.00	1.00	1.00		
	90	0.99	0.99	0.99	0.99	0.99	0.99	0.99	0.99	1.00	1.00	
	100	0.97	0.98	0.98	0.98	0.98	0.98	0.98	0.98	0.99	1.00	1.00

Table shows values of r

Shaded correlations are significant at $p \leq 0.05$

4.7.2 Effect of size of SCP actual concentration on correlation with predicted SCP deposition

A change in the actual sediment SCP size fraction produces a range of values of r for each modelled deposition size (Table 4.8). For example, 5.13-15.38 µm has a range of r between 0.44 and 0.48 compared with 35.90-46.15 µm where r = 0.59-0.62. The relationship between SCP concentrations in the fraction 0-5.13 µm and any of the predicted deposition SCP sizes is small, negative and not significant at $p \leq 0.05$. The same relationship is true for the correlations between SCP concentrations in the size fraction larger than 105.13 µm and any of the predicted deposition SCP sizes.

4.7.3 Relationships between summary statistics and modelled deposition

Table 4.10 shows the correlation matrix of selected summary statistics and modelled deposition of power station and other Part A Process emissions. Comparing the statistical properties of the distribution with SCP deposition will further test whether it is possible to relate predicted deposition to the shape of the distribution.

Table 4.10: Correlation matrix of summary statistics and modelled deposition of SCPs from all sources

		Mean	Median	Mode	Kurtosis	Skewness	Min	Max
Modelled deposition (µm)	5	0.29	0.31	0.16	-0.07	-0.04	0.13	0.12
	10	0.29	0.32	0.16	-0.07	-0.05	0.13	0.12
	20	0.29	0.32	0.16	-0.07	-0.05	0.13	0.12
	30	0.29	0.32	0.16	-0.07	-0.05	0.13	0.12
	40	0.29	0.32	0.16	-0.07	-0.05	0.13	0.12
	50	0.29	0.32	0.16	-0.07	-0.05	0.13	0.12
	60	0.30	0.32	0.16	-0.07	-0.04	0.13	0.13
	70	0.30	0.33	0.17	-0.06	-0.04	0.12	0.13
	80	0.30	0.33	0.17	-0.05	-0.03	0.11	0.14
	90	0.32	0.36	0.17	-0.04	-0.02	0.11	0.16
	100	0.36	0.39	0.18	-0.04	-0.03	0.14	0.18

Table shows values of r.
Shaded correlations are significant at $p \leq 0.05$

The correlations between deposition and statistical values are weak and insignificant with one exception between 100 µm deposition and median ($r=0.39$, $p\leq0.05$). This shows that there is a weak relationship between the middle of the distribution and the deposition of 100 µm particles at each site. It has been shown (Section 4.3.1) that the pattern of modelled deposition does not vary considerably with SCP size. This is reflected in the correlation matrix (Table 4.2) where the range of values of r is small for changing SCP size. In general r increases with SCP size for mean, median, mode and maximum and decreases for kurtosis and skewness. The relationship of minimum with size is more complex but since r is low and insignificant it does not merit further discussion.

4.7.4 PCA of SCP concentration, environmental data and SCP deposition data at twenty-four sites

Since the environmental variables do not explain the spatial variation in SCP concentration the hypothesis that SCP concentration is driven by deposition was tested. The correlations between SCP concentration and modelled deposition are described in Section 4.3.1. The environmental variables will have no bearing on modelled deposition and vice versa since the two data sets are independent. However, inclusion of deposition data in a PCA in addition to the environmental variables may contribute to a better explanation of SCP concentration.

Figure 4.7 shows a PCA biplot of SCP concentration, environmental data and modelled SCP deposition. The 1st axis explains 65.0% of the variation in the data and the 2nd axis explains 26.5%. The 3rd and 4th axes were not significant when tested using BSTICK. All deposition variables score highly along axis 1 and are all highly correlated (see Table 4.2).

Figure 4.7: PCA biplot of SCP concentration, environmental data and modelled SCP deposition

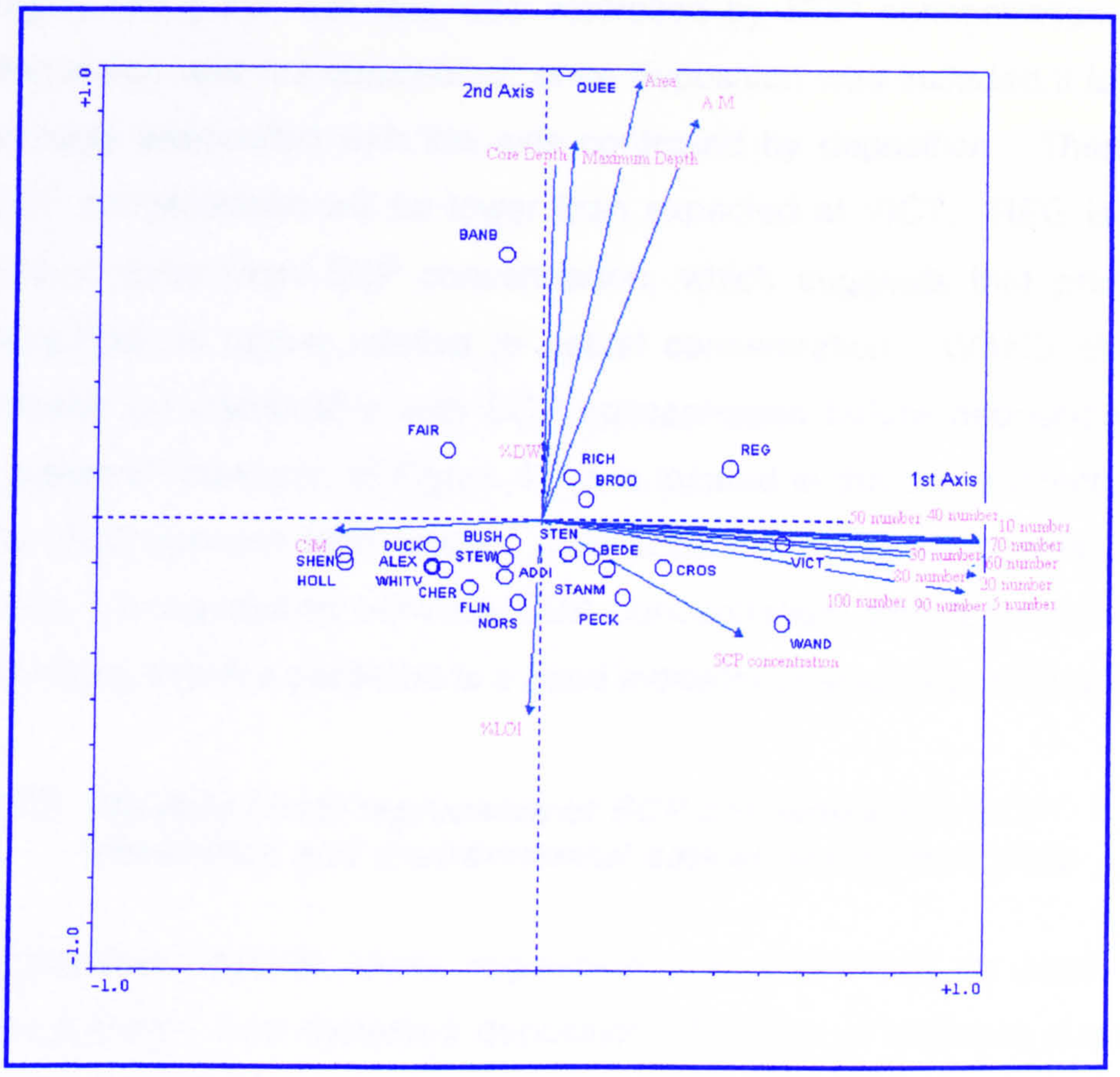

The arrow for SCP concentration lies in a similar direction to predicted deposition of all size fractions, which confirms the relationship between SCP concentration and predicted deposition as discussed in Section 4.3.1. Area, maximum depth, water depth and area/maximum depth have no relationship with the deposition data and score highly along the 2nd axis. %DW lies along the 2nd axis but the arrow is not as long and therefore the data do not show so much variation. %LOI also lies along the 2nd axis but in the opposite direction to the other environmental variables due to its negative correlation with %LOI. C:M is negatively correlated with predicted deposition suggesting a link between these two variables. However, this relationship is coincidental because neither of these two variables is dependent on the other.

The locations of sites on the biplot in comparison with their locations in the previous biplot without modelled SCP deposition (Figure 4.5) show how the predicted diverges from the actual. Whereas VICT scored highly along the axis that was controlled by SCP concentration when deposition was not considered, once deposition was included it is more strongly associated with the axis controlled by deposition. Therefore, SCP concentration will be lower than expected at VICT. REG is even further away from SCP concentration, which suggests that predicted deposition is higher relative to actual concentration. WAND showed virtually no relationship with SCP concentration before deposition was considered however, in Figure 4.7 it is located in the same direction as the SCP concentration arrow. This shows that WAND scores highly along the correlation between SCP concentration and deposition and, therefore, that the predicted is a good indicator of actual concentration.

4.7.5 Multiple linear regression of SCP concentration, SCP deposition and environmental data at twenty-four sites

A stepwise multiple linear regression was performed on total SCP concentration and modelled deposition of SCPs of different sizes for twenty-four lakes and ponds with SCP as the dependent variable (Table 4.11). The environmental variables were included in the analysis to determine whether any of the variation could be explained by environmental factors once any contribution from deposition had been accounted for.

Table 4.11: Significant environmental variables selected by the step-wise multiple regression for twenty-four lakes and ponds with SCP as the dependent variable

Variable	Coefficient	Standard deviation	*p*-value	Simple r^2	Sequential r^2
100 μm SCP dep^n	0.94	0.10	0.015	0.27	0.27
C:M	131009.50	144606.97	0.050	0.14	0.41

This result shows that deposition of 100 µm SCPs is the main predictor of total SCP concentration. Since predicted deposition of different sized SCPs are highly correlated with each other (Figure 4.6), another size fraction could be substituted for 100 µm. The deposition variables are not contributing uniquely to the explanation of the variance in SCP concentration. The forward selection procedure will only select one environmental variable that best explains the variation in the dependent variable and, therefore, removes any spurious explanations due to co-linear variations in the deposition data. Therefore, 100 µm is selected by the step-wise regression because correlation increases with predicted deposition size (see Table 4.8). Selection of C:M by the model shows that the depth at which a core is taken is related to SCP concentration.

4.8 Discussion

4.8.1 SCP concentrations in lake and pond surface sediments

Lake and pond sediments are a dynamic environment affected by within-lake or pond processes and within-sediment processes in addition to external forces such as atmospheric and catchment inputs. The effects of climate, altitude and nutrient input as well as many other factors combine to make each lake and pond into a unique environment. Despite these lake specific processes, this study has shown that total SCP concentration has a good relationship with predicted deposition from all sources for all size fractions ($r=0.52$-0.56, $p \leq 0.05$).

The forward selection procedure incorporating twenty-four sites (Table 4.11) showed that 100 µm SCP deposition explained 27% of the total variance in SCP concentration. However, in combination, the environmental variables explained 75% of the total variation in SCP concentration. This shows that although SCP deposition is the driving force behind SCP concentration there is still a contribution from the lake and pond processes.

Core depth to maximum lake depth ratio (C:M) was the only lake and pond environmental variable identified as contributing significantly to variation in SCP concentration (14% of the total).

However, in this study there was not much variation in bathymetry because most of the lakes and ponds used were artificial. Most of the cores were taken from the deepest point but this may have been similar in depth to the rest of the lake or pond. Therefore, the relationship between C:M and concentration may be coincidental. The remaining 34% of the variation not accounted for by significant individual variables is caused by the remaining variables in combination, in particular some of the explanation is due to correlations between deposition variables.

The unexplained variation in SCP concentration is due to other environmental variables that have not been considered or errors in either the SCP concentration data or the predicted deposition data. The causes of the unexplained variation are discussed in the following sections.

4.8.2 Environmental variables

The environmental variables used in the forward selection for twenty-four sites were lake area, maximum depth, core depth, %DW and %LOI. There are a number of other lake and pond variables that would possibly affect the concentration of SCPs in the study sites. For example, lake altitude, sulphur deposition, annual rainfall and lake area had a significant relationship with SCP deposition in Scottish lakes (Rose and Juggins, 1994). Site altitude was not included in this study because it was almost constant across London and, therefore, would not have contributed to the explanation of SCP concentration. Sulphur deposition data were not available in this study. Annual rainfall will affect sedimentation through the amount of run-off in the catchment that carries sediment into the lake or pond. The effects of run-off in London are not known. The presence of paved areas surrounding the lakes and

ponds may make run-off more significant, or alternatively the presence of drainage systems around each site might divert run-off into the sewage system. It was not included in the model because it was impossible to determine the rainfall at each site over the areas covered by the M25. The rainfall in 1996 was not identical at the three meteorological stations in London (Gatwick, Heathrow and the London Weather Centre). To what extent one of the sites in this study is influenced by the meteorology at a particular weather centre is uncertain.

Lake area was extracted as the only significant predictor variable in the forward selection involving the eight sites that had accumulation rate data. This analysis contained the sites BREN, BANB and QUEE which are reservoirs that have very large surface areas upon which SCPs will fall from the atmosphere. These sites do not have correspondingly large catchments to provide particulate matter because they are located in very artificial environments. Both BANB and QUEE are raised basins that sit on top of the surrounding landscape and are surrounded by a rim that is only a few metres wide. The predominant source for particles is atmospheric deposition. BREN differs slightly to QUEE and BANB in that it was created by flooding an existing river valley, however, it is surrounded by a complex network of roads and drainage systems that will channel the water away from the reservoir to protect water quality from polluting run-off. As a result, SCP concentrations are not diluted by sediment from the catchment and this is confirmed by the relationship between accumulation rate and lake area such that accumulation rate decreases as lake area increases. Once deposition is included as an environmental variable in a forward selection analysis for the twenty-four sites then the relationship between lake area and SCP concentration becomes insignificant.

4.8.3 Within-site spatial patchiness

Accumulation rate varies across the lake basin and is affected by the properties of the lake or pond, in particular by the bathymetry of the

basin, it's size and orientation and by climatic conditions (Sly, 1978). Studies of varved sediments from a Swedish Lake (Petterson et al., 1993) showed that spatial variability of sediment accumulation was very low. Although Downing and Rath (1988) showed that there was considerable spatial heterogeneity in the water and organic matter content, pigment and phosphorous concentrations of sediments from the same site with up to 320 times greater variance than caused by analytical or microscale variation. Spatial non-uniformity of sediments was also indicated in diatom studies of a small lake in Northern Ireland (Anderson, 1990) implicating the importance of diatom source communities to the sediment record and that whole-lake mixing and resuspension do not effectively create uniform diatom concentrations. SCP concentration has been shown to vary within the surface sediments within the small area of a basin of a remote lake in Scotland (Rose et al., 1999b). Wik and Renberg (1991) showed that SCPs are focussed into the deepest part of the lake basin in their study of three Swedish lakes. Models have been developed that predict sediment distribution in large lakes (Håkanson and Jansson, 1983).

There are many other studies that have investigated spatial patchiness using approaches that include volcanic ash (Kimmel, 1978) and pollen (Davis and Ford, 1982) but these studies have all been carried out on natural systems. The models proposed by Håkanson and Jansson do not apply to small lakes or ponds. Bennion et al. (2001) linked poor radionuclide records in small, natural lakes to sediment disturbance by wind stress and sediment resuspension due to the shallow nature of the lakes.

The lakes and ponds used in this study have all been modified in some way and have catchments that are limited by the surrounding artificial urban drainage system. Therefore, comparison with natural systems is not strictly relevant, although these studies are referred to in the absence of similar studies on artificial systems. Catchment was not included as a variable in the analyses because the catchment area was

impossible to measure without undertaking a detailed study of the drainage system, which was beyond the scope of this project. It may be more realistic to treat lakes and ponds in the urban environment as if they are individual basins without a significant catchment.

SCP concentration of the sediments of even the largest lakes in this study will not depend on variation of atmospheric input within a site. However, the C:M ratio used in forward selection of the twenty-four variables showed that core location has a significant influence on SCP concentration (accounting for 14% of the variation once the effects of deposition or 100μm particles has been removed), therefore suggesting that the SCP concentration may not be uniform across each site. Where possible in this study the sediment sample was taken from the centre of the lake or pond for both consistency and because the SCP cores taken from the deepest point usually provide the best historical records in natural systems (Rose, 1999b). These results indicate that there may be local catchment effects and inflows that have not been taken into account that are having an effect on SCP concentration.

4.8.4 Inter-lake sediment variability

The action of bioturbation within the surface sediment (e.g. Davis, 1974; Fisher et al., 1980), and mixing caused by water currents and gas bubbles creates a time averaging effect on the SCP record (Rose, 1991). The majority of the lakes sampled by Rose had very low accumulation rates in comparison with the rates known for the sites in this study (0.63 mm yr^{-1} in Scotland compared with between 2.90 and 34.88 mm yr^{-1} in London). Therefore it is likely that the sediments in this study are less likely to suffer from the effects of mixing. The consequences of mixing may have a significant effect at sites where there is a long temporal record (e.g. BANB and BREN) since the spatial distribution of power stations, the fuels combusted and the abatement technology has changed considerably in the last 100 years (see Chapter 1 for more details). At most sites the sediment only covers a short time

period and so the effects of mixing will not be so severe. A more significant problem is that of physical disturbance through dredging or if the sediments are directly disturbed if the lake or pond has dried out.

4.8.5 Local meteorological factors

The local meteorology of each site is complex and will influence SCP concentration by affecting the transporting air currents. For example, if buildings or trees surround a site, their size and proximity will control the airflow and affect SCP deposition (see Chapter 3). A detailed meteorological study was not undertaken in this study and so the effects are unknown.

4.8.6 Deposition errors

The lack of variation in the predicted spatial deposition pattern for different SCP size fractions (see Chapter 3) accounts for the consistency seen in the correlation coefficients produced by comparing actual concentrations with predicted. Dispersion modelling can only reflect an idealised environment. For example, in this study the effects of topography were not taken into account because the Thames Corridor is relatively uniform (see Figure 3.4) but considering the extent of the study area it is likely that topography will have an effect even if it is relatively minor. In particular, the presence of hills between Didcot and London will present a barrier to the movement of pollution but this has not been accounted for in the model. The urban topography will also affect movement of pollution (see Section 3.9.1) and has not been taken into account.

Small size fractions in sediments may be under-represented because they may agglomerate close to the source and then behave as larger particles that cannot travel as far. Alternatively, it is difficult to identify small (<2.5 μm) SCPs using an optical microscope at a magnification of 400x and so that fraction may be missed. Another explanation is that

the high temperatures, long residence times and oxidising conditions inside modern boilers effectively remove the elemental carbon content of fly ash from pulverised coal combustion (Ohlstrom et al., 2000), and the same may be true for oil combustion. Although the presence of SCP in the environment shows that elemental carbon cannot be completely removed.

4.8.7 Relationship of SCP size fraction and SCP source

The SCP data are in percentage form, which means that if a site has a high score for a particular size fraction it is high relative to the other size fractions and not just high due to elevated levels in all size fractions. BREN, NORS, FLIN, STEN, STEW, QUEE and DUCK score highly in the n1-n2 (0.00-10.26 μm) direction. In comparison with the modelled deposition data these sites are not significantly affected by power stations or other Part A Processes. Similarly, CHER, SHEN and FAIR score highly in the direction if n3-n4 (10.26-20.51 μm), and ALEX lies along the line of n5-n7 (20.51-35.90 μm), these sites also do not expect to receive high levels of deposition. These SCPs are relatively small and will be able to travel for long distances (see Chapter 3) and therefore may have a more distant source. The arrow for n25 (123.08-128.21 μm) lies in the same direction as n1 and n2 but this is probably co-incidental due to the small numbers of SCPs found in the n25 size fraction.

In contrast, VICT, CROS and BROO score highly in the direction of n8-n21 (35.90-107.69 μm) and n24 (117.5-123.08 μm) and these are located at sites that are predicted to receive greater levels of SCP deposition. These sites are close to Littlebrook power station and Ford in East London (see Figure 3.4) and the larger particles will originate from these sources.

REG, WHITV and WAND all lie mid-way between the n8-n22, n28 cluster of arrows and the n5-7 (20.51-35.90 μm) arrows, but do not score

particularly highly for each. Therefore, both the medium sized and larger SCPs are equally important. These sites are located close to each other in the centre of London and are surrounded by London Underground Chelsea, London Underground Greenwich and Citigen. They are all predicted to have high levels of deposition of all sizes of SCPs. The n5-7 (20.51-35.90 μm) size fraction appears to be important for both high and low levels of deposition. This fraction will be able to travel for moderately long distances and the results suggest that these sized SCPs are being reasonably well dispersed from the sources in London.

4.8.8 Summary

The results of this chapter have shown that actual concentrations of SCPs in lakes and ponds agrees well with the dispersion modelling footprint of SCPs across London from Chapter 3. In general, the environmental variables do not contribute much to the explanation of variation in SCP concentrations. The SCP size distribution in the lakes and ponds shows some relationship with proximity to source. SCP sources is discussed further in Chapters 5 and 6.

CHAPTER 5: SCP AND IAS POLLUTION EPISODES ACROSS LONDON

5.1 Introduction

There are many studies that look at the quantities and types of contemporary pollution in London (e.g. SEIPH 1999; LRC, 1997; Long, 1998) but specific sources are less well understood. Modelling studies, pollution inventories and particle chemistry studies go part of the way towards understanding the sources of gaseous and particulate pollution, however the specific impacts of individual sources in London are uncertain due to the complex cocktail of pollution that London is inundated with (see Chapter 1). It is generally accepted that the impacts of power stations and other high-temperature fossil-fuel combustion sources do not have a large overall impact on urban areas in comparison with the vast emissions from road transport. However, these point sources may have a significant impact on the character and intensity of episodic pollution.

SCPs and IASs are uniquely produced by the high-temperature combustion of fossil fuels (see Section 3.3.2) and therefore are ideal to trace the impact of pollution in London from power station and other Part A fossil-fuel combustion sources. Chapter 3 has shown that predicted deposition of SCPs from these sources varies across London and Chapter 4 has confirmed that there is a similar spatial pattern of SCPs in lake and pond sediments. These Chapters were both focused on long-term deposition and concentrations, on a scale of years, however the short-term impacts of pollution from power station and other Part A Processes are less well understood. The Burkard Trap was first used by Boehm and Leuschner (1979) to evaluate fly ash pollution and it was suggested by Mackay and Rose (1998) in a study of all pollution particles that SCPs and IASs collected on Burkard Traps may show the presence of episodic pollution plumes in London. Therefore, the short-term impact of SCP and IAS is now addressed in this Chapter.

5.1.1 Aims

The data in Chapter 3 showed that non-power station Part A Processes have the greatest deposition of SCPs to London over a period of one year. However, the balance between emissions from non-power station Part A Processes and emissions from power stations may be different when considering episodes of pollution over short time periods. The specific aims of this Chapter are:

- To determine the impact of SCPs and IASs in London over short time periods at high temporal resolution. This is a unique study of particles on this scale of resolution that can be attributed to a specific type of source; and

- To evaluate the spatial differences in SCP and IAS concentration along a transect of sites in order to test the hypothesis that short-term episodes of SCP and IAS pollution are dominated by emissions from power stations.

5.2 IAS and SCP episodes

SCPs and IASs were counted on Burkard Trap tapes at four sites across London on a transect connecting the centre of London to the power stations along the Thames Corridor. The term 'episode' in this study refers to the period of time that Burkard Trap tapes were counted for. Shorter periods of time, where there were elevated concentrations of particles or gases, are referred to as pollution 'events'. All episodes were selected based on hourly average SO_2 concentrations exceeding 35 ppb at monitoring stations close to the Burkard Trap transect sites at London Bloomsbury, London Eltham, Thurrock and Rochester (see Section 2.7). Altogether five pollution episodes were selected for analysis.

Numbers of SCPs and IASs were counted for each microscope field of view along each tape of an episode and the counts were then added together to

obtain a count per hour (hr^{-1}) (see Section 2.6.4). Where possible, a day before and after the elevated concentration was also counted.

Figures 5.1-5.11 show the counts of SCPs and IASs from Burkard Trap tapes at UCL, Thamesmead, Dartford and Northfleet for Episodes 1 and 2 and at UCL for Episodes 3, 4 and 5. SO_2 and NO_2 are plotted for the closest monitoring station to the Burkard Trap site for the same period. The IAS/SCP record is not complete in Episodes 1 and 2 where the record is missing due to Burkard Trap operational problems.

Correlation matrices (Tables 5.1-5.13) were calculated for the IAS, SCP, SO_2 and NO_2 profiles at each site and for each episode. Significant correlations ($p \leq 0.05$) are indicated by grey shaded boxes. The IAS and SCP time-series at Northfleet are compared with the SO_2 and NO_2 concentrations at both Rochester and Thurrock because Northfleet lies approximately equidistant from both.

The NO_2 profiles have been included for comparison so that the influence of road transport can be eliminated. If there is a co-incident peak of NO_2 and SO_2 then the source is likely to be vehicular. Road transport accounts for over 75% of NO_2 emissions in London (AQS, 1999) and so the contribution of other sources of NO_2 is likely to be swamped by the vehicular contribution.

5.2.1 Episode 1 (4/3/99-9/3/99)

This episode was selected because there were two dates at two sites where SO_2 exceeded the 35 ppb limit; the first was on 5/3/99 at UCL and the second at Thamesmead on 8/3/99. There was no single time when SO_2 was elevated at all four sites, however there were slightly raised levels of SO_2 at Thurrock at approximately the same time as the episode at Bloomsbury. The whole period was chosen to determine whether these two incidences were part of one larger episode and to gain some insight on the movement of plumes of particles from high temperature combustion sources.

Figures 5.1-5.4 show the time-series profiles of SO_2 and NO_2 concentrations and SCP and IAS counts at the transect sites for Episode 1. Correlations between variables are shown in Tables 5.1-5.5.

The flow rate of air into the Burkard Trap is 10 litres per minute (Burkard Manufacturing Company operation manual) and this corresponds to a flow rate of 0.6 m^3 hr^{-1} (see Section 2.6.1). The numbers of particles per volume of air are reported in the text alongside the count of particles for each hour.

UCL

The SO_2 profile (Figure 5.1a) shows a peak of 46 ppb in the afternoon on 5/3/99, a decrease in the early evening and a rise just before midnight, following which concentrations drop to 4-5 ppb in the early hours of 6/3/99. The SO_2 levels at Bloomsbury are moderately high for most of the day on 6/3/99, with concentrations around 30 ppb. There are two further peaks of just below 30 ppb at around midnight on 7/3/99 and in the early evening on 8/3/99. The NO_2 profile (Figure 5.1b) has a diurnal structure with higher concentrations during the daytime and into the evening and a drop in the early hours of the morning, typical of vehicle activity.

Table 5.1: Correlation matrix showing the relationships between IAS and SCP at UCL and SO_2 and NO_2 at Bloomsbury for Episode 1

	SCP	IAS	SO_2	NO_2
SCP	1			
IAS	0.02	1		
SO_2	-0.18	0.16	1	
NO_2	-0.27	0.23	0.16	1

Figure 5.1a-d: Plots of SCP and IAS (UCL) with SO_2 and NO_2 (Bloomsbury) for Episode 1

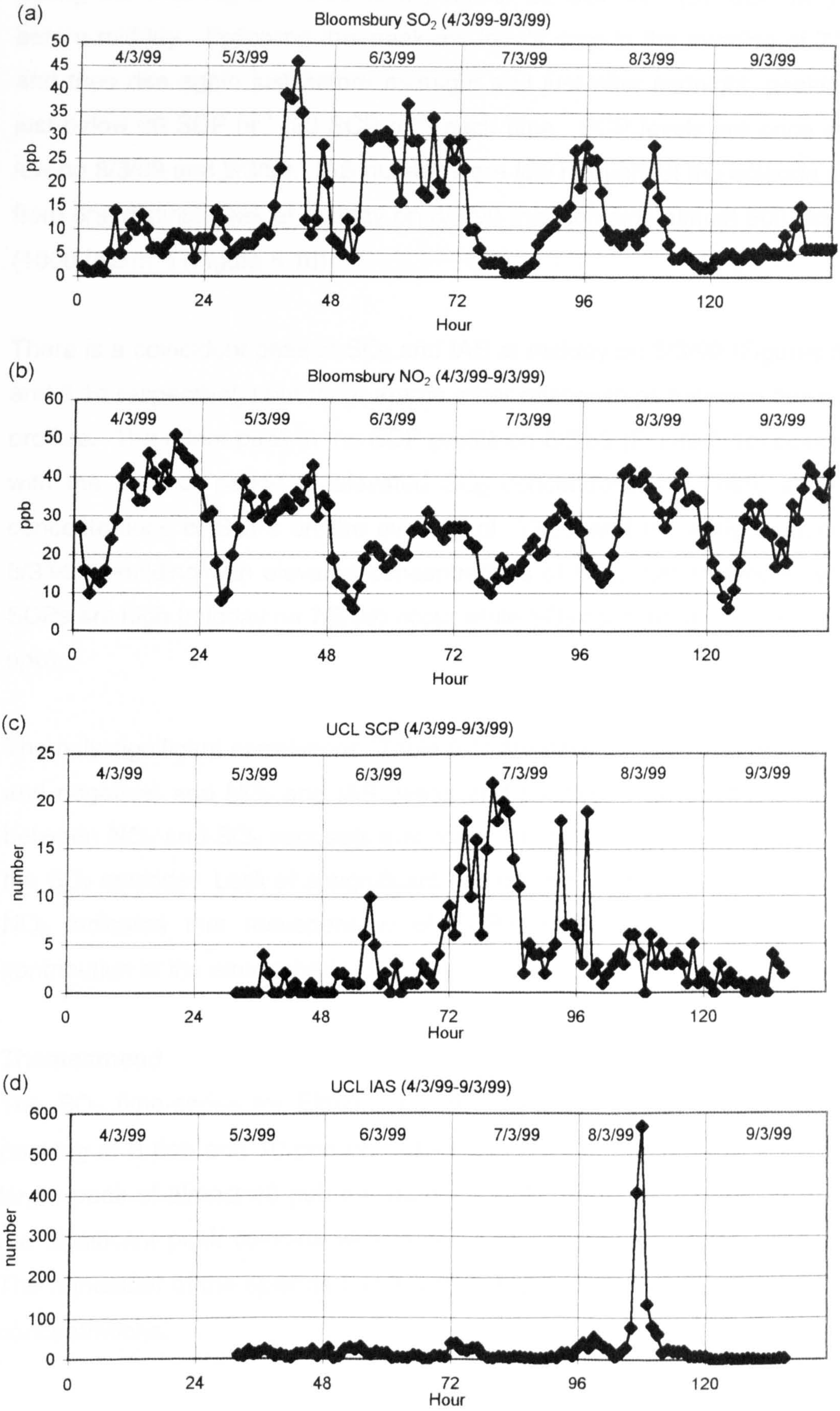

SCP numbers are low on 5/3/99 and 6/3/99 (Figure 5.1c) with a small peak of 10 SCP hr^{-1} (17 SCP m^{-3}) just before midday on 6/3/99. The numbers rise during the morning of 7/3/99 to a peak of 22 SCP hr^{-1} (37 SCP m^{-3}) just before midday. Following this peak the levels drop in the evening of 7/3/99 and then rise again just before midnight and just after midnight, peaking at just below 20 SCP hr^{-1} (33 SCP m^{-3}) each time. SCP levels are once again low on 8/3/99 and 9/3/99. IAS numbers are low throughout the episode apart from one distinct peak at midday on 8/3/99 that contains almost 600 IAS hr^{-1} (1000 IAS m^{-3}) (Figure 5.1d).

There is a coincident peak in SO_2 and IAS at midday on 8/3/99 (Figures 5.1a and 5.1d respectively) but there are no other relationships between these two profiles. The minor peak in the SCP profile on 6/3/99 (Figure 5.1c) coincides with the start of period of elevated SO_2 concentrations. There are high concentrations of SCPs on the evening of 7/3/99 and the early morning of 8/3/99 coinciding with elevated concentrations of SO_2. Other periods where SCPs are high (midday on 7/3/99) occur while SO_2 concentrations are low (<5 ppb).

The only significant correlations (Table 5.1) are between NO_2 and SCP (weak and negative) and NO_2 and IAS (weak and positive). The poor relationship between NO_2 and SO_2 suggests that road transport is not the only source of the SO_2 episode. Lack of a significant relationship between SCP or IAS with NO_2 indicates that resuspension of SCPs or IASs is not a significant contribution to the atmospheric load.

Thamesmead

The SO_2 time-series for Eltham (Figure 5.2a) has slightly elevated levels peaking at 8 ppb and 10 ppb on 4/3/99 and 5/3/99 respectively. A second, larger peak of almost 40 ppb occurs on 8/3/99. Both the elevated level and the significant peak coincide with features on the Thamesmead IAS profile. The remainder of the episode has low (5 ppb or less) and fairly constant SO_2 concentrations.

Figure 5.2a-d: Plots of SCP and IAS (Thamesmead) with SO_2 and NO_2 (Eltham) for Episode 1

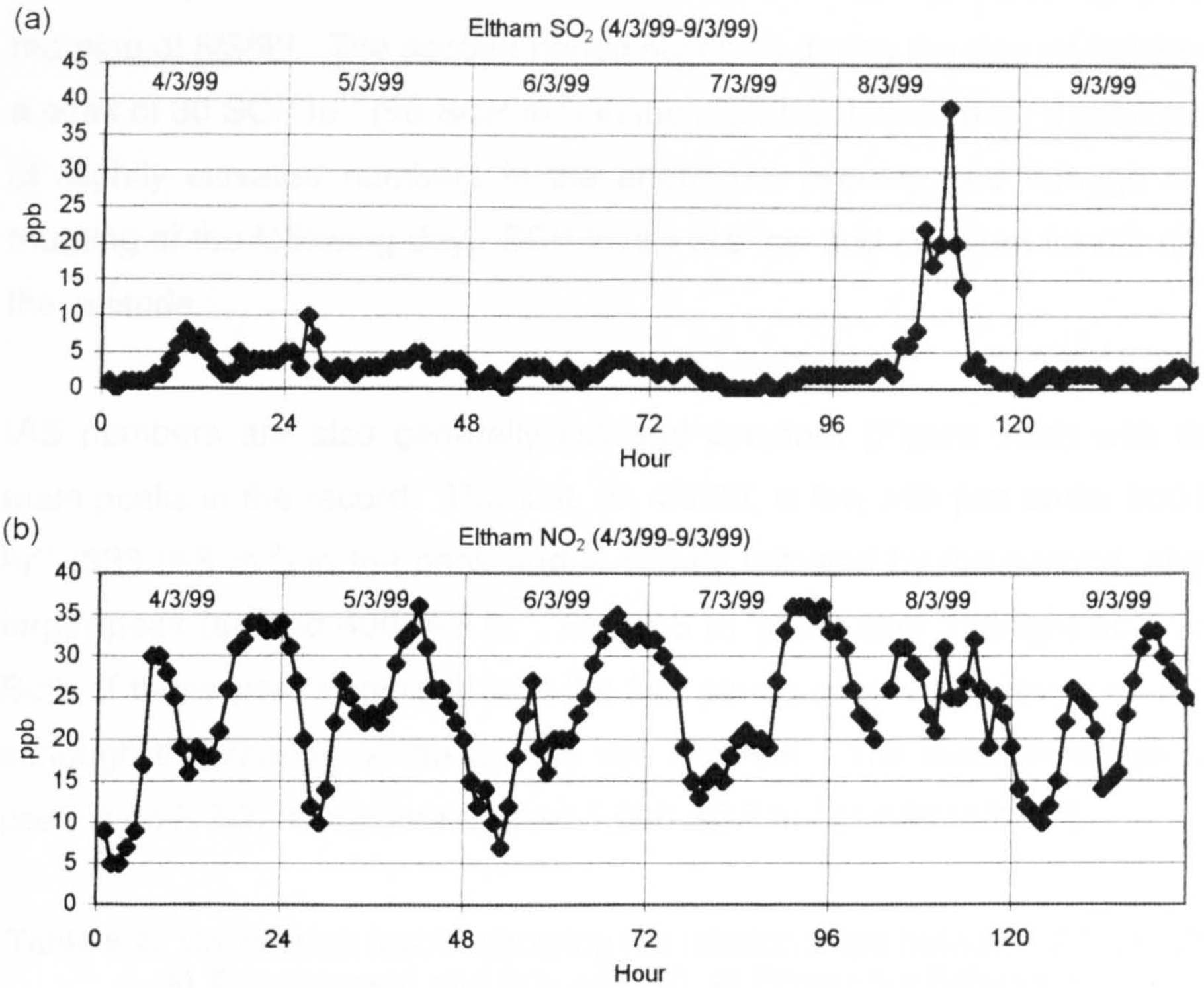

There are two main periods where SCP levels are high (Figure 5.2c). The first in the evening of 4/3/99, with a peak of over 50 SCP hr^{-1} (83 SCP m^{-3}) followed by a smaller peak of just over 20 SCP hr^{-1} (33 SCP m^{-3}) in the morning of 5/3/99. The second period occurred during the day on 8/3/99 with a peak of 30 SCP hr^{-1} (50 SCP m^{-3}) in the morning, followed by a short period of slightly elevated numbers in the afternoon, evening and through to the morning of the following day. SCP levels are low and constant for the rest of the episode.

IAS numbers are also generally low and constant (Figure 5.2d) with three main peaks in the record. The first, on 4/3/99, is low with just under 200 IAS hr^{-1} (333 IAS m^{-3}) in the peak and is shortly followed by the second, slightly larger peak (around 400 IAS hr^{-1}, 666 IAS m^{-3}) just after midnight on 5/3/99. Both of these peaks coincide with the first period of elevated levels of SCPs, although the shapes of the profiles are different. The most significant IAS peak is on 8/3/99 and contains over 1,000 SCP hr^{-1} (1,666 IAS m^{-3}).

Table 5.2: Correlation matrix showing the relationships between IAS and SCP at Thamesmead and SO_2 and NO_2 at Eltham for Episode 1

	SCP	IAS	SO_2	NO_2
SCP	1			
IAS	0.25	1		
SO_2	0.29	0.71	1	
NO_2	0.17	0.05	0.19	1

Figure 5.3a-d: Plots of SCP and IAS (Dartford) with SO_2 and NO_2 (Thurrock) for Episode 1

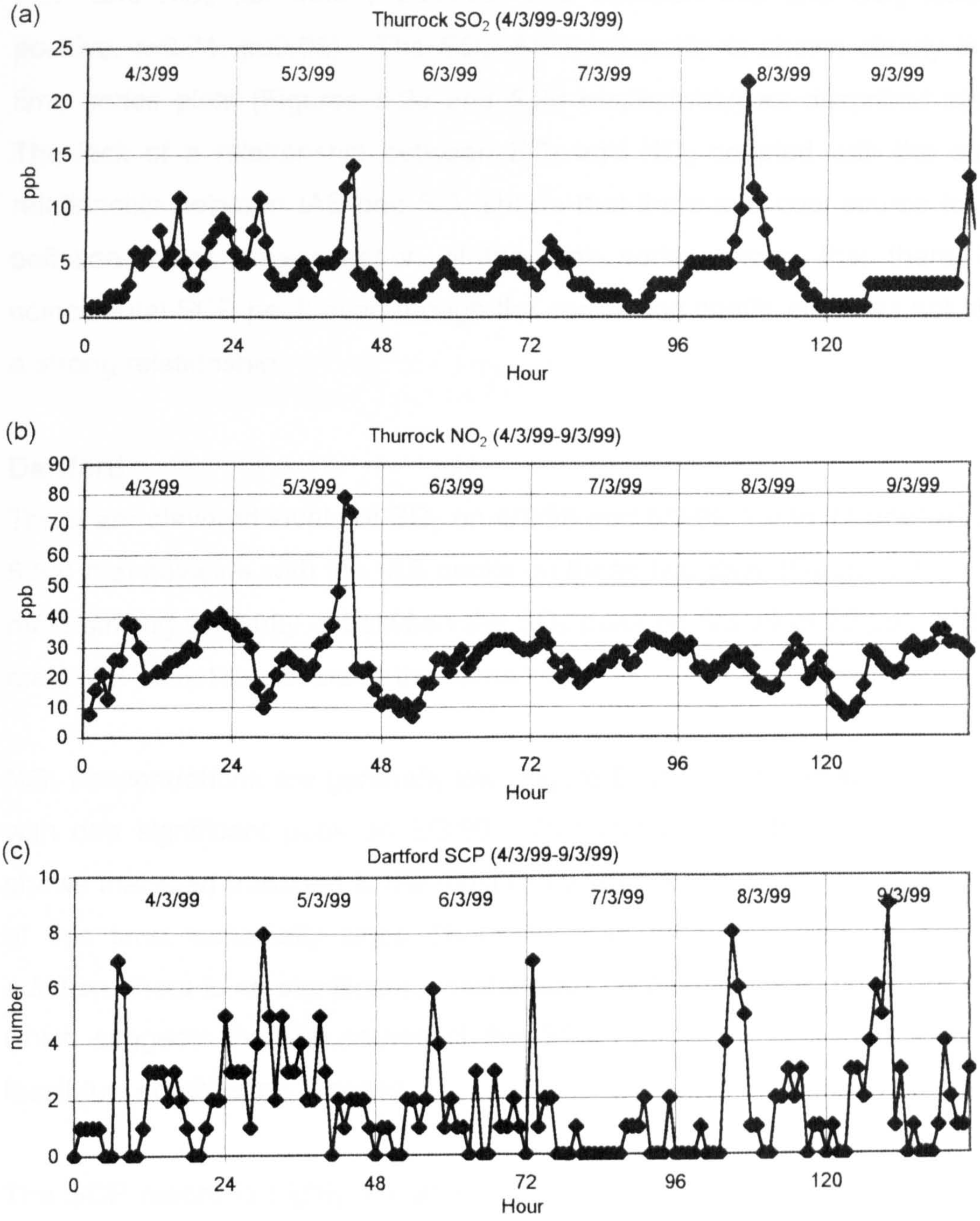

The correlation data between Eltham and Thamesmead (Table 5.2) has a number of significant relationships, between SCP and IAS, SCP and SO_2, SCP and NO_2 (all weakly positive) and between IAS and SO_2 (strongly positive, $r=0.71$, $p\leq0.05$). The SO_2-IAS relationship is shown clearly in the time series plots (Figures 5.2a and 5.2d respectively) as described above. The lack of a relationship between SO_2 and NO_2 coupled with the strong relationship between IAS and SO_2 shows that there is a coal source for this pollution event. Examination of the time series shows that there is a coincidental SCP peak even though the correlation coefficient does not show a strong relationship.

Dartford

There are elevated levels of SO_2 on 4/3/99 and 5/3/99 (up to 14 ppb) (Figure 5.3a) that coincide with the IAS peaks on those two days (Figure 5.3d). The most striking similarity is between the SO_2 peak on 8/3/99 of 22 ppb and the main IAS peak that occurs at the same time.

NO_2 concentrations are generally low (Figure 5.3b), averaging around 25 ppb with one significant peak on 5/3/99. This coincides with a SO_2 peak and shows that road transport is the most likely source of both of these pollutants at this time, especially since Thurrock is an urban background site. In addition, there is no significant simultaneous peak in the SCP or IAS profiles, which suggests that the source of this SO_2 peak is not a high-temperature fossil-fuel combustion process.

The SCP record is highly variable with many peaks and troughs due to low numbers (Figure 5.3c). There are no distinctive peaks in the profile but there are slightly higher numbers coinciding with similar features on the Thamesmead SCP profile. The SCP peak (9 SCP hr^{-1}, 15 SCP m^{-3}) occurs at about midday on 9/3/99. The IAS profile contains two major peaks, the first in the early hours of the morning on 5/3/99 which has a maximum count of 240 IAS hr^{-1} (400 IAS m^{-3}), and the second on 8/3/99 which has a maximum of 707 IAS hr^{-1} (1178 IAS m^{-3}). There are other minor peaks on 4/3/99, in the

evening of 5/3/99 and on 6/3/99 that have maximum concentrations of around 100 IAS hr^{-1} (167 IAS m^{-3}).

There are three significant relationships between Dartford IAS and SCP and Thurrock SO_2 (Table 5.3). SCP-IAS and SCP-SO_2 are weakly positive (r=0.22 and r=0.25, $p \leq 0.05$ respectively). The best relationship is between SO_2 and IAS (r=0.51, $p \leq 0.05$) and can be clearly seen in the profiles shown in Figures 5.3a and 5.3d respectively.

Table 5.3: Correlation matrix showing the relationships between IAS and SCP at Dartford and SO_2 and NO_2 at Thurrock for Episode 1

	SCP	IAS	SO_2	NO_2
SCP	1			
IAS	0.22	1		
SO_2	0.25	0.51	1	
NO_2	0.07	-0.01	0.41	1

Northfleet

The SO_2 profile at Rochester (Figure 5.4a) has a peak of 22 ppb that coincides with the end of the first IAS peak at Northfleet (Figure 5.4d). For the rest of the episode the SO_2 concentrations are generally low, with some minor fluctuations that peak at around 15 ppb.

The SCP levels are low at the beginning of the episode (Figure 5.4c) and then increase slightly with occasional peaks of over 10 SCP hr^{-1} (17 SCP m^{-3}) between the evening of 4/3/99 and the early morning of 6/3/99. Once again this is the same period of time that has elevated SCP concentrations at both Dartford and Thamesmead. On 8/3/99 the SCP concentrations are high with a major peak of 24 SCP hr^{-1} (40 SCP m^{-3}) around midday.

There is a second IAS peak (423 IAS hr^{-1}, 705 IAS m^{-3}) (Figure 5.4d) that occurs at the same time as the SCP peak but has no corresponding elevated levels in the SO_2 profile. Rochester and Northfleet are not co-located which

might explain a lack of relationship; the plume may pass over both Rochester and Northfleet during the first episode but not during the second episode.

Table 5.4: Correlation matrix showing the relationships between IAS and SCP at Northfleet and SO_2 and NO_2 at Rochester for Episode 1

	SCP	IAS	SO_2	NO_2
SCP	1			
IAS	0.46	1		
SO_2	0.27	0.23	1	
NO_2	-0.14	-0.02	0.09	1

Table 5.5: Correlation matrix showing the relationships between IAS and SCP at Northfleet and SO_2 and NO_2 at Thurrock for Episode 1

	SCP	IAS	SO_2	NO_2
SCP	1			
IAS	0.50	1		
SO_2	0.46	0.63	1	
NO_2	-0.06	0.02	0.41	1

SCP and IAS have the best statistical relationship ($r=0.46$, $p\leq0.05$) when comparing Northfleet IAS and SCP with Rochester SO_2 and NO_2 (Table 5.4). Table 5.5 shows the correlation coefficients from the relationship between IAS and SCP from Northfleet and SO_2 and NO_2 from Thurrock. The IAS-SO_2 relationship is much stronger than that shown in Table 5.4 ($r=0.63$, $p\leq0.05$).

Figure 5.4a-d: Plots of SCP and IAS (Northfleet) with SO_2 and NO_2 (Rochester) for Episode 1

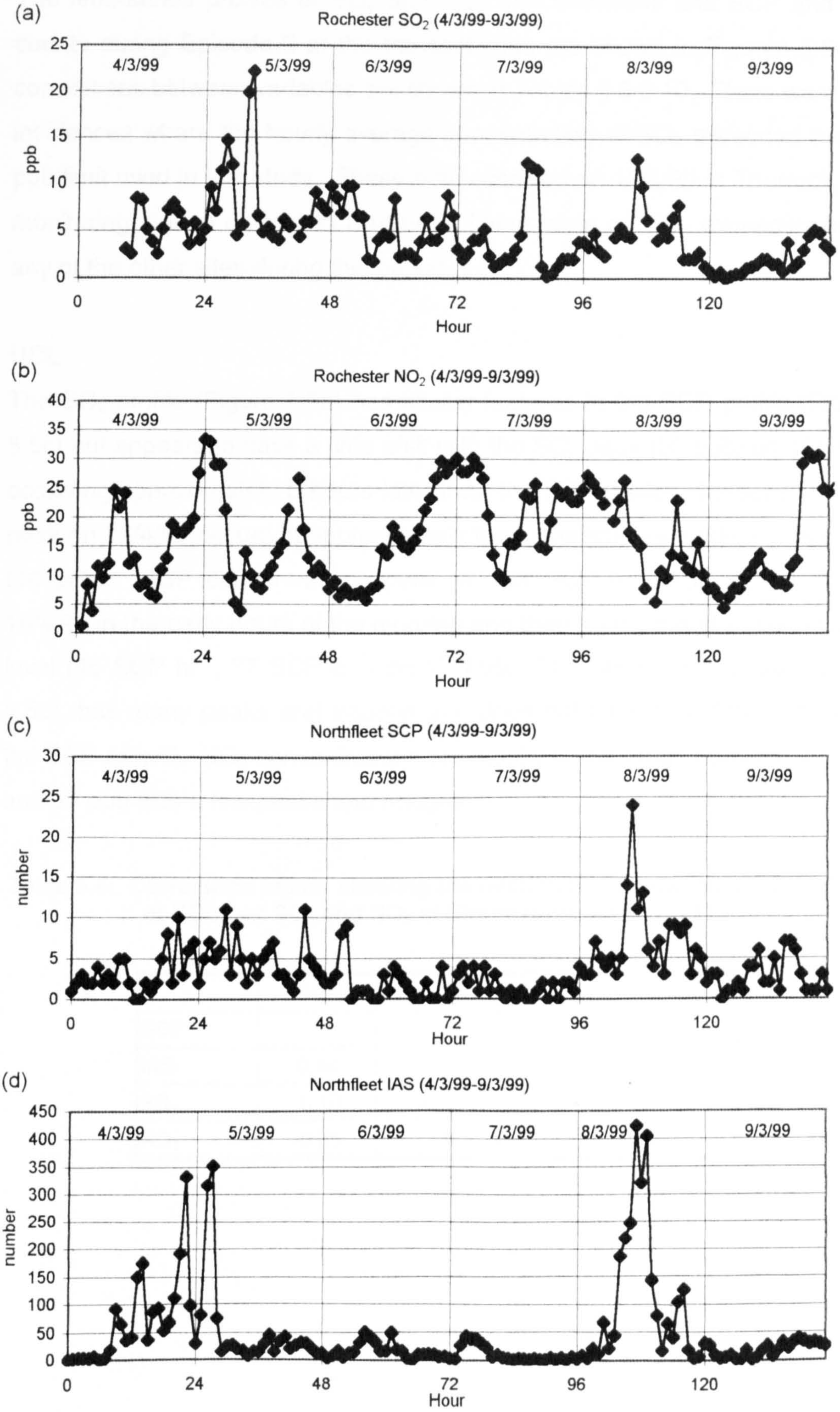

5.2.2 Episode 2 (15/4/99-17/4/99)

The time-series profiles of SO_2 and NO_2 concentrations and SCP and IAS counts during Episode 2 at the transect sites are shown in Figures 5.5-5.8; correlations between variables are shown in Tables 5.6-5.10. There were two incidences where the hourly average concentration of SO_2 exceeded the 35 ppb limit used in this study. These both occurred on 16/4/99 at Thurrock, the monitoring station closest to Dartford. There were no SO_2 exceedances at any of the other sites during this period.

UCL

The SO_2 profile (Figure 5.5a) has similar features to the SCP profile (Figure 5.5c) but appears to have a time shift with the SO_2 peak (20 ppb) on 16/4/99, occurring approximately 5 hours later than the SCP peak. The second SCP peak on 17/4/99 occurs at approximately the same time as a minor SO_2 peak (16 ppb). SCP concentrations peak at 153 SCP hr^{-1} (255 SCP m^{-3}) on 16/4/99 in the early hours of the morning and then again, but at a much lower level (46 SCP hr^{-1}, 77 SCP m^{-3}) on 17/4/99. The IAS record is low (Figure 5.5d), has many peaks and troughs and does not have any similarities with the SCP record. NO_2 concentrations are mostly in the range between 40 ppb and 50 ppb with a few peaks and troughs.

Table 5.6: Correlation matrix showing the relationships between IAS and SCP at UCL and SO_2 and NO_2 at Bloomsbury for Episode 2

	SCP	IAS	SO_2	NO_2
SCP	1			
IAS	0.14	1		
SO_2	-0.10	0.25	1	
NO_2	-0.28	-0.22	0.20	1

Figure 5.5a-d: Plots of SCP and IAS (UCL) with SO_2 and NO_2 (Bloomsbury) for Episode 2

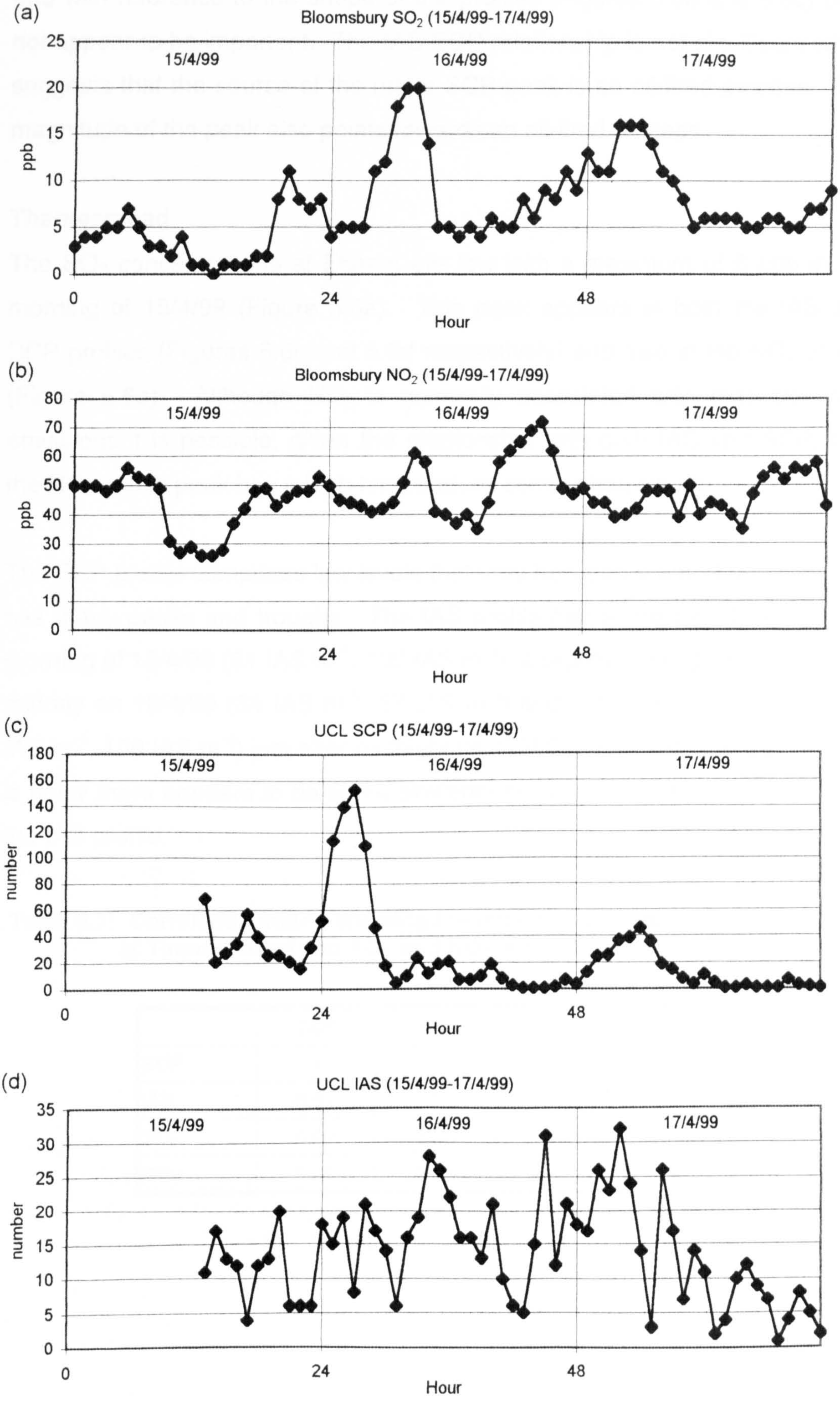

The correlation matrix (Table 5.6) shows only one significant relationship and that is between SCP and NO_2. However, this relationship is weakly negative and with reference to the shape of the profiles (Figures 5.5b and 5.5c) does not appear to be important. The IAS-SCP relationship is not significant which suggests that the source of the major SCP peak is an oil-fired process. The magnitude of the peak also points towards an oil-fired process.

Thamesmead

The SO_2 concentrations at Eltham are low with a maximum of 6 ppb in the morning of 15/4/99 (Figure 5.6a). This peak appears in both the IAS and SCP profiles (Figures 5.6c and 5.6d respectively) and also in the NO_2 profile (Figure 5.6b). Although NO_2 is generally associated with road transport emissions it is possible, given the relationship with both IAS and SCP, that the NO_2 in this peak has a high temperature combustion source.

The SCP profile comprises low levels that vary between 0 and 9 particles and has many peaks and troughs. The IAS profile has some high levels in the morning of 15/4/99 (61 IAS hr^{-1}, 102 IAS m^{-3}), a slightly lower peak just before midday on 16/4/99 (34 IAS hr^{-1}, 57 IAS m^{-3}) and then a third high peak (60 IAS hr^{-1}, 100 IAS m^{-3}) just after midnight on 17/4/99. Although the SCP profile is noisy there appears to be some similarity in its structure to the structure of the IAS profile.

Table 5.7: Correlation matrix showing the relationships between IAS and SCP at Thamesmead and SO_2 and NO_2 at Eltham for Episode 2

	SCP	IAS	SO_2	NO_2
SCP	1			
IAS	0.51	1		
SO_2	0.07	0.27	1	
NO_2	0.25	0.23	0.21	1

Figure 5.6a-d: Plots of SCP and IAS (Thamesmead) with SO_2 and NO_2 (Eltham) for Episode 2

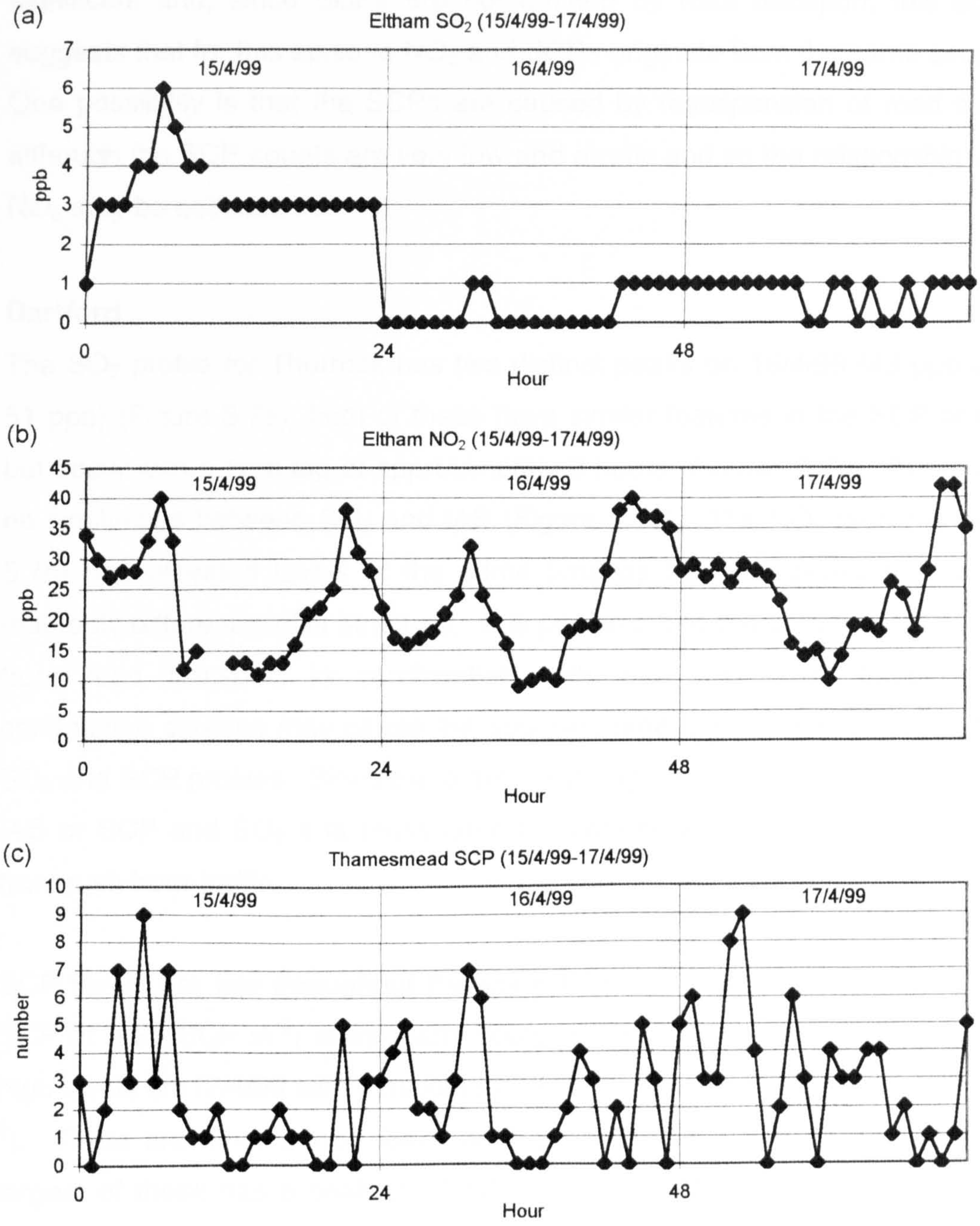

The correlation matrix (Table 5.7) shows that IAS and SCP have a statistically significant relationship ($r=0.51$, $p\leq0.05$). The SCP-NO_2 relationship is also significant and, since SCPs are not emitted by road transport, this again suggests that for this episode NO_2 and SCPs originate from the same source. One possibility is that the SCPs are caused by resuspension of road dusts although the SCP counts are very low and erratic and so the relationship with NO_2 may be coincidental.

Dartford

The SO_2 profile for Thurrock has two distinct peaks on 16/4/99 (43 ppb and 51 ppb) (Figure 5.7a); both of these have similar features in the SCP profile but occur with a time lag of approximately 3 hours (Figures 5.7c). There are no similarities between SO_2 and IAS (Figure 5.7d). The NO_2 profile (Figure 5.7b) has elevated levels at the same time as the SO_2 peaks but has a markedly different profile structure. It is possible that the contribution of SO_2 from road transport in combination with SO_2 from high temperature combustion sources may cause the apparent time-lag between peaks in the SO_2 and SCP profiles. Since there are no strong relationships between either IAS or SCP and SO_2 it is reasonable to suppose that the source of SO_2 is from rush hour traffic.

SCP levels are low throughout the episode with a relatively large peak (15 SCP hr^{-1}, 25 SCP m^{-3}) in the early hours of 15/4/99 and a second period of high levels on 17/4/99 with a maximum SCP count of 16 SCP hr^{-1} (27 SCP m^{-3}). There are other minor peaks during the middle of the episode but the largest of these has a peak of 10 SCP hr^{-1} (17 SCP m^{-3}) in the evening of 16/4/99. The IAS record has a high peak in the afternoon of 16/4/99 (173 IAS hr^{-1}, 288 IAS m^{-3}) with a secondary and much smaller peak (58 IAS hr^{-1}, 97 IAS m^{-3}) in the evening of that day. There are two further peaks (111 and 107 IAS hr^{-1}, 185 and 178 IAS m^{-3} respectively) on 17/4/99 at around midday, occurring at the same time as elevated SCP numbers. A further low peak (70 IAS hr^{-1}, 117 m^{-3}) occurs in the evening of 17/4/99.

Figure 5.7a-d: Plots of SCP and IAS (Dartford) with SO_2 and NO_2 (Thurrock) for Episode 2

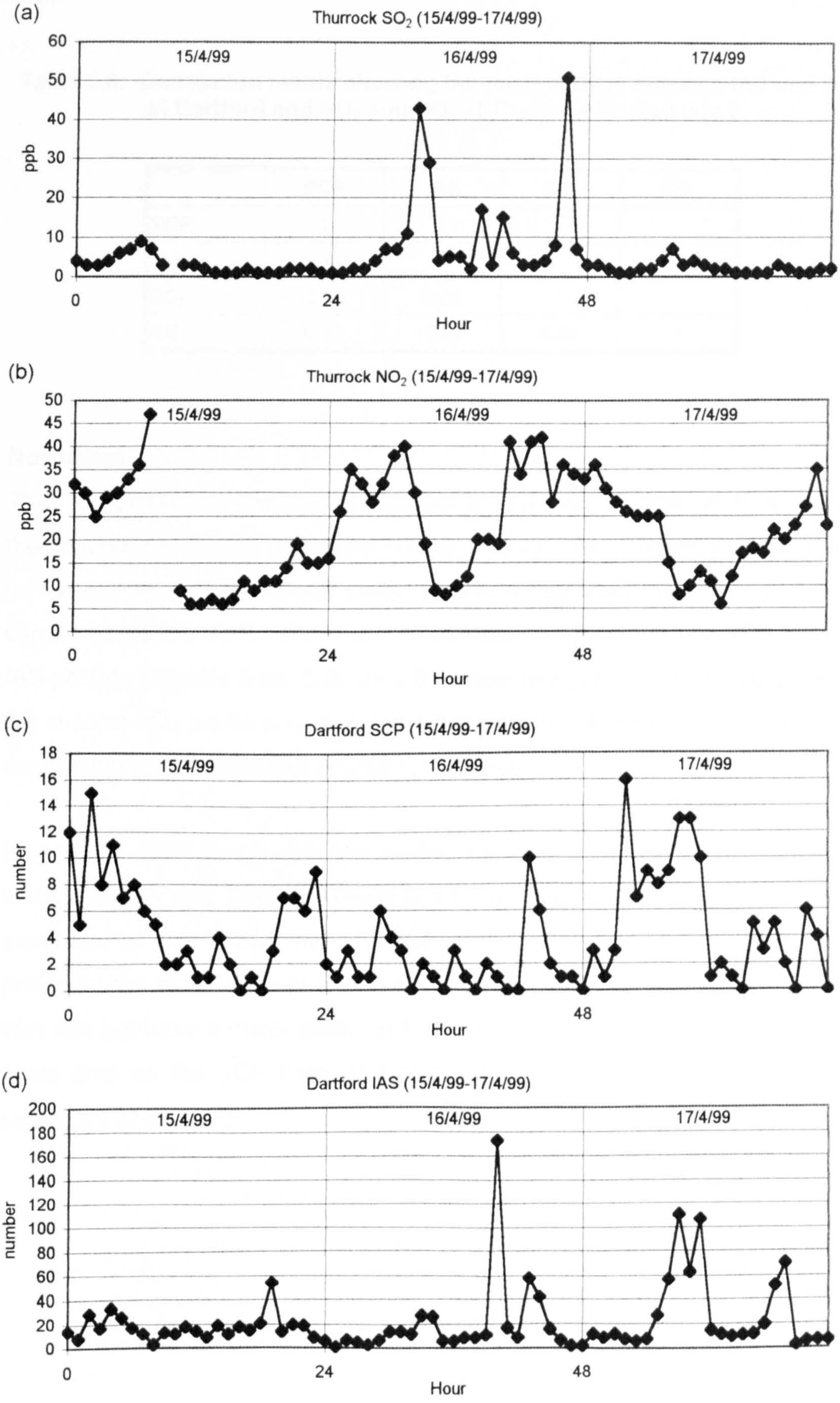

There are no significant correlations between the SCP and IAS collected at Dartford and the SO_2 and NO_2 concentrations detected at Thurrock (Table 5.8).

Table 5.8: Correlation matrix showing the relationships between IAS and SCP at Dartford and SO_2 and NO_2 at Thurrock for Episode 2

	SCP	IAS	SO_2	NO_2
SCP	1			
IAS	0.11	1		
SO_2	-0.19	0.08	1	
NO_2	0.27	-0.02	0.26	1

Northfleet

The SO_2 profile has two peaks, the first at just over 16 ppb on 15/4/99, and the second, on 16/4/99 at around 10 ppb (Figure 5.8a). There is missing data in the middle of the second peak, therefore the exact peak concentration cannot be determined. There are no coincidental peaks in the NO_2, SCP or IAS profiles (Figures 5.8b, 5.8c an 5.8d respectively) for the first SO_2 peak but the second SO_2 peaks occurs at approximately the same time as a NO_2 peak, suggesting a road transport source for the SO_2.

In general, SCP levels are low during Episode 2 at Northfleet, especially during 15/4/99 and 16/4/99. There is a broad peak on 17/4/99 but this has a maximum of only 8 SCP hr^{-1} (13 SCP m^{-3}). This peak covers some of the period of the main peak in SCPs at Dartford. The IAS levels are generally very low but have a major peak (311 IAS hr^{-1}, 518 IAS m^{-3}) on 17/4/99, at the same time as the SCP peak and at a similar time to the IAS peak on the same day at Dartford.

Figure 5.8a-d: Plots of SCP and IAS (Northfleet) with SO_2 and NO_2 (Rochester) for Episode 2

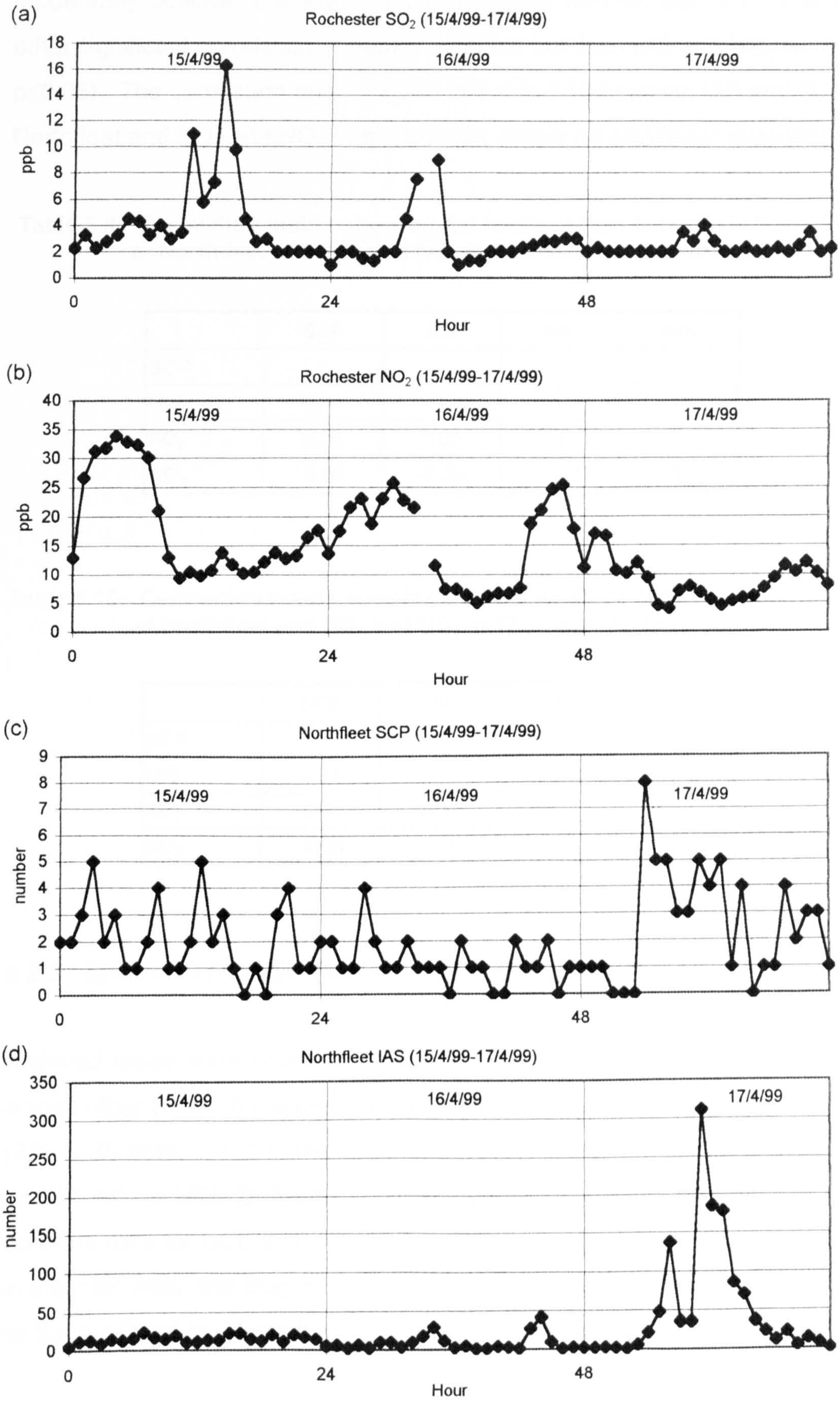

The SO_2 peak appears to have no relationship with either SCP or IAS and this is supported by the correlations shown in Table 5.9. The IAS-SCP has a moderately positive and significant relationship ($r=0.44$, $p\leq0.05$). The only other significant correlation is weakly negative between IAS and NO_2 ($r=-0.30$, $p\leq0.05$). The correlation matrix shown in Table 5.10 between IAS and SCP at Northfleet and SO_2 and NO_2 from Thurrock shows no significant relationships.

Table 5.9: Correlation matrix showing the relationships between IAS and SCP at Northfleet and SO_2 and NO_2 at Rochester for Episode 2

	SCP	IAS	SO_2	NO_2
SCP	1			
IAS	0.44	1		
SO_2	0.05	0.00	1	
NO_2	-0.09	-0.30	0.07	1

Table 5.10: Correlation matrix showing the relationships between IAS and SCP at Northfleet and SO_2 and NO_2 at Thurrock for Episode 2

	SCP	IAS	SO_2	NO_2
SCP	1			
IAS	0.01	1		
SO_2	-0.21	-0.18	1	
NO_2	-0.08	-0.09	0.26	1

5.2.3 Episode 3 (13/3/96-14/3/96)

Archived tapes were counted for Episodes 3, 4 and 5 to extend the study across other years. Episodes were selected using the same criteria as before (SO_2 > 35 ppb). Prior to the 1999 transect study, tapes were only collected consistently at UCL (between 1995 and 2000). Each episode therefore only contains data for UCL and London Bloomsbury. There were several periods in the past when the SO_2 limit was exceeded, however choice was restricted by the quality of the tapes that were available for analysis.

Figure 5.9a-d: Plots of SCP and IAS (UCL) with SO_2 and NO_2 (Bloomsbury) for Episode 3

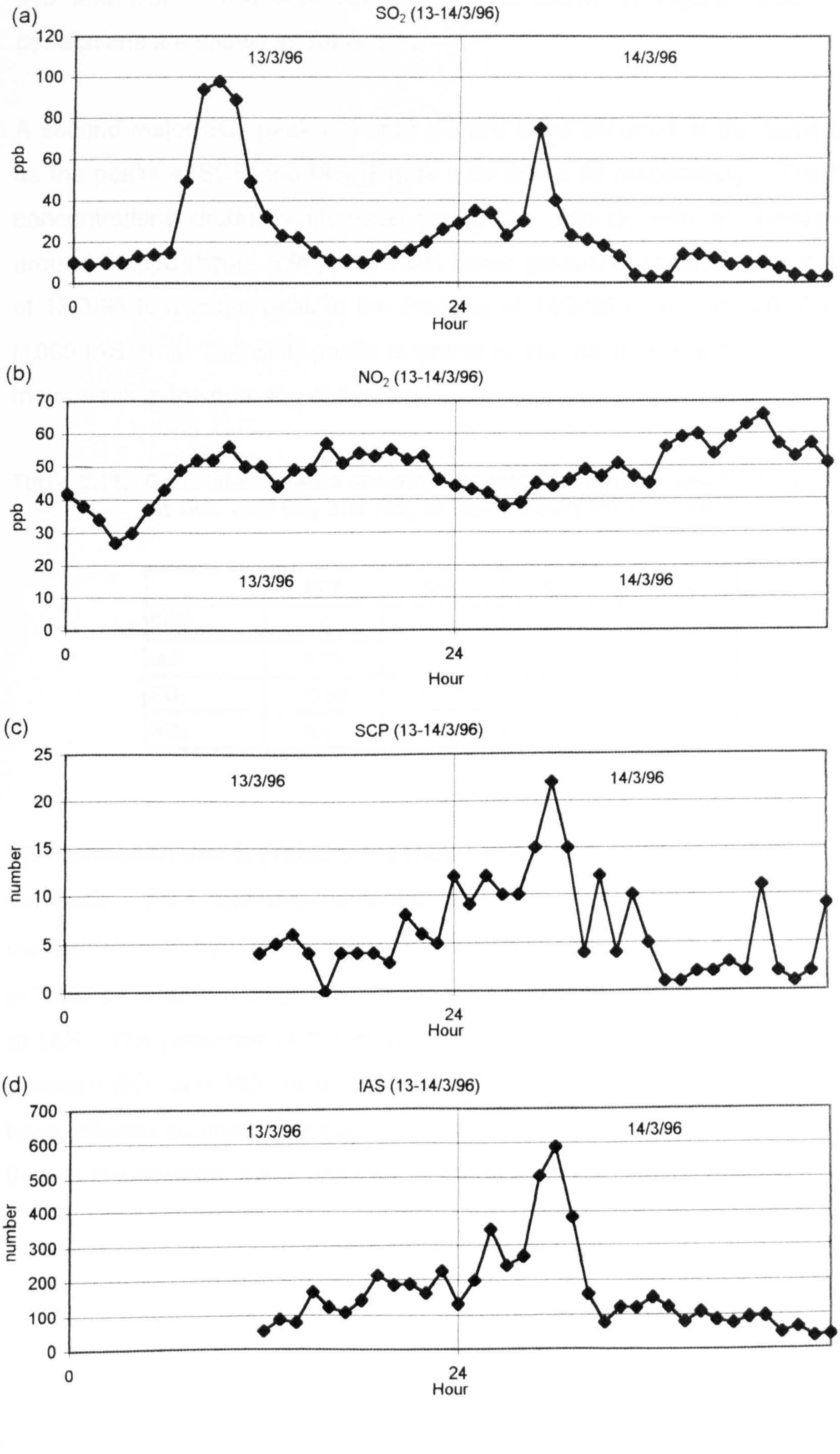

The major feature of the episode is on 13/3/96 with a concentration of 98 ppb but the Burkard Trap tape was not available to compare SO_2 with counts of IAS and SCP. The time series plots are shown in Figures 5.9a-d and correlations are shown in Table 5.11.

A second major SO_2 peak (75 ppb) (Figure 5.9a) occurred at the same time as the peaks in SCP and IAS (Figure 5.9c and 5.9d respectively). The NO_2 concentrations gradually increase during the episode with an average of around 50 ppb (figure 5.9b). The IAS levels gradually increase from midday of 13/3/96 to a major peak in the morning of 14/3/96 of almost 600 IAS hr^{-1} (1000 IAS m^{-3}). The SCP profile is similar to the IAS profile with a coincident major peak in the morning of 14/3/96.

Table 5.11: Correlation matrix showing the relationships between IAS and SCP at UCL and SO_2 and NO_2 at Bloomsbury for Episode 3

	SCP	IAS	SO_2	NO_2
SCP	1			
IAS	0.75	1		
SO_2	-0.58	-0.52	1	
NO_2	0.62	0.73	-0.54	1

The correlation matrix (Table 5.11) shows significant relationships between all variables. SCP and IAS have the strongest correlation ($r=0.75$, $p\leq0.05$) closely followed by IAS and NO_2 ($r=0.73$, $p\leq0.05$) and SCP and NO_2 ($r=0.62$, $p\leq0.05$) although, visually, the profiles are not similar for NO_2 with either SCP or IAS. The presence of the major peak on 13/3/96 causes the correlation between SO_2 and NO_2 to be strongly negative showing that SO_2 and NO_2 have different sources. The distinct similarities between IAS and SCP suggest that, in this episode, these particles originate from the same source.

Figure 5.10a-d: Plots of SCP and IAS (UCL) with SO_2 and NO_2 (Bloomsbury) for Episode 4

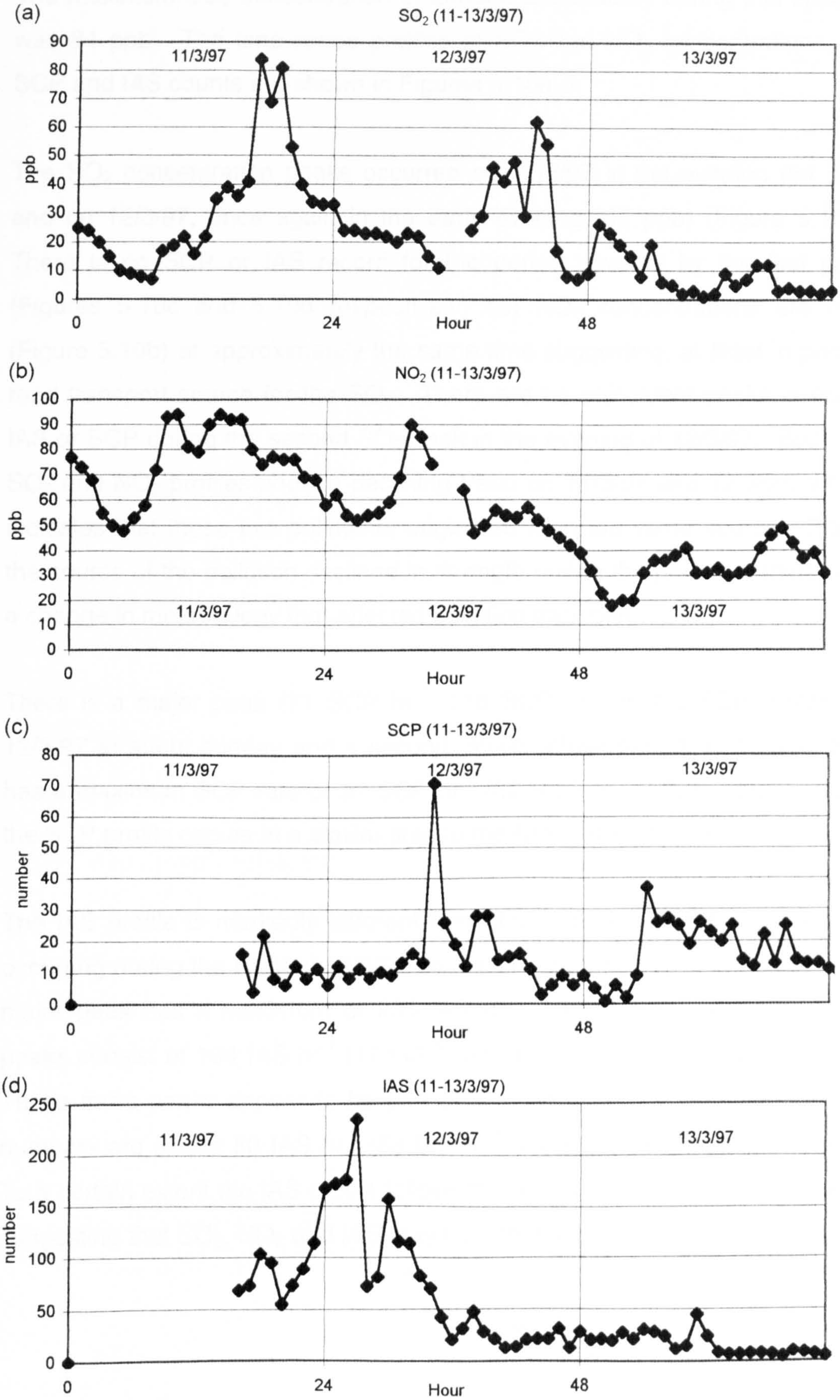

5.2.4 Episode 4 (11/3/97-13/3/97)

The maximum SO_2 concentration at London Bloomsbury during this episode was 84 ppb. The time-series profiles of SO_2 and NO_2 concentrations and SCP and IAS counts are shown in Figures 5.10a-d.

The SO_2 concentration peaks occurred on 11/3/97 in the evening (84 ppb) and on 12/3/97, once again in the early evening (62 ppb) (Figure 5.10a). There is no SCP or IAS record for the period covered by the first peak (Figures 5.10c and 5.10d respectively) but NO_2 concentrations are high (Figure 5.10b) at approximately the same time suggesting, at least in part, a road transport source for the SO_2. There are no coincident peaks in either IAS or SCP during the second SO_2 peak in the evening of 12/3/97. Both the SO_2 and NO_2 profiles show a declining trend on 11/3/97 and 12/3/97, which indicates that these two pollutants originated from the same source. Either the source of the pollution declined in strength during the period or there was a change in meteorology that affected pollution transport.

There is a major peak (71 SCP hr^{-1}, 118 SCP m^{-3}) in the SCP profile on 12/3/97 at about midday and a second, more diffuse period on 13/3/97 that has a maximum SCP rate of 37 SCP hr^{-1} (62 SCP m^{-3}). The major peak in the SCP profile occurs at a similar time to the NO_2 peak on 12/3/97.

The IAS profile is markedly different from the SCP profile with three peaks occurring during the night of 11/3/97 and finishing at midday on 12/3/97. The major peak has a maximum of 235 IAS hr^{-1} (392 IAS m^{-3}) and the minor peaks consist of 104 IAS hr^{-1} (173 IAS m^{-3}) and 157 IAS hr^{-1} (252 IAS m^{-3}). These three peaks appear to be part of a single pollution event where IAS numbers are above 50 IAS hr^{-1} (83 IAS m^{-3}) for a period of eighteen hours. To a certain extent the IAS profile follows the declining trend of SO_2 and NO_2, suggesting that SO_2, NO_2 and IAS may be from the same source.

Table 5.12: Correlation matrix showing the relationships between IAS and SCP at UCL and SO_2 and NO_2 at Bloomsbury for Episode 4

	SCP	IAS	SO_2	NO_2
SCP	1			
IAS	-0.11	1		
SO_2	0.05	0.53	1	
NO_2	-0.25	0.34	0.60	1

Table 5.12 shows correlations between SCP and IAS from UCL with SO_2 and NO_2 measured at Bloomsbury. The statistical relationships confirm the patterns seen in the pollutant profiles (Figures 5.10a-d). There are positive and significant relationships between IAS and SO_2 ($r=0.53$, $p\leq0.05$) and between SO_2 and NO_2 ($r=0.60$, $p\leq0.05$). These relationships suggest that, although there is a component of SO_2 from the same source as the NO_2, there is also a component that can be associated with high-temperature combustion of fossil fuels. A weaker significant relationship exists between IAS and NO_2 ($r=0.34$, $p\leq0.05$), suggesting the possibility that some of the NO_2 may originate from the IAS source. Alternatively the relationship between IAS and NO_2 may be a by-product of the relationship between IAS and SO_2, or between NO_2 and SO_2.

5.2.5 Episode 5 (19/12/97-22/12/97)

The peak SO_2 concentrations during Episode 5 was 57 ppb. Figures 5.11a-d show the time-series profiles of IAS and SCP counts and NO_2 and SO_2 concentrations. The correlation matrix for these variables is shown in Table 5.13. The SO_2 profile has many similarities with the IAS profile, with a peak (34 ppb) that coincides with the major IAS peak (Figures 5.11a and 5.11d respectively). The main SO_2 peak (57 ppb) occurs in the beginning of the episode and finishes just as the SCP peak begins to appear (Figure 5.11c). NO_2 remains fairly constant throughout the episode (Figure 5.11b).

Figure 5.11a-d: Plots of SCP and IAS (UCL) with SO_2 and NO_2 (Bloomsbury) for Episode 5

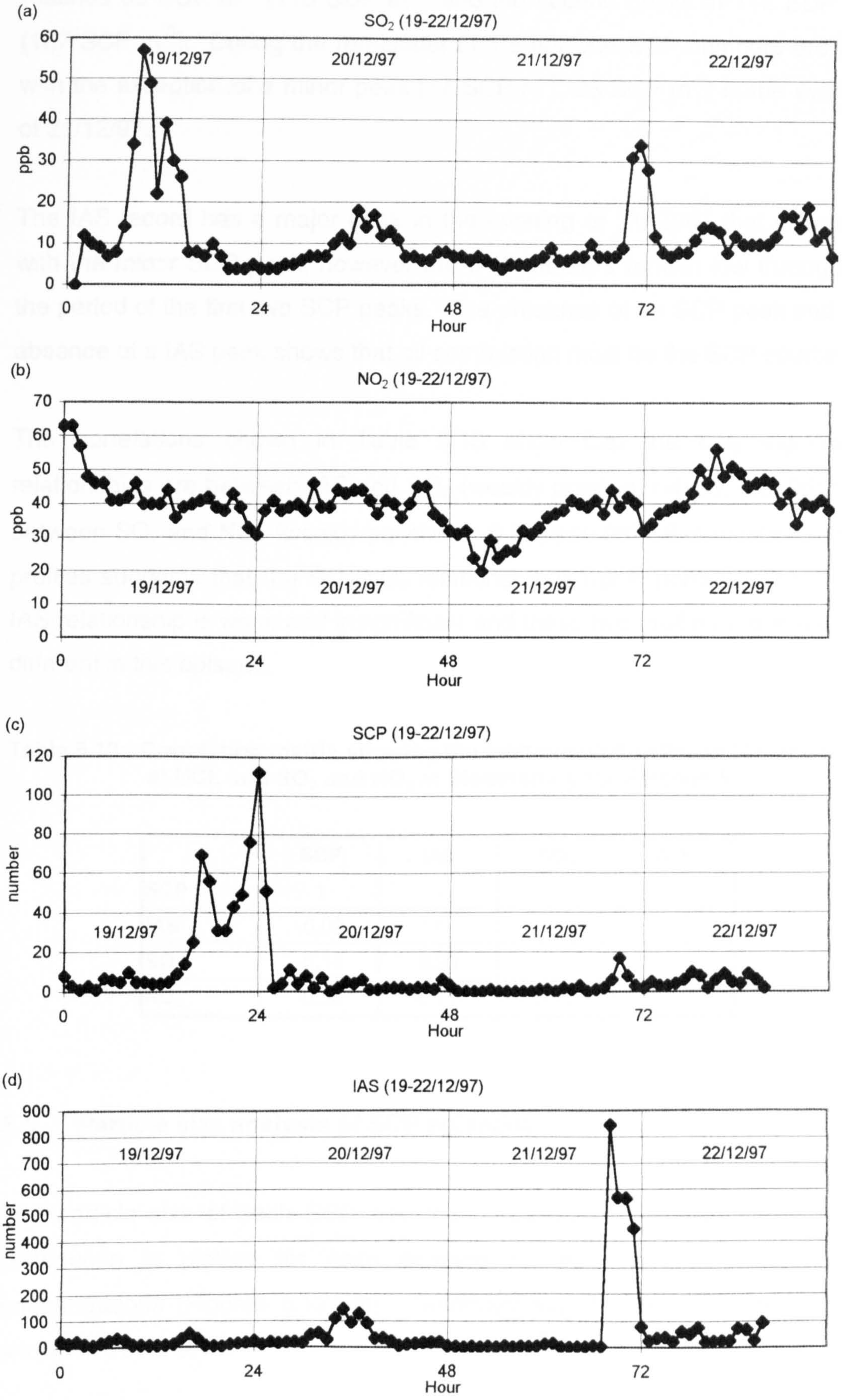

There is a major and distinct period of elevated SCP concentrations in the evening of 19/12/97 and until 01.00 in the following morning. The first peak reaches 69 SCP hr^{-1} (115 SCP m^{-3}) and the second peaks at 112 SCP hr^{-1} (187 SCP m^{-3}). During the remainder of the episode SCP numbers are low, with the exception of a minor peak (17 SCP hr^{-1}, 28 SCP m^{-3}) in the evening of 21/12/97.

The IAS record has a major peak in the evening of 21/12/97 that coincides with the minor SCP peak, however the IAS numbers remain low throughout the period of the first two SCP peaks. The presence of an SCP peak and the absence of a IAS peak shows that oil-combustion must be the SCP source.

The correlations shown in Table 5.13 show that the only significant relationships are between IAS and SO_2 (weakly positive, $r=0.39$, $p\leq0.05$) and between SO_2 and NO_2 (weakly positive, $r=0.22$, $p\leq0.05$). Examination of the profiles suggests that the SO_2-NO_2 relationship is not important. The SCP-IAS relationship is weak and insignificant and these two profiles are markedly different in this episode.

Table 5.13: Correlation matrix showing the relationships between IAS and SCP at UCL and SO_2 and NO_2 at Bloomsbury for Episode 5

	SCP	IAS	SO_2	NO_2
SCP	1			
IAS	-0.02	1		
SO_2	-0.14	0.39	1	
NO_2	-0.06	0.11	0.21	1

5.3 Particle size analysis of SCP episodes

The particle size of each SCP was measured (see Section 2.6.4) and the distribution is plotted for each episode for periods of elevated SCP concentrations (Figures 5.12a-m). Summary statistics for each period are shown in Table 5.14.

Particle size was used by Rickard et al. (1999) to suggest that the particles collected at two sites in London originated from different sources. Periods were selected visually from the time-series profiles. There were no periods selected for Dartford in Episode 1 (Figure 5.3c) or Thamesmead in Episode 2 (Figure 5.6c) because the SCP time-series show very low counts with no major peaks. In each case the distribution profile is positively skewed and has a positive kurtosis.

5.3.1 Episode 1

The distributions of SCPs in the Northfleet profile (Figure 5.12b) and in both Thamesmead profiles (Figure 5.12c and d) are similar, with the majority of the SCPs less than about 20 μm in size. The average particle size for all three are similar at 9.68, 11.70 and 12.53 μm respectively. The distribution profile for UCL (Figure 5.12a) is more dispersed, with an average particle size of 16.08 μm. In each case the greatest number of particles are in the size fractions between 2.56 μm and 7.68 μm.

5.3.2 Episode 2

The three periods at UCL that have elevated SCP counts do not have the same distribution profile of SCP sizes. The first period (14-22 hours) (Figure 5.12e) has the highest mean SCP size (14.68 μm) and maximum SCP size (94.87 μm). This profile has an elongated tail to the distribution. The second period occurs immediately after the first (22-31 hours) (Figure 5.12f) and has a much narrower distribution profile. This is reflected in the lower average SCP size of 9.52 μm and a lower maximum SCP size of 76.92 μm. The first two periods are contiguous but they have been treated as two separate events in order to determine whether they were caused by different pollution sources. The size distribution data indicate that this is probably the case. The third period (48-61 hours) (Figure 5.12g) has a similar distribution profile to the second period with a mean of 10.85 μm.

Table 5.14: Summary statistics of SCP size (μm) for periods of elevated SCP counts

	Episode 1				Episode 2					Episode 3	Episode 4		Episode 5
Site	UCL	Northfleet	Thamesmead		UCL			Northfleet	Dartford	UCL	UCL		UCL
Hours	72-99	103-117	15-27	100-129	14-22	22-31	48-61	53-62	48-60	23-37	29-43	51-71	13-27
Mean	16.08	9.68	11.70	12.53	14.68	9.52	10.85	11.57	17.55	12.86	12.73	14.05	10.68
Standard Error	0.61	0.50	0.67	0.51	0.69	0.24	0.45	1.10	1.59	0.91	0.53	0.53	0.31
Median	12.82	7.69	7.69	10.26	10.26	7.69	7.69	10.26	12.82	7.69	10.26	10.26	7.69
Mode	7.69	5.13	7.69	7.69	7.69	5.13	5.13	5.13	10.26	7.69	5.13	5.13	7.69
Standard Deviation	10.32	5.85	8.75	8.18	11.28	6.28	7.14	7.05	14.53	10.97	9.11	10.33	7.51
Sample Variance	106.59	34.17	76.52	66.92	127.33	39.40	51.04	49.68	211.11	120.25	82.97	106.74	56.37
Kurtosis	1.56	1.76	9.34	1.82	11.89	26.25	13.15	0.26	16.27	9.17	4.65	4.05	8.68
Skewness	1.23	1.47	2.68	1.46	2.76	3.85	2.80	1.15	3.33	2.76	1.94	1.79	2.65
Range	56.41	28.21	51.28	38.46	89.74	71.79	58.97	23.08	100.00	58.97	53.85	61.54	51.28
Minimum	5.13	5.13	5.13	5.13	5.13	5.13	5.13	5.13	5.13	5.13	5.13	5.13	5.13
Maximum	61.54	33.33	56.41	43.59	94.87	76.92	64.10	28.21	105.13	64.10	58.97	66.67	56.41

Figures 5.12a-d: SCP size distributions for periods of elevated SCP counts in Episode 1

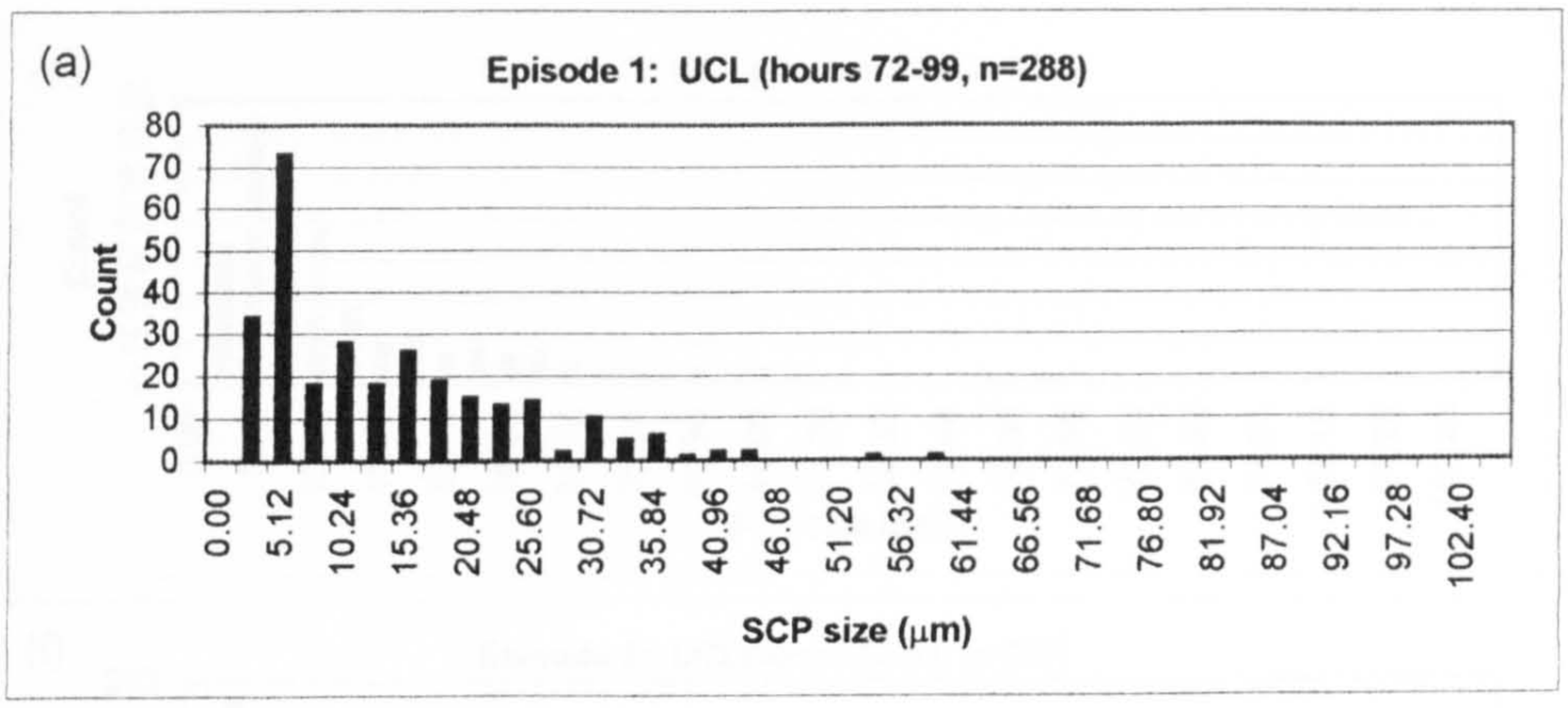

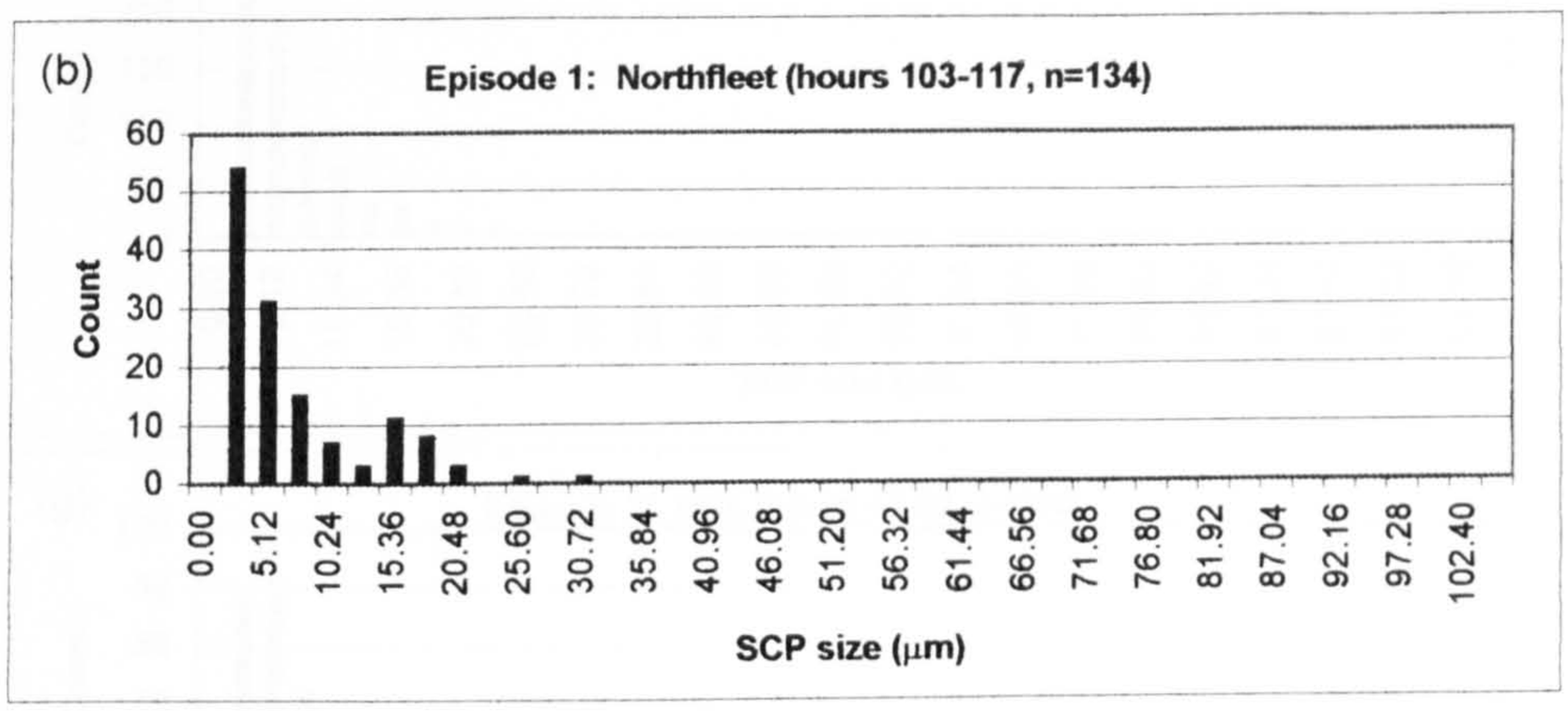

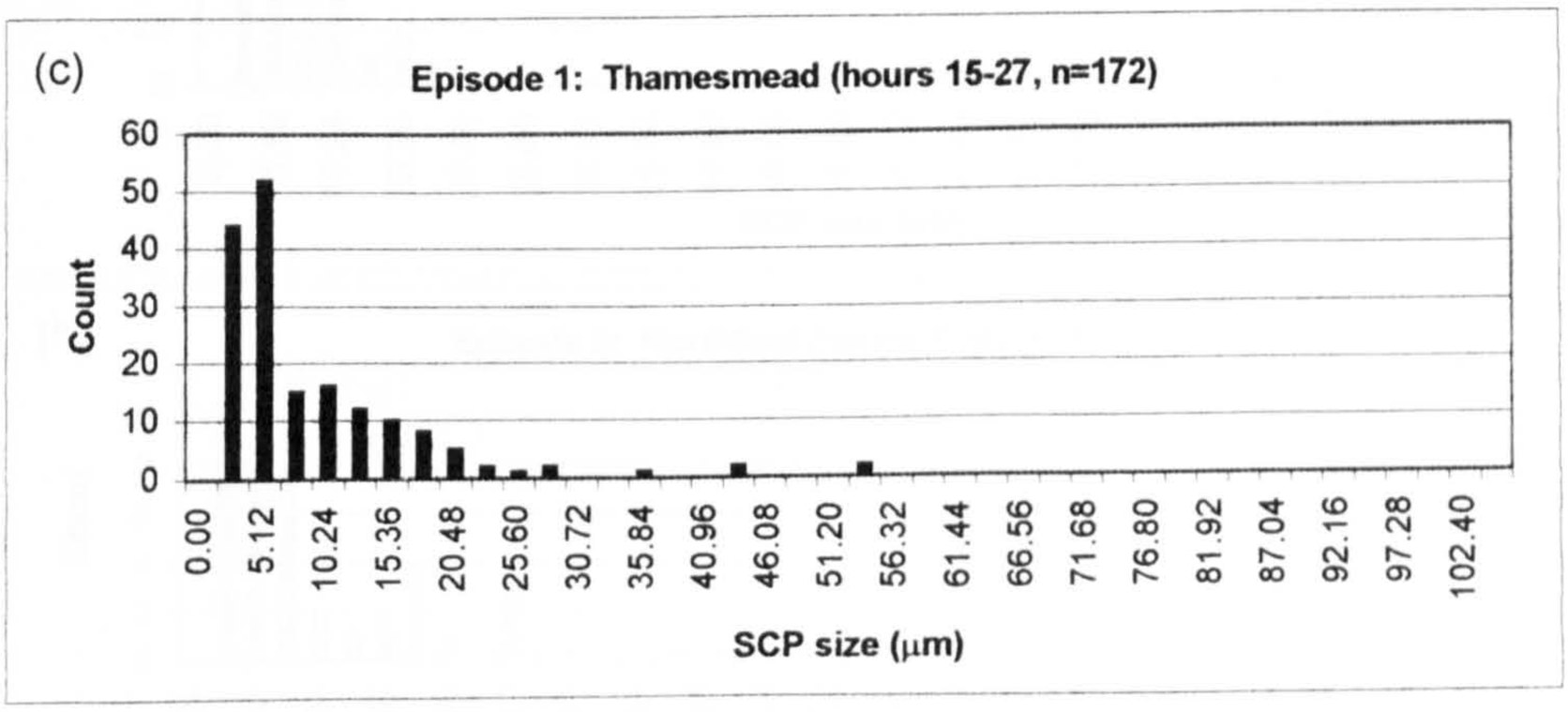

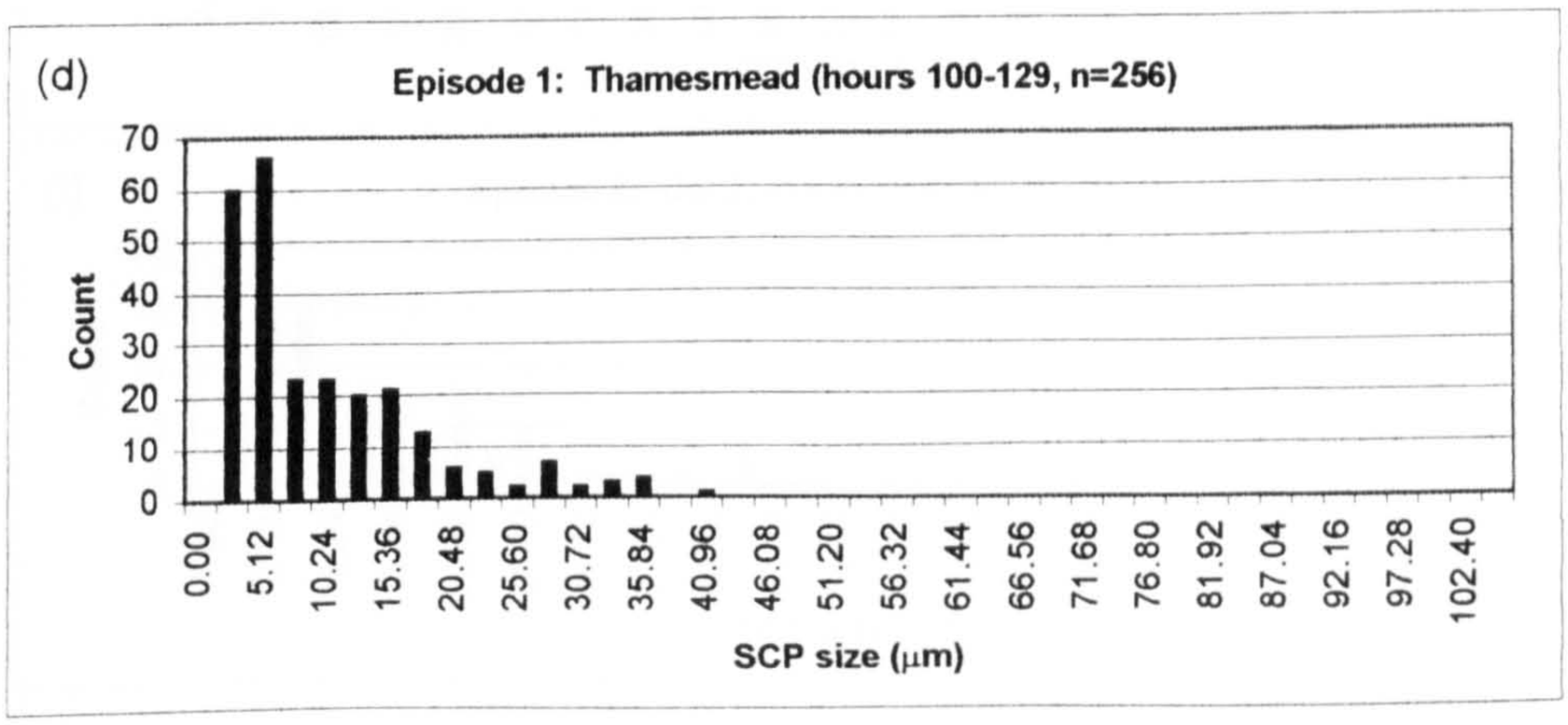

Figures 5.12e-i: SCP size distributions for periods of elevated SCP counts in Episode 2

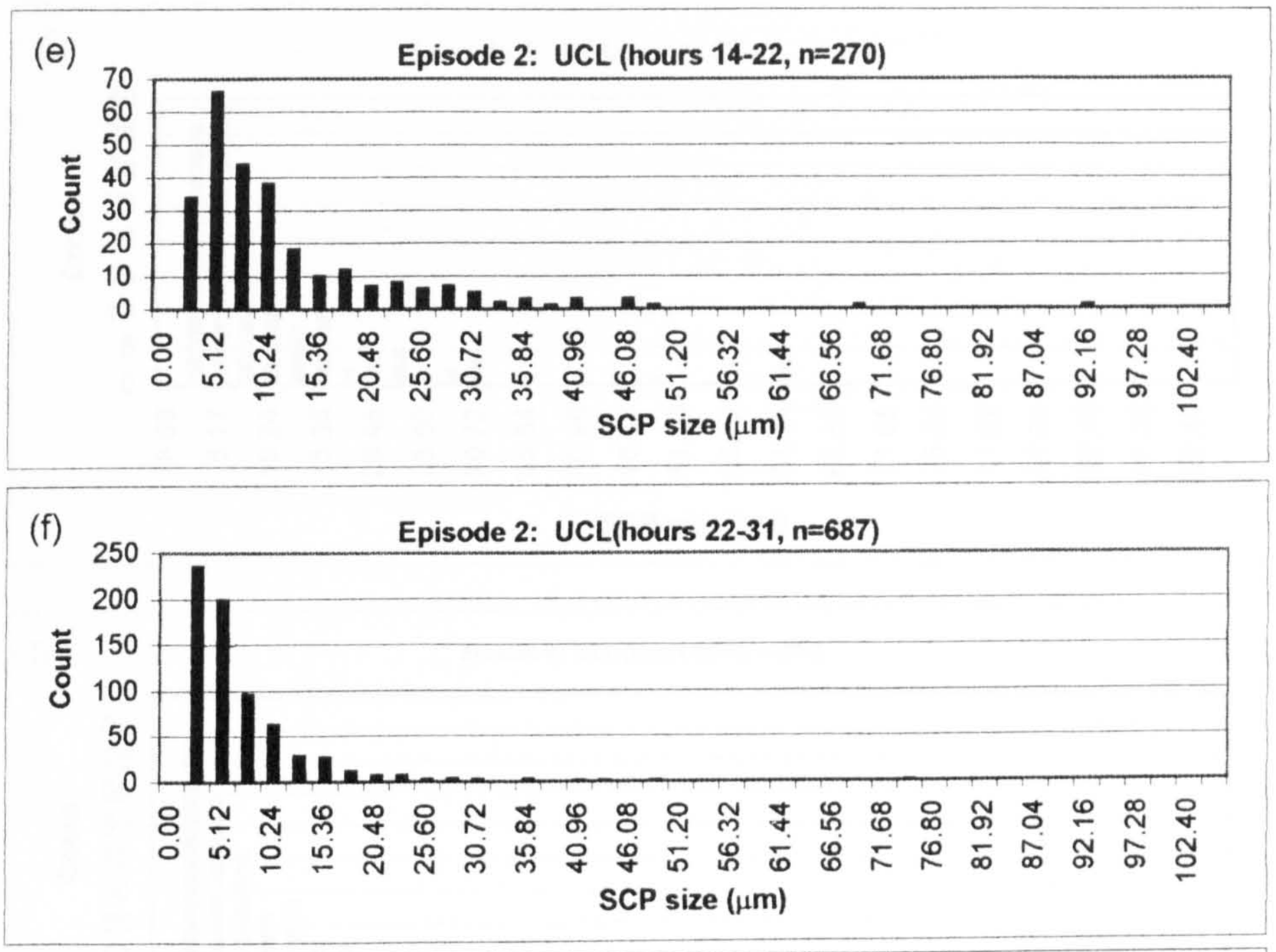

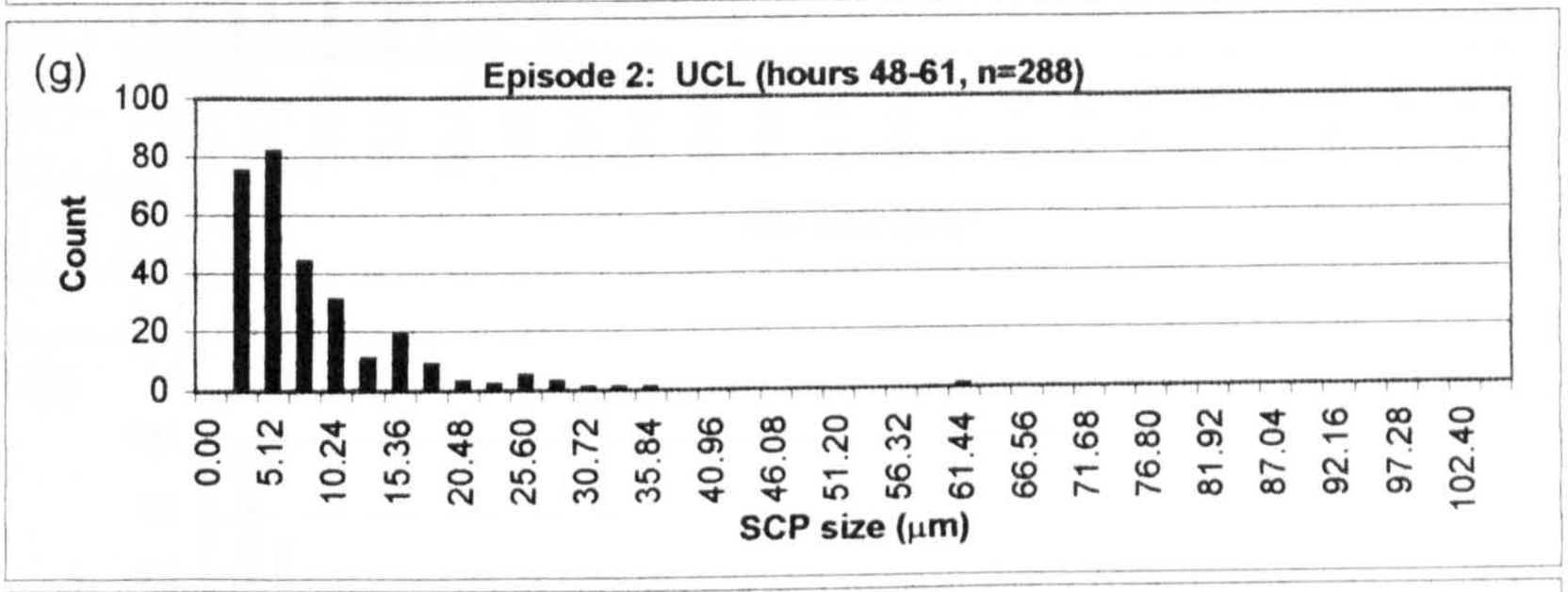

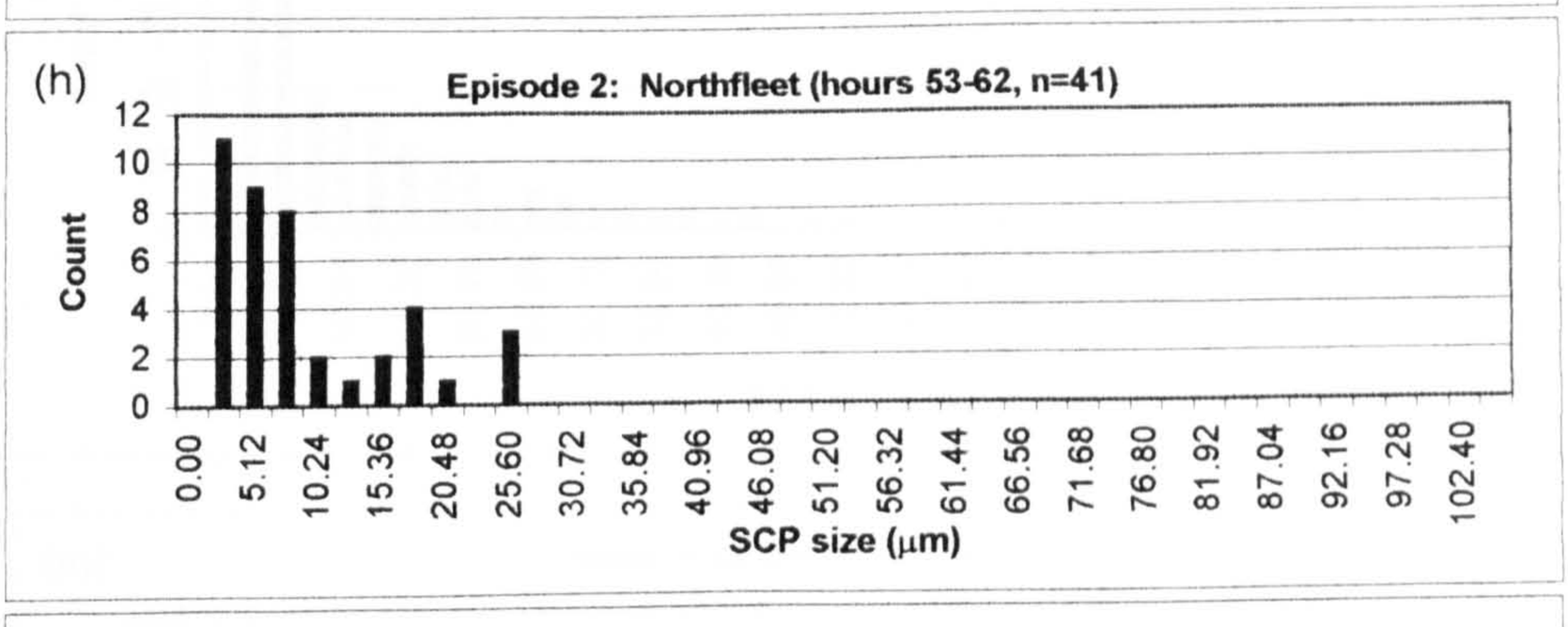

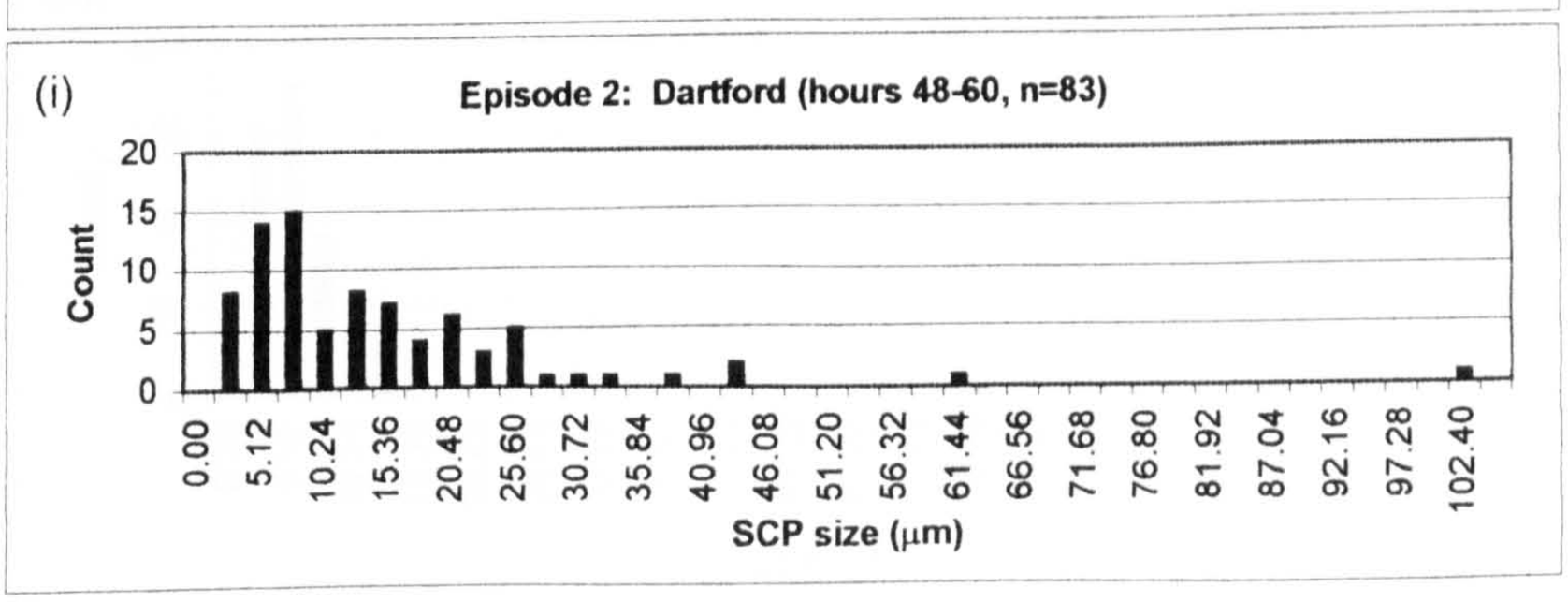

Figures 5.12j-m: SCP size distributions for periods of elevated SCP counts in Episodes 3, 4 and 5

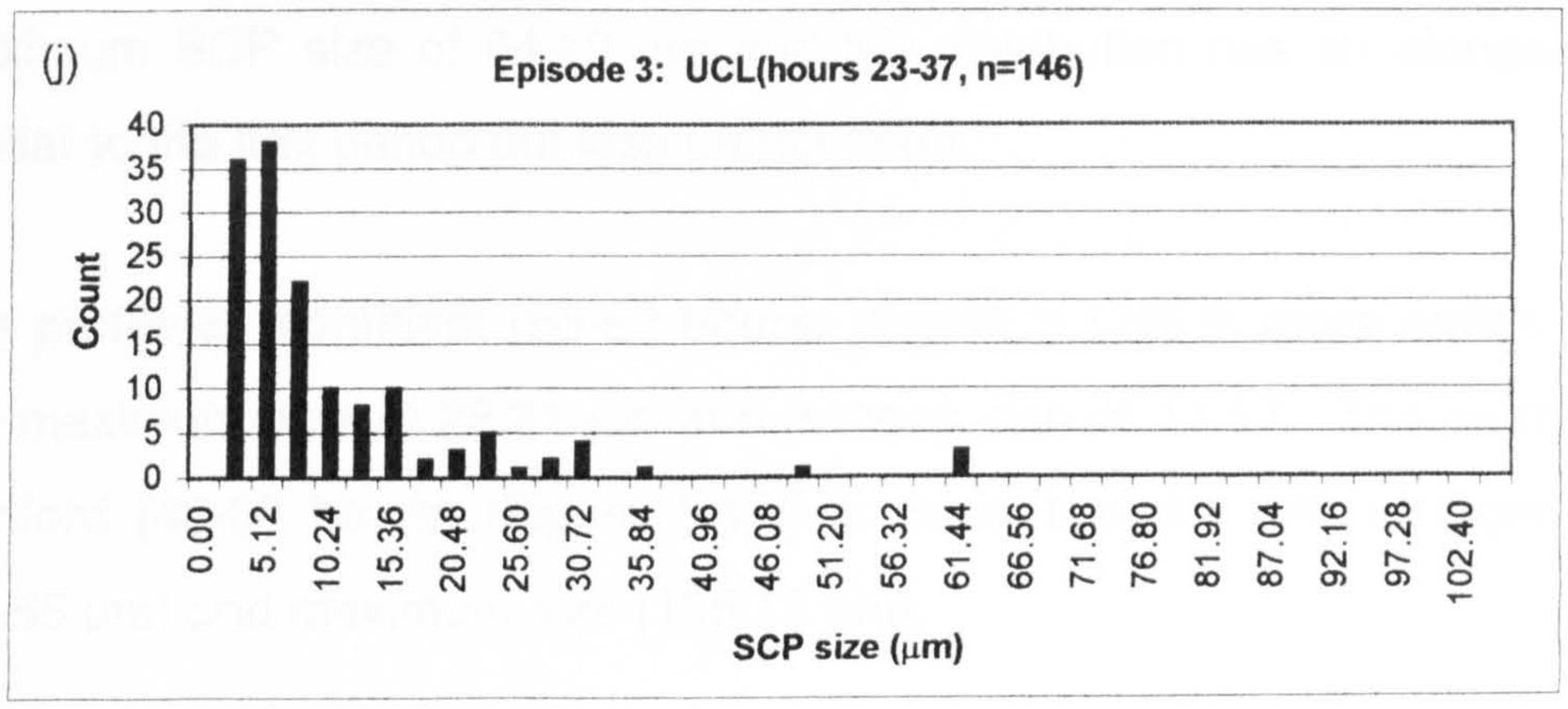

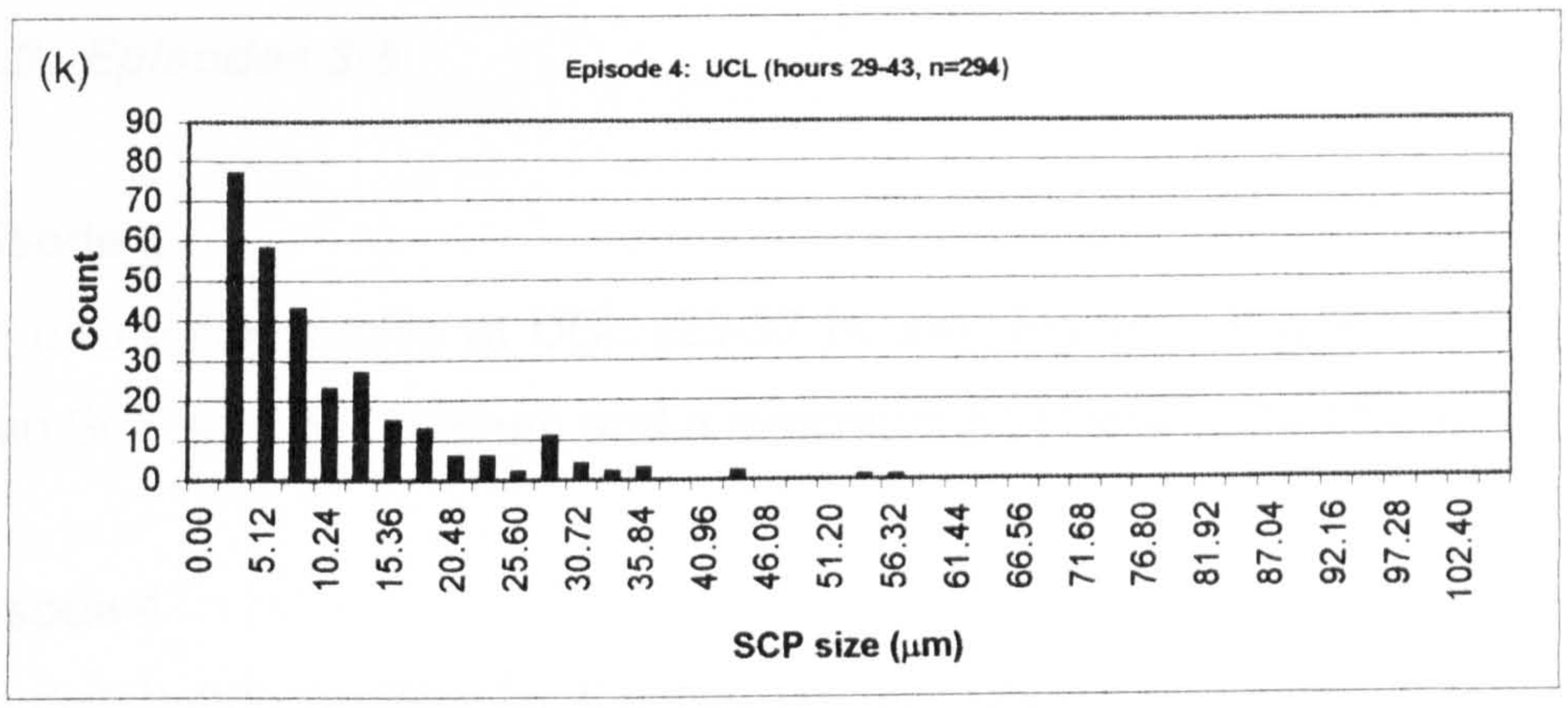

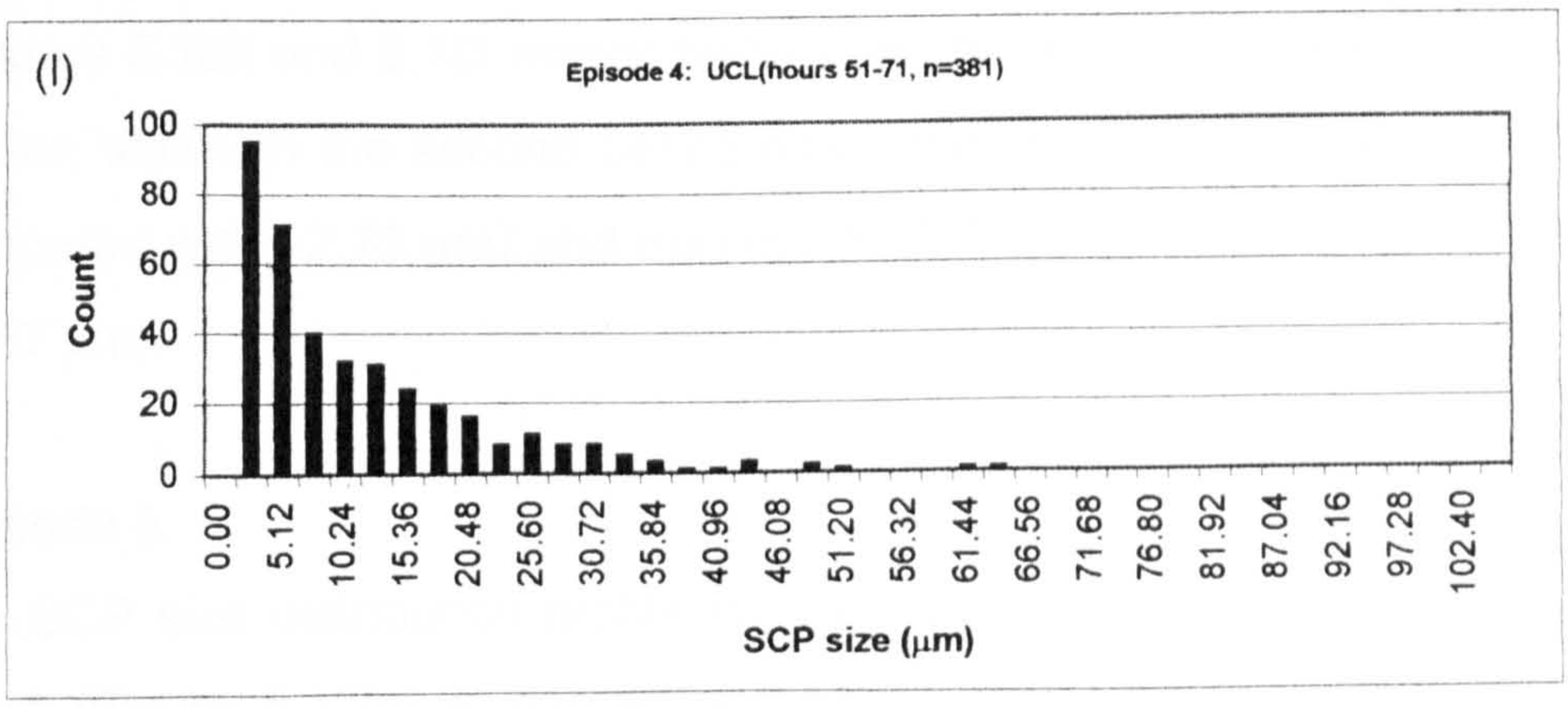

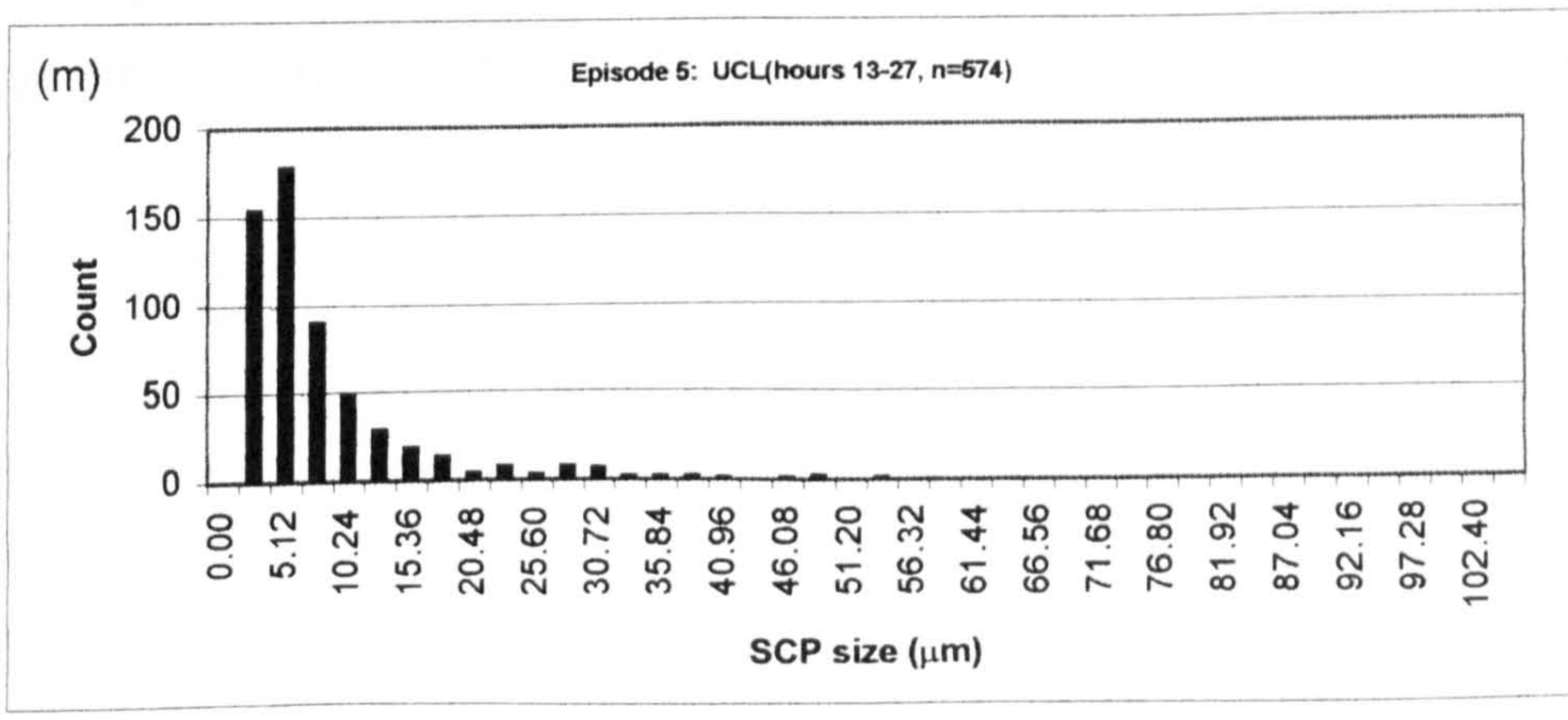

The counts in the second period are much higher than first (n=687 and n=270 respectively). The third period (48-61 hours) has a mean size of 10.85 μm, a maximum SCP size of 64.10 μm and the distribution has an elongated tail similar to the first period but less pronounced.

The profile at Northfleet (53-62 hours) (Figure 5.12h) is more erratic with a low maximum size of 28.21 μm and a mean size of 11.57. The profile from Dartford (48-60 hours) (Figure 5.12i) is much broader with a larger mean (17.55 μm) and maximum size (105.13 μm).

5.3.3 Episodes 3-5

Episode 3

The distribution profile at UCL (23-37 hours) (Figure 5.12j) is narrow with a mean SCP size of 12.86 μm and a maximum SCP size of 64.10 μm.

Episode 4

The distribution profiles for the two periods (29-43 hours and 51-71 hours) (Figures 5.12k and 5.12l respectively) selected during Episode 4 are visually similar, although the second period has a marginally larger mean (14.05 μm compared with 12.73 μm) and maximum SCP size (58.97 μm compared with 66.67 μm).

Episode 5

The SCP size distribution profile for the period at UCL between 13 and 27 hours (Figure 5.12m) is narrow and has a correspondingly low mean size (10.68 μm) and maximum size (56.41 μm).

5.4 Relationships between IAS and SCP across London for Episodes 1 and 2

The relationships between IAS and SCP deposition (in terms of number of particles per hour) at the different transect sites show the spatial relationship of power station pollution episodes. Correlations between the IAS and SCP time-series were calculated and are shown in Tables 5.15. and 5.16.

Table 5.15: Correlation matrix showing the relationships between IAS and SCP at all sites in Episode 1

	UCL SCP	UCL IAS	T'MEAD SCP	T'MEAS IAS	D'FORD SCP	D'FORD IAS	N'FLEET SCP	N'FLEET IAS
UCL SCP	1							
UCL IAS	0.02	1						
T'MEAD SCP	-0.10	0.16	1					
T'MEAS IAS	0.00	0.84	0.33	1				
D'FORD SCP	-0.21	0.07	0.26	0.18	1			
D'FORD IAS	0.00	0.88	0.21	0.93	0.24	1		
N'FLEET SCP	-0.14	0.43	0.40	0.49	0.33	0.43	1	
N'FLEET IAS	-0.04	0.75	0.48	0.91	0.25	0.85	0.61	1

5.4.1 Episode 1

IAS-IAS relationships

Strong, positive and significant relationships exist between IAS deposition (particles per hour) at all sites with the strongest relationships occurring between Thamesmead and Dartford ($r=0.93$, $p\leq0.05$) and Thamesmead and Northfleet ($r=0.91$, $p\leq0.05$). This pattern can be clearly seen on the time-series profiles (Figures 5.2d, 5.3d and 5.4d) for these sites. The IAS profile at Dartford is almost identical to the one at Thamesmead, however the third major IAS peak at Thamesmead spans more time than its corresponding peak in the Dartford profile. The IAS record shows a number of peaks early in the episode that are synchronous with peaks in the IAS profiles from Dartford and Thamesmead but of much greater magnitude. The second IAS peak is present on 8/3/99 and coincides with the peaks at Dartford, Northfleet and

UCL, however at Northfleet it is smaller (just over 420 SCP hr^{-1} compared with over 1000 at Thamesmead) and wider, therefore spanning a greater amount of time.

IAS-SCP relationships

The relationships between SCP and IAS vary from site to site. The correlation between SCP deposition at UCL and the IAS profiles at UCL, Thamesmead, Dartford and Northfleet ranges with non-significant r between 0.02 and –0.04. The UCL IAS profile has only one significant relationship with the SCP profile at another site and this is with Northfleet (r=0.43). Generally IAS and SCP relationships in Episode 1 are positive with the highest correlations between Northfleet IAS and Northfleet SCP (r=0.61, $p \leq 0.05$) and between Northfleet SCP and Thamesmead IAS (r=0.49, $p \leq 0.05$).

SCP-SCP relationships

The SCP-SCP correlations between UCL and Thamesmead and between UCL and Northfleet are not significant; between UCL and Dartford the relationship is significant but weakly negative (r=-0.21, $p \leq 0.05$). The large SCP peak at UCL (Figure 5.1c) has no counterparts in the SCP profiles from the other transect sites. The SCP-SCP relationships between Thamesmead, Dartford and Northfleet are all significant and weakly positive (r ranges between 0.26 and 0.40).

5.4.2 Episode 2

IAS-IAS relationships

There are only 2 significant correlations between IAS counts in Episode 2, between Thamesmead and UCL (r=0.34, $p \leq 0.05$) and between Northfleet and Dartford (r=0.33, $p \leq 0.05$). The profile for Thamesmead has some very distinct peaks whereas the UCL profile is much noisier, although those same peaks can be seen occurring at the same time. The profiles of Dartford and Northfleet are less noisy but there is evidence of a peak in the profile at Dartford that is not present at Northfleet. The secondary peak at Dartford is present in both profiles.

Table 5.16: Correlation matrix showing the relationships between IAS and SCP at all sites in Episode 2

	UCL SCP	UCL IAS	T'MEAD SCP	T'MEAS IAS	D'FORD SCP	D'FORD IAS	N'FLEET SCP	N'FLEET IAS
UCL SCP	1							
UCL IAS	0.14	1						
T'MEAD SCP	0.07	0.21	1					
T'MEAS IAS	-0.19	0.34	0.40	1				
D'FORD SCP	-0.07	0.07	0.20	0.12	1			
D'FORD IAS	-0.21	0.00	-0.03	-0.01	0.34	1		
N'FLEET SCP	0.05	-0.20	-0.14	-0.15	0.24	0.08	1	
N'FLEET IAS	-0.19	-0.13	-0.09	0.06	0.22	0.33	0.48	11

IAS-SCP relationships

Thamesmead ($r=0.40$, $p\leq0.05$), Dartford ($r=0.34$, $p\leq0.05$) and Northfleet ($r=0.48$, $p\leq0.05$) all have significant correlations between their SCP and IAS time-series. Although the relationships are weak they show that the source for some of the IAS peaks and the SCP peaks is the same. There are no significant correlations between the IAS and SCP profiles from different sites.

SCP-SCP ratios

There are no significant correlations of SCP profiles between any of the sites.

5.5 Discussion

This discussion focusses on the differences and relationships between the counts and size distributions of IAS and SCP at each site and during each episode. An attempt has been made to suggest potential sources for each pollution event. The relationship between IAS and SCP with SO_2 and NO_2 is also discussed. The meteorological conditions at the time of the episode are not considered fully in this chapter, although meteorology will have a major effect on SCP and IAS numbers and distribution. Any discussion of pollution time-series would be incomplete without a consideration of the meteorology and, therefore, this is analysed fully in Chapter 6.

5.5.1 Episode 1

The similarities in the IAS profiles across the transect indicate the presence of two periods within the episode where deposition of IAS occurs simultaneously at all four sites. IAS are almost exclusively produced by high temperature combustion of coal and therefore these periods are almost certainly caused by a single source that is fuelled by coal.

The relationship between IAS and SCP is weaker, especially between the IAS and SCP counts from UCL and those from all other transect sites. There are coincidental IAS and SCP peaks at Thamesmead, Dartford and Northfleet for both periods, although the Dartford SCP profile is very noisy. The SCP levels are low at Dartford compared to the other three sites. The mean SCP size and maximum are both smaller at Northfleet than at Thamesmead suggesting that the source is closer to Thamesmead. The closest coal-fired process that fulfils the criterion is Tilbury power station. The Ford plant at Dagenham was switched from coal to natural gas in 1997 so will not have an impact on these episodes. There may be an impact from Didcot on London, however the dispersion modelling results from Chapter 3 showed that this will be minor and is unlikely to have a significant impact at the transect sites which are in the centre and east of London.

The lack of a simultaneous SCP peak at UCL may be due to site specific factors. For example, the urban canyons and trees that are relatively close to the UCL site may affect the movement of SCPs more than IASs due to the larger SCP size. The Dartford site is significantly higher than the other transect sites (9.1 m compared with 5.0 m at Thamesmead, 3.0 m at UCL and just 2.0 m at Northfleet) and, once again, this may affect SCP numbers and cause the effects of the episode to be dampened. A study in Milan, Italy showed that under good atmospheric mixing conditions the concentration of particulate matter from an episodic long-range transport event was found to be almost constant up to 100 m (Marcazzan et al., 1994). However, fly ash larger than 0.5 μm emitted by coal power plants in the region of north-west Bohemia was shown to increase in concentration with height (Havlíček et al.

2000). In a study in Loughborough, UK the effect of height on particle concentrations from the ground, to a height of 2.88m, in a variety of locations, was found to vary (Micallef et al.,1998). The precise effect of sampling height on SCP and IAS concentrations in this study is uncertain but it does not appear to affect the spatial impact of peaks.

The time-series for UCL has only one significant correlation with IAS at other sites and that is between UCL IAS and Northfleet SCP. Visual examination of the profiles (Figure 5.1d and 5.4c) shows that there is little relationship between these two sites and indicates that the correlation is likely to be spurious. Since there is no relationship between IAS and SCP at UCL, the unique SCP profile suggests that the elevated period (hours 72-99) is caused by a local oil-fired source. The particle size data for this period confirms that the source is likely to be local with a large SCP mean size and a relatively large maximum SCP size, therefore, possibly Citigen or London Underground Chelsea.

5.5.2 Episode 2

The similarities between profiles in Episode 2 are less obvious than in Episode 1. There are IAS peaks at all sites on 17/4/99 but these are lower and more diffuse than those in Episode 1. In general, the IAS peaks of Episode 2 are associated with low SCP peaks, consistent with emissions from a coal source. The single IAS peak at Thamesmead on 15/4/99 is also coincident with a low SCP peak, but this feature does not appear at all sites, suggesting a local source for these particles.

The major period of elevated SCP counts at UCL on 16/4/99, and the minor peak immediately preceding it, are not associated with peaks in the IAS profile. These periods are therefore produced by an oil combustion source. However, the SCP size profiles for these peaks are different (Figures 5.12e and 5.12f) with the smaller peak (14-22 hours) associated with a wider distribution profile, higher average SCP size and larger maximum SCP size than the larger peak (22-31 hours). One possibility is that the small peak

reflects emissions from a more local source, whereas the source of the SCPs in the large peak is more distant and, therefore, the two peaks are the result of two separate pollution events. However, the absence of large SCPs does not necessarily indicate that the source is not local, it is feasible that larger particles were just not collected. That said, in this case the number of SCPs in the major peak (n=687) indicates that if large particles were emitted then it is likely that they would be present on the Burkard Trap tapes.

The third UCL period coincides with elevated concentrations of SCPs at Northfleet (53-62 hours) and Dartford (48-60 hours). At both Dartford and Northfleet the distribution profile is broader than that of UCL with a larger mean SCP size (UCL = 10.85 μm compared with Dartford = 17.55 μm and Northfleet = 11.57 μm). The profile and the means would suggest that the SCP source is local to Dartford and Northfleet and further from UCL, however the maximum particle size at Northfleet is only 28.21 μm compared with 64.10 μm at UCL. Since the number of SCPs counted in the peak at Northfleet is so low (n=41) then it is possible that larger SCPs may be present in the atmosphere but not collected by the Burkard Trap. The numbers of SCPs counted at Dartford (48-60 hours) is also small (n=83) compared with 288 SCPs counted in the peak at UCL. The greater magnitude of the UCL peak points to the source of the peak being local to UCL.

The time periods covered by the SCP events are almost identical for Northfleet and Dartford, however these slightly lag behind the peak at UCL. This can be explained either by the source of the particles being local to UCL and their being a time delay during transport of the SCPs particles over to Thamesmead and Dartford, or by there being two separate sources that cause SCP events at a similar time (i.e. one event causing an SCP peak at UCL and a second causing an SCP peak at Dartford and Northfleet). The IAS profile confirms that the latter is true with a peak in IAS that coincides with the peak in SCP at both Dartford and Northfleet. At both these sites the onset of the SCP peak occurs slightly before the IAS peak and this is consistent with a coal-fired source being fired up using oil and then switching to coal fuel. The most likely sources would be Kingsnorth or Tilbury although

the absence of a similar profile at Thamesmead indicates that the source is more likely to be Kingsnorth since Tilbury is closer to Thamesmead.

5.5.3 Episode 3

There is a clear relationship between the SO_2, SCP and IAS profiles during Episode 3, showing that the source of the particle event is coal-fired. The SCP peak contains a few large particles (maximum = 64.10 μm) which indicates that the source must be relatively local. The SCP peak might be due to low emissions from an oil-fired source (e.g. Citigen) or alternatively due to resuspension of SCPs previously deposited.

5.5.4 Episode 4

There are no clear relationships between SO_2 and either IAS or SCP during Episode 4. Both SCP and IAS peaks occur during periods where SO_2 concentrations are very low. IAS and SCP peaks also occur at different times indicating that there are two sources causing two separate pollution events during the episode. The IAS peak is caused by a coal-fired source but without the extra information from other transect sites the origin of the event is unclear. Examination of the meteorological conditions at the time may provide more insight about the source (see Chapter 6).

The first SCP peak (29-43 hours) occurs at the end of the IAS peak but is probably unrelated due to the high number of SCPs counted (see Section 5.5.4). The SCP size distribution profile is similar to the profile for the second SCP event (51-71 hours), the second peak having slightly higher mean (14.05 μm compared with 12.73 μm). Both peaks have a number of relatively large SCPs and, therefore, the source for these two peaks must be a local oil-fired source, probably Citigen or London Underground Chelsea. The first SCP peak is associated with a peak in NO_2 and therefore an alternative source might be resuspension of road dusts.

5.5.5 Episode 5

The two particle events that occur during Episode 5 are clearly caused by different sources. The first SCP peak is not associated with an IAS peak and, therefore, the SCPs are emitted by an oil-fired process. There are few large SCPs in the size distribution and so it is possible that the source is less local than the sources of the SCP peaks in other episodes. Possibly Littlebrook or Grain in the east Thames corridor may be the source. Both IAS peaks are associated with relatively low levels of SCPs, as in other episodes, which indicates that the source is coal-fired.

5.5.6 Comparison of episodes

UCL

The only significant relationship (r=0.75) between IAS and SCP at UCL occurs during Episode 3 when there are synchronous peaks in both types of particle. During all the other episodes the correlations are insignificant, however there is evidence during Episode 5 on 21/12/97 (Figure 5.9c) of a small SCP peak at the same time as the major IAS peak. This relationship is masked by other non-synchronous features that occur in the SCP and IAS profiles during Episode 5. There are peaks in IAS during all episodes at UCL and these indicate the impact of a coal-fired source on the centre of London, i.e. Didcot, Tilbury or Kingsnorth. Although the results from Chapter 3 show that it is unlikely to be Didcot.

There is evidence for an oil-fired source during Episodes 1, 2, 4 and 5 with SCP peaks that do not have an associated IAS peak. The magnitude of the peaks varies between episodes but there is no consistent relationship with the size distribution. This might have indicated whether the magnitude of the peak is related to proximity to a source. For example, the major peak from Episode 2 (22-31 hours), and one of the minor peaks (48-61 hours), have similar size distributions despite the major peak having around three times as many SCPs hr^{-1}. Episode 4, on the other hand has a relatively high major peak (71 SCP hr^{-1}) (51-71 hours) and a much broader size distribution profile

than the peak in Episode 5 (13-27 hours), which is also large, with over 110 SCP hr^{-1}.

The size distributions for the UCL SCP peaks can be visually grouped into two types. One has a narrow distribution characterised by a low average SCP size (around 10 μm) and the other has a larger distribution with an average size of around 13 μm or larger. This indicates that there are two different sources for the episodes at UCL. One that is local (Citigen, London Underground Chelsea or London Underground Greenwich) and another that is more distant (Littlebrook, Grain, Kodak or Heathrow). Alternatively there may be only one source with larger SCPs becoming resuspended at certain times but not at others. An analysis of the meteorology (Chapter 6) will improve the interpretation of these data.

Thamesmead

The major peaks at Thamesmead during Episodes 1 and 2 occur at the same time as IAS peaks therefore showing that the source of the particle events is a coal-fired process. Potential sources are Tilbury and Kingsnorth in the east Thames corridor. There are no oil-related SCP peaks during either of the Episodes at Thamesmead. The size of the major IAS peak during Episode 1 is much greater the peaks of Episode 2 (over 1000 IAS hr^{-1} and around 60 IAS hr^{-1} respectively). The minor peak during Episode 1 is about 400 IAS hr^{-1} but is associated with a SCP peak that is higher (70 SCP hr^{-1}) than the SCP peak that occurs at the same time as the major IAS peak (30 SCP hr^{-1}). This may be due to the impact of an oil-fired source at the same time as the coal-fired one. Alternatively, these SCP and IAS peaks are slightly offset and therefore the SCP peak may be due to the use of oil in a coal-fired power station during firing-up. This explanation is less likely due to the presence of a small IAS peak a few hours before the major SCP peak.

Dartford

The IAS peaks in Episode 1 are potentially associated with minor peaks in the SCP profile whereas in Episode 2 the relationship is less straightforward with only two of the IAS peaks (42-46 hours and 54-60 hours) having coincident

SCP peaks. However, there are low levels of SCPs at all times when there are IAS peaks. Lack of a synchronous SCP peak may indicate that a source is further away than if there is a high SCP occurring at the same time as an IAS peak. The SCP peak (48-60 hours) has a very broad distribution profile which suggests that the potential sources for the coincident IAS peak is a local coal-fired power station, probably Tilbury. The low SCP peaks that do not have a significant IAS peak are possibly due to Littlebrook power station, which is located on the outskirts of Dartford. However, the SO_2 and NO_2 profiles show that there is a build up of road transport derived pollution and therefore SCP levels maybe due to resuspension of road dust.

The SCP counts are slightly lower in Episode 1 (maximum 9 SCP hr^{-1}) compared with Episode 2 (maximum 16 SCP hr^{-1}). However, the peaks in IAS are higher in Episode 1 with just over 700 IAS hr^{-1} in the major peak compared with just over 100 IAS hr^{-1} in the second peak (i.e. the one that coincides with the SCP peak) in Episode 2. There is not enough information at this site to determine a relationship between relative peak height and source, although there is no relationship between IAS and SCP peak heights and particles size at UCL.

Northfleet

The major IAS peaks during both Episodes 1 and 2 with associated SCP peaks suggest a coal-fired source. The size distribution of the SCP peak at 103-117 hours during Episode 1 has a lower average (9.69 µm) compared with 11.57 µm during Episode 2 (53-62 hours) and therefore these two events may originate from separate sources, possibly Kingsnorth for Episode 1 and Tilbury for Episode 2. Kingsnorth lies to the east of Northfleet and Tilbury lies to the north-west, so once again, examination of meteorological data may provide more information about the likely source.

There is a more diffuse, low level, SCP event that occurs during, and after the same time as the first IAS peak during Episode 2 (12-53 hours). Elevated SCP levels after the IAS levels have reduced to the background (29-53 hours) and may indicate resuspension. However there is a large SO_2 peak during

the first SCP and IAS event of Episode 2 but not during the second. This may indicate two different sources, the first event being associated with a source where the flue gas desulphurisation (FGD) equipment is not very efficient or even switched off. More information about FGD at each source would be necessary to make a better evaluation.

5.5.7 Magnitude of particulate pollution events

The magnitude of IAS peaks varies from site to site. During Episode 1, where the major IAS peaks occur synchronously at all sites, the highest counts are at Thamesmead. The IAS source is likely to be the same at each site since the peaks seem to be part of one wide-spread event that impacts across the east of London at the same time.

It is feasible that a plume could move quickly enough across London to deposit IASs that feature as peaks on Burkard Trap tapes at different sites at the same time. At the start of this major IAS event in Episode 1 the wind is easterly and has a speed of 2.75 ms^{-1} (see Section 6.2.1) which is equivalent to 9.27 km hr^{-1}. The distance from Northfleet to UCL is approximately 35 km. At this speed a plume would take approximately 4 hours to reach UCL after passing over Northfleet. This agrees well with the onset of the IAS peak at UCL occurring a few hours after the increase at Northfleet.

IASs have the largest impact at Thamesmead and so this site may be closest to the source. However, the source has a similar impact to both the east and west of Thamesmead with similar peak counts at UCL and Dartford and this is not easily explained. In contrast, during Episode 2 the IAS counts increase with increasing distance east from the centre of London. The peaks do not occur at the same time and, therefore, it is not possible to determine any further relationships between peak size and source for this episode.

The highest SCP peak occurs at UCL during Episode 2 with no IAS peak and is assumed to be from an oil-fired source. There are also other high SCP peaks at UCL during Episodes 3 and 4 that do not have associated peaks in

IAS. It has been assumed that the source of these is a local oil-fired source and this is consistent with the results from Chapter 4 where REG and VICT had the highest SCP concentrations in their surface sediments, thought to be caused by a local source.

5.5.8 SO_2 concentrations

Generally, elevated counts of IAS and SCP are associated with high levels of SO_2. There are incidences where SO_2 and NO_2 have the same peaks, for example during Episode 1 at UCL there is a coincident SO_2 and NO_2 peak (40-45 hours), which indicates road transport derived pollution. In Episode 4 the SO_2, NO_2 and IAS profiles follow similar patterns for the first two days of the Episode. This may indicate that the NO_2 is from the same source as both the SO_2 and IAS, or that IAS levels are high due to meteorological conditions that favour a build up of NO_2 and SO_2 and resuspension of particles. Analysis of the meteorology during this period may suggest an explanation.

There are a few examples (e.g. Episode 1 at Northfleet, Episode 4 at UCL) where there is a peak in IAS or SCP, or both, which is not associated with a SO_2 peak. This can be explained at Thamesmead, Dartford and Northfleet because the pollution monitoring stations and the Burkard Traps were not co-located and pollution plumes could affect each site differently. However, during Episodes 4 and 5 at UCL, the peaks in SO_2 are not well related to SCP concentration. The UCL Burkard Trap is situated within 500 m of the Bloomsbury monitoring station and the input of SCPs and SO_2 should be the same at each site. The relationships between IAS and SCP are also poor during Episodes 4 and 5 (see Table 5.12 and 5.13) and the reasons for this are not clear.

In general, analysis of SO_2 and NO_2 concentrations can be used as an indicator of the presence of a pollution event from high-temperature combustion sources and, to some extent, can provide an indication of the magnitude of the event. For example, the major IAS peak in Episode 1 contains over 1000 SCP hr^{-1} in Episode 1 and is associated with a high peak

in SO_2 (almost 40 ppb). In contrast, the major IAS peaks in Episode 2 are much lower (around 60 SCP hr^{-1}) and are associated with much lower levels of SO_2.

There are other factors that have not been taken account in this analysis, such as the motion of the plume, which may loop up and down or side-to-side (see Section 3.1.4) or errors made in cutting up the Burkard Trap tapes. The Burkard Trap tape method has a resolution of one hour in each 2 mm section of tape. A measurement error of 1 mm would therefore shift the time-series by half an hour. In addition, the tape moves continuously and at any one time on the tape there is a spread of particles that covers a 2 mm band. This means that particles deposited at any time may be counted in a section half an hour earlier or later. These errors in combination could account for a time shift and it would be surprising if any events occurred at exactly the same time, even if they were measured at the same site.

This Chapter has attempted to extract patterns from the SCP and IAS profiles collected on tapes from a transect of Burkard Traps across London. It is clear that there is a lot of information in the profiles of SCP and IAS that can be used to determine the source of pollution events. Comparison of particle counts and SCP size distributions has enabled a general discussion of likely sources for the SCP and IAS event. However, it is also clear that for a more detailed analysis of each pollution event then meteorology must be considered. The meteorology of each episode is the subject of Chapter 6.

CHAPTER 6: METEOROLOGY OF POLLUTION EPISODES

6.1 Introduction

In the past, pollution episodes have been linked to source by the meteorological conditions prevailing at the time. For example, using a synoptic climatology approach Cheng and Lam (2000) showed that wind direction and speed are the most important variables affecting pollution concentrations in Hong Kong, and in Birmingham, UK, continental anticyclonic airmass types were associated with high pollution concentrations (McGregor and Bamzelis, 1995). Application of a Kalman filter to meteorological data improves the explanation of the variance in PM_{10} in the Netherlands, compared with linear regression analysis (van der Wal and Janssen, 2000). They found that PM_{10} concentrations were characterised by low temperatures, dry weather and winds from the east and south in winter. Other research using a number of different statistical techniques has been used to apportion sources and important meteorological variables for pollution concentrations (e.g. Olcese and Toselli, 1998; Chueinta et al., 2000; Mukerjee et al., 2001; Oh and Ghim, 2001; Chan and Kwok, 2001; Triantafyllou, 2001; Physick and Goudey, 2001).

South-easterly winds have been shown to be important for PM_{10} concentrations in London. The contribution of secondary particles from the south-east to a PM_{10} episode in March 1996 was described by Stedman (1998). Smith et al. (2001) used multivariate statistics to explain the variance in PM_{10} in London and found that by plotting PM_{10} against trajectory wind speed a clear PM_{10} peak could be ascribed to the south-easterly direction. Power station pollution was cited as the cause of an SO_2 episode in July 1996 due to easterly winds bringing power station plumes over London from the sources in the East Thames Corridor (SEIPH, 1997). Boundary layer height in combination with low wind speeds from the east was linked to an SO_2 episode in London in 1994. The highest SO_2 concentrations were measured at monitoring stations in the east of London with a decrease towards the west (SEIPH, 1995).

The IAS and SCP time-series results from Chapter 5 are a result of the quantities of emissions from high-temperature combustion sources and dispersion by the meteorological processes in the atmosphere at the time. The presence of a peak in SCP or IAS relies on both a source of sufficient magnitude and the right meteorological conditions to bring the particles from the source to the Burkard Trap. There are similar patterns in SCP and IAS time-series from different sites across London, which would suggest that simultaneous peaks originate from the same source and are driven by the same meteorological conditions. However, there are peaks in both IAS and SCP that do not have coincidental peaks at all or some of the other sites.

The aims of this Chapter are:

- To simplify the meteorology of the episodes from Chapter 5 using multivariate statistics and to determine the significant meteorological variables that influence the SCP and IAS profiles;
- To evaluate the common themes that cause IAS and SCP episodes in London; and
- To test the hypothesis that sampling site has an effect on SCP and IAS concentrations.

6.1.1 Definitions of meteorological parameters

The meteorological data were taken from the London Weather Centre via the British Atmospheric Data Centre available through the Internet (http://www.badc.rl.ac.uk), the same source as for the meteorological data used in the dispersion model discussed in Chapter 3.

Wind strength and direction

Wind direction is measured as an averaged direction from which the wind is blowing to the nearest 10 degrees. Wind speed is measured in knots (1 knot is equivalent to 0.515 ms^{-1}). Both speed and direction data used in this study are hourly averaged values. Direction data are discontinuous at 360 degrees i.e. 0 degrees and 360 degrees are the same direction. In order to use the wind direction data in further statistical analyses it was necessary to split the

direction into a north-south component and an east-west component using a sine-cosine transformation. These new directions were then combined with the wind speed to create north-south (NORTH) and east-west (EAST) speed vectors. Both the direction vectors and the original wind speed and direction data are used in the time-series plots (Figures 6.1, 6.4, 6.7, 6.10 and 6.13).

Cloud cover

Total cloud amount (TCA), cloud base amount (CBA) and cloud amount - level 1 (CA1) are measured in eighths of the sky (Oktas) and are estimated manually. CA1 is the amount of low-level cloud and includes cumulus, cumulonimbus, stratus and stratocumulus (Met. Office, 2001). Cloud base height (CBH) and cloud base - level 1 (CB1), the height of the low clouds, are measured in decametres (100's of meters) (dams) either manually or using a Laser Cloud Base Recorder.

Horizontal visibility

Visibility (VIS) is measured in decametres and is defined as the greatest distance at which an object can be seen in daylight, or could be seen and recognised at night if the light was raised to daylight levels. The measurements made at night are the most prone to error and the measurement is usually made using fixed lights as reference points. If the visibility varies in different directions then the minimum value of visibility is reported.

Temperature

Temperature (TEMP) is measured in degrees Celcius to the nearest 0.1 °C.

Humidity

The wet-bulb temperature (WETB) is the lowest temperature that is measured when the water surrounding the thermometer bulb evaporates into the air. The dew point (DEW) is the temperature at which the air becomes saturated. Both dew point temperature and wet-bulb temperatures are measures of humidity. Measurements are given in degrees Centigrade to the nearest 0.1 °C.

Mean sea-level pressure

The mean sea-level pressure (MSLP) is calculated by applying a correction to the atmospheric pressure measured by an aneroid barometer. Pressure is measured in millibars (mb)

Rainfall

Rainfall (RAIN) at the London Weather Centre is collected using a tipping bucket gauge and is reported in units of 0.1mm.

6.2 Meteorology

A principle component analysis (PCA) was performed on the meteorological variables of each episode (see Section 4.5.3) to extract a smaller number of new components that explain the variance in the original. In each case the PCA was performed on $\log_{10}$ transformed data to normalise the data. The data were centred and standardised and divided by the standard deviation so that all species receive equal weight (Birks pers. comm.). This is appropriate since the meteorological variables are in different units. Where there were missing data then the whole hour was deleted from the analysis.

The length of the arrows on each plot is a function of the variability of that variable. The angle between arrows indicates the correlation between those two variables. A right angle between two arrows shows that those two variables have no relationship to each other. Arrows that point in opposite directions are negatively correlated variables (see Chapter 4 for further information). In each case only the 1st and 2nd axes are shown since they account for the majority of the variance in the data.

6.2.1 Episode 1 (4/3/99-9/3/99)

The meteorological data of Episode 1 covers the same period as Episode 1 in Chapter 5 and are plotted in Figures 6.1a-o. Figure 6.2 shows a summary of IAS and SCP peaks collected by Burkard Trap tapes in Episode 1 described in Chapter 5.

Figure 6.1a-h: Meteorological time-series for Episode 1

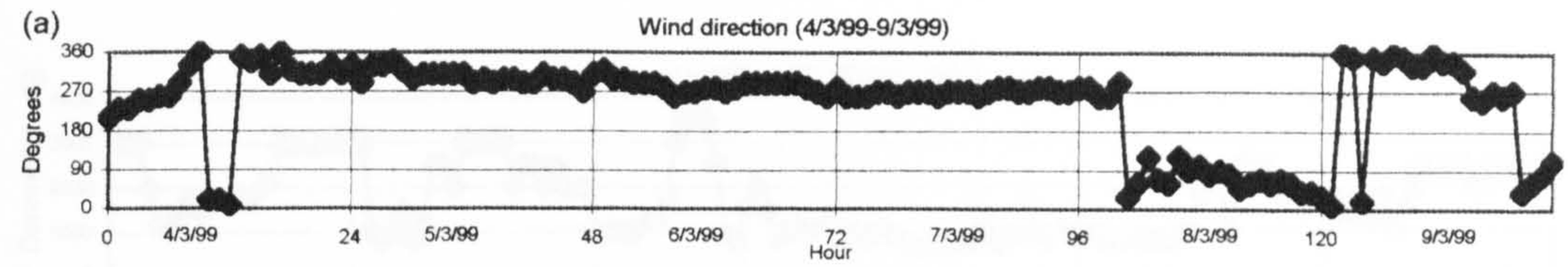

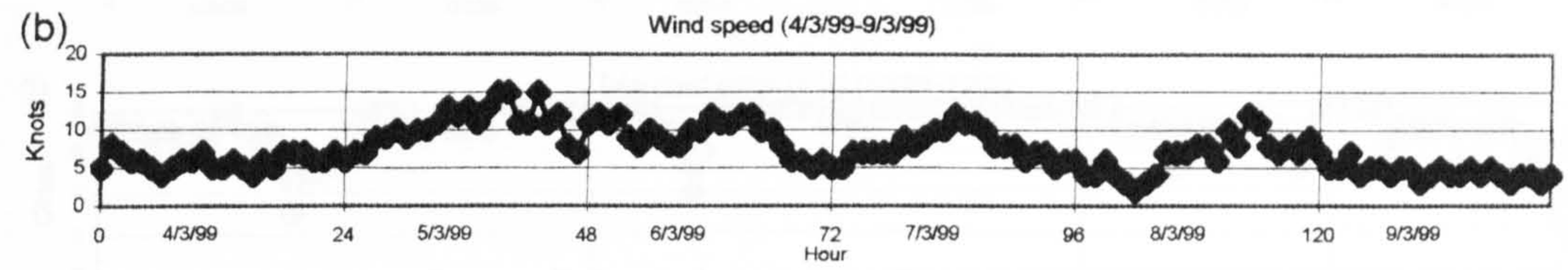

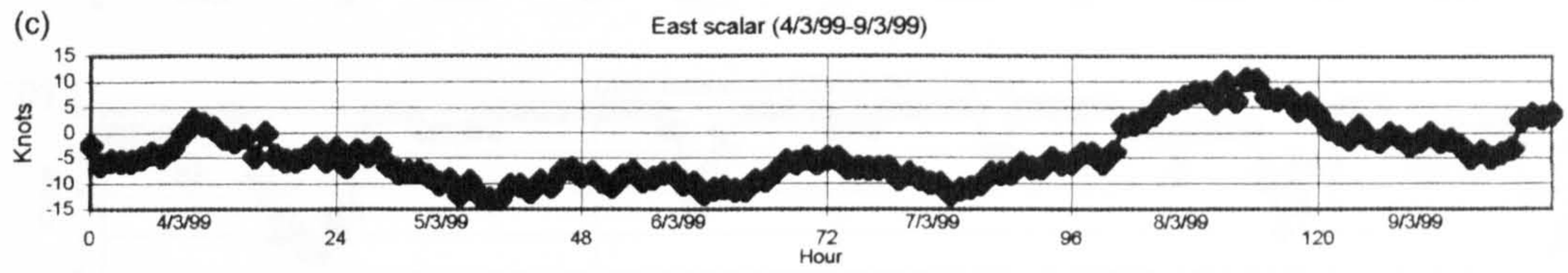

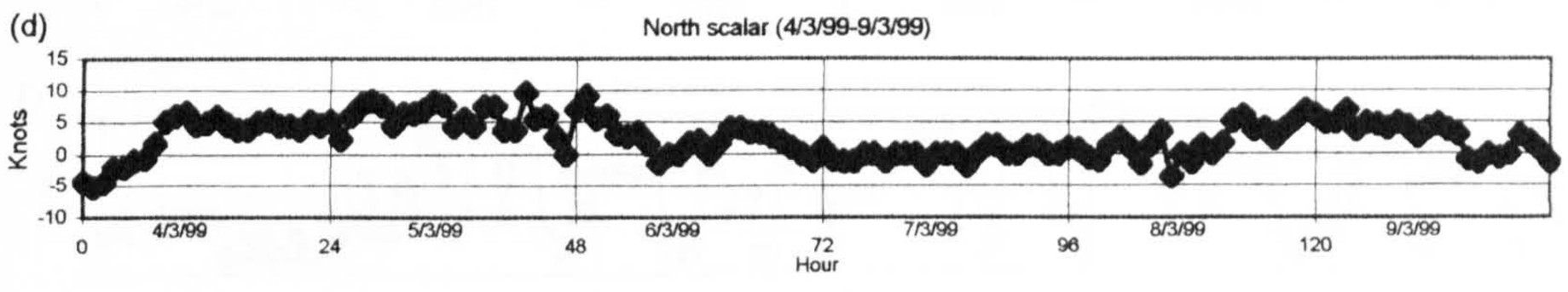

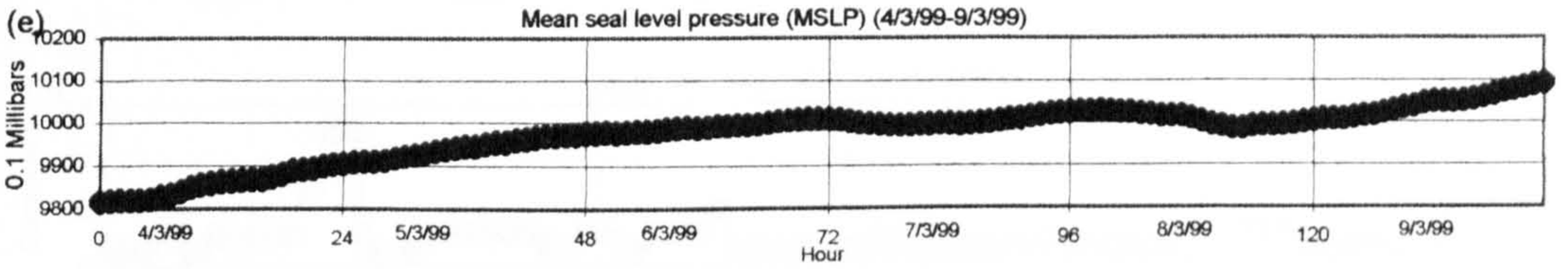

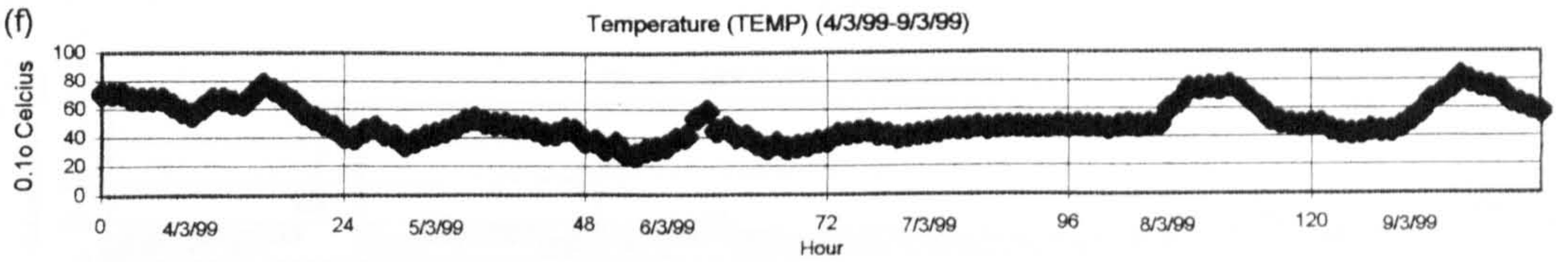

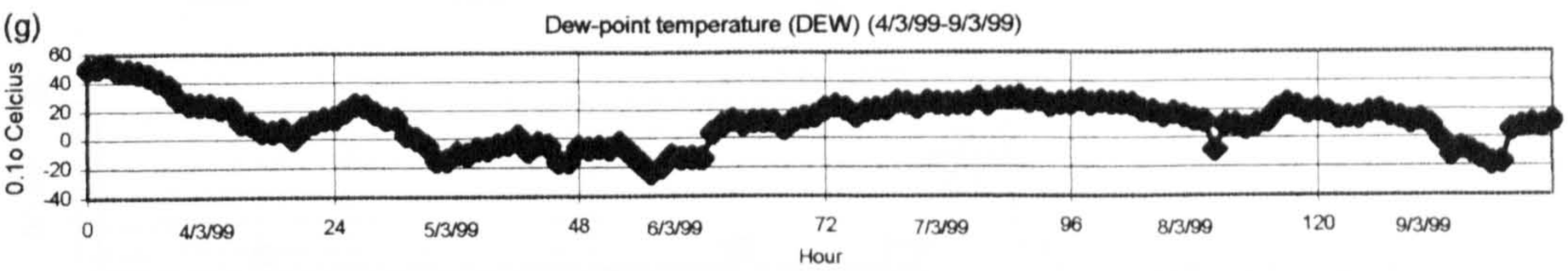

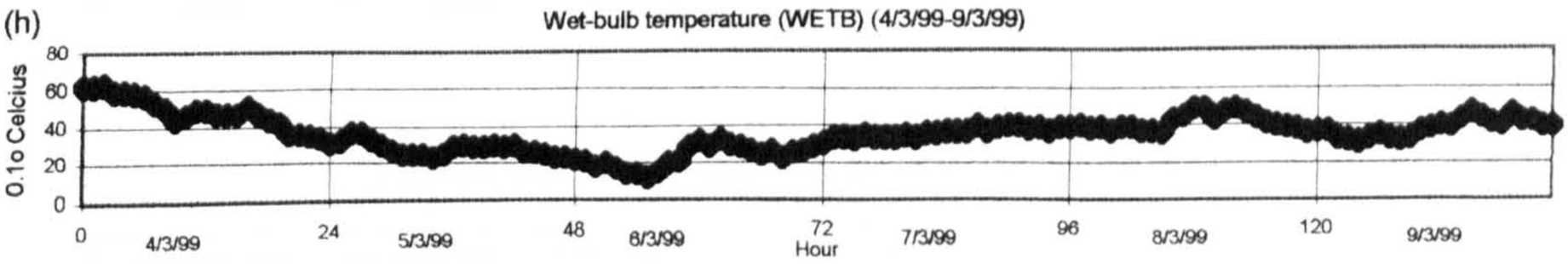

Figure 6.1i-o: Meteorological time-series for Episode 1

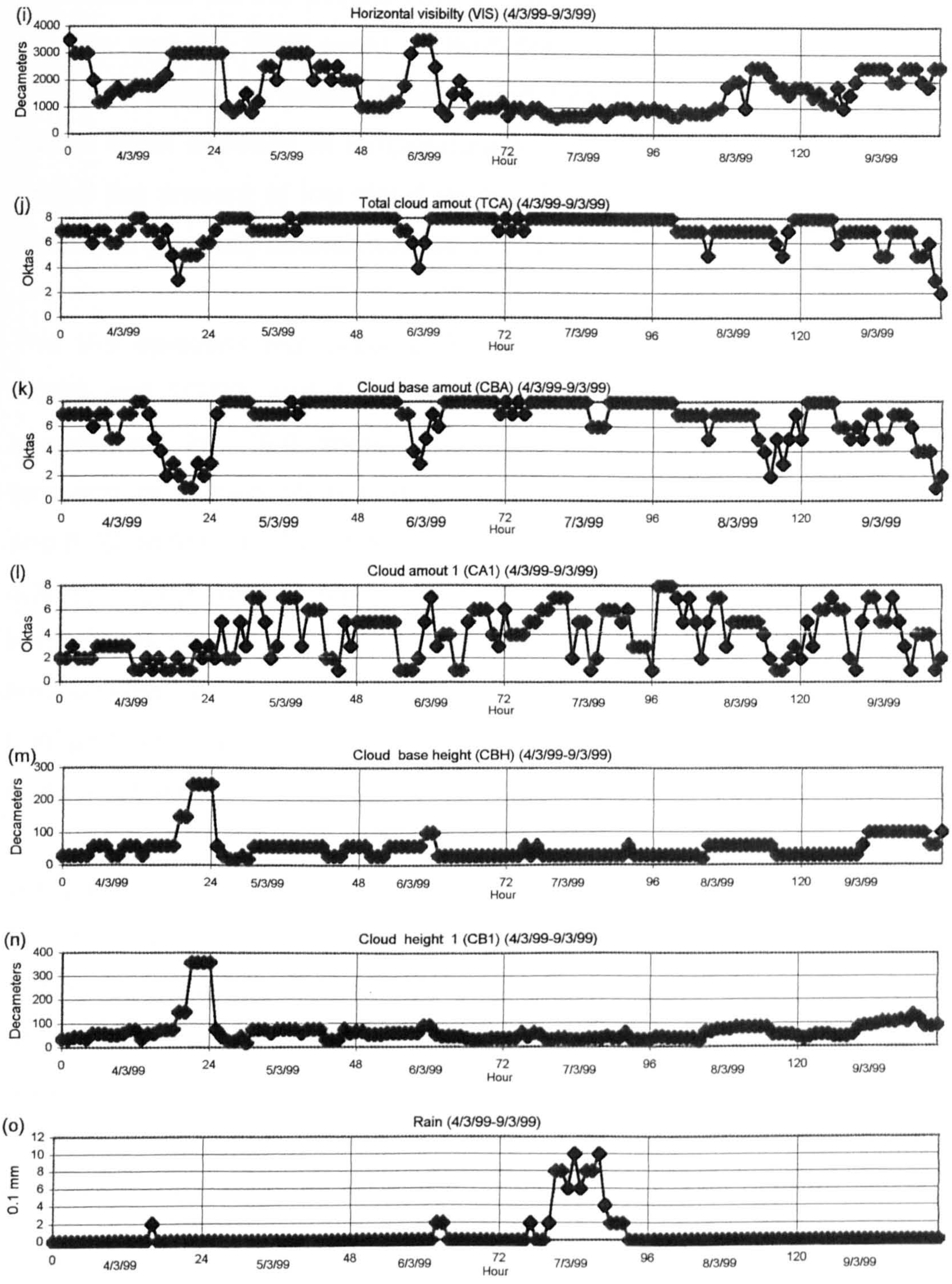

Figure 6.2: SCP and IAS peaks for Episode 1

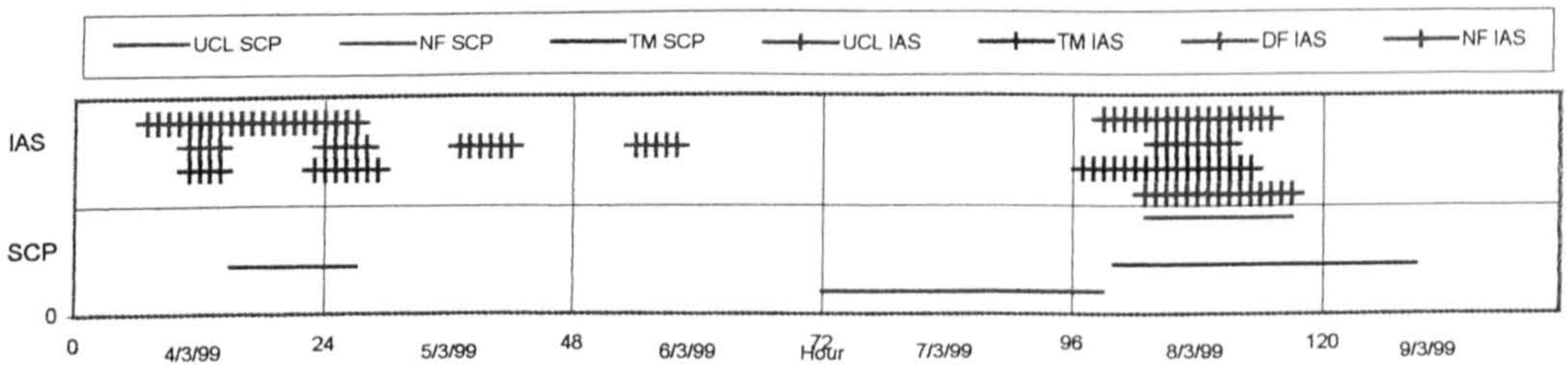

The wind direction during Episode 1 is predominantly from the north and west apart from a period on 8/3/99 when the wind is easterly. This period coincides with the IAS pollution event that affects all Burkard trap sites across London and the SCP event at Northfleet (Figure 6.2). The wind speed increases during the period, from around 7 knots to a peak of 13 knots along with a slight increase in temperature to 8 °C and towards the end of the period the amount of low cloud drops. During this period the atmospheric stability is generally neutral (see Section 3.1.3).

The IAS episodes that occur at Thamesmead, Dartford and Northfleet on 4/3/99 and 5/3/99, and the SCP event at Thamesmead occur while wind speeds are low (5-6 knots) and from the north to north-west. The temperature is relatively high (6-8 °C on 4/3/99) but drops to between 4 °C and 6 °C on 5/3/99. The atmosphere becomes more stable in the evening of 4/3/99. CBA drops and there is a corresponding increase in CBH immediately preceding the second peak at Dartford and Thamesmead. The time between the two peaks at Dartford and Thamesmead coincides with a brief period of rain. In contrast, the SCP peak at UCL occurs on 7/3/99 during a period of rain.

Throughout the episode there is an increase in MSLP, a downward trend in TEMP and DEW on 4/3/99 and 5/3/99 then a gradual rise for the rest of the episode. DEW follows a similar pattern but decreases again on 9/3/99. Cloud heights are generally low except for the period mentioned above. VIS is varied and bears some relation to TCA in that VIS is low when there is a lot of cloud. The highest wind speed occurs during the middle of the episode when the wind is from the north-west.

The corresponding PCA is shown in Figure 6.3. The first two axes explain 52.9% of the variance in the original data. The 3rd and 4th axes account for a further 29.4% (Table 6.1). All four component axes are significant (see Section 4.5.3). The most important variables on the 1st axis are VIS, CB1, CBH and EAST and these are negatively correlated with RAIN, TCA, CA1 and CBA.

Figure 6.3: A PCA of the meteorology of Episode 1

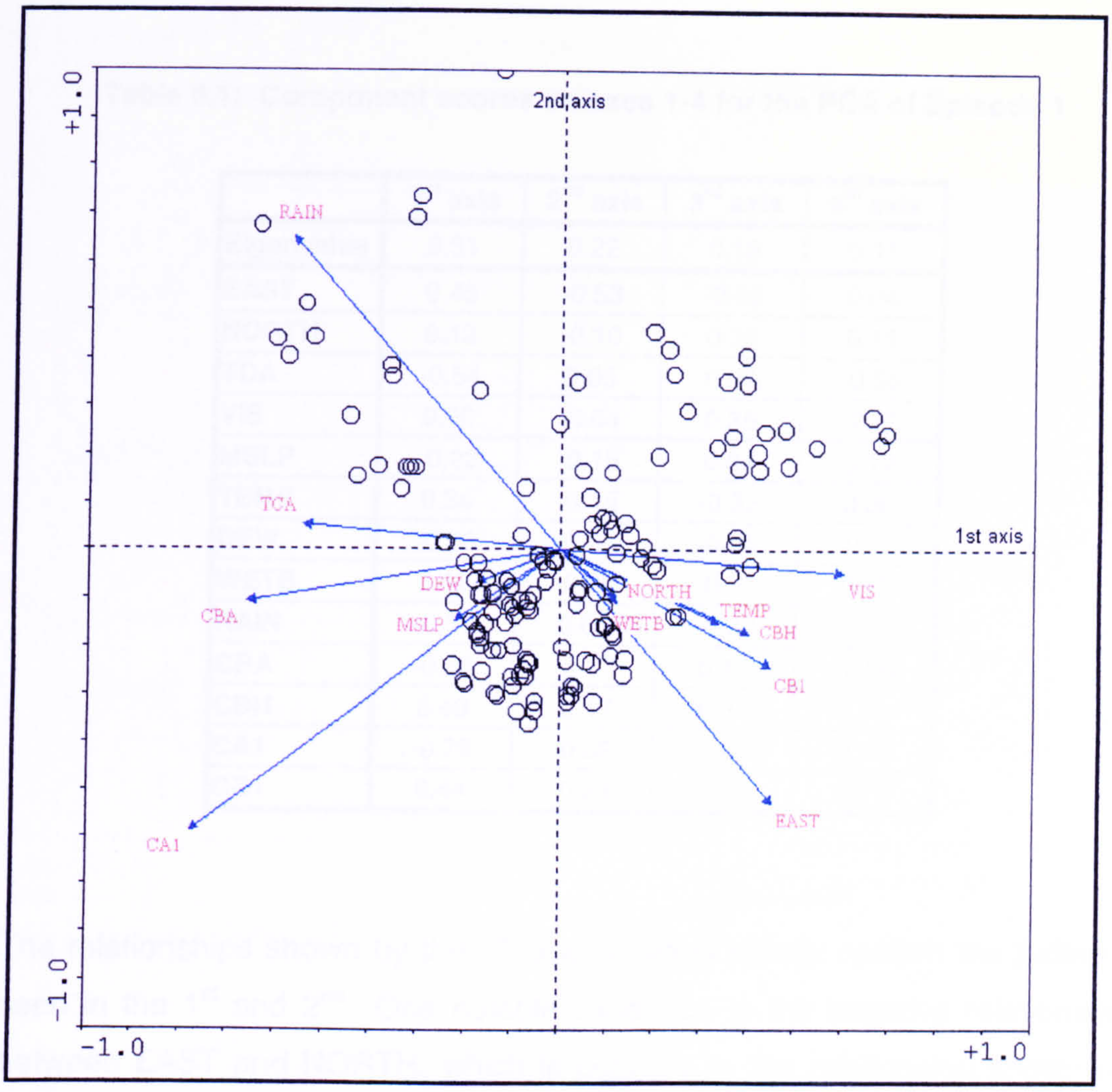

The relationship between TCA, CBA, CB1, CBH and RAIN shows that as cloud base height increases there is less rain and fewer clouds.

RAIN, CA1 and EAST are also important along the 2nd axis. RAIN and EAST are negatively correlated showing that there is no rain when the winds have a strong easterly component. NORTH, TEMP and WETB show less variation in their values and are correlated with CBH and CB1 showing that, during this episode, higher temperatures and high humidity can be associated with a strong northerly component and high clouds. MSLP and DEW show a similar amount of variation but have no relation with NORTH, TEMP and WETB. WETB is dependent on TEMP, which explains their relationship. DEW is not dependent on TEMP, but is related to a combination of the amount of vapour

in the atmosphere and the atmospheric pressure, thus explaining the lack of relationship between these two variables and also the relationship between MSLP and DEW.

Table 6.1: Component scores on axes 1-4 for the PCA of Episode 1

	1st axis	2nd axis	3rd axis	4th axis
Eigenvalue	0.31	0.22	0.18	0.11
EAST	0.45	-0.53	-0.63	0.04
NORTH	0.12	-0.10	0.38	0.11
TCA	-0.54	0.05	0.09	-0.50
VIS	0.60	-0.04	0.35	0.27
MSLP	-0.22	-0.15	0.04	0.12
TEMP	0.34	-0.15	-0.32	0.30
DEW	-0.18	-0.07	-0.80	-0.11
WETB	0.12	-0.11	-0.71	0.12
RAIN	-0.57	0.65	-0.33	0.32
CBA	-0.66	-0.11	0.12	-0.60
CBH	0.40	-0.17	0.33	0.73
CA1	-0.78	-0.59	0.07	0.21
CB1	0.44	-0.24	0.26	0.72

The relationships shown by the 3rd and 4th axes mostly confirm the patterns seen in the 1st and 2nd. One notable exception is the negative relationship between EAST and NORTH, which is contrary to the relationship shown on the plot of the 1st and 2nd axes. Therefore, a proportion of the variance in the meteorological data is caused by days when the northerly component is small and the easterly component is large or vice versa.

6.2.2 Meteorology of Episode 2 (15/4/99-17/4/99)

The meteorological data of Episode 2 are shown in Figure 6.4.

Figure 6.4a-h: Meteorological time-series for Episode 2

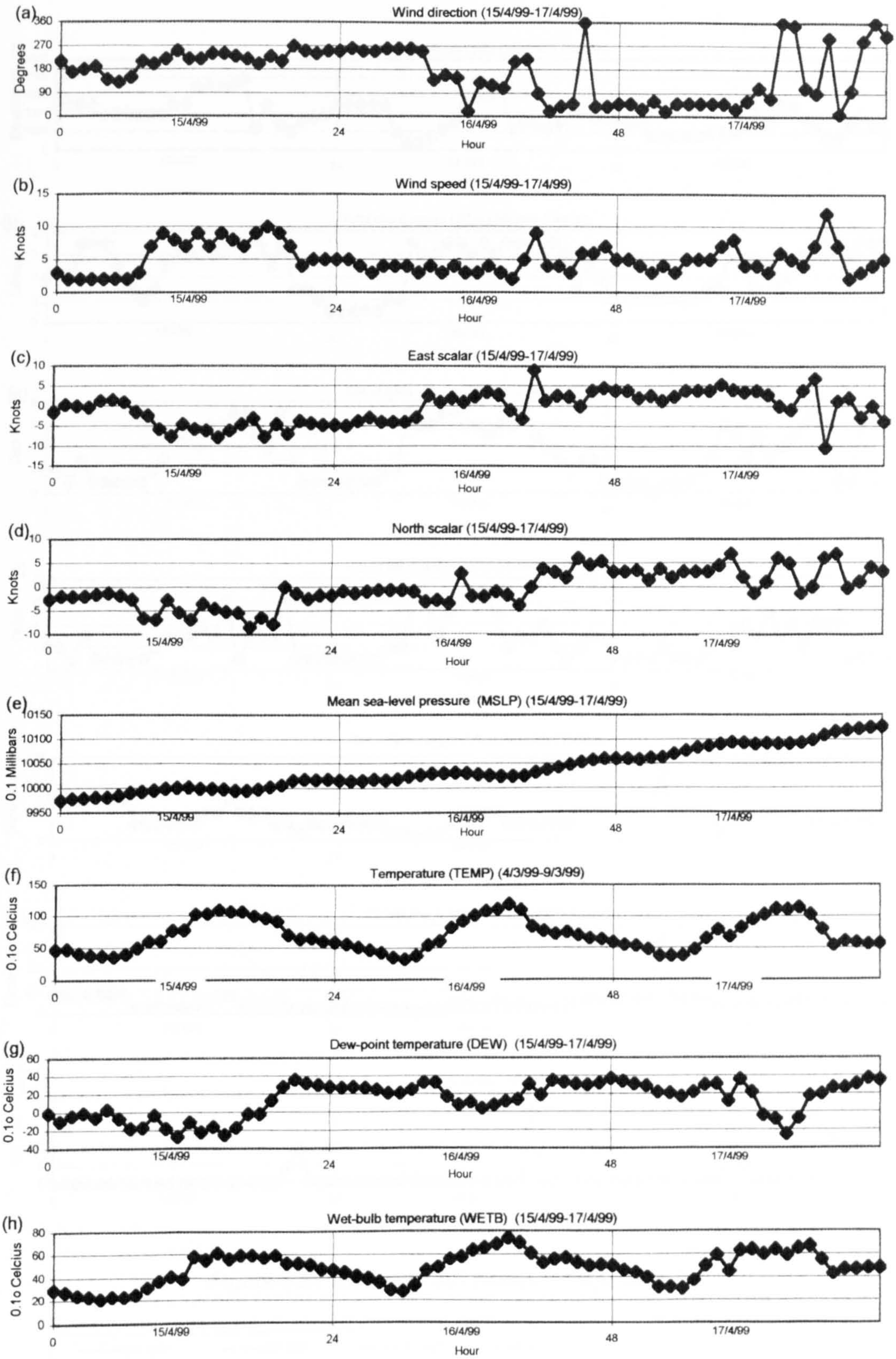

Figure 6.4i-o: Meteorological time-series for Episode 2

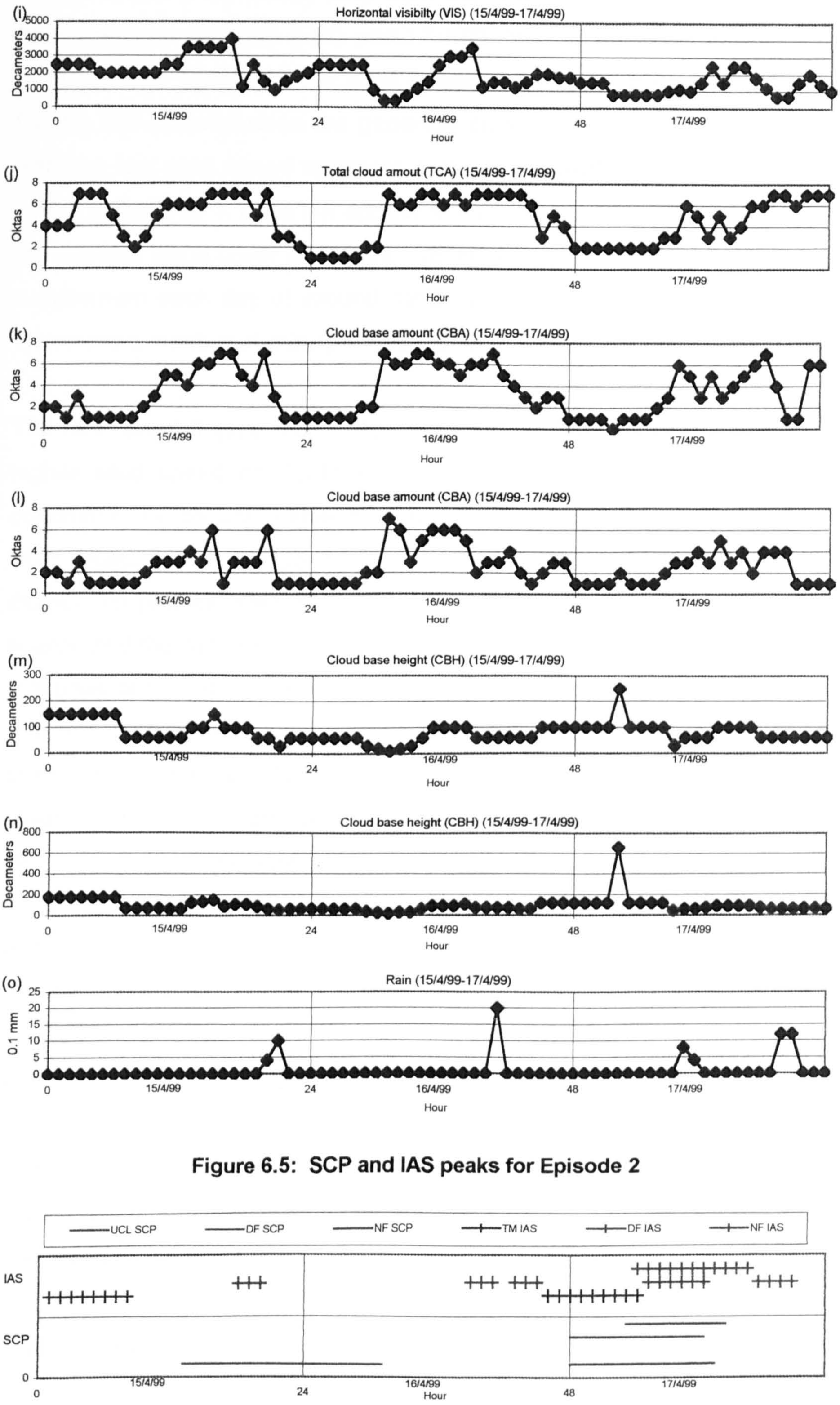

Figure 6.5: SCP and IAS peaks for Episode 2

There is a shift from generally south and westerly winds in the first part of the episode to north-easterly winds in the second part. There is a period of higher speed (7-10 knots) wind from the south-west on 15/4/99, and a two brief spells on 16/17/99 (SW) and 17/4/99 (NW) which reach 9 and 12 knots respectively. Otherwise the wind speed is generally low (around 5 knots). During this episode skies are generally clear at night which, in combination with the low wind speed suggests a stable atmosphere. VIS is varied but, unlike in Episode 1, does not appear to have a relationship with TCA. During the daytime cloud cover increases. TEMP varies on a diurnal time-scale with a maximum each day of around 12°C and WETB follows a similar pattern. There are a number of rainy periods that last for 2-3 hours each time.

The SCP event (Figure 6.5) on 15-16/4/99 at UCL begins during the period of higher wind speed on 15/4/99. The atmosphere will be well mixed and conditions will be favourable for resuspension of particles. There are two SCP peaks within this period (see Section 5.5.2) and, based on the size distribution profiles, the first peak (14-22 hours) could be attributed to a local source and the second (22-31 hours) to a more distant source. However, the first peak occurs at the same time as the period of higher south-westerly wind and the second peak occurs when the wind drops in speed and changes direction to westerly. Therefore, the first period may then be caused by resuspension due to atmospheric turbulence, which would contribute larger SCPs to the atmosphere and explain the wide distribution profile. The implication of this is that when the conditions favour resuspension, it is not possible to use the size distribution as an indication of proximity to source. At around midday on 16/4/99 the wind direction switches to westerly and the SCP counts decrease at almost the same time. The source of the SCP event will therefore lie to the west of UCL.

The second SCP event at UCL is attributed to a local oil-fired source. This occurs at the same time as SCP peaks at Dartford and Northfleet, although these were related to a coal-fired source. The wind direction is north-easterly at this time which does not pass over any potential sources for the SCP peaks at any of the sites.

The IAS peak at Thamesmead on 15/4/99 is from a coal-fired source (see Section 5.5.2). It occurs during a calm (2-3 knots) period of south to south-easterly winds. Dartford SCP levels are elevated at the same time, but not IAS. The end of this event occurs when the wind speed increases and changes direction. The IAS peaks that occur at similar times to the SCP events at Dartford and Northfleet also occur during the period of north-easterly winds. The peak at Northfleet occurs slightly later than the one at Dartford and coincides with an increase in wind speed, with a maximum of 8 knots.

Figure 6.6: A PCA of the meteorology of Episode 2

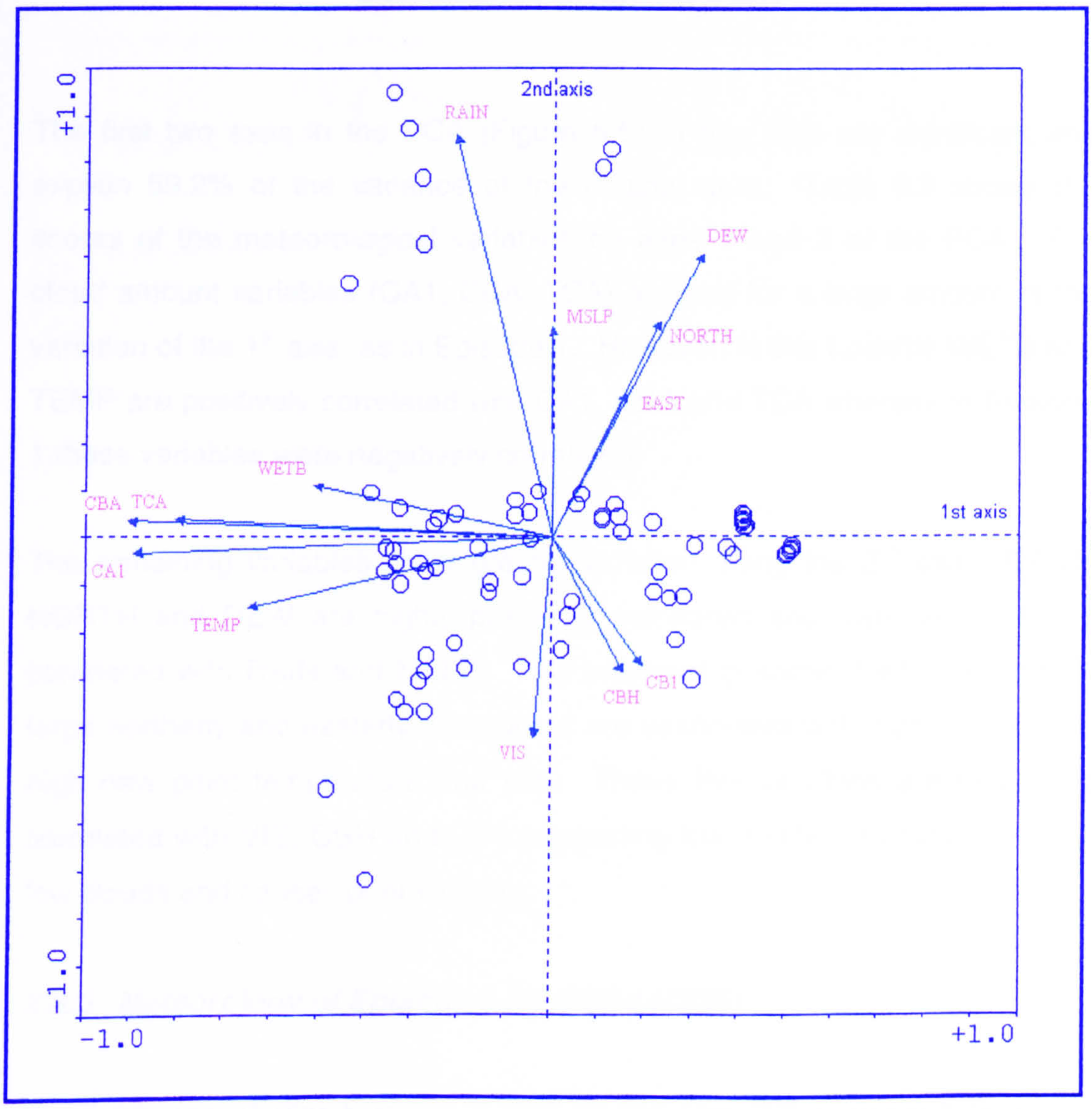

Table 6.2: Component scores on axes 1 and 2 for the PCA of Episode 2

	1st axis	2nd axis
Eigenvalue	0.38	0.21
EAST	0.16	0.31
NORTH	0.23	0.46
TCA	-0.81	0.04
VIS	-0.03	-0.42
MSLP	0.00	0.45
TEMP	-0.65	-0.15
DEW	0.32	0.61
WETB	-0.51	0.11
RAIN	-0.21	0.86
CBA	-0.91	0.04
CBH	0.15	-0.28
CA1	-0.90	-0.03
CB1	0.20	-0.27

The first two axes in the PCA (Figure 6.6) of this data are significant and explain 59.2% of the variance of the original data. Table 6.2 shows the scores of the meteorological variables on axes 1 and 2 of the PCA. The cloud amount variables (CA1, CBA, TCA) account for a large amount of the variation of the 1st axis, as in Episode 1. However, in this Episode WETB and TEMP are positively correlated with CA1, CBA and TCA whereas in Episode 1 these variables were negatively correlated.

The remaining variables show greater variation along the 2nd axis. EAST, NORTH and DEW are highly positively correlated and also are positively correlated with RAIN and MSLP. This relationship shows that winds with a large northerly and easterly component are associated with high pressure, a high dew point temperature and rain. These five variables are negatively correlated with VIS, CBH and CB1 suggesting that rainfall is associated with low clouds and causes poor visibility.

6.2.3 Meteorology of Episode 3 (13/3/96-14/3/96)

It did not rain during Episode 3 and so the rain plot is omitted from the meteorology time-series plots (Figure 6.7).

Figure 6.7a-h: Meteorological time-series for Episode 3

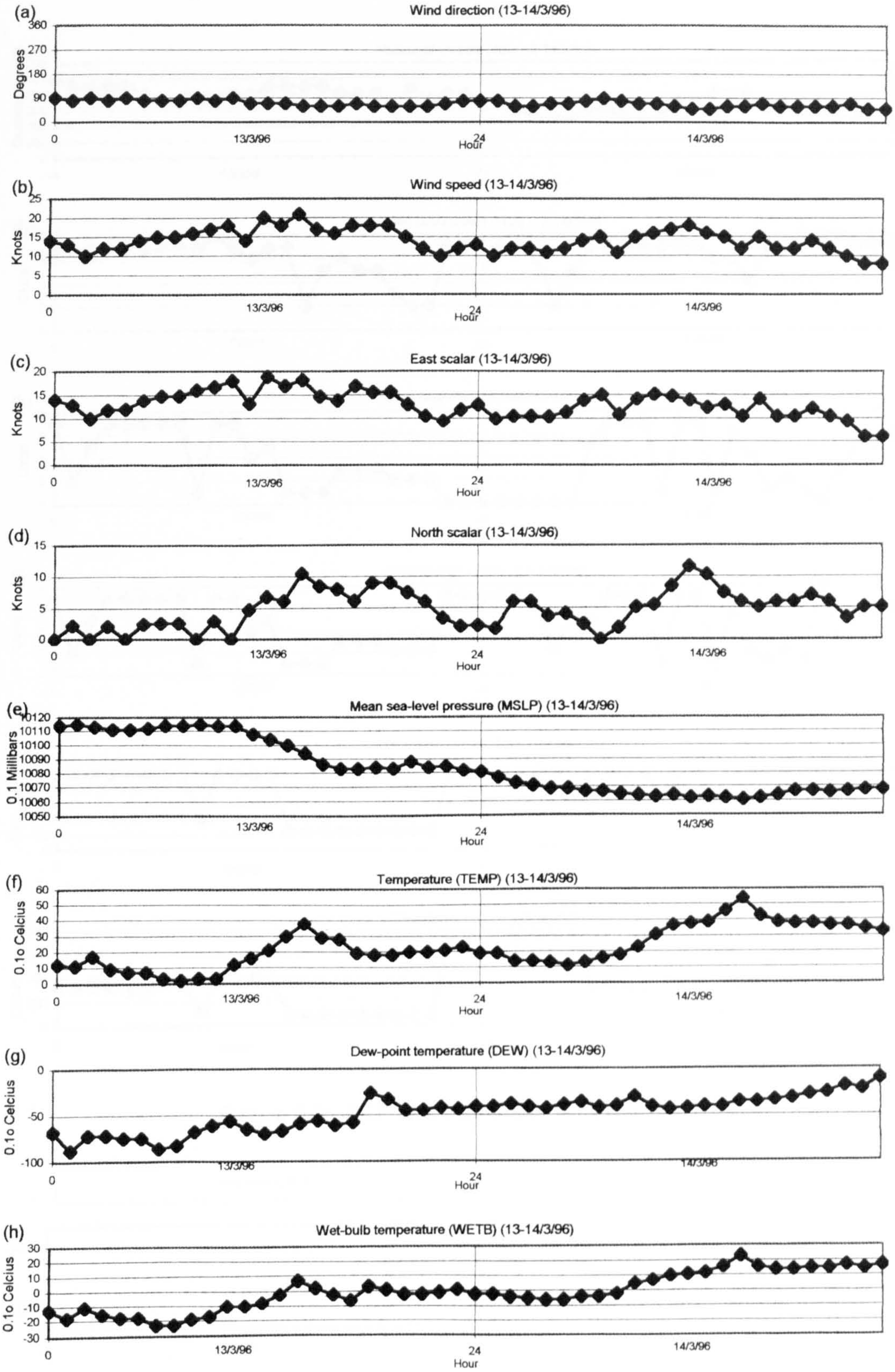

Figure 6.7i-n: Meteorological time-series for Episode 3

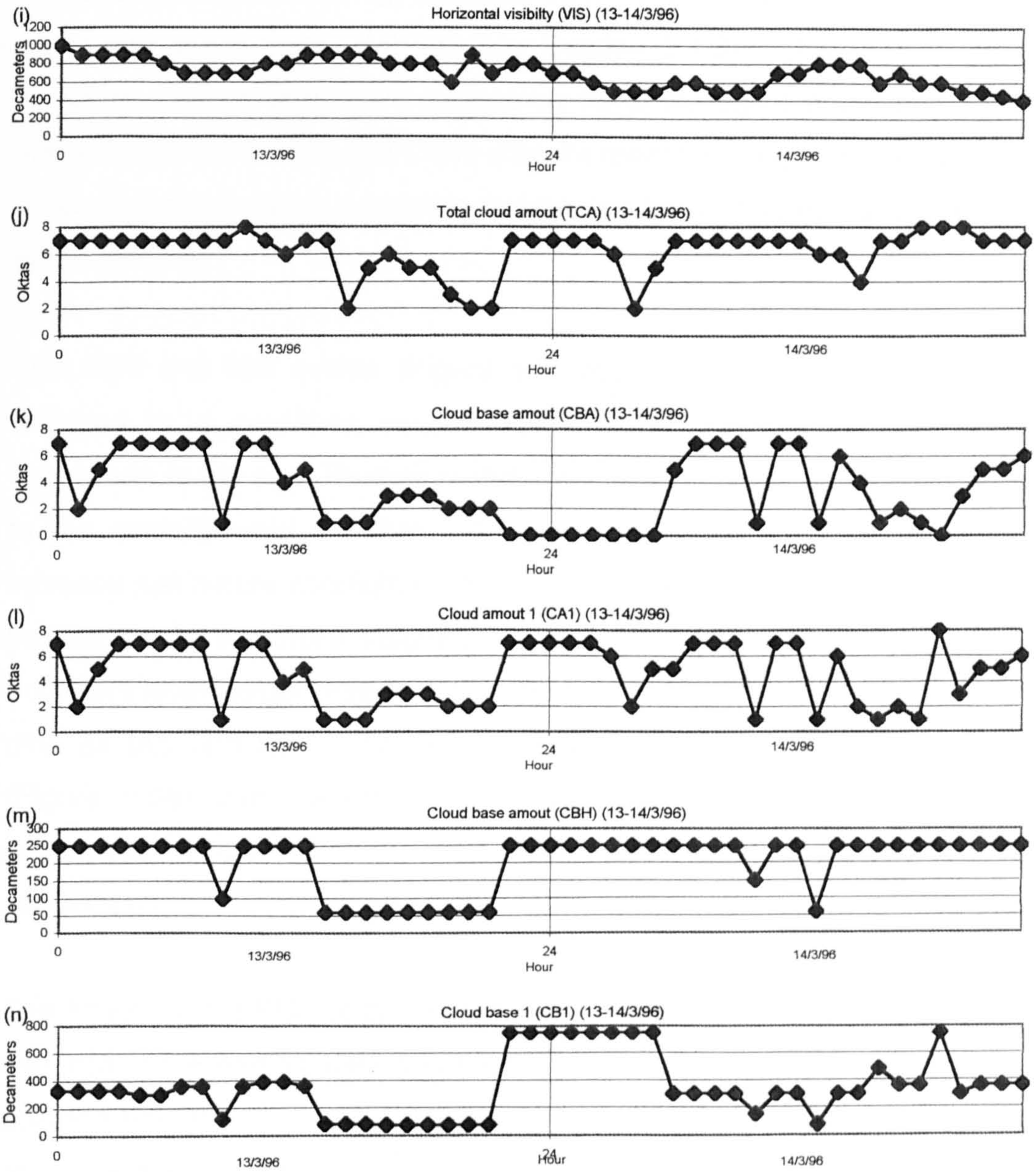

Figure 6.8: SCP and IAS peaks for Episode 3

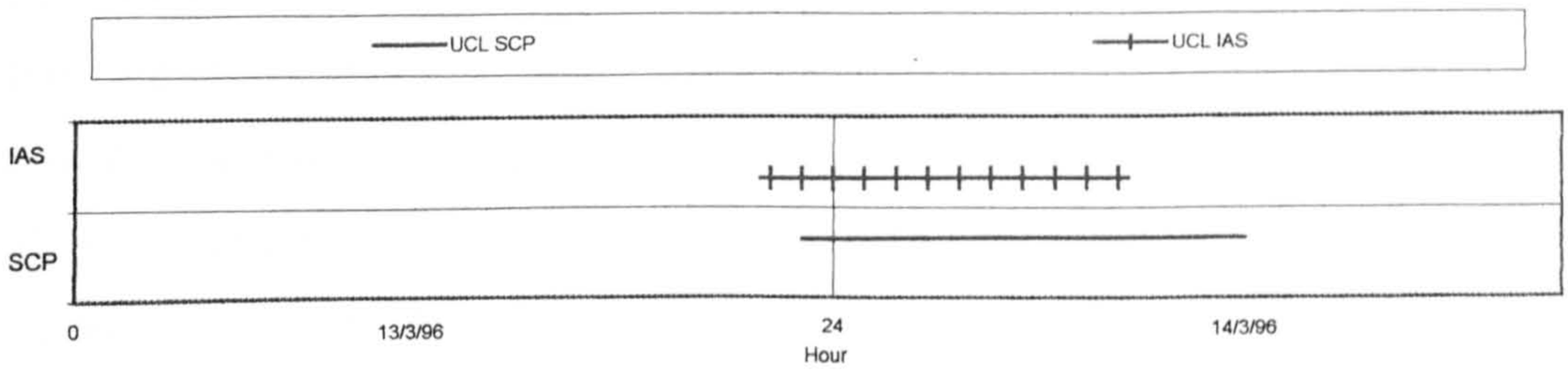

The wind direction was almost constant and from the east and north-east during the episode with slightly elevated speeds during the day (just over 20 knots) compared with at night (around 10 knots). These conditions are typical of neutral atmospheric stability (see Section 3.1.3). TEMP shows diurnal structure with an underlying increasing trend through the episode. WETB shows a similar profile and DEW also increases through the episode. The amount of cloud varies according to type and level. VIS decreases with time in the episode.

The SCP and IAS events (Figure 6.8) occur at the same time and were ascribed to a coal-fired source (see Section 5.5.3). Either Tilbury or Kingsnorth in the east Thames corridor will be the source of the particles due to the easterly wind direction. The levels of both SCP and IAS start to increase just before midnight when the wind speed drops. This will probably be caused by a relative stagnation of the atmosphere and the decreasing boundary layer height (Figure 3.1). The SO_2 levels are elevated at the same time as IAS and SCP. There is a second SO_2 event during the episode (Figure 5.9a) that appears to be caused by the same meteorological conditions, unfortunately the IAS and SCP record does not exist for comparison.

The 1st axis in the PCA of this meteorology (Figure 6.9) explains 67.6% of the variance in the original data and the 2nd axis explains a further 9.8%. In this episode only the 1st axis is significant. As in Episodes 1 and 2, CBA, CA1 and TCA account for a large amount of variation on the 1st axis. These two variables are positively correlated with CBH and CB1, contrary to the negative correlation seen in Episodes 1 and 2. Therefore, in this episode, as cloud base height increases then so does the amount of cloud. EAST and NORTH are almost unrelated and both have a moderate amount of variation along the 1st axis. The PCA scores on the 1st axis for the meteorological variables of Episode 3 are shown in Table 6.3.

WETB is important on the 2nd axis as in Episodes 1 and 2. TEMP is once again correlated with WETB and also with CBA. MSLP and VIS are strongly

correlated with EAST showing that, in this Episode, winds with a strong easterly component are associated with a clear atmosphere and high pressure. The profiles of these three variables show a general decrease as the Episode progresses and they are negatively correlated with TCA and CA1 showing that, when there are winds with a large easterly component, there are few clouds. This is not borne out by the specific profiles for these variables, however, and it should be borne in mind that the 2nd axis does not explain a significant amount of the variation in the meteorological data.

Figure 6.9: A PCA of the meteorology of Episode 3

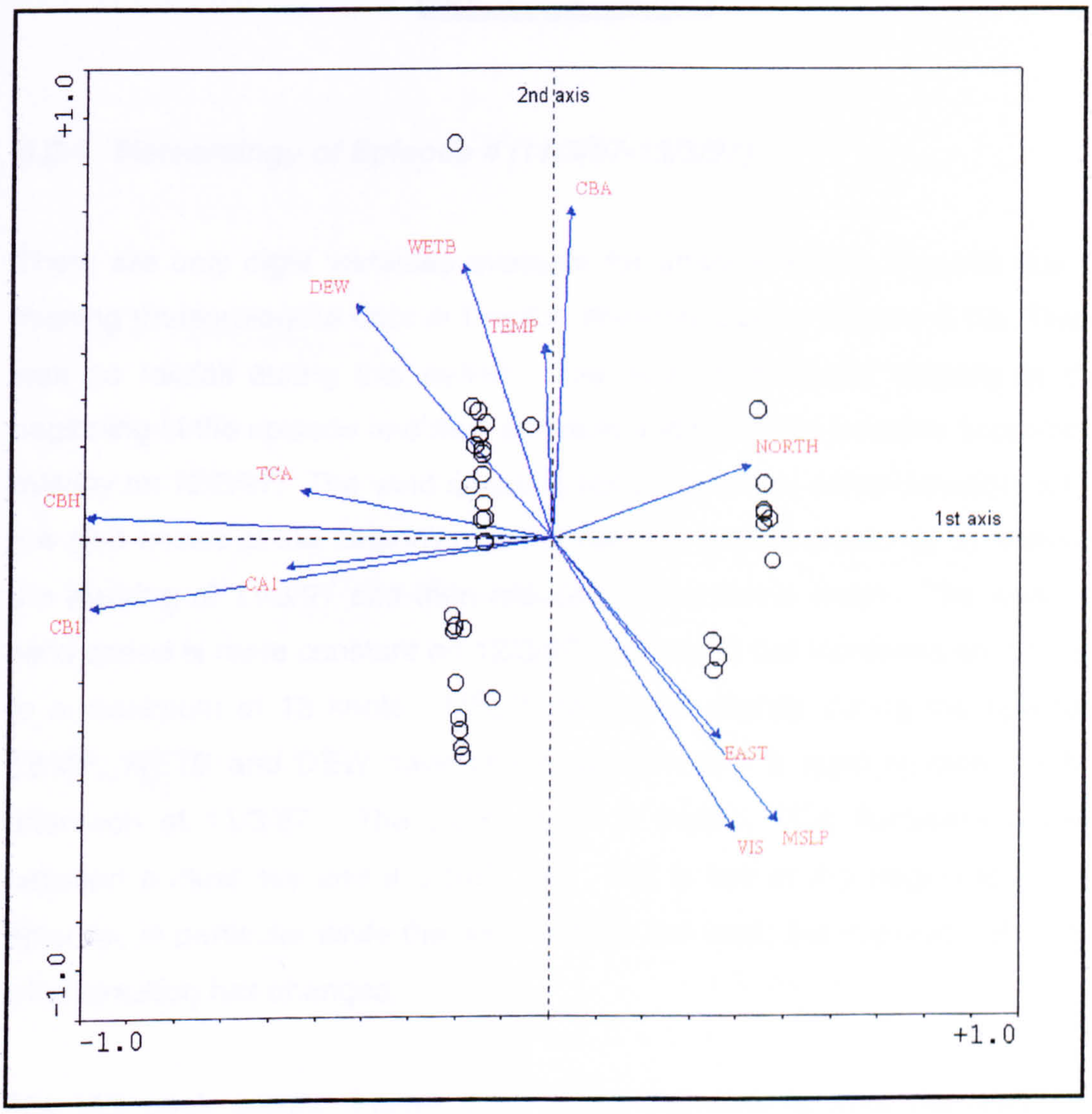

Table 6.3: Component scores on axis 1 for the PCA of Episode 3

	1st axis
Eigenvalue	0.68
EAST	0.36
NORTH	0.43
TCA	-0.54
VIS	0.31
MSLP	0.45
TEMP	-0.02
DEW	-0.40
WETB	-0.20
CBA	0.07
CBH	-0.99
CA1	-0.54
CB1	-0.97

6.2.4 Meteorology of Episode 4 (11/3/97-13/3/97)

There are only eight variables available for analysis in this Episode due to missing meteorological data at London Weather Centre (Figure 6.10). There was no rainfall during this period. The wind is generally easterly at the beginning of the episode and then switches and becomes westerly from about midday on 12/3/97. The wind speed is not constant for either direction but is low (2-3 knots) at the beginning of the easterly period, peaks at 11 knots in the evening of 11/3/97 and then reduces to low levels again. The westerly wind speed is more constant on 12/3/97 (7-8 knots) but increases on 13/3/97 to a maximum of 13 knots. MSLP decreases slightly during the episode. TEMP, WETB and DEW have similar profiles with a rapid increase in the afternoon of 11/3/97. The cloud cover is erratic, TCA fluctuates quickly between a clear sky and a cloudy sky. VIS is low at the beginning of the episode, in particular while the wind is from the east, but improves after the wind direction has changed.

The IAS peak occurs (Figure 6.11) when the wind is from the east and immediately following the increase in speed. The source of this peak will be a coal-fired source and the direction data shows that the location of the source will be Kingsnorth or Tilbury in the east Thames.

Figure 6.10a-h: Meteorological time-series for Episode 4

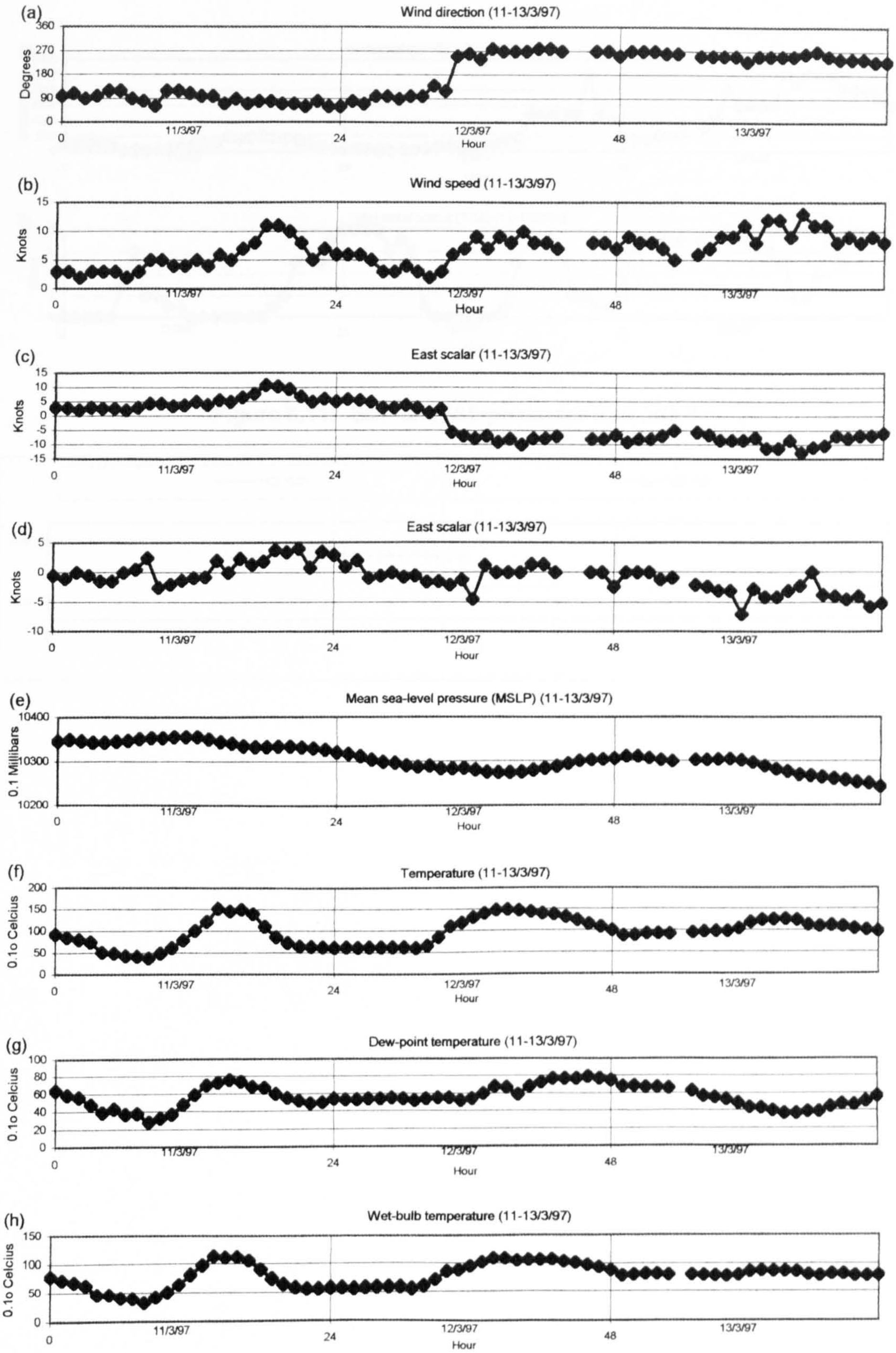

Figure 6.10i-j: Meteorological time-series for Episode 4

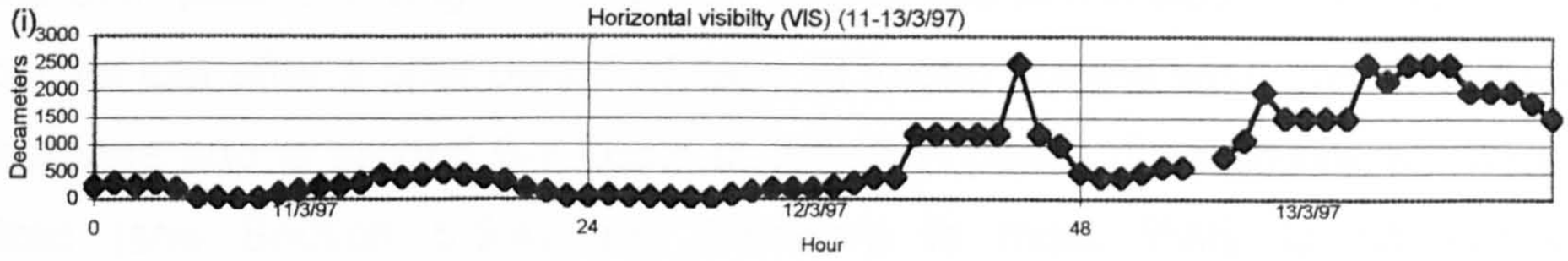

Figure 6.11: SCP and IAS peaks for Episode 4

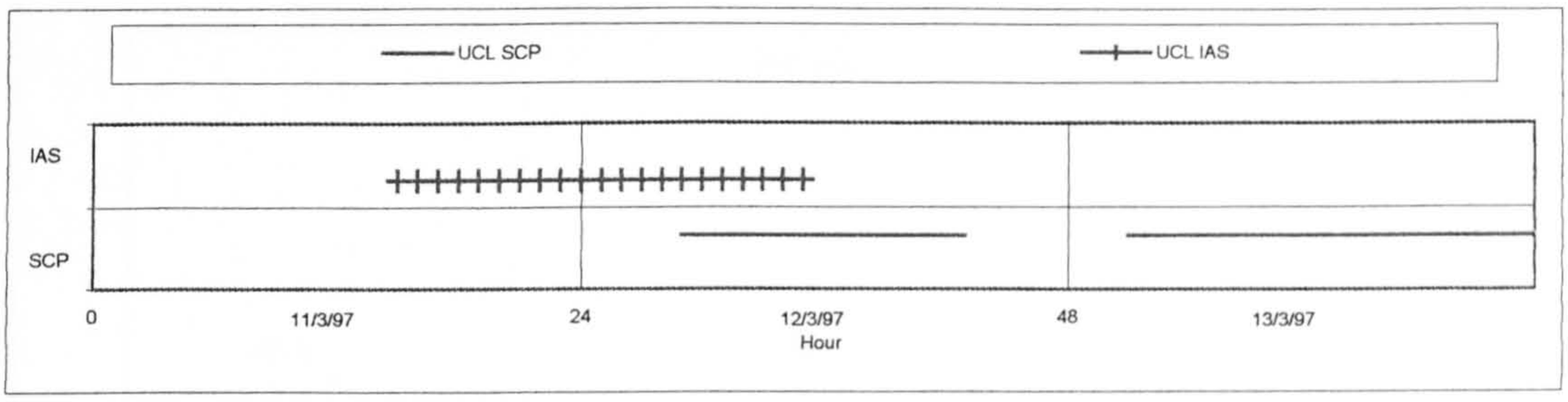

IAS levels drop as the wind changes direction and this coincides with start of the SCP peak showing that the SCP source lies to the west. The SCP peak occurs just after a brief period of calm (2 knots) but the wind speed starts to increase and is around 6-7 knots at the SCP peak. This source will be oil-fired (see Section 5.5.4) and therefore is most likely to be London Underground Chelsea. The second SCP event occurs while the wind is from the west and peaks at the point when there is a drop in wind speed.

Figure 6.12: A PCA of the meteorology of Episode 4

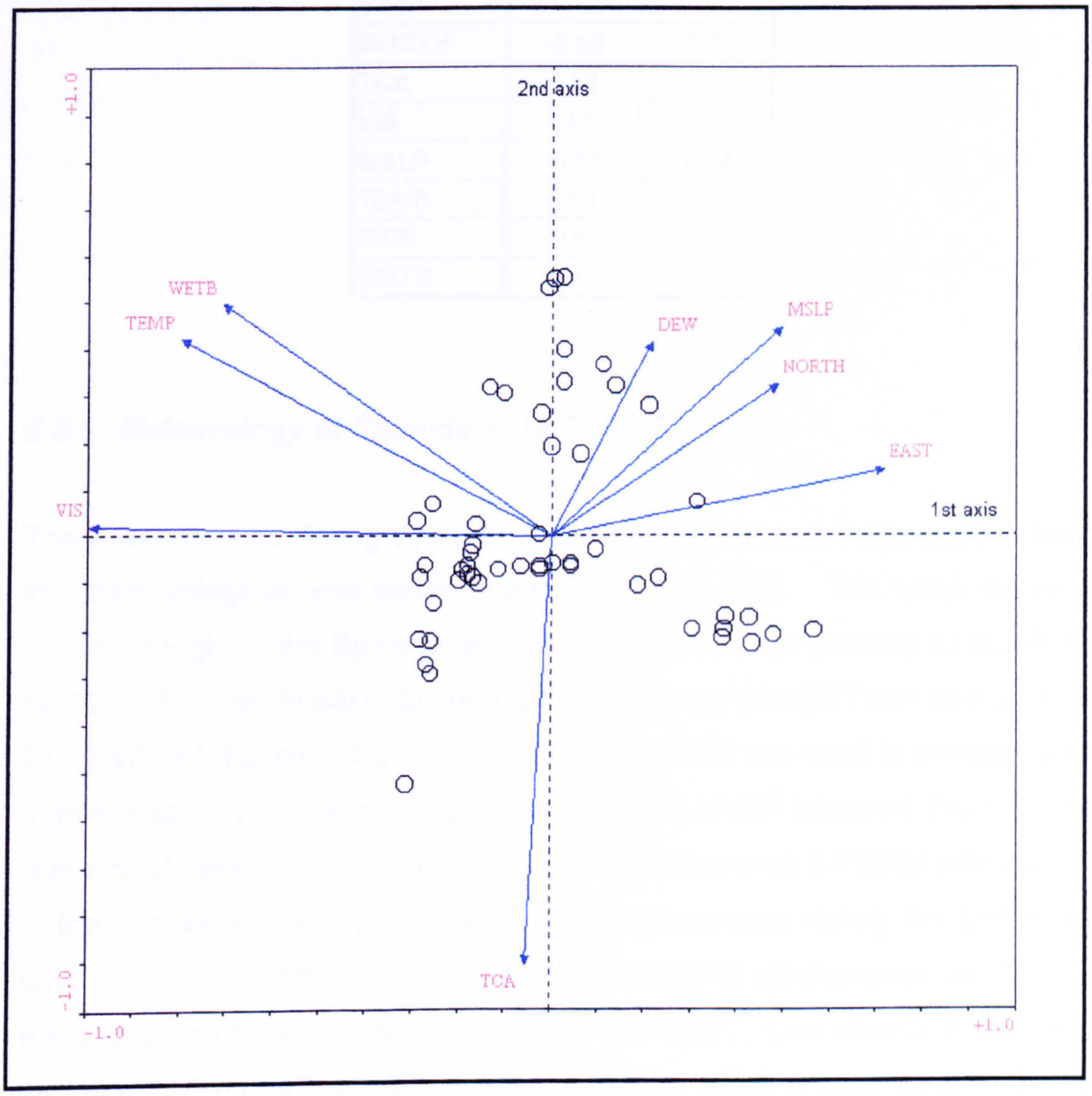

Figure 6.12 shows the PCA biplot for the meteorology of Episode 4. The 1st and 2nd axes are significant and together they explain 71.5% of the variance in the original data. VIS, TEMP and WETB are negatively correlated with

EAST, NORTH and MSLP and they all have a large amount of variation along the 1st axis. TCA makes the largest contribution to the 2nd axis and is negatively correlated with all other variables, with the exception of VIS with which TCA has little relationship. This indicates that TCA is varying independently to the other variables. Table 6.4 shows the scores of each of the meteorological variables on the 1st and 2nd axes of the PCA.

Table 6.4: Component scores on axes 1 and 2 for the PCA of Episode 4

	1st axis	2nd axis
Eigenvalue	0.41	0.30
EAST	-0.82	-0.23
NORTH	-0.63	-0.03
TCA	0.48	-0.86
VIS	0.80	0.46
MSLP	-0.56	-0.04
TEMP	0.53	0.67
DEW	-0.41	0.10
WETB	0.42	0.67

6.2.5 Meteorology of Episode 5 (19-22/12/97)

There was no rain during Episode 5 and so this plot has been omitted from the meteorological time-series shown in Figure 6.13. The wind direction varies throughout the Episode and switches from north-westerly to southerly on 19/12/97, then to easterly and north-easterly on 20/12/97 and is erratic on 21/12/97. At the end of 21/12/97 and on 22/12/97 the wind is constant and from the east. Wind speed is generally low (2-6 knots) between 19-21/12/97, with a brief peak (9 knots) on 19/12/97, but increases on 22/12/97 with a peak in the middle of the day (10 knots). MSLP increases during the first three days and then levels off. TEMP, DEW and WETB all decrease on the first three days and then increase again on 22/12/97. Low clouds fill the sky between 19-21/12/97, with the exception of CA1, which is more erratic. There is a large amount of cloud cover on 22/12/97 but the height of the clouds increases. The meteorology of this episode appears to have two phases, the

first between 19-21/12/97 where the conditions are mostly neutral and the second on 22/12/97 when the conditions are more unstable.

The SCP peak is on 19/12/99 (Figure 6.14) in the first meteorological phase. The start of the peak coincides with the elevated wind speed (9 knots) and the direction is south-westerly. This source is oil-fired and was suggested (see Section 5.5.5) to arise from Littlebrook or Grain in the east Thames corridor based on the SCP size distribution, however the wind direction shows that London Underground Chelsea is the source (see Figure 3.3). The first IAS peak is relatively small (around 150 IAS hr^{-1}) (see Section 5.2.5) and is associated with a coal-fired source. The wind (2-6 knots) during this event is generally from the east and, therefore, the source is likely to be Tilbury or Kingsnorth in the east Thames corridor. The second IAS peak (Figure 6.10) occurs at the beginning of the second meteorological phase when the wind is from the east. Wind speed is around 4 knots during the peak. Once again, the source of the IAS peak will be Tilbury or Kingsnorth. The magnitude of the second peak is larger (over 800 IAS hr^{-1})

The first two axes in the PCA for Episode 5 (Figure 6.15) are significant and explain 67.6% of the variance in the original data. TEMP and WETB are highly correlated and are the most important variables along the 1^{st} axis. Negatively correlated with these variables are NORTH, TCA and CBA which show little variation in their values. NORTH and EAST have little relation to each other, in contrast with Episode 2. EAST and MSLP are once again highly correlated and these account for a large amount of variation in both the 1^{st} and 2^{nd} axes. These two variables are highly dependent on each other for most of the episodes, with the exception of Episode 1. EAST and MSLP are negatively correlated with WETB and TEMP, as in Episodes 3 and 4, and with DEW, similar to Episode 3 but contrary to Episode 4.

Figure 6.13a-h: Meteorological time-series for Episode 5

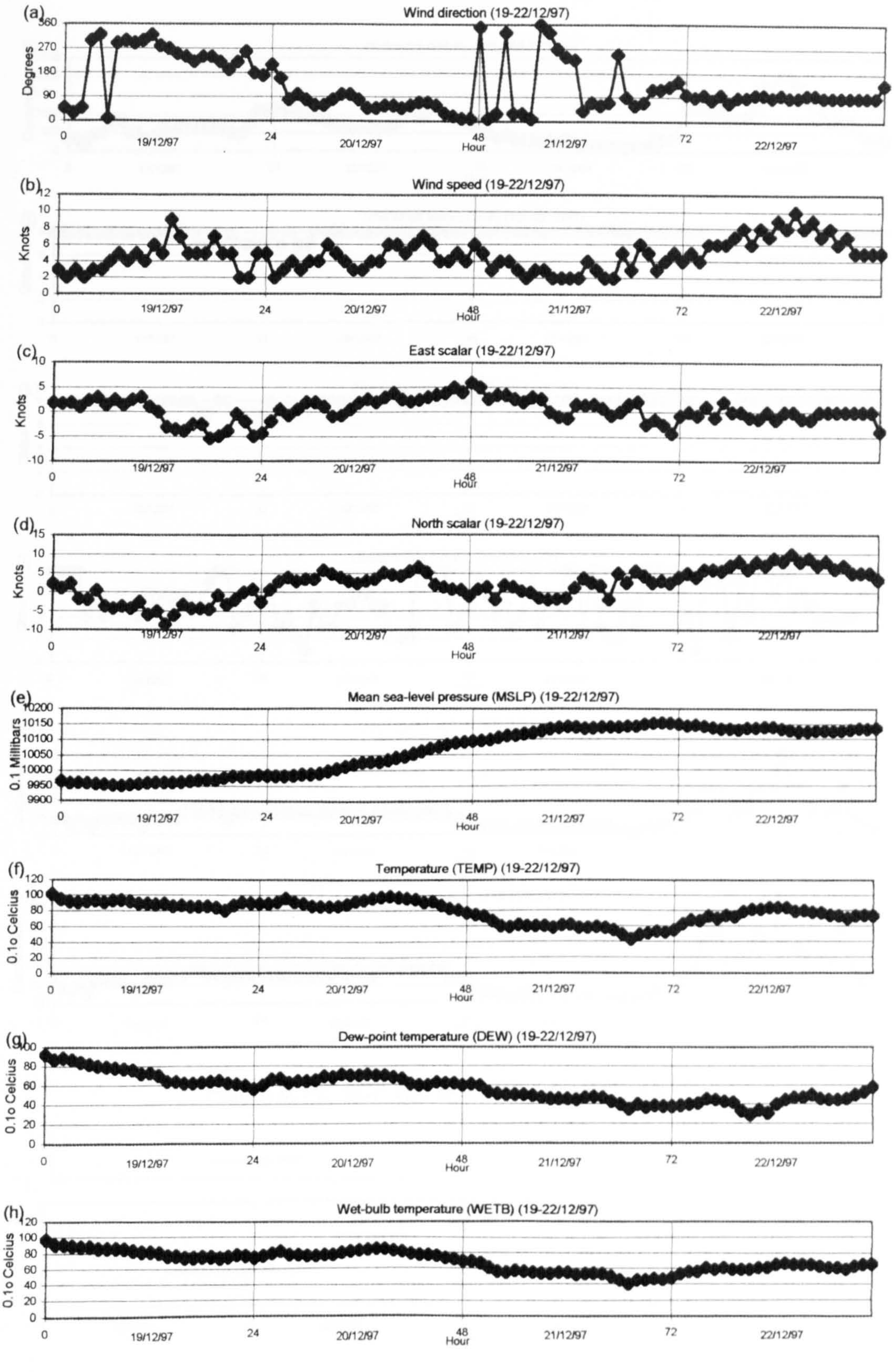

Figure 6.13i-n: Meteorological time-series for Episode 5

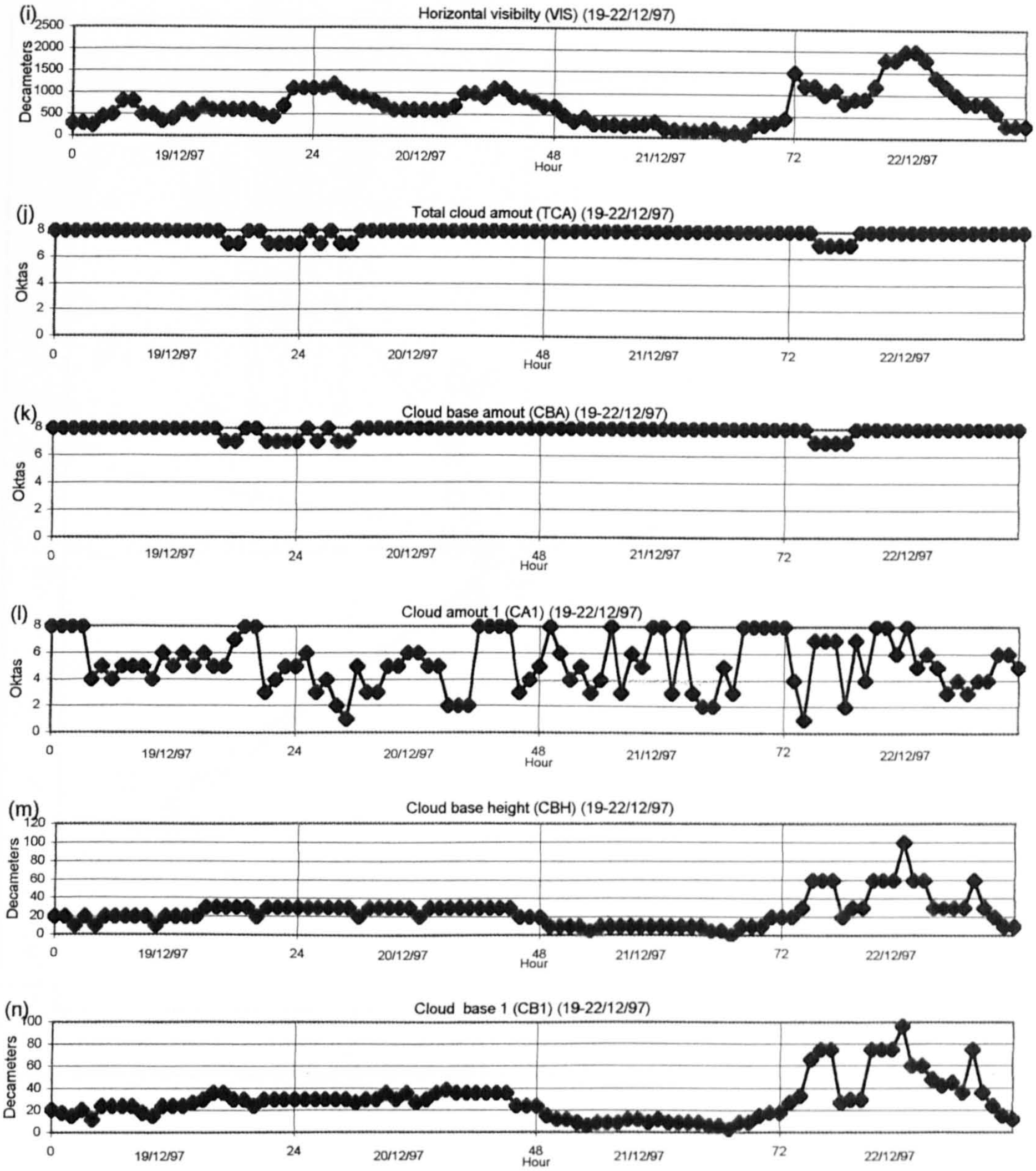

Figure 6.14: SCP and IAS peaks for Episode 5

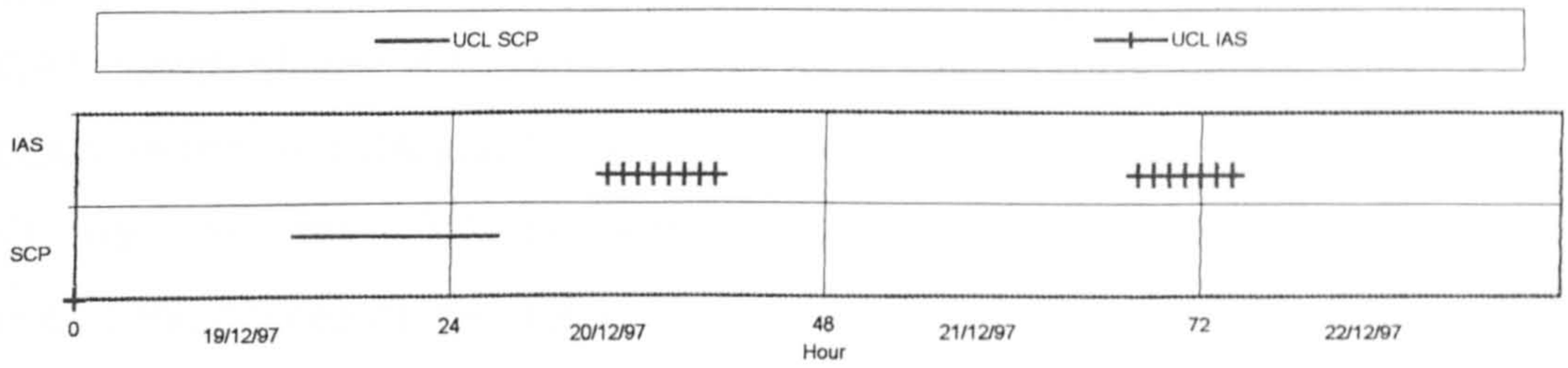

Figure 6.15: A PCA of the meteorology of Episode 5

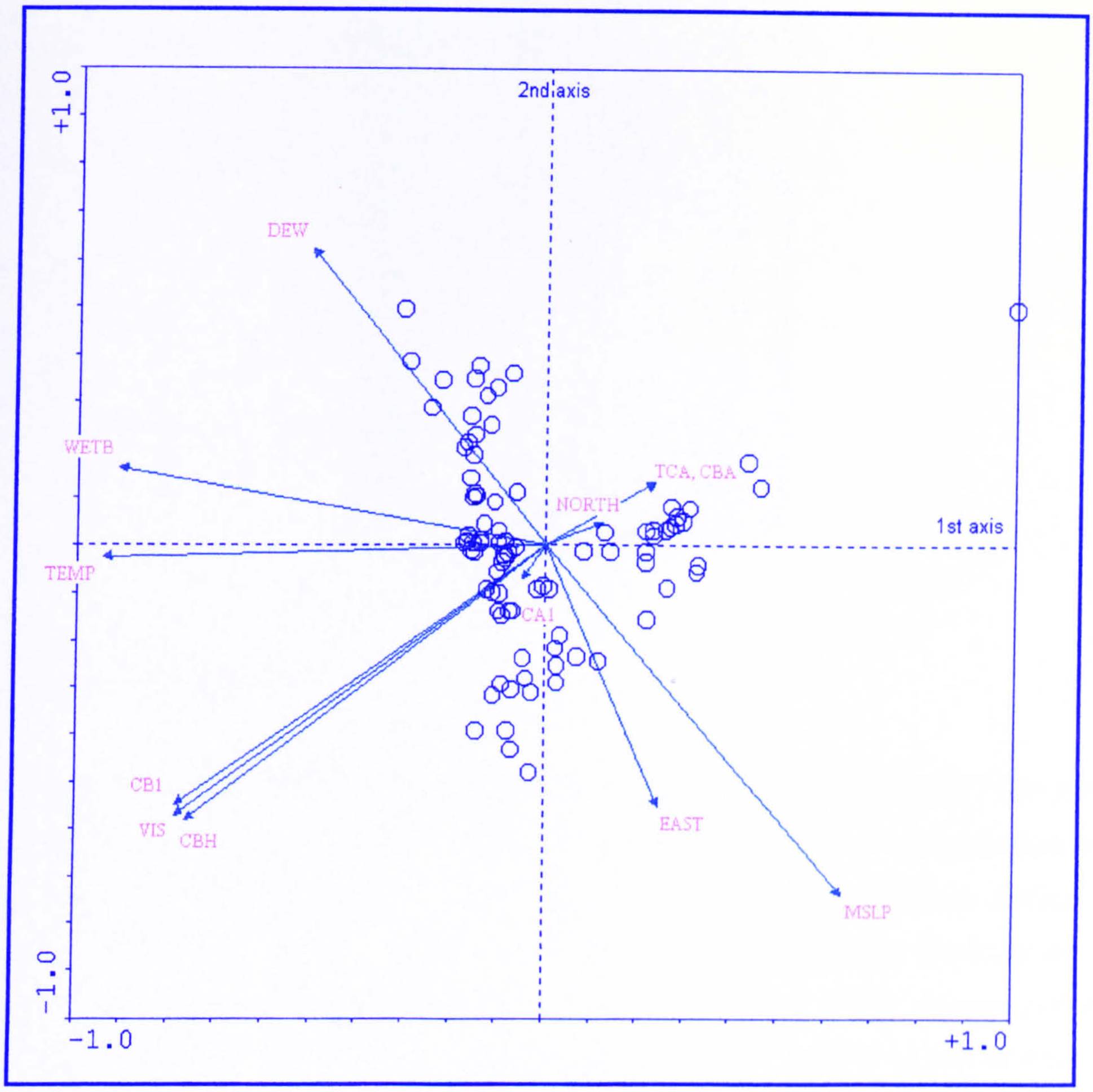

CB1, CBH and VIS are strongly related and have a large amount of variance along both the 1st and 2nd axes. These three variables are correlated with CA1, which shows little variation, but have negative correlation with the other cloud variables TCA and CBA. Therefore, as in all Episodes (except Episode 4), there are fewer clouds as the cloud base height increases. Table 6.5 shows the scores of the meteorological variables on axes 1 and 2 of the PCA.

Table 6.5: Component scores on axes 1 and 2 for the PCA of Episode 5

	1st axis	2nd axis
Eigenvalue	0.38	0.21
EAST	0.16	0.31
NORTH	0.23	0.46
TCA	-0.81	0.04
VIS	-0.03	-0.42
MSLP	0.00	0.45
TEMP	-0.65	-0.15
DEW	0.32	0.61
WETB	-0.51	0.11
RAIN	-0.21	0.86
CBA	-0.91	0.04
CBH	0.15	-0.28
CA1	-0.90	-0.03
CB1	0.20	-0.27

6.2.6 Summary

IAS peaks are generally associated with winds of varying speeds from the east, or when there is a strong easterly component, and can be attributed to the coal-fired sources, Kingsnorth and Tilbury, in the east Thames corridor. However, the minor IAS peak in Episode 1 at Thamesmead, Dartford and Northfleet is associated with winds from the north to north-west. Peaks in the SCP profile occur when the wind speed is low or just after a period of calm. The SCP peaks that are associated with IAS peaks have the same source but the ones that are not associated with IAS peaks, i.e. derived from oil-fired sources, have wind directions that have a strong south-easterly component. These events are associated with a local source. The relationships between other meteorological variables and SCP and IAS peaks are less clear.

6.3 Statistical relationships between meteorological variables and IAS/SCP

This section describes the use of multivariate statistics to attempt extract the meteorological variables that have a meaningful relationship with the SCP and IAS concentrations presented in Chapter 5.

A step-wise multiple regression procedure (see Chapter 4) was used to determine the meteorological variables that have a significant relationship with SCP and IAS (as single response variables in multiple linear regression analysis) (Jongman et al. 1995). Monte Carlo permutation tests were used to determine the statistical significance of each meteorological variable. The model created by the step-wise analysis was also tested for significance at the 95% level. All analyses were performed using Canoco for Windows version 4 (ter Braak and Smilauer, 1998). Tables 6.6a and 6.6b show the grouped results for SCP and IAS.

The amount of variance in the dependent variable accounted for by the meteorological variables extracted by the step-wise analysis has been included Tables 6.6a and 6.6b. For comparison the total variance that all meteorological variables account for has also been included.

6.3.1 SCP

The results of the step-wise multiple regression analyses with SCP as the dependent variable are shown in Table 6.6a. The amount of variance that each variable explains is shown in each cell. The greatest amount of variance is explained by the variable selected first, the next greatest amount by the variable selected second and so on.

Episode 1

There are few significant meteorological variables that explain the SCP record and these are different for each site. RAIN is the variable that is the most consistent (UCL, Thamesmead and Dartford), followed by EAST at Thamesmead and Northfleet. EAST explains the greatest amount of the variance (0.19) at Thamesmead and RAIN only accounts for a further 0.06 whereas at Northfleet RAIN explains more variance than EAST (0.09 compared with 0.02 respectively). Dartford is the only non-significant model across all the sites and for all episodes. Therefore, RAIN does not significantly predict the variance the SCP data. The total variance that all the meteorological variables explain is small for each site.

Episode 2

The significant meteorological variables are different during Episode 2 than during Episode 1 with WETB emerging as the most common variable at UCL, Thamesmead and Dartford. However, WETB (21%) only explains the greatest amount of variance in SCP at Dartford whereas MSLP (39%) is the most important at UCL and NORTH explains the most variance at Thamesmead. MSLP is also extracted at Dartford but it only explains 6% of the variance. NORTH (7%) is significant at UCL but again only explains a small amount of the variance. The variables selected for Northfleet are different to those selected at other sites and they account for a smaller proportion of the total variance.

The model created by the step-wise analysis at UCL explains 72.4% of a possible 77.8% of the variation in SCP counts. MSLP and TCA are the most important predictor variables and together account for 63% of the total. The other models explain a relatively small amount of the variation in SCP.

Episode 3

Only two variables are selected by the analysis but these account for a relatively large amount of the variance in the SCP data (52.5% of a total of 68.2%). TEMP is the most important of these and explains 45% of the variance alone.

Episode 4

DEW (11%) and TCA (7%) are selected by the analysis of SCP counts from Episode 4, however these two variables explain a much smaller amount of the total variance (18.2% of 40.9%). The unexplained variance is caused by the meteorological variables that do not have a significant relationship with the remaining variation in SCP counts once the TCA and DEW have been included in the model. There are fewer meteorological variables available for analysis in Episode 4, however the total variance that can be explained by these (40.9%) is higher than during other episodes where more meteorological variables are taken into account (e.g. Northfleet, Episode 1, total variance = 21.6%).

Table 6.6a: Results of the step-wise multiple regression for all episodes and sites with SCP as the dependent variable

Episode	Site	EAST %	NORTH %	TCA %	VIS %	MSLP %	TEMP %	DEW %	WETB %	CT1 %	LCT %	RAIN %	CBA %	CBH %	CA1 %	CB1 %	Variance (%)*	Total variance (%)**	Sig?
1	UCL		31									6					36.5	48.5	yes
	TM	19				4								6			29.4	33.8	yes
	DF											4					4.0	10.0	no
	NF	2										9					10.9	21.6	yes
2	UCL		7	24		39			3								72.4	77.8	yes
	TM		17						9								27.4	39.9	yes
	DF					6			21								26.8	46.2	yes
	NF											8				8	15.9	40.2	yes
3	UCL						45									8	52.5	68.2	yes
4	UCL			7				11									18.2	40.9	yes
5	UCL		45	9		6											59.8	62.7	yes

sig? significance of model ($p \leq 0.05$)

* Variance explained by environmental variables selected by the forward selection procedure

** Variance explained by the environmental variables if all were selected

grey shading indicates missing environmental variables in Episodes 3, 4 and 5

Table 6.6b: Results of the step-wise multiple regression for all episodes and sites with IAS as the dependent variable

Episode	Site	EAST %	NORTH %	TCA %	VIS %	MSLP %	TEMP %	DEW %	WETB %	CT1 %	LCT %	RAIN %	CBA %	CBH %	CA1 %	CB1 %	Variance (%)*	Total variance (%)**	Sig?
1	UCL		11									12		7			29.7	51.6	yes
	TM				4							10		5			18.7	26.8	yes
	DF											6					5.9	17.8	yes
	NF	4	2									7				17	30.1	41.5	yes
2	UCL		7			14										7	28.4	42.4	yes
	TM	8			4				18								29.8	39.2	yes
	DF			17	6												22.7	31.0	yes
	NF						6										5.9	33.5	yes
3	UCL				7	11	56										73.8	82.0	yes
4	UCL	6			74	10											89.6	91.5	yes
5	UCL	13			3	5	6	3						8			38.3	46.1	yes

sig? significance of model ($p \leq 0.05$)

* Variance explained by environmental variables selected by the forward selection procedure

** Variance explained by the environmental variables if all were selected

grey shading indicates missing environmental variables in Episodes 3, 4 and 5

Episode 5

NORTH, TCA and MSLP explain a relatively large amount of the variation in SCP counts, 59.8% of the possible 62.7%. NORTH is the most important variable and accounts for 45% of the variation whereas TCA and MSLP only explain 9% and 6% respectively.

6.3.2 IAS

The results of the step-wise multiple regression analyses with IAS as the dependent variable are shown in Table 6.6b. The format is the same as in Table 6.6a.

Episode 1

At each site the meteorological variables selected by the step-wise analysis only explain a small amount of the variance, varying from 30.1% of 41.5% at Northfleet to 5.9% of 17.8% at Dartford. Although the amount of variance in IAS explained at Dartford is very low the model is significant, whereas the model was not a significant predictor of SCP at Dartford (Table 6.6a). RAIN is extracted at all sites as a significant predictor of IAS concentration and it explains the greatest amount of the variation at UCL (12%), Thamesmead (10%) and Dartford (6%). CB1 is the most important variable at Northfleet. NORTH is significant at UCL (11%) and also at Northfleet where it only explains 2% of the variance. The other meteorological variables are less consistent and CBH is the only other variable selected at more than one site.

Episode 2

VIS is the only variable that is extracted as a significant predictor of IAS at more than one site in Episode 2. However, the amount of variance explained by VIS low, 4% at Thamesmead and 6% at Dartford. There are some similarities with the analyses of Episode 2 that have SCP as the dependent variable. For example, MSLP is the most important variable extracted at UCL. WETB is extracted at Thamesmead and it explains the greatest amount of variance in IAS but not SCP. This shows that there are few similarities in the SCP and IAS profiles. Both the total variance explained by all the

meteorological variables and the variance accounted for by the extracted variables are lower than when SCP is the dependent variable, suggesting that there is more noise in the IAS profile that is caused by other factors.

Episode 3

VIS, MSLP and TEMP significantly predict a large amount (73.8%) of the variation in the IAS data. TEMP accounts for 56% or the variation on its own. The total variation that all the meteorological variables can account for is 82.0%, the small difference between the two shows that the other meteorological variables in the analysis do not contribute much to the explanation. The large total variation indicates that there is little variation in the IAS profile caused by variables not included in the model.

Episode 4

VIS and MSLP are also significant predictors of the IAS profile in Episode 4 with the substitution of EAST for TEMP, compared to in Episode 3. In this episode the most important predictor is VIS (74%). However, it is possible that VIS is an effect of the pollution event rather than the cause. Once again the model explains a large amount of the variation, 89.6% of a possible 91.5% showing that there are no other major factors causing variation in the IAS profile.

Episode 5

There are six variables (EAST, VIS, MSLP, TEMP, DEW, CBH) selected as significant predictors of the IAS profile in Episode 5 and these account for only 38.3% of a total variance possible of 46.1%. EAST was selected first and explains 13% of the variation. This episode has the largest number of variables selected in the step-wise regression and therefore is the least easy to interpret with the meteorology available.

6.3.3 Summary

With one exception the models created by the step-wise analyses during Episodes 1 and 2 explain little of the variation in SCP or IAS. The exception

is at UCL in Episode 2 where MSLP and TCA are the most important predictors and together explain 63% of the variation in SCP concentration. The models best explain the variation in IAS during Episodes 3 and 4 and in SCP during Episodes 3 and 5. There are few variables that consistently account for the variation in SCP or IAS data at different sites during these episodes. NORTH is the most important variable in explaining the variation in SCP at three sites, UCL (Episode 1), Thamesmead (Episode 2) and UCL (Episode 5). The most variation in IAS is accounted for by EAST at Thamesmead (Episode 2) and UCL (Episode 5). TEMP explains the most variation in IAS at Northfleet (Episode 2) and UCL (Episode 3).

6.4 The effect of site on SCP and IAS concentration

The SCP and IAS profiles vary from site to site during the same Episode (see Chapter 5) even though the meteorological data are the same. This indicates that either the impact of SCPs and IASs changes spatially due to the locations of power stations and other Part A sources (see Chapters 3 and 4) or that there are site specific meteorological conditions that are not taken into account that affect SCP and IAS concentrations locally. This section will test the hypothesis that site has an effect on SCP and IAS concentrations by creating a site identity data set that will remove the effect of site (see ter Braak, (1988) for details of partial redundancy analyses).

A data set was created that contained all the SCP and IAS data from each site and for each episode. A co-variable data set was created that contained the corresponding meteorological variables for each site and episode. The co-variable data set is dummy data that comprises four columns (one for each site) with 1/0 data to represent presence or absence of a site in each column (Jongman et al. 1995). The data were compared using step-wise multiple linear regression and redundancy analysis as before (see Section 6.3).

6.4.1 SCP

Table 6.7a shows the significant variables selected by the step-wise multiple regression analysis with SCP as the dependent variable; Table 6.7b shows the significant variables from the same analysis with the inclusion of the co-variable data. Both models were significant ($p \leq 0.05$).

Table 6.7a: Results of the step-wise multiple regression for all episodes and sites in combination with SCP as the dependent variable

Variable	Coefficient	Standard deviation	*p*-value	sequential r^2
TCA	0.83	0.18	0.005	0.05
VIS	3.10	0.34	0.005	0.07
NORTH	1.01	0.17	0.005	0.09

Table 6.7b: Results of the step-wise multiple regression for all episodes and sites in combination with SCP as the dependent variable and including site predictor as a co-variable

Variable	Coefficient	Standard deviation	*p*-value	sequential r^2
TCA	0.83	0.18	0.005	0.05
NORTH	1.01	0.17	0.005	0.06
DEW	1.93	0.17	0.040	0.06*

*the output from CANOCO gives r^2 to two decimal places and in this case since the values are very low then the sequential r^2 does not increase due to rounding errors

The results show a very poor relationship between the meteorological data and SCP as the only dependent variable. The total variance explained by the model without co-variables is 9% of a possible 12% of all the meteorological variables combined. The effect of adding in the site identity co-variable is to reduce the explanation of the variance to 6% of a possible 7%. The difference between the variances explained by the models is the effect of site. In this case the difference is 3%.

6.4.2 IAS

The significant values identified by the step-wise multiple regression of all data with IAS as the dependent variable are shown in Table 6.8a and with site identity as a co-variable in Table 6.8b. Both models were significant ($p \leq 0.05$).

Table 6.8a: Results of the step-wise multiple regression for all episodes and sites in combination with IAS as the dependent variable

Variable	Coefficient	Standard deviation	*p*-value	sequential r^2
EAST	1.01	0.28	0.005	0.06
WETB	1.68	0.20	0.005	0.12
RAIN	0.08	0.25	0.005	0.14
VIS	3.10	0.33	0.005	0.16
TEMP	1.65	0.22	0.005	0.19
DEW	1.92	0.16	0.005	0.20
NORTH	1.01	0.18	0.025	0.21

Table 6.8b: Results of the step-wise multiple regression for all episodes and sites in combination with IAS as the dependent variable and including site predictor as a co-variable

Variable	Coefficient	Standard deviation	*p*-value	sequential r^2
EAST	1.01	0.28	0.005	0.06
WETB	1.68	0.20	0.005	0.12
RAIN	0.08	0.25	0.005	0.14
VIS	3.10	0.33	0.005	0.15
TEMP	1.65	0.22	0.005	0.18
DEW	1.92	0.16	0.005	0.19
NORTH	1.01	0.18	0.025	0.20

The significant meteorological variables selected by both models explain almost all of the variance (21% and 20%) that would be possible if all the meteorological variables were included in the regression (21% and 20% respectively). These figures are identical due to rounding errors, the significant variables explain slightly less than the total possible. The results

show that the two analyses are very similar with only 1% accounted for by site specific differences.

6.4.3 PCA

A PCA was performed on the environmental data for all episodes used in this Section (Figure 6.16). The 1st axis explains 28.0% of the variation in the meteorological data and the 2nd axis explains a further 22.4%, these are the only two significant axes. WETB, TEMP and DEW score highly on the 1st axis and are negatively correlated with NORTH, which also shows most of its variation on the 1st axis. Therefore, winds with a strong northerly component are associated with low temperatures and low humidity. EAST scores highly on both axes and has some positive correlation with NORTH. EAST is highly correlated with MSLP, which lies along the 2nd axis. These two variables are negatively correlated with RAIN, TCA and VIS showing that strong easterly winds do not bring rain and that rain is associated with the presence of clouds and poor visibility.

The location of episode hours on the PCA shows that different meteorological variables are important to each episode. The hours of Episode 1 are located in the centre of the plot and show the greatest variation in RAIN, TCA and VIS. Episode 2's hours are positioned centrally and also show variation in RAIN, TCA and VIS. Episodes 1 and 2 are the only episodes that had rainfall. Episode 2, 3 and 5 show some variation in WETB, TEMP and DEW although the hours of Episode 3 are much more dispersed and show variation in MSLP as well. Episode 3 is the most distinct group and accounts for the variation in NORTH, thus indicating that there is a component of the wind that fluctuates from north to south during this Episode.

Figure 6.16: A PCA of the meteorology of all episodes

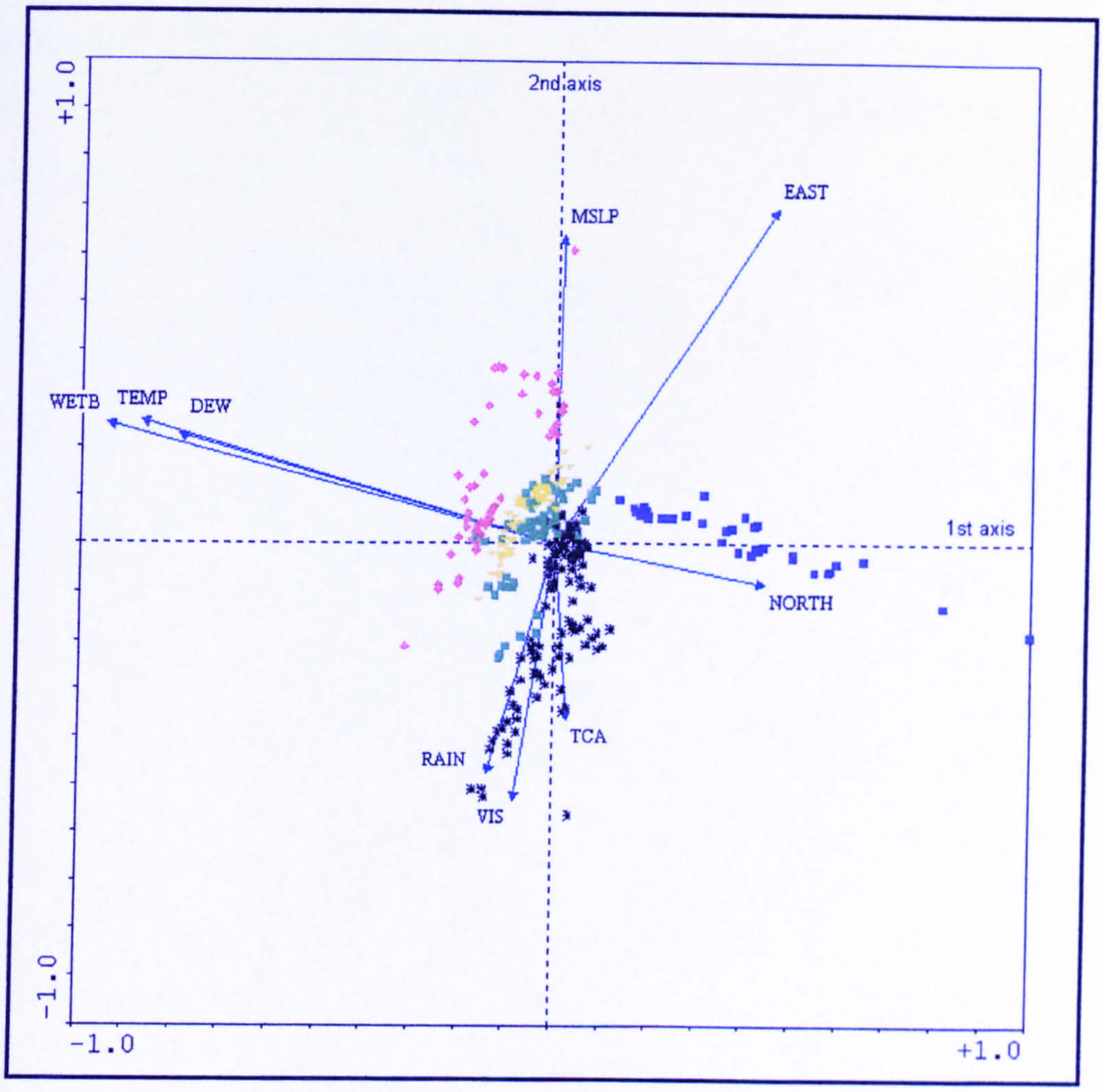

Black stars Episode 1 Green squares Episode 2

Purple squares Episode 3 Red diamonds Episode 4

Yellow triangles Episode 5

6.5 Discussion

6.5.1 Meteorological time series

Visual analysis of the meteorological data for each episode with reference to the peaks in IAS and SCP from Chapter 5 shows that IAS-derived events from coal-fired sources occur at all sites in the transect when winds are from the east. This shows that the Kingsnorth and Tilbury, the coal-fired sources in the east Thames Corridor, have an episodic impact on London and confirms the analysis from Chapter 5. The size of IAS peaks bears some relationship

to wind speed at UCL, with higher speeds being associated with IAS peaks of greater magnitude from the east. This is consistent with stronger winds being able to carry IAS further before deposition occurs and therefore causing a greater impact on the centre of London. There is not enough information to determine a relationship between the size of IAS peaks and wind speed at the other transect sites.

Not all IAS events are caused by winds from the east; there is an IAS event during Episode 1 at Thamesmead, Dartford and Northfleet that coincides with winds from the north and north-west and its origin is not clear. The particle size data for the SCP peak at the same time at Northfleet (Table 5.14) show a relatively small mean size which indicates that the source is not local. Although, as discussed in Chapter 6, the absence of large particles does not necessarily mean that these particles are absent as they just might not have been collected. In addition, the SCP and IAS events may not originate from the same source. The only source that lies in a westerly direction is Didcot but the modelling data from Chapter 3 showed that it will have a small impact on London, especially in the east of London. However, the modelling study was based on the dispersion of SCPs which are relatively large (SCPs over 100 μm were collected in lakes sediments in this study - see Table 4.3). In comparison, IASs are small (typically less than 5μm) and would easily be carried over long distances, i.e. from Didcot to the east of London. Long range transport of material contributes to the atmospheric load in London (Stedman, 1998) but the source of this material is associated with winds from the south-east. Other potential sources are the large coal fired power stations in the East Midlands which lie to the north of London and may contribute to the fine fraction of SCPs and IASs.

This analysis does not take into account any effects that previous weather may have on pollution. A plume may originate to the east of London and initially be carried away from the city. A change in wind direction might then bring the plume back towards London and, based on an analysis of the wind direction, it would not be possible to identify the source. Comparison of pollution peaks with previous wind trajectories on different time scales (e.g.

Smith et al, 2001) may provide further information on the impact to London of high-temperature combustion derived particle pollution.

A change in meteorological conditions might also be associated with pollution events. For example, in Episode 2 the SCP episode is immediately preceded by strong winds from the south-west which are probably ensuring that the pollution is being transported out of London. The following decrease to the relatively low wind speeds of the SCP peak cause stagnation of the air and then elevated concentrations, possibly due to a local source.

The SCP peaks that occur at UCL are evidence of a local source based on size distribution data. The impact of Part A processes in London was shown to be local in Chapter 3 and there is evidence from Chapter 4 of a significant local source of SCPs to lake sediments. The wind direction is generally from the south-east and the potential sources are Citigen and London Underground Chelsea. However, the wind direction data are not consistent during each event, which once again may be caused by the effect of previous wind directions. Resuspension of particles is favoured when the atmosphere is turbulent. For example in Episode 4 (52-64 hours) the diffuse but elevated counts of SCP occur during the day with a period of high wind speed which would suggest a relatively turbulent atmosphere. The average particle size is relatively high (Table 5.14) and large particles are more easily resuspended (Hinds, 2000).

The relationships with rain are not conclusive because there are not very many rain data points. Since rain is generally associated with removing particles a study of particulate pollution events will probably coincide with an absence of rain and it will therefore be difficult to study both at the same time. That said, there is a significant SCP peak in Episode 1 at UCL during a period of rain. Rain type determines the efficiency with which particles are removed (Mircea and Stefan, 1998) and heavier rain is less efficient at removing pollution particles. However, the rain during this period was not particularly heavy (see Figure 6.1o), only reaching around 1mm hr^{-1}. Alternatively, the source of this SCP event may be very close to UCL, i.e. Citigen, and the rain

may have had the effect of washing the particles out very close to the source, thereby causing a pollution event.

6.5.2 Statistically significant meteorological variables

There are few similarities in the results between the significant meteorological variables that explain the IAS and SCP profiles. Further, the total amount of variance explained by the models is, with a few exceptions, generally low. These exceptions are at UCL in Episodes 2, 3 and 5 with SCP as the dependent variable and at UCL in Episodes 3 and 4 with IAS as the dependent variable. The model created for each of these Episodes reduces the input meteorology into a small number (between two and four) of significant meteorological variables that could be used to predict a proportion of the variance. Only Episodes 2 and 5 with SCP as the dependent variable are similar in terms of the meteorological variables; NORTH, TCA and MSLP are all selected by both but the relative importance of these variables in terms of the amount of variance they explain in SCP is different for each episode.

RAIN is important for Episode 1 at all sites with IAS as the dependent variable, and for SCP as the dependent variable at all sites with the exception of Thamesmead. As mentioned above, rain has the effect of washing particles out of the air. Rain appears to have had this effect on IASs but it does not appear to have had much effect on the SCP event that occurred at UCL in Episode 1.

There is no consistency between Episodes and sites in the statistically significant meteorological variables. In some cases the effect of correlation between variables may complicate the interpretation when one variable is selected to explain variation in one case and a different variable that is related to the first is selected to explain the variation in the second case. If the first variable was selected both times the explanation of the variance may not be reduced by much but patterns between cases would be easier to interpret. For example, if TEMP is the most important variable for explaining the variance in one case and WETB is the most important in another then it may

be appropriate to select TEMP at both sites because these have a good relationship. To refine the approach used in this Chapter analyses should be carried out on a reduced set of variables to remove inter-variable correlations.

6.5.3 The effect of site and time

The results show that there are site specific factors that will affect the explanations of variance by the meteorological variables. These will include localised meteorological processes, site height, surrounding trees, buildings and changes in the atmospheric loading of SCPs and IASs. The amount of variance explained by meteorological variables in the site analysis is very low for all dependent variables and indicates the complexity of the system.

The PCA shows that there are different meteorological variables important during each Episode. All the episodes selected occurred in the winter and spring but differences may be caused by the effects of season that have not been taken into account in these analyses.

6.5.4 Model

The relationship between meteorology and SCP and IAS is complex and, therefore, it is not possible to develop a single model predicting IAS or SCP concentrations using this approach. The unexplained variation in SCP and IAS profiles is either caused by changes in meteorology or in the SCP or IAS input or is due to other factors that have not been taken into account in these analyses. The meteorology that would ordinarily cause a SCP or IAS episode will not be important if there is no source emitting these particles at the right time. Other variables, such as the previous weather conditions, have not been considered but may also be the cause of variation not explained by the meteorological variables selected. The contribution of resuspended particles to the particle size spectra is also a complicating factor. Therefore, it is not possible to create an overarching meteorological model to explain the pollution episodes seen. However, use of a longer data-set, consideration of the contribution that alternative variables such as previous wind direction will

have to the explanation of the variance or simplification of the model to remove correlations between variables may improve the analysis. Use of a synoptic climatalogical approach (e.g. Kalkstein and Corrigan, 1986) was attempted but was not successful due to the relatively small IAS and SCP time series.

CHAPTER 7: SUMMARY AND CONCLUSIONS

7.1 Introduction

This study has evaluated the spatial and temporal distribution of SCPs and IASs from high-temperature combustion point sources in and around London. The main aims of this project were to determine the footprint of pollution from high-temperature fossil fuel combustion sources using dispersion modelling; to compare predicted deposition with actual concentrations of SCP in lake and pond sediments in London; to assess the short term variations of emissions from fossil-fuel combustion source using Burkard Traps across London; to determine spatial differences in SCPs and IAS using a transect of Burkard Traps across London; and to identify the meteorological conditions under which high concentrations of particles from high-temperature combustion sources impact on London.

7.2 SCPs in lakes and ponds in London

The hypothesis that SCP deposition would decrease from east to west London was disproved and shown to be related to source location. The spatial deposition pattern of SCPs modelled using ADMS 3 shows that Part A processes have the most significant impact in London due to lower stack heights causing SCPs to be deposited locally despite having lower emissions than power stations. Power stations in the east Thames corridor and the coal-fired power station in Didcot are responsible for contributing to the SCP background levels in London with the exception of south-east London where power stations are the dominant source of SCPs. Each power station shows a decrease in its impact across London away from the source. Littlebrook has the potential to have the greatest impact on London because it is the only power station located inside the M25. However, it is in operation for less than 2% of the time and therefore its impact is relatively minor in comparison with the other power stations and the non-power station Part A processes.

The main weakness of dispersion modelling is the large number of assumptions that have to be made. The qualitative deposition results from

this study should be treated with caution. Bearing in mind all the assumptions made the model produces a reasonable representation of the relative differences in deposition of SCPs across London and was therefore suitable for comparison with actual concentrations of SCPs in lakes and ponds.

The footprint of SCP deposition agrees well with actual SCP concentrations in the surface sediments of 27 lakes and ponds across London. Deposition of SCPs 100 μm in diameter was found to significantly predict 27% of the total variance in SCPs in lake and pond surface sediments. Deposition of all SCP size fractions were well correlated with each other and so were not selected by a step-wise regression analysis, however any of the SCP deposition fractions would predict a similar amount of the variance in the actual SCP concentration data.

The only environmental variable that was a significant predictor of the variation in SCP concentration data was the core depth to maximum lake depth ratio, which explained 14% of the variation and suggested that SCP accumulation may not be uniform across each site. However, accumulation rate data was only available at eight sites and was shown to not have a significant influence on SCP concentration data. The remainder of the variation was accounted for by the other environmental variables in combination.

Analysis of the SCP size distribution shows that size has some relationship with proximity to source and predicted SCP deposition.

7.3 SCPs, IASs and meteorology

Identification of IAS and SCP episodes using SO_2 concentrations is not a fail-safe method for finding IAS and SCP pollution events but in combination with NO_2 levels is a reasonably accurate technique. SO_2 and NO_2 data are widely available and, for the most part, SCP and IAS events are associated with elevated SO_2 concentrations. Incorporating an examination of the NO_2 levels at the time proves this to be a good method for screening Burkard Trap tapes.

Examination of the time-series of SCP and IAS alone can identify the fuel type used in the high-temperature fossil fuel combustion source. By considering the size distribution for each SCP peak it is possible to suggest a likely source for the event. A local oil-fired source was identified in the centre of London based on the SCP events that are not associated with IAS events. This agrees with the evidence from Chapter 3 which predicts high levels of deposition from Part A processes in the centre of London and in Chapter 4 which shows that large numbers of SCPs are collected in the lakes in the centre of London.

Inclusion of meteorology in the analysis in Chapter 6 allows sources to be identified with more certainty. There is significant evidence based on wind direction data that IAS events are caused by episodic pollution from power stations in the east Thames corridor.

This is the first study of emissions of particulate pollution from power stations and other Part A processes for specific episodes in London and it has shown that high-temperature combustion sources have a specific impact that can be separated from the complex atmospheric aerosol load. Burkard Traps and lakes and ponds are not the only places where episodes of pollution have an impact. Between these sites are people, buildings and the natural environment, which are sensitive to the impact of particulate pollution. SCPs and IASs smaller than 5 μm can be deposited in the bronchioles and the alveoli. Not enough is known about these particles to assess their potential health impacts or to determine the precise effect that these pollution events have. Therefore it is vital that the health effects of IASs and SCPs are studied in more detail.

7.4 Recommendations for further work

There is some variability in SCP concentrations in the lake and pond sediments that cannot be explained by modelled deposition from power stations. One variable that has not been incorporated in the model is lake or pond catchment due to the complex drainage systems that surround urban sites. Therefore, a detailed catchment study of a lake in an urban area is suggested.

A study was attempted that co-located a deposition gauge with a Burkard Trap so that the SCPs collected could be compared with the flux of SCPs collected using a sediment trap in a close-by lake. This attempt was unsuccessful due to the disturbed nature of the lake but this approach would produce valuable information linking atmospheric concentrations with deposition.

Dispersion modelling is complex due the numbers of input variables that are required and the lack of suitable meteorological data. There are other dispersion models that might be more useful for modelling particles (for example the Meteorological Office NAME model) and a study should be carried out to compare ADMS 3 with other models.

To remove the unknown effect of the urban heat island a similar study should be undertaken to model the emissions from an individual power station in a rural area and to compare the local impacts on Burkard Traps and lakes. This would remove some of the uncertainty in the model.

A more detailed modelling study should also be carried out in conjunction with a power station operator to determine the impact of emissions over a shorter time period so that these can be directly compared with SCPs and IASs collected on Burkard Traps.

To better understand the effects of meteorology on IAS and SCP peaks collected in the Burkard Trap transect a longer record of tapes should be

counted, rather than just episodes, and the analysis should be re-run including other explanatory variables such as previous weather conditions.

A study of the contribution of SCPs and IASs to PM_{10} and $PM_{2.5}$ should be carried out in combination with an investigation into the impacts on health of inhalation of SCPs and IASs.

BIBLIOGRAPHY

Abbott J and J Stedman, 1999: *Dispersion modelling and mapping studies for review and assessment of PM_{10}.* Report produced for the Department of the Environment, Transport and the Regions. AEAT 5273 Issue 2. pp18

Anderson H R, A Ponce de Leon, J M Bland, J S Bower and J P Strachan, 1996: Air pollution and daily mortality in London: 1987-92. *British Medical Journal*, 312(March), 665-669

Anderson N J, 1990: Variability of diatom concentrations and accumulation rates in sediments of a small lake basin. *Limnology and Oceanography,* 35(2), 497-508

Anfossi D, F Desiato, G Tinarelli, G Brusasca, E Ferreros and D Sacchetti, 1998: Transalp 1989 experimental campaign - II simulation of a tracer experiment with Lagrangian particle models. *Atmospheric Environment*, 32(7), 1157-1166

APEG, 1999*: Source apportionment of airborne particulate matter in the United Kingdom.* Report of the Airborne Particles Expert Group. DETR, UK. pp157

Appleby P G and F Oldfield, 1978: The calculation of 210Pb dates assuming a constant rate of supply of unsupported 210Pb to the sediment. *Catena.*, 5, 1-8

Appleby P G, P Nolan, D W Gifford, M J Godfrey, F Oldfield, N J Anderson and R W Battarbee, 1986: 210Pb dating by low background gamma counting. *Hydrobiologia.* 141, 21-27

Applestone P, 1997: *An investigation into the sources of particulate matter in the Kings Cross area.* Unpublished Dissertation for the MRes in Environmental Science, University College London

AQS, 1999: *The air quality strategy for England, Scotland, Wales and Northern Ireland.* Consultation Document, DETR in partnership with the Scottish Executive, The National Assembly for Wales and the Department of the Environment for Northern Ireland, pp103

Arya S P, 1999: *Air pollution meteorology and dispersion.* Oxford University Press. New York, pp310

Barnes R A and A E J Eggleton, 1977: The transport of atmospheric pollutants across the North Sea and English Channel. *Atmospheric Environment*, 11, 879-892

Barratt M, 2000: *The worst and the best. Atmospheric emissions from large point sources in Europe.* The Swedish NGO Secretariat on Acid Rain, 39pp

Barratt M and R Protheroe, 1994: *Sulphur emissions from large point sources in Europe.* Air pollution and climate series No. 3, The Swedish NGO Secritariat on Acid Rain.

Battarbee J L, N L Rose and X Long, 1997: A continuous, high resolution record of urban airborne particulates suitable for retrospective microscopical analysis. *Atmospheric Environment*, 31(2), 171-181

Battarbee R W and I Renberg, 1990: The surface water acidification project (SWAP) palaeolimnology project. *Philosophical Transactions of the Royal Society of London.* B(327), 227-232

Battarbee R W, V J Jones, R J Flower, P G Appleby, N L Rose and B Rippey, 1995: Palaeolimnological evidence for the atmospheric contamination and acidification of high Cairngorm lochs with special reference to Lochnagar. *Botanical Journal of Scotland,* 48(1), 79-87

BEI, 1991: *Modern power station practice.* British Electricity International, Volume D

Bennett M and G C Hunter, 1997: Some comparisons of LIDAR estimates of peak ground-level concentrations with the predictions of UK-ADMS. *Atmospheric Environment*, 31(3), 429-439

Bennion H, P G Appleby and G L Phillips, 2001: Reconstructing nutrient histories in the Norfolk Broads, UK: implications for the role of diatom-total phosphorous transfer functions in shallow lake management. *Journal of Paleolimnology*, 26, 181-204

BéruBé K A, T P Jones, B J Williamson and R J Richardson, 1999: The physiochemical characterization of urban airborne particulate matter. In: *Particulate Matter.* Ed Maynard R L and C V Howard. BIOS Scientific Publishers, Oxford. Chapter 4, 39-62

Boehm G and R M Leuschner, 1979: A simple procedure for the photometric evaluation of incidental findings on the recording strips of the Burkard pollen-and-spore trap. *Experientia*, 35, 1415-141

Boni C, E Caruso, E Cereda, G Lombardo, G M B Marcazza and P Redaelli, 1988: Particulate matter elemental characterization in urban areas: Pollution and source identification. *Journal of Aerosol Science*, 19(7), 1271-1274

Brazdil R and M Budikova, 1999: An urban bias in air temperature fluctuations at the Klementinium, Prague, The Czech Republic. *Atmospheric Environment*, 33, 4211-4217

Briggs D J, C de Hoogh, J Gulliver, J Wills, P Elliot, S Kingham and K Smallbone, 2000: A regression based method for mapping traffic-related air pollution: application and testing in four contrasting urban environments. *The Science of the Total Environment*, 253, 151-167

Brimblecombe P, 1977: London air pollution, 1500-1900. *Atmospheric Environment*, 11, 1157-1162

Brimblecombe P, 1988: *The big smoke. A history of air pollution in London since medieval times.* Routledge, London and New York

Burkard Manufacturing Co Ltd., *Burkard Volumetric Spore Trap operating instructions.* Burkard Manufacturing Co Ltd. Rickmansworth, Hertfordshire

Carruthers D J, A M Mckeown, D J Hall and S Porter, 1999: Validation of ADMS against wind tunnel data of dispersion from chemical warehouse fires. *Atmospheric Environment*, 33, 1937-1953

CERC, 1999: *ADMS User Guide.* CERC Limited, Cambridge

Cereda E, G M B Marcazzan, M Pedretti, G W Grime and A Baldacci, 1995: The microscopic nature of coal fly ash particles investigated by means of nuclear microscopy. *Atmospheric Environment,* 29, 2323-2329

Chan L Y, W S Kwok, 2001: Roadside suspended particulates at heavily trafficked urban sites of Hong Kong - Seasonal variation and dependence on meteorological conditions. *Atmospheric Environment*, 35, 3177-3182

Chan Y C, P D Vowles, G H McTainsh, R W Simpson, D D Cohen, G M Bailey and G D McOrist, 2000: Characterisation and source identification of PM_{10} aerosol samples collected with a high volume cascade impactor in Brisbane (Australia). *The Science of the Total Environment*, 262, 5-19

Cheng S and K-C Lam, 2000: Synoptic typing and its application to the assessment of climatic impact on concentrations of sulfur dioxide and nitrogen oxides in Hong Kong. *Atmospheric Environment*, 34, 585-594

Chueinta W, P K Hopke and P Paatero, 2000: Investigation of sources of atmospheric aerosol at urban and suburban residential areas in Thailand by positive matrix factorization. *Atmospheric Environment*, 34, 3319-3329

Clark J S, 1988: Stratigraphic charcoal analysis on petrographic thin sections: application to fire history in north-western Minnesota. *Quaternary Research*, 30, 81-91

Colls J, 1997: *Air pollution - an introduction.* E & F N Spon, London, pp341

Davis M B and M S Ford, 1982: Sediment focusing in Mirror Lake, New Hampshire. *Limnology and Oceanography,* 27(1), 137-150

Davis R B, 1974: Stratigraphic effects of tubificids in profundal lake sediments. *Limnology and Oceanography*, 19, 466-488

Deboudt K, P Flament, D Weis, J-P Mennessier and P Maquinghen, 1999: Assessment of pollution aerosols sources above the Straits of Dover using lead isotope geochemistry. *The Science of the Total Environment*, 236, 57-74

Del Monte M, C Sabbioni and O Vittori, 1984: Urban stone sulphation and oil-fired carbonaceous particles. *The Science of the Total Environment*, 36, 369-376

Del Monte M and O Vittori, 1985: Air pollution and stone decay: the case of Venice. *Endeavour,* 9(3), 117-122

Diociaiuti M, F Bordi, L Gatelata, G Baldo, P Crateri and L Paoletti, 1999: Morphological and functional alterations of human erythrocytes induced by SiO2 particles: An electron microscopy and dielectric spectroscopy study. *Environmental Research Section A*, 80, 197-207

Dockery D W, C A Pope, X Xipeng, J D Spengler, J H Ware, M E Fay, B G Ferris and F E Speizer, 1993: An association between air pollution and mortality in six US cities. *The New England Journal of Medicine*, 329(24), 1753-1759

Dockery D W and C A Pope, 1994: Acute respiratory effects of particulate air pollution. *Annual Review of Public Health*, (15), 107-132

Downing J A, L C Rath, 1988: Spatial patchiness in the lacustrine sedimentary environment. *Limnology and Oceanography*, 33(3), 447-458

EA, 1996: *Appendix 1. Modelling of power station impacts on local air quality.* 1-45

EA, 1998: *Guidance for estimating the air quality impact of stationary sources.* Environment Agency, pp30

EA, 2000: *Report into an air pollution episode. Sulphur dioxide, September 2nd 1998, Midlands and South Yorkshire.* Environment Agency. pp109

Evelyn J, 1661: *Fumifugium.* National Smoke Abatement Society, UK. pp42

Fast J D and S Zhong, 1998: Meteorological factors associated with inhomogeneous ozone concentrations within the Mexico City basin. *Journal of Geophysical Research.* 103(D15), 18927-18946

Fisher J B, W J Lick, P L McCall and J A Robbins, 1980: Vertical mixing of lake sediments by tubificid oligochaetes. *Journal of Geophysical Research*, 85, 3997-4006

Gardner M W and S R Dorling, 1999: Neural network modelling and prediction of hourly NOx and NO2 concentrations in urban air in London. *Atmospheric Environment*, 33, 709-719

Glew J R, 1991: Miniature gravity corer for recovering short sediment cores. *Journal of Paleolimnology*, 5, 285-287

Goldberg E D, V F Hodge, JJ Griffin, M Koide and D N Edgington, 1981: Impact of fossil fuel combustion on the sediments of Lake Michigan. *Environmental Science and Technology,* 15(4), 466-470

Goldberg E D, 1985: *Black carbon in the environment: properties and distribution.* New York: Wiley Interscience.

Goldstein H L and C W Siegmund, 1976: Influence of heavy fuel oil composition and boiler combustion conditions on particuate emissions. *Environmental Science and Technology*, 10(12), 1109-1114

Griest W H, L A Harris, 1985: Microscopic identification of carbonaceous particles in stack ash from pulverised-coal combustion. *Fuel,* 64, 821-826

Griffin J J and E D Goldberg, 1979: Morphologies and origin of elemental carbon in the environment. *Science*, 206, 563-565

Griffin J J and E D Goldberg, 1981: Sphericity as a characteristic of solids from fossil fuel burning in a Lake Michigan sediment. *Geochimica et Cosmochimica Acta*, 45, 763-769

Haan P, 1999: On the use of density kernels for concentration estimations within particle and puff dispersion models. *Atmospheric Environment*, 33, 2007-2021

Håkanson L and M Jansson, 1983: *Principles of lake sedimentology.* Springer-Verlag, Berlin Heidelberg New York Tokyo. pp 316

Hall D and A Spanton, 1999: Meteorological data and dispersion modelling. *Clean Air.* 29(5), 130-137

Hall D J, A M Spanton, F Dunkerley, M Bennett and R F Griffiths, 2000a: *A review of dispersion model inter-comparison studies using ISC, R91, AERMOD and ADMS.* Environment Agency, UK. pp69

Hall D J, A M Spanton, F Dunkerley, M Bennett and R F Griffiths, 2000b: *An inter-comparison of the AERMOD, ADMS and dispersion models for regulatory applicaitons.* Environment Agency, UK. pp110

Hamilton R, 1993: *Effects of airborne particulate matter in historic buildings.* ECHNLR 7(1-4), 39-42

Harrison R M, D J T Smith, C A Pio and L M Castro, 1997a: Comparative receptor modelling study of airborne particulate pollutants in Birmingham (United Kingdom), Coimbra (Portugal) and Lahore (Pakistan). *Atmospheric Environment*, 31(20), 3309-3321

Harrison R M, A R Deacon, M R Jones and R S Appleby, 1997b: Sources and processes affecting concentrations of PM_{10} and $PM_{2.5}$ particulate matter in Birmingham (UK). *Atmospheric Environment*, 31(24), 4103-4117

Harrison R M, J P Shi and M R Jones, 1999a: Continuous measurements of aerosol physical properties in the urban atmosphere. *Atmospheric Environment*, 33, 1037-1047

Harrison R M, M Jones and G Collins, 1999b: Measurements of the physical properties of particles in the urban atmosphere. *Atmospheric Environment*, 33, 309-321

Hatano Y, N Hatano, H Amano, T Ueno, A K Sukhoruchkin and S V Kazakov, 1998: Aerosol migration near Chernobyl: long term data and modelling. *Atmospheric Environment,* 32(14-15), 2587-2594

Havlíček D, R Přibil, O Dubovský, L Dobiášová and P Sedlák, 2000: Chemical and mineralogical composition of solid fraction of ambient aerosol at different levels (Kopisty near Most, NW Bohemia). *Atmospheric Environment,* 34, 3237-3244

Henry R C, C W Lewis, P K Hopke and H J Williamson, 1984: Review of receptor model fundamentals. *Atmospheric Environment*, 18(8), 1507-1515

Hien P D, N T Binh, Y Truong, N T Ngo and L N Sieu, 2001: Comparative receptor modelling study of TSP, PM2 and PM2-10 in Ho Chi Minh City. *Atmospheric Environment*, 35, 2669-2678

Hinds W C, 2000: *Aerosol technology.* Wiley-Interscience. pp483

Hirst M J, 1952: An automatic volumetric spore trap. *Annals of Applied Biology*, 39, 257-265

HMIP, 1996: *An assessment of the effects of industrial releases of nitrogen oxides in the East Thames corridor.* Executive Summary. HMIP Environment Series, HMSO.

Huang S, R Arimoto and K A Rahn, 2001: Sources and source variations for aerosol at Mace Head, Ireland. *Atmospheric Environment*, 35, 1421-1437

Jackson D A, 1993: Stopping rules in PCA: a comparison of historical and statistical approaches. *Ecology*, 74, 2204-2214

Javitz H S, J G Watson, J P Guertin and PK Mueller, 1988: Results of a receptor model feasibility study. *JAPCA*, 661-667

Jones T P, B J Williamson, K A BeruBe and R J Richards, 2001: Microscopy and chemistry of particles collected on TEOM filters: Swansea, south Wales, 1998-1999. *Atmospheric Environment*, 35, 3573-3583

Jongman R H, C J F ter Braak and O F R van Tongeren, 1995: *Data analysis in community and landscape ecology.* Cambridge University Press, UK. pp299

Kalkstein L S and P Corrigan, 1986: A synoptic climatological approach for geographical analysis: Assessment of sulfur dioxide concentrations. *Annals of the Association of American Geographers*, 76(3), 381-395

Kalkstein L S, G Tan and J A Skindlov, 1987: An evaluation of three clustering procedures for use in synoptic climatologial classification. *Journal of climate and applied meteorology*, 26, 717-730

Katsouyanni K, G Touloumi, C Spix, J Schwartz, F Balducci, S Medina, G Rossi, B Wojtyniak, J Sunyer and L Bacharova, 1997: Short term effects of ambient sulphur dioxide and particulate matter on mortality in 12 European cities: results from time series data from the APHEA project. *British Medical Journal*, 314, 1658-1665

Kimmel B L, 1978: An evaluation of recent sediment focusing in Caste Lake (California) using a volcanic ask layer as a stratigraphic marker. *Verhandlungen (Internatinonale Vereinigung für Theoretische und Angewandte Limnologie)*, 20, 393-400

Kolehmainen M, H Martikainen and J Ruuskanen, 2001: Neural networks and periodic components used in air quality forecasting. *Atmospheric Environment*, 35, 815-825

Laxen D, 1996: *Generating emissions? Studies of the local impact of gaseous power station emissions.* Report on the findings of the extensive air pollution monitoring programs carried out around coal and oil fired power stations during the period 1963-1994 by the CEGB and by National Power PLC and Poweren plc under their Joint Environmental Program. pp 74

Long X, 1998: *Particulate air pollution in central London: characterisation, temporal patterns and source apportionment.* Unpublished PhD Thesis, University of London.

LRC, 1997: *London atmospheric emissions inventory.* London Research Centre. Environment and Transport Studies. pp81

Mackay A, 1998: *Temporal trends of fungal spores in central London and their functional relationships with environmental factors.* JEI working paper (No.2.), 32pp

Mackay A W and N L Rose, 1998: Characterisation and temporal distribution of atmospheric particulates (PM10's) in central London *Air Pollution VI, Air Pollution '98.* Ed C A Brebbia, C F Rabb and H Power. 948-957

Malcolm A L, R G Derwent and R H Maryon, 2000: Modelling the long-range transport of secondary PM_{10} to the UK. *Atmospheric Environment*, 34, 881-894

Malcolm A L and A J Manning, 2001: Testing the skill of a Lagrangian dispersion model at estimating primary and secondary particualtes. *Atmospheric Environment*, 35, 1677-1685

Mamane Y, J L Miller and T G Dzubay, 1986: Characterisation of individual fly-ash particles emitted from coal- and oil-fired power plants. *Atmospheric Environment*, 20(11), 2125-2135

Marcazzan G M B, B Bellagamba, M Bellotto, C Boni, A Caridi, E Cereda and C Chemelli, 1990: Fly ash from a coal power plant: Correlation of elemental and structural composition with electrostatic precipitator collection efficiency. *Journal of Aerosol Science (Supplement 1)*, 21(1), S697-S701

Marcazzan G M B, B Balossi, S Pasello, N Petriccioli and F Apadula, 1994: Study of aerosol-particle transport by means of particulate-matter elemental composition. *Nuovo Cimento Della Societa Italiana Di Fisica C-Geophysics and Space Physics*, 17(4), 393-406

Maugeri M, M Valentini and G M B Marcazzan, 1990: Elemental characterisation of atmospheric aerosol collected in an urban center of northern Italy. *Journal of Aerosol Science (supplement 1)*, 21(1), S339-S342

McCrone W C and J G Delly, 1973: *The Particle Atlas. An encyclopedia of techniques for small particle identification.* Ann Arbor Science Publishers, Michigan, USA

McElroy M W, R C Carr, D S Ensor and G R Markowski, 1982: Size distribution of fine particles from coal combustion. *Science*, 215(4528), 13-18

McGregor G R and D Bamzelis, 1995: Synoptic typing and its application to the investigation of weather air pollution relationships, Birmingham, United Kingdom. *Theoretical and Applied Climatology*, 51, 223-236

McMurray P H, 2000: A review of atmospheric aerosol measurements. *Atmospheric Environment*, 34, 1959-1999

Met Office, 2001: http://www.met-office.gov.uk/education/training/clouds.html

Micallef A, C N Deucher and J J Colls, 1998: Indoor and outdoor measurements of vertical concentration profiles of airborne particulate matter. *The Science of the Total Environment*, 215, 209-216

Middleton D R, 1997: *Manual on modelling: a guide for local authorities.* Met Office (APR) Turbulence and Diffusion Note No. 241. pp41

Mirccea M and S Stefan, 1998: A theoretical study of the microphysical parameterization of the scavenging coefficient as a function of precipitation type and rate. *Atmospheric Environment*, 32, 2931-2938

Moreno-Grau S, A Perez-Tornell, J Bayo, J Moreno, J M Angosto and J Moreno-Clavel, 2000: Particulate matter and heavy metals in the atmospheric aerosol from Cartagena, Spain. *Atmospheric Environment*, 34, 5161-5167

Morrison G F, 1986: *Understanding pulverised coal combustion.* IEA Coal Research. 14-15 Lower Grosvenor Place, London. pp46

Mukerjee S, D S Shadwick, L A Smith, M C Somerville and K E Dean, J J Bowser, 2001: Techniques to assess cross-border air pollution and application to a US-Mexico border region. *The Science of the Total Environment*, 276, 205-224

National Power, 1997: *Environmental performance review 1997.* National Power. pp16

Nef J U, 1932: *The rise of the British coal industry.* George Routledge & Sons Limited, London. pp448

Nettleton M A, 1979: Particulate formation in power station boiler furnaces. *Progress in Energy Combustion Science*, 5, 223-243

Nimko J, J-P Tuovinen, J Kukkonen and I Valkama, 1999: A hybrid plume model for local-scale atmospheric dispersion. *Atmospheric Environment*, 33, 4389-4399

Nriagu J O and C J Bowser, 1969: The magnetic spherules in sediments of Lake Mendota, Wisconsin. *Water Research*, 3, 833-842

Odgaard B V, 1993: The sedimentary record of spheroidal carbonaceous fly-ash particles in shallow Danish lakes. *Journal of Paleolimnology*, 8, 171-187

Oh H S and Y S Ghim, 2001: Numerical study of atmospheric dispersion of a substance released from an industrial complex in the southern coast of Korea. *Atmospheric Environment*, 35, 3103-3111

Ohlstrom M O, K E J Lehtinen, M Moisio and J K Jokiniem, 2000: Fine-particle emissions of energy production in Finland. *Atmospheric Environment*, 34, 3701-3711

Oke T R, 1987: *Boundary layer climates - 2nd ed. 1. Microclimatology. 2. Planetary boundary layer.* Routeledge, 11 New Fetter lane, London, EC4P 4EE.

Olcese L E and B M Toselli, 1998: Statistical analysis of PM_{10} measurements in Cordoba City, Argentina. *Meteorology and Atmospheric Physics*, 66, 123-130

Oza R B, N S Panchal, K S V Nambi and T M Krishnamoorthy, 2001: Coupling of mesoscale meteorological model with particle trajectory model to study the atmospheric dispersion under sea breeze conditions. *Environmental Modelling and Software*, 16, 63-71

Paciga J J and R E Jervis, 1976: Multielement size characterization of urban aerosols. *Environmental Science and Technology*, 10(12), 1124-1128

Parkin D W, D R Phillips and R A Sullivan, 1970: Airborne dust collections over the North Atlantic. *Journal of Geophysical Research*, 75(9), 1782-1793

Perez P, A Trier and J Reyes, 2000: Prediction of $PM_{2.5}$ concentrations several hours in advance using neural networks in Santiago, Chile. *Atmospheric Environment*, 34, 1189-1196

Petterson G, I Renberg, P Geladi, A Lindberg and F Lindgren, 1993: Spatial uniformity of sediment accumulation in varved lake sediments in northern Sweden. *Journal of Paleolimnology*, 9, 195-208

Physick W L and R Goudey, 2001: Estimating an annual-average RSP concentration for Hong Kong using days characteristic of the dominant weather patterns. *Atmospheric Environment*, 35, 2697-2705

PowerGen, 1996: *Environmental performance report 1996.* PowerGen Plc. pp44

Prati P, A Zucchiatti, F Lucarelli and P A Mando, 2000: Source apportionment near a steel plant in Genoa (Italy) by continuous aerosol sampling and PIXE analysis. *Atmospheric Environment*, 34, 3149-3157

Pyatt F B, 1973: Some aspects of plant contamination by air borne particulate pollutants. *International Journal of Environmental Studies*, 5, 215-220

QUARG, 1993: *Urban air quality in the United Kingdom.* First Report of the Quality of Urban Air Review Group. DOE, UK. pp201

QUARG, 1996*: Airborne particulate matter in the United Kingdom.* Third report of the Quality of Urban Air Review Group. DETR, UK. pp176

Raask E, 1968: Cenospheres in pulverised-fuel ash. *Journal of the Institute of Fuel,* Sep, 339-344

Raask E, 1984: Creation, capture and coalescence of mineral species in coal flames. *Journal of the Institute of Energy*, 57, 231-239

Raeymaekers B, M Demuynck, W Dorrine and F Adams, 1988: Characterisation of oil fly-ash particles by electron probe microanalysis. *International Journal of Environmental Analytical Chemistry*, 32, 291-312

Raga G B, D Baumgardner, G Kok and I Rosas, 1999: Some aspects of boundary layer evolution in Mexico City. *Atmospheric Environment*, 33, 5013-5021

Ramsden A R and M Shibaoka, 1982: Characterisation and analysis of individual fly-ash particles from coal-fired power stations by a combination of optical microscopy, electron microscopy and quantitative electron microprobe analysis. *Atmospheric Environment*, 16(9), 2191-2206

Renberg I and M Wik, 1984: Dating recent lake sediments by soot particle counting. *Verhandlungen (Internatinonale Vereinigung für Theoretische und Angewandte Limnologie)*, 22, 712-718

Renberg I and M Wik, 1985: Soot particle counting in recent lake sediments. An indirect dating method. *Ecological Bulletins*, 37, 53-57

Rickard A, C Milliken and S Neville, 1999: *The mass concentrations and size distributions of particles in central London using non-continuous gravimetric sampling techniques.* London Borough of Camden. pp14

Rodriguez S, X Querol, A Alastuey, G Kallos and O Kakaliagou, 2001: Saharan dust contributions to PM_{10} and TSP levels in Southern and Eastern Spain. *Atmospheric Environment.* 35, 2433-2447

Rojas C M and R E V Grieken, 1992: Electron microprobe characterisation of individual aerosol particles collected by aircraft above the Southern Bight of the North Sea. *Atmospheric Environment*, 26A(7), 1231-1237

Rose N L, 1991*: Fly-ash particles in lake sediments: extraction, characterisation and distribution.* Unpublished Ph.D. Thesis, UCL

Rose N L, 1994: A note on further refinements to a procedure for the extraction of carbonaceous fly-ash particles from sediments. *Journal of Paleolimnology*, 11, 201-204

Rose N L, 1995: Carbonaceous particle record in lake sediments from the Arctic and other remote areas of the Northern Hemisphere. *The Science of the Total Environment,* 160/161, 487-496

Rose N L, 1996: Inorganic fly-ash spheres as pollution tracers. *Environmental Pollution*, 91(2), 245-252

Rose N L, T Alliksaar, J J Bowman, J Fott, S Harlock, J M Punning, K St.Clair-Gribble, J Vukic and J Watt, 1998c: The FLAME project: General discussion and conclusions *Water, Air and Soil Pollution*, 106, 329-351

Rose N L, P G Appleby, J F Boyle, A W Mackay, and R J Flower, 1998b: The spatial and temporal distribution of fossil-fuel derived pollutants in the sediment record of Lake Baikal, eastern Siberia *Journal of Paleolimnology*, 20, 151-162

Rose N L and S Harlock, 1998: The spatial distribution of characterised fly-ash particles and trace metals in lake sediments and catchment mosses in the United Kingdom *Water, Air and Soil Pollution*, 106, 287-308

Rose N L, S Harlock and P G Appleby, 1999a: The spatial and temporal distributions of spheroidal carbonaceous fly-ash particles (SCP) to the sediment records of European mountain lakes. *Water, Air and Soil Pollution*, 113, 1-32

Rose N L, S Harlock and P G Appleby, 1999b: Within basin profile variability and cross correlation of lake sediment cores using the spheroidal carbonaceous particle record *Journal of Paleolimnology*, 21, 85-96

Rose N L and S Juggins, 1994: A spatial relationship between carbonaceous particles in lake sediments and sulphur deposition. *Atmospheric Environment*, 28(2), 177-183

Rose N L, S Juggins, J Watt and R Battarbee, 1994: Fuel-type characterisation of spheroidal carbonaceous particles using surface chemistry. *Ambio*, 23(4-5), 296-299

Rose N L, S Juggins and J Watt, 1996a: Fuel-type characterisation of carbonaceous fly-ash particles using EDS-derived surface chemistries and its application to particles extracted from lake sediments. *Proceedings of the Royal Society of London.* A(452), 881-907

Rose N L, J M Punning, J Fott, J Bowman, J Watt, T Alliksaar, S Harlock, S Juggins, K St.Clair-Gribble and J Vukie, 1996b: *Fly ash and metals in Europe: implications for human and environmental health (FLAME).* EU Copernicus Programme. Contract Number: CIPA-CT93-0090. Final report.

Rosenfeldt and Rudich, May 2001: http://www.gsfc.nasu.gov/gsfc/earth/dust/rainfall.html.

Russell Bullock Jr O, K A Brehme and G R Mapp, 1998: Lagrangian modelling of mercury air emission, transport and deposition: An analysis of model sensitivity to emissions uncertainty. *The Science of the Total Environment*, 213, 1-12

Sabbioni C and G Zappia, 1991: Particle elemental characterisation on urban monuments. *Journal of Aerosol Science*, 22(Supp 1), S681-S684

Sabbioni C and G Zappia, 1992: Decay of sandstone in urban areas correlated with atmospheric aerosol. *Water, Air and Soil Pollution*, 63, 305-316

Sadasivan S and B S Negi, 1990: Elemental characterisation of atmospheric aerosols. *The Science of the Total Environment*, 96, 269-279

Scaperdas A and R N Colville, 1999: Assessing the representativeness of monitoring data from an urban intersection site in central London, UK. *Atmospheric Environment*, 33, 661-674

Schure M R, P A Soltys, D F S Natusch, and T Mauney, 1985: Surface area and porosity of coal fly ash. *Environmental Science and Technology*, 19, 82-86

Seaton A, W MacNee, K Donaldson and D Godden, 1995: Particulate air pollution and acute health effects. *The Lancet*, 345(January), 176-178

Seika M, R M Harrison and N Metz, 1998: Ambient background model (ABM): development of an urban gaussian dispersion model and its application to London. *Atmospheric Environment*, 32(11), 1881-1891

SEIPH, 1995: *Air quality in London 1994. The second report of the the London Air Quality Network.* Association of London Authorities, London Boroughs Association and South East Institute of Public Health. Chapter 5

SEIPH, 1996: *The third report of the London Air Quality Network.* Chapters 2, 5 and 7. SEIPH.

SEIPH, 1997: *The AIM Project and air quality in London, 1996.* Chapters 3, 4, 7 and Executive Summary. SEIPH.

SEIPH, 1999: *Air quality in London 1998. The sixth report of the London Air Quality Network.* SEIPH - Environmental Research Group, Kings College London, pp62

Sitzmann B, M Kendall, J Watt and I Williams, 1999: Characterisation of airborne particles in London by computer-controlled scanning electron microscopy. *The Science of the Total Environment*, 241, 63-73

Sharan M, S G Gopalakrishnan, R T McNider and M P Singh, 2000: A numerical investigation of urban influences on local meterological conditions during the Bhopal gas incident. *Atmospheric Environment*, 34, 539-552

Shen T T, R J Cheng, V A Mohnen, M Current and Hudson J B, 1976: *Characterisation of differences between oil-fired and coal-fired power plant emissions. III-10.* The Fourth International Clean Air Congress.

Shu J, J A Dearing, A P Morse, L Yu and N Yuan, 2001: Determining the sources of atmospheric particles in Shanghai, China, from magnetic and geochemical properties. *Atmospheric Environment*, 35, 2615-2625

Sly E G, 1978: Sedimentary processes in lakes. *Lakes Chemistry, Geology, Physics*, 65-89

Smith S, F T Stribley, P Milligan and B Barratt, 2001: Factors influencing measurements of PM_{10} during 1995-1997 in London. *Atmospheric Environment*, 35, 4651-4662

Sofiev M, 2000: A model for the evaluation of long-term airborne pollution transport at regional and continental scales. *Atmospheric Environment*, 34, 2481-2493

Stedman J R, 1998: The secondary particle contribution to elevated PM_{10} concentrations in the UK. *Clean Air*, 28, 87-93

Stedman J R, E Linehan and B Conlan, 2001: Receptor modelling of PM_{10} concentrations at a United Kingdom national network monitoring site in central London. *Atmospheric Environment*, 35, 297-304

Stirling R, 1997: *The weather of Britain.* Giles de la Mare Publishers Limited, 3 Queen Square, London, WC1N 3AU.

ter Braak C J F, and P Smilauer, 1998: *CANOCO reference manual and user's guide to Canoco for Windows.*

Triantafyllou A G, 2001: PM_{10} pollution episodes as a function of synoptic climatology in a mountainous industrial area. *Environmental Pollution*, 112, 491-500

Van der Wal J T and L H J M Janssen, 2000: Analysis of spatial and temporal variations of PM_{10} concentrations in the Netherlands using Kalman filtering. *Atmospheric Environment*, 34, 3675-3687

Van Malderen H, C Rojas and R Van Grieken, 1992: Characterisation of individual giant aerosol particles above the North Sea. *Environmental Science and Technology*, 26, 750-756

Watson J G and J C Chow, 2001: Source characterization of major emission sources in the Imperial and Mexicali Valleys along the US/Mexico border. *The Science of the Total Environment*, 276, 33-47

Webb A H, R J Bawden, A K Busby and J N Hopkins, 1992: Studies on the effects of air pollution on limestone degradation in Great Britain. *Atmospheric Environment*, 26B(2), 165-181

Webster R and M A Oliver, 1990: *Sampling and estimation. Statistical methods in soil and land resource survey.* Chapter 3. Oxford University Press.

Wik M and J Natkanski, 1990: British and Scandinavian lake sediment records of carbonaceous particles from fossil fuel combustion. *Philosophical Transactions of the Royal Society of London*, B(327), 319-323

Wik M, I Renberg and J Darley, 1986: Sedimentary records of carbonaceous particles from fossil fuel combustion. *Hydrobiologia*, 143, 387-394

Wik M and I Renberg, 1991: Recent atmospheric deposition in Sweden of carbonaceous particles from fossil-fuel combustion surveyed using lake sediments. *Ambio*, 20(7), 289-292

Wordley J, S Walters and J G Ayers, 1997: Short term variations in hospital admissions and mortality and particulate air pollution. *Occupational Environmental Medicine*, 54, 108-116

Xia J and D Y C Leung, 2001: Pollution dispersion in urban street canopies. *Atmospheric Environment*, 35, 2033-2043

Xie S, J A Dearing, J Bloemendal and J Boyle, 1999: Association between the organic matter content and magnetic properties in street dust, Liverpool, UK. *The Science of the Total Environment*, 241, 205-214

Yang H, 2000: *Trace metal storage in lake system and its relationship with atmospheric deposition with particular reference to Lochnagar, Scotland.* Unpublished PhD thesis, University of London

APPENDIX

A detailed size breakdown of all SCPs in the twenty-seven lakes and ponds is included below.

Site	Percentage of SCPs in size fraction (μm)									
	0-2.56	2.56-5.13	5.13-7.69	7.69-10.25	10.26-12.82	12.82-15.38	15.38-17.95	17.95-20.51	20.51-23.08	23.08-25.64
ADDI	0.00	0.93	5.12	10.70	10.70	13.02	12.09	9.77	7.44	4.19
ALEX	0.00	0.00	1.61	1.61	6.45	14.52	17.74	14.52	6.45	6.45
BANB	0.00	3.09	5.15	7.22	7.22	10.31	19.59	11.34	7.22	6.19
BEDE	0.00	3.28	8.20	6.56	9.84	4.92	6.56	9.84	4.92	13.11
BREN	0.00	3.95	13.16	14.47	10.53	7.89	9.21	7.89	9.21	2.63
BROO	0.00	0.00	3.28	5.74	4.51	5.74	6.15	9.43	9.43	5.74
BUSH	0.00	0.60	5.72	8.43	7.53	7.53	12.05	8.13	6.93	5.42
CHER	0.00	0.00	1.96	5.88	19.61	15.69	9.80	9.80	7.84	7.84
CROS	0.00	0.00	2.14	8.02	11.23	6.42	8.02	8.02	8.56	5.88
DAGN	0.00	1.67	2.50	10.42	8.75	10.00	10.42	9.58	8.33	4.58
DUCK	0.00	0.93	8.41	11.53	15.26	13.08	8.72	7.17	8.41	7.17
EALI	0.00	0.86	3.43	7.14	11.14	10.57	11.71	8.57	7.43	5.14
FAIR	0.00	0.63	8.81	10.69	18.87	15.09	11.32	10.06	5.03	6.29
FLIN	0.00	2.06	10.31	14.43	9.28	13.40	8.25	10.31	5.15	4.12
HOLL	0.30	1.51	3.93	8.16	13.60	11.48	8.16	10.88	11.18	5.44
NORS	0.00	3.02	9.37	12.08	13.60	9.06	12.99	9.37	6.65	4.23
PECK	0.52	0.00	3.09	6.70	11.34	12.89	14.43	10.82	6.70	7.22
QUEE	0.00	0.51	9.23	12.31	13.33	7.69	11.28	10.26	4.62	3.08
REG	0.00	0.16	3.32	9.18	8.86	13.45	9.49	8.54	6.80	7.12
RICH	0.00	1.35	4.05	10.81	13.51	9.46	12.16	8.11	8.11	2.70
SHEN	0.00	0.00	3.23	4.84	9.68	12.90	11.29	8.06	8.06	8.06
STANM	0.00	1.03	4.44	8.89	13.68	11.79	10.77	7.01	7.52	5.47
STEN	0.00	5.59	8.39	6.29	14.69	9.09	11.89	10.49	4.20	4.20
STEW	0.00	1.04	8.33	12.50	7.29	11.46	10.42	8.33	5.21	4.17
VICT	0.00	0.65	3.07	7.28	8.74	9.71	7.61	8.58	8.74	7.61
WAND	0.00	0.00	2.83	8.13	10.95	11.66	10.25	10.25	9.89	5.30
WHITV	0.00	0.00	4.21	8.74	10.68	9.71	9.39	9.39	8.74	7.44

Site	Percentage of SCPs in size fraction (μm)									
	25.64-28.21	28.21-30.77	30.77-33.33	33.33-35.90	35.90-38.46	38.46-41.03	41.03-43.59	43.59-46.15	46.15-48.72	48.72-51.28
ADDI	4.65	5.58	3.26	2.33	2.79	2.33	0.93	0.93	0.93	0.47
ALEX	3.23	3.23	6.45	3.23	3.23	1.61	3.23	0.00	1.61	0.00
BANB	4.12	3.09	1.03	4.12	1.03	0.00	2.06	2.06	0.00	2.06
BEDE	8.20	1.64	6.56	4.92	1.64	3.28	1.64	1.64	0.00	0.00
BREN	7.89	1.32	1.32	2.63	2.63	3.95	0.00	0.00	0.00	0.00
BROO	6.56	4.10	4.10	5.33	3.28	1.23	2.05	1.64	1.23	2.46
BUSH	6.93	6.33	2.71	4.22	3.61	3.31	1.81	1.81	0.60	1.20
CHER	5.88	5.88	3.92	5.88	0.00	0.00	0.00	0.00	0.00	0.00
CROS	6.95	4.81	5.35	2.14	1.07	4.81	1.60	1.60	2.67	2.14
DAGN	4.58	4.17	1.67	3.33	4.17	1.67	2.92	0.83	1.67	2.08
DUCK	2.49	2.18	2.18	2.80	2.18	1.25	1.56	0.31	0.93	0.62
EALI	3.14	4.86	4.00	3.71	4.29	1.71	3.43	0.86	1.14	2.00
FAIR	4.40	1.89	1.89	1.26	0.00	0.00	1.26	0.00	0.00	0.00
FLIN	5.15	2.06	3.09	1.03	1.03	2.06	1.03	1.03	1.03	0.00
HOLL	6.65	2.11	4.23	3.63	1.51	1.21	0.91	0.60	1.21	0.60
NORS	3.32	3.32	2.42	3.63	0.30	1.21	0.91	0.60	0.91	0.60
PECK	5.15	4.64	4.12	3.09	2.58	0.52	0.52	0.52	1.03	1.03
QUEE	5.13	5.13	3.08	2.56	3.59	1.54	0.51	0.51	0.51	0.51
REG	5.38	6.49	5.54	2.85	3.80	1.42	2.22	1.27	0.63	0.79
RICH	5.41	5.41	5.41	1.35	0.00	0.00	1.35	2.70	2.70	2.70
SHEN	3.23	8.06	11.29	4.84	4.84	0.00	0.00	0.00	1.61	0.00
STANM	5.81	3.42	5.13	2.74	2.91	1.37	1.37	1.54	0.85	0.34
STEN	3.50	1.40	2.80	2.80	3.50	1.40	1.40	2.80	0.70	1.40
STEW	7.29	6.25	4.17	0.00	1.04	2.08	0.00	2.08	4.17	2.08
VICT	5.34	3.56	4.21	4.53	4.53	2.91	2.27	2.27	1.62	1.13
WAND	8.48	4.24	1.77	3.18	2.47	1.06	1.77	2.83	0.35	1.41
WHITV	6.15	5.18	3.88	3.56	2.91	2.59	1.94	1.29	1.29	0.00

Site	Percentage of SCPs in size fraction (μm)									
	51.28-53.85	53.85-56.41	56.41-58.97	58.97-61.54	61.54-64.10	64.10-66.67	66.67-69.23	69.23-71.79	71.79-74.36	74.36-76.92
ADDI	0.00	0.47	0.00	0.47	0.00	0.47	0.00	0.00	0.00	0.00
ALEX	1.61	1.61	0.00	1.61	0.00	0.00	0.00	0.00	0.00	0.00
BANB	1.03	0.00	0.00	0.00	0.00	1.03	0.00	0.00	0.00	0.00
BEDE	0.00	1.64	0.00	0.00	0.00	1.64	0.00	0.00	0.00	0.00
BREN	0.00	0.00	0.00	1.32	0.00	0.00	0.00	0.00	0.00	0.00
BROO	1.64	1.23	0.82	2.46	2.87	0.82	2.05	0.41	0.82	0.41
BUSH	1.81	0.90	0.30	0.60	0.60	0.30	0.00	0.00	0.30	0.00
CHER	0.00	0.00	0.00	0.00	0.00	0.00	0.00	0.00	0.00	0.00
CROS	0.53	1.07	0.53	2.14	0.53	1.07	0.53	0.53	0.53	0.00
DAGN	0.83	0.42	1.67	0.00	0.83	1.25	0.00	0.42	0.00	0.83
DUCK	0.31	0.31	0.31	0.31	0.62	0.31	0.00	0.31	0.00	0.31
EALI	1.14	1.43	0.29	0.29	0.57	0.57	0.00	0.00	0.00	0.00
FAIR	0.00	0.63	0.00	1.89	0.00	0.00	0.00	0.00	0.00	0.00
FLIN	0.00	1.03	1.03	0.00	0.00	1.03	1.03	1.03	0.00	0.00
HOLL	0.30	0.91	0.30	0.30	0.00	0.00	0.00	0.00	0.30	0.00
NORS	0.00	0.30	1.21	0.00	0.30	0.00	0.00	0.30	0.30	0.00
PECK	1.03	0.00	0.00	0.00	0.52	0.52	0.00	0.00	0.00	0.00
QUEE	0.51	1.03	1.03	0.00	0.00	0.00	0.51	1.03	0.00	0.00
REG	1.27	0.16	0.32	0.32	0.00	0.16	0.00	0.00	0.00	0.00
RICH	1.35	0.00	0.00	1.35	0.00	0.00	0.00	0.00	0.00	0.00
SHEN	0.00	0.00	0.00	0.00	0.00	0.00	0.00	0.00	0.00	0.00
STANM	1.03	0.34	0.34	0.17	0.51	0.34	0.68	0.00	0.34	0.00
STEN	0.00	0.70	1.40	0.00	0.00	0.00	0.00	0.00	0.00	0.00
STEW	0.00	0.00	0.00	0.00	1.04	0.00	1.04	0.00	0.00	0.00
VICT	0.65	0.81	0.49	1.29	0.32	0.32	0.49	0.00	0.32	0.32
WAND	0.35	0.35	0.35	0.71	0.35	0.00	0.35	0.00	0.00	0.71
WHITV	0.65	0.32	0.97	0.32	0.00	0.32	0.00	0.00	0.00	0.32

Site	Percentage of SCPs in size fraction (μm)									
	76.92-79.49	79.49-82.05	82.05-84.62	84.62-87.18	87.18-89.74	89.74-92.31	92.31-94.87	94.87-97.44	97.44-100.00	100.00-102.56
ADDI	0.00	0.00	0.00	0.00	0.00	0.00	0.00	0.00	0.00	0.47
ALEX	0.00	0.00	0.00	0.00	0.00	0.00	0.00	0.00	0.00	0.00
BANB	0.00	0.00	1.03	0.00	0.00	0.00	0.00	0.00	0.00	0.00
BEDE	0.00	0.00	0.00	0.00	0.00	0.00	0.00	0.00	0.00	0.00
BREN	0.00	0.00	0.00	0.00	0.00	0.00	0.00	0.00	0.00	0.00
BROO	0.41	1.23	0.00	0.00	0.82	0.00	0.41	0.82	0.00	0.41
BUSH	0.00	0.00	0.30	0.00	0.00	0.00	0.00	0.00	0.00	0.00
CHER	0.00	0.00	0.00	0.00	0.00	0.00	0.00	0.00	0.00	0.00
CROS	0.53	0.53	0.00	0.00	0.00	0.00	0.00	0.00	0.00	0.00
DAGN	0.00	0.00	0.00	0.00	0.00	0.00	0.00	0.00	0.00	0.00
DUCK	0.00	0.00	0.00	0.00	0.00	0.00	0.00	0.00	0.00	0.00
EALI	0.00	0.00	0.00	0.00	0.29	0.00	0.00	0.00	0.29	0.00
FAIR	0.00	0.00	0.00	0.00	0.00	0.00	0.00	0.00	0.00	0.00
FLIN	0.00	0.00	0.00	0.00	0.00	0.00	0.00	0.00	0.00	0.00
HOLL	0.30	0.30	0.00	0.00	0.00	0.00	0.00	0.00	0.00	0.00
NORS	0.00	0.00	0.00	0.00	0.00	0.00	0.00	0.00	0.00	0.00
PECK	1.03	0.00	0.00	0.00	0.00	0.00	0.00	0.00	0.00	0.00
QUEE	0.00	0.00	0.00	0.00	0.00	0.00	0.00	0.00	0.00	0.51
REG	0.00	0.00	0.00	0.00	0.32	0.00	0.00	0.00	0.00	0.00
RICH	0.00	0.00	0.00	0.00	0.00	0.00	0.00	0.00	0.00	0.00
SHEN	0.00	0.00	0.00	0.00	0.00	0.00	0.00	0.00	0.00	0.00
STANM	0.00	0.00	0.00	0.00	0.00	0.00	0.00	0.00	0.00	0.00
STEN	0.70	0.00	0.00	0.00	0.00	0.00	0.00	0.00	0.00	0.00
STEW	0.00	0.00	0.00	0.00	0.00	0.00	0.00	0.00	0.00	0.00
VICT	0.16	0.49	0.00	0.00	0.00	0.00	0.00	0.00	0.00	0.00
WAND	0.00	0.00	0.00	0.00	0.00	0.00	0.00	0.00	0.00	0.00
WHITV	0.00	0.00	0.00	0.00	0.00	0.00	0.00	0.00	0.00	0.00

Site	Percentage of SCPs in size fraction (μm)									
	102.56-105.13	105.13-107.69	107.69-110.26	110.26-112.82	112.82-115.38	115.38-117.95	117.95-120.51	120.51-123.08	123.08-125.64	125.64-128.21
ADDI	0.00	0.00	0.00	0.00	0.00	0.00	0.00	0.00	0.00	0.00
ALEX	0.00	0.00	0.00	0.00	0.00	0.00	0.00	0.00	0.00	0.00
BANB	0.00	0.00	0.00	0.00	0.00	0.00	0.00	0.00	0.00	0.00
BEDE	0.00	0.00	0.00	0.00	0.00	0.00	0.00	0.00	0.00	0.00
BREN	0.00	0.00	0.00	0.00	0.00	0.00	0.00	0.00	0.00	0.00
BROO	0.41	0.00	0.00	0.00	0.00	0.00	0.00	0.00	0.00	0.00
BUSH	0.00	0.00	0.00	0.00	0.00	0.00	0.00	0.00	0.00	0.00
CHER	0.00	0.00	0.00	0.00	0.00	0.00	0.00	0.00	0.00	0.00
CROS	0.00	0.00	0.00	0.00	0.00	0.00	0.00	0.00	0.00	0.00
DAGN	0.00	0.00	0.00	0.00	0.00	0.00	0.00	0.42	0.00	0.00
DUCK	0.00	0.00	0.00	0.00	0.00	0.00	0.00	0.00	0.00	0.00
EALI	0.00	0.00	0.00	0.00	0.00	0.00	0.00	0.00	0.00	0.00
FAIR	0.00	0.00	0.00	0.00	0.00	0.00	0.00	0.00	0.00	0.00
FLIN	0.00	0.00	0.00	0.00	0.00	0.00	0.00	0.00	0.00	0.00
HOLL	0.00	0.00	0.00	0.00	0.00	0.00	0.00	0.00	0.00	0.00
NORS	0.00	0.00	0.00	0.00	0.00	0.00	0.00	0.00	0.00	0.00
PECK	0.00	0.00	0.00	0.00	0.00	0.00	0.00	0.00	0.00	0.00
QUEE	0.00	0.00	0.00	0.00	0.00	0.00	0.00	0.00	0.00	0.00
REG	0.16	0.00	0.00	0.00	0.00	0.00	0.00	0.00	0.00	0.00
RICH	0.00	0.00	0.00	0.00	0.00	0.00	0.00	0.00	0.00	0.00
SHEN	0.00	0.00	0.00	0.00	0.00	0.00	0.00	0.00	0.00	0.00
STANM	0.00	0.00	0.00	0.00	0.17	0.00	0.00	0.00	0.00	0.00
STEN	0.00	0.00	0.00	0.00	0.00	0.00	0.00	0.00	0.70	0.00
STEW	0.00	0.00	0.00	0.00	0.00	0.00	0.00	0.00	0.00	0.00
VICT	0.00	0.00	0.00	0.00	0.00	0.00	0.00	0.00	0.00	0.00
WAND	0.00	0.00	0.00	0.00	0.00	0.00	0.00	0.00	0.00	0.00
WHITV	0.00	0.00	0.00	0.00	0.00	0.00	0.00	0.00	0.00	0.00